FABRICATION AND CHARACTERIZATION OF METAL OXIDE NANOSTRUCTURED THIN FILM FOR PHOTOVOLTAIC APPLICATION

By

UKOBA, Kingsley Ogheneovo (*B. Eng.; M. Eng.*)

216075239

Supervisor: Prof. Freddie L. Inambao

Thesis submitted in fulfilment of the requirements for the degree of DOCTOR OF PHILOSOPHY IN ENGINEERING (PhD)

(MECHANICAL ENGINEERING)

College of Agriculture, Engineering and Science, University of KwaZulu-Natal,
Durban, South Africa

2018

As the candidate's supervisor, I have approved this thesis for submission.

Signed:  Date: 2nd May, 2018

Name: Prof. Freddie L. Inambao

Declaration 1 – Plagiarism

I, **Ukoba, Kingsley Ogheneovo**, declare that:

1. The research reported in this thesis, except where otherwise indicated is my original research.

2. This thesis has not been submitted for any degree or examination at any other university.

3. This thesis does not contain other persons' data, pictures, graphs or other information, unless specifically acknowledged as being sourced from other persons.

4. This thesis does not contain other persons' writing, unless specifically acknowledged as being sourced from other researchers. Where other written sources have been quoted, then:

a) Their words have been re-written but the general information attributed to them has been referenced.

b) Where their exact words have been used, then their writing has been placed in italics and inside quotation marks, and referenced.

5. This thesis does not contain text, graphics or tables copied and pasted from the internet, unless specifically acknowledged, and the source being detailed in the thesis and in the References sections.

Signed…  …… Date: 27th March, 2018

Declaration 2 - Publications

This section presents the articles that form part and/or include the research presented in this thesis. The following papers have been published, accepted or under review:

ISI/SCOPUS/DoHET Accredited Journals

1. **Ukoba, O.K.,** Eloka-Eboka, A.C. and Inambao F.L. (2018). "Review of nanostructured NiO thin film deposition using Spray pyrolysis technique", *Renewable and Sustainable Energy Reviews ISSN: 13640321,* vol 82, pp 2900 - 2915. DOI: 10.1016/j.rser.2017.10.041, Elsevier publishers (**Published**).

2. **Ukoba, O.K.,** Inambao F.L. and Eloka-Eboka, A.C. (2017) "Influence of annealing on properties of spray deposited nickel oxide films for solar cells", *Energy Procedia,* vol 142, December 2017, pp. 244–252. DOI: 10.1016/j.egypro.2017.12.039, Elsevier publishers (**Published**).

3. **Ukoba, O.K**., Eloka-Eboka, A.C. and Inambao F.L. (2017) "Influence of concentration on properties of spray deposited nickel oxide films for solar cells", *Energy Procedia,* vol 142, pp. 236–243. DOI: 10.1016/j.egypro.2017.12.038, Elsevier publishers (**Published**).

4. **Ukoba, O.K.,** Inambao F.L. and Eloka-Eboka, A.C. (2018) "Experimental optimization of nanostructured nickel oxide deposited by spray pyrolysis for solar cells application" *International Journal of Applied Engineering Research,* vol 13(6), pp. 3165-3173 (**Published**).

5. **Ukoba, O.K**., Inambao F.L. and Eloka-Eboka, A.C. "Study of deposition temperature on properties of aged nanostructured nickel oxide for solar cells", *International Journal of Renewable Energy Research,* vol 8, no 2, pp 724 – 732, June 2018 (**Published**).

6. **Ukoba, K. O**., Inambao, F. L., & Eloka-Eboka, A. C. (2018) "Fabrication of affordable and sustainable solar cells using NiO/TiO2 PN heterojunction" *International Journal of Photoenergy,* vol. 2018, pp 1-7, Hindawi publishers (**Published**).

7. **Ukoba, O.K.,** and Inambao F.L. (2018) "Modeling of Properties of Fabricated NiO/TiO_2 heterojunction solar cells". *International Journal of Applied Engineering Research* ISSN 09734562, vol. 13, number 11, pp. 9701-9705 (**Published**).

8. Ukoba, O.K; and Inambao FL. (2018) “Solar Cells and Global Warming Reduction”. International Journal of Applied Engineering Research, ISSN 09734562, vol. 13 (10), pp. 8303-8310 (**Published**).

9. **Ukoba, O.K.,** Eloka-Eboka, A.C. and Inambao F.L. “Review of solar energy inclusion in Africa; case study of Nigeria” Proceedings of *ISES Solar World Congress 2017*, pp 962 – 973, Abu Dhabi, UAE, 2017. DOI:10.18086/swc.2017.16.05 (**Published**).

10. **Ukoba, O.K.,** Eloka-Eboka, A.C. and Inambao F.L. Optimizing aged nanostructured nickel oxide thin films for solar cells. *Journal of Physical Science* (Accepted).

11. **Ukoba, O.K.,** and Inambao, F.L “Investigation of Optoelectronic Properties of Nanostructured TiO_2/NiO Heterojunction Solar Cells” *International Journal of Green Energy*, (Under review).

International and DHET accredited conferences

1. **Ukoba, O.K.,** Eloka-Eboka, A.C. and Inambao F.L. “Optimizing properties of nanostructured NiO thin films for affordable and sustainable solar energy” presented at *5th Nano Today* conference organized by Elsevier and held on December 6-10, 2017, Waikoloa Beach Marriott, Hawaii, USA.

2. **Ukoba, O.K** “The Role of Solar Cells in Reducing Air Pollution” Presented at NewtonFund/British Council (UK/South Africa/Kenya) Trilateral Workshop entitled *Air Pollution in Emerging Mega-Cities: Sources, Evolution and Impacts* from April 16 – 20, 2018 at Silver Spring Hotel, Nairobi, Kenya.

3. **Ukoba, O.K.,** Inambao, F.L and Adeoye A.E. “Modeling and simulation of metal oxide solar cells: an overview” 15th Industrial and Commercial Use of Energy held at Cape Peninsula University of Technology, Cape Town, South Africa, 13 – 15 August, 2018.

4. **Ukoba, O.K** and Inambao, F.L. “Solar Energy and Post-Harvest Loss Reduction in Roots and Tubers in Africa” Accepted for presentation at World Congress on Engineering and Computer Science 2018 (WCECS 2018), San Francisco, USA, 23-25 October, 2018.

5. **Ukoba, O.K** and Inambao, F.L “Study of Properties of Nanostructured TiO_2/NiO Heterojunction Solar Cells” Accepted for presentation and book chapter by World Congress on Engineering and Computer Science 2018 (WCECS 2018), San Francisco, USA, 23-25 October, 2018.

The candidate is the main and corresponding author for all the publications and Prof. Freddie L. Inambao is the supervisor.

Dedication

This thesis is dedicated to every young person, especially the African child, who is struggling to make it in life. Never give up on your dreams. And to my family members and friends for sharing in my pains and joy all the time.

Acknowledgements

I give glory to God that lifts the commoner from the dunghill and places him among the princes and nobles. To my family for the love and support before and during the course of my studies. To my very wonderful Onome, my parents, bros Daniel, Roland, Austine, The Alamu's, Uzuokoh's, Favour, I love you guys.

I am grateful to the National Research Foundation and The World Academy of Science (NRF/TWAS) for believing in the work and funding it.

To other institutes, agencies and individuals that supported me one way or the other especially staff and management of EMDI, Akure especially my oga Dr. Olusunle, NDDC, MMU UKZN, iThembaLab, Geology XRD, UKZN – I appreciate you all.

To my friends too numerous to mention especially Dr. Adeoye Abiodun who mentored and helped me from development to completion, God will reward you for me. To Dr. Imoisili, Dr. Ogunmola, Jolly, Dr. Ezekiel, Akpan, Dr. Akuru Bola, Olumide, Tolulope Adebiyi, Fatounde, Raymond, Dr. Oyelami, Engr. Ogunkoya, Pst Komolafe, Mrs. Komolafe, Mrs. Yusuf, Mr and Mrs Iruobe and others that space would not allow me to mention, you are appreciated. All the DMS staff is acknowledged.

I also appreciate members of Winners Chapel both in Nigeria and Durban especially Pst. Adeniyi Olukotun family, Kolawole Muyiwa, Dcn Niyi Ayeleso, Ubaba and family, Ibukun Fatoyibo and Popoola Ayo, members of my research group (Green Energy Solutions) especially my lab mates Amina, Samwell, Salma, Femi Ige, Gloria, Dr. Onuh, Dr Ebhota, Omolara, Akande, Omojola.

Special appreciation to Dr Richard Steele for his professional editing service in this research.

I also appreciate Dr Richard Loubser for the opportunity to tutor his courses in both semesters.

Others staff of UKZN and mechanical engineering in general, I appreciate you all. A big thank you to HoS Prof. Bright, Kogie Naicker, Shaun, among others. I want to appreciate Dr Andrew for all the help and guidance. And a special appreciation to the supervising team ably led by a father and a mentor, Prof. Freddie Inambao. Pardon me if your name is omitted, but your effort is acknowledged.

Table of Contents

List of Figures

List of Tables

List of Appendices

Nomenclature

Symbol	Description	Unit
I-V	Current-voltage	Ampere-volts
J-V	Current density-voltage	Amperes/m^2- volts
J_{sc}	Short-circuit current density	Amperes
P_{in}	Power in	Watts
Pmax	Maximum power	Watts
V_{oc}	Open-circuit voltage	volts
Au	Gold	
CuO	Copper oxide	
FF	Fill factor	
In_2O_3	Indium oxide	
ITO	Indium tin oxide	
Ni	Nickel	
NiO	Nickel oxide	
O	Oxygen	
Ti	Titanium	
TiO_2	Titanium oxide	
ZnO	Zinc oxide	

Acronyms/Abbreviations

Au	Gold
CuO	Copper Oxide
EDX	Energy Dispersive X-ray Spectrometer
FEGSEM	Field Emission Gun Scanning Electron Microscope
FF	Fill Factor
GDP	Gross Domestic Product
In_2O_3	Indium Oxide
ITO	Indium Tin Oxide
Jsc	Short-circuit current density
MO	Metal Oxide
Ni	Nickel
NiO	Nickel Oxide
NREL	National Renewable Energy Laboratory
O	Oxygen
P_{in}	Power in
Pmax	Maximum Power
PV	Photovoltaic
SCAP	Solar Cell Analysis Programs
SPT	Spray Pyrolysis Technique

Ti	Titanium
TiO_2	Titanium oxide
XRD	X-ray Diffractometer
ZnO	Zinc Oxide

Abstract

This study focused on fabrication and characterization of nanostructured metal oxide heterojunction solar cells for photovoltaic application. The study involved experimental fabrication of the device and modelling and theoretical validation of the fabricated device. The laboratory experiment was carried out by fabricating and characterizing nanostructured metal oxide thin film based solar cells using chemical spray pyrolysis and magnetron sputtering deposition techniques. The study included device design, materials tuning, process development, device characterization, device simulation, device reliability testing, and device circuit demonstration. The study covers the whole course of the device lithography and development.

The spray pyrolysis method was used for depositing nickel oxide (NiO) thin films. Scanning electron microscope (SEM), energy dispersive X-ray powder diffraction (XRD), and Fourier transform infrared microscopy (FTIR) were used to characterize the films and four-point probe for the final device. Experimental optimization was conducted on the films with a focus on pre-deposition, deposition and post-deposition. The optimized result was used to fabricate a metal oxide NiO/TiO_2 P-N heterojunction solar cell using spray pyrolysis and magnetron sputtering techniques. The optoelectronic properties of the heterojunction were determined. The fabricated solar cell exhibited 16.8 mA for the short circuit current, 350 mV open circuit voltage, 0.39 fill factor and conversion efficiency of 2.30 % under 100 mW/cm^2 illumination.

The result obtained from the experiment was compared and evaluated with the simulated results. The theoretical understanding of the device was modelled and theoretically validated. Theoretical understanding of the solar cell was established and thereafter the fabricated device modelled using solar cell analysis programs (SCAPxD). The working points used for the modelling included a temperature of 350 ^oC, illumination of $100mW/cm^2$, the voltage range of 0 volts to 1.5 volts. The output gave filled factor (FF) of 0.38 % which validated the experimental results.

This study is a boosts in the quest to develop low-cost, environmentally friendly and sustainable solar cells materials and deposition method especially in developing and low-income countries that are experiencing electricity shortage using nanostructured metal oxide.

CHAPTER 1: INTRODUCTION

1.1 Introduction

There is a growing need for energy sources that are affordable, sustainable and environmentally benign. This arises from the fast depletion of present energy sources which are mainly fossil fuels. This has brought about a huge interest in alternative sources of energy. These alternate sources are mainly renewable energy such as wind, solar, tidal, geothermal, etc. Single or combined usage of such energy has been proven to be economically and socially acceptable worldwide.

Solar energy stands out among these alternate energy sources because of its potential global availability. Solar energy is infinite in relation to human existence. Today, there is a huge interest in increasing solar energy efficiency. The conversion of solar energy to affordable useable energy is one of the most promising ways of overcoming global energy challenges. There has been a reduction in prices of solar technologies around the world but it is still out of the reach of developing and low-income countries.

Studies are being channelled towards affordable, sustainable and environmentally benign methods and materials that will lead to easy availability of solar technologies. Nanostructured metal oxide is one such material. Studies have confirmed that p-type metal oxides exhibit better carrier mobility and greater stability compared to organic materials [1-3].

Nickel Oxide (NiO) is a p-type metal oxide with great promise. It has great air stability, and large open circuit voltage when compared with poly (3,4-ethylenedioxythiophene) polystyrene sulfonate (PEDOT: PSS). It can be deposited by physical and chemical methods. However, research is being conducted in search of a low-cost and sustainable deposition method that requires little or no electricity usage. This is owing to the fact that most developing and low-income countries have little or no constant power supply.

1.2 Research motivation

Solar energy has been tipped to be a better replacement for fossil fuels owing to its renewability and environmental benign nature. Solar cells are the building blocks of solar energy. The current solar energy market is dominated by silicon based solar cells. Such solar cells are effective but have drawbacks that hinder full utilization in developing and low-income countries. Silicon based solar cells are single band gap. One of the drawbacks is heat generation that tends to reduce the efficiency. This is because solar radiation with less energy than the band gap of silicon passes straight through. Further, the solar cells are unable to utilize the extra energy from radiation with higher energy than silicon. Another drawback is that the production process is expensive since it requires the use of high power consumption equipment such as a furnace, vacuum pumps and so on. It also involves the use of chemicals that are environmentally harmful. Thus, there is a need to find a new approach to photovoltaic (PV) cells that will be cheap, sustainable and environmentally benign with good efficiency. In the course of the past decade, different approaches have been developed to compete with traditional silicon based PV devices by employing p-n junctions with emphasis on low-cost materials and manufacturing techniques [4]. This motivated this study to focus on nanostructured metal oxide for possible usage in heterojunction solar cell fabrication owing to their cheap material costs and manufacturing techniques.

1.3 Problem statement

As the worldwide demand for energy is becoming greater than the supply, the cost of supplying electricity becomes expensive. Also, it is a growing concern that global warming (greenhouse effect) and climate changes are being caused by usage of fossil fuels like coal, oil and gas. These fossil fuels are the major source for about 66% of electricity supply globally, and accounts for 95% of total energy demands on earth [5]. Hence it is important to find a source of renewable energy which is clean, efficient, and sustainable. Among the various renewable energy sources which include biomass, geothermal, solar, wind and mini hydro, solar energy stands out owing to its infinite nature and global availability. Solar energy is useful for generating electricity both on small and large scales. However, cost and storage are major drawbacks hindering its usage worldwide [6]. Therefore, the search is on for ways to reduce the cost of solar cells and solar panels to a competitive level with conventional ways of generating electricity. This can be achieved by fabrication of solar cells while maintaining higher efficiency.

Increasing solar cell efficiency can be achieved in two ways:

1. Careful material selection with suitable energy gaps that match the solar spectrum and fine-tuning the material optoelectronic properties.

2. Novel device development for charge collection and better solar spectrum utilization by employing single, ternary and quaternary semiconductor materials.

Hence, this work developed a nanostructured metal oxide thin film based solar cell system for PV and optoelectronic device.

1.4 Background to the study

This work lies within the field of renewable energy and nanotechnology. The study aims to contribute to the achievement of global climate and energy goals. PV will have a momentous influence on the energy market when the energy conversion efficiency of solar cells is enhanced. Most types of PV cells use efficient thin films. Solar cell efficiency can be enhanced by modifying the properties of such films. Major challenges of solar cells are to enhance photon absorption, reduce electron-hole recombination and improve charge transport [7]. Metal oxide semiconductors are promising materials for PV applications [8]. The benign, stable and abundant nature of metal oxides encourage deposition even in ambient conditions [9]. Metal oxides are found in applications as active or passive components in a variety of commercial applications [10]. Metal oxides are used as transport layers or transparent conducting electrodes in solar cells [11]. There is currently huge interest in heterojunction metal oxide solar cells because of their low-cost potential due to the inexpensive materials and manufacturing techniques involved [12, 13]. Nanostructured oxides can play a crucial role in energy challenges faced by new sustainable and renewable energy resources. Their infinite varied structural architecture and morphological features present new hope and prospects for energy harvesting, conversion, and storage devices.

1.4.1 Development of the solar cell

Humanity has interacted with solar technology for a long time dating as far back as the 7th century BC [14]. Human beings started experimenting with the sun by focusing the sunlight with glass and mirrors to light fires and burn ants [15]. Today, this has evolved into more advanced technologies like solar powered vehicles and solar powered airplanes.

The super powers of the 3rd century (Romans and the Greeks) used sunlight focused on mirrors to light religious torches and this was also done by the Chinese in 20 A.D. [16]. The 1st to 4th Century A.D. saw the sun being used to warm water in the famous Roman bathhouses through the use of large windows that were designed to face south in order to let in the sun's rays. The Anasazi of North America lived in houses that faced the south to capture the winter sun which demonstrated passive solar design in the 1200s A.D.

The world's first solar collector was built by Horace de Saussure. Sir John Herschel took this collector to South Africa in his expedition in the 1830s for his cooking [17]. A minister in the Church of Scotland, Robert Stirling, applied for a patent in September 27, 1816, for his heat engine known as the 'eEonomizer' at the Chancery in Edinburgh, Scotland [18, 19]. This heat engine was used in a solar thermal electric technology to produce power [20]. It focused the sun's thermal energy in its operation to produce power.

It was not until 1839 that the photovoltaic effect was discovered. Edmond Becquerel, a French scientist, discovered it while experimenting with an electrolytic cell [21]. The electrolytic cell comprised two metal rods placed in an electricity-conducting solution. Electricity generation improved when exposed to light. August Mouchet, a French mathematician, and his assistant, constructed the predecessor of a modern parabolic dish collector known as a solar-powered engine which was used for various applications in the 1860s [22].

Willoughby Smith in 1873 discovered selenium photoconductivity while Williams A. Grylls alongside Richard Evans Day discovered the electricity generation ability of selenium when exposed to light in 1876, thus proving that a solid material could change light into electricity without heat or moving parts. Although selenium solar cells failed to convert enough sunlight to power electrical equipment, these researchers later went on to publish a paper on the selenium cell entitled 'The action of light on selenium,' in *Proceedings of the Royal Society*, A25, 113. Charles Fritts was able to describe the first solar cells made from selenium wafers in 1883. In 1887 Heinrich Hertz discovered that ultraviolet light altered the lowest voltage capable of causing a spark to jump between two metal electrodes.

In 1904, Wilhelm Hallwachs discovered that a metal oxide is photosensitive, namely, copper and cuprous oxide. He made a semiconductor-junction solar cell out of it. A year later, Albert Einstein published his paper on the photoelectric effect in relation to quantum mechanics. About a decade after Albert Einstein's publication, the existence of a barrier layer in PV devices was discovered, while Robert Millikan in 1916 was able to experimentally prove the

photoelectric effect. Jan Czochralski developed a method of growing single-crystal silicon (Czolchraski, 1885 – 1953).

In 1932, Audobert and Stora discovered the photovoltaic effect in cadmium selenide (CdSe), a PV material still used today. In 1948 Gordon Teal and John Little adapted the Czochralski method of crystal growth to produce single-crystalline germanium and, later, silicon [23]. On April 25, 1954, Bell Labs announces the invention of the first practical silicon solar cell [24, 25]. These cells had about 6% efficiency. Western Electric licensed commercial solar cell technologies in 1955. That same year, Hoffman Electronics‘s Semiconductor Division created a 2% efficient commercial solar cell for $25/cell or $1,785/watt. Mandelkorn T of U.S. Signal Corps Laboratories, created n-on-p silicon solar cells in 1958. These are more resistant to radiation damage and are better suited for space. Hoffman Electronics created 9% efficient solar cells. Vanguard I, the first solar powered satellite, was launched with a 0.1 W, 100 cm^2 solar panel.

In 1976, David Carlson and Christopher Wronski of RCA Laboratories created the first amorphous silicon PV cells, which had an efficiency of 1.1%. The Institute of Energy Conversion at University of Delaware developed the first thin film solar cell exceeding 10 % efficiency using Cu_2S/CdS technology in 1980. In 1985, a 20% efficient silicon cell was achieved by the Centre for Photovoltaic Engineering at the University of New South Wales. The dye-sensitized solar cell was created by Michael Grätzel and Brian O'Regan (chemist) in 1988. These photo electrochemical cells worked from an organic dye compound inside the cell and cost half as much as silicon solar cells. A new world record was achieved in solar cell technology in 2006 by breaking the “40 percent efficient” sunlight-to-electricity barrier [26]. 2008 heralded a new record in solar cell efficiency when National Renewable Energy Laboratory (NREL) Scientists achieved a PV device with a 40.8 % conversion rate of the light that hit it into electricity. However, it was only under the concentrated energy of 326 suns that this was achieved. The inverted metamorphic triple-junction solar cell was designed, fabricated and independently measured at NREL [27]. In 2011, fast-growing factories in China pushed manufacturing costs down to about $1.25 per watt for silicon PV modules and installations doubled worldwide.

PV research and development continues with intense interest in new materials, cell designs, and novel approaches to solar material and product development. It is a future where the clothes

you wear and your mode of transportation can produce power that is clean and safe. The price of PV power will be competitive with traditional sources of electricity within a few years [28].

1.4.2 History and origin of solar cells

Photo is the Greek word for ‘light’ while voltaic refers to electricity (from Alessandro Volta, the Italian physicist who invented the electric battery). Therefore, the term ‘photovoltaic’ is commonly used to mean the process of transformation of light energy (or solar energy) into electric energy. The basic science behind the photovoltaic effect was first observed in 1839 by the nineteen-year-old French physicist Alexandre Edmond Becquerel. Becquerel observed a physical phenomenon allowing light-electricity conversion while experimenting with metal electrodes and electrolytes. In 1883 Charles Fritts, an American inventor described the first solar cells made from selenium wafers. In 1888 Edward Weston received the first US patent for a "solar cell". In 1901 Nikola Tesla received a US patent for a "method of utilizing, and apparatus for the utilization of, radiant energy" [29]. The pace of advancement increased dramatically after the publication of Einstein's paper entitled “On a Heuristic Viewpoint Concerning the Production and Transformation of Light”. This paper, published in 1905, proposed a theoretical explanation for the photoelectric effect [30]. Some years later, in 1916, Robert Millikan provided experimental proof of Einstein's theory of the photoelectric effect. Due to this success, Einstein received the 1922 Physics Nobel Prize for his work on the photoelectric effect. Approximately three decades later, a Bell Labs team discovered that silicon had photoelectric properties and quickly developed Si solar cells achieving efficiency of 6%. Early satellites were the primary use for these first solar cells. The commercial solar age had then begun. On the next years the advancements concentrated on space-related applications. In the 1970s oil crisis, also referred to as the oil shock, when the price of the oil quadrupled in less than half a year, alternative sources of energy gained in importance.

More recently, global warming and climate change have become issues of ever-growing concern. The use of renewable sources of energy has been encouraged. The rising attention that global warming has gained has forced world leaders to embrace certain goals in order to minimize its effect. The Kyoto Protocol is an example of how the leaders decided to face the problem. In the Kyoto Protocol the goal was the reduction, by 2012, of at least 5.2% on the emissions of greenhouse gases by developed countries compared to levels recorded in 1990. Those conditions, together with major subsidy programs, have provided the means for an extraordinary growth of the PV industry for a sustained period of time. Nowadays the PV

industry is one of the fastest growing industries in the world and exists largely without subsidies [31].

1.4.3 Energy

Energy is crucial for the survival of humanity. Every human interaction is linked directly or indirectly to energy [32]. The major sources of energy, especially in developing countries, are fossil fuel. These include sources like petroleum, coal, and natural gas that are non-renewable and harmful to the environment. Energy supply is expected to hit 30 TW by 2050 worldwide [33]. This will mount pressure on the fossil fuel sources that will be shared by the over 10 billion people that are projected to be living on earth by 2050. Fossil fuels are consumed/produced at a rate of 5 to 1 at which rate it is expected to be depleted by 2050 [34-36]. Bookout [37] predicted a deficit in energy supply from fossil fuels and energy demand unless steps are taking to remedy the situation. This problem is in addition to the challenge of global warming caused by the continuous usage of fossil fuel.

This has encouraged research on diversification of energy sources. Most of such research has been targeted at energy sources that do not possess the disadvantages of the fossil fuels. The main focus is on renewability and reduction of harm to the environment [38]. Renewable energy has an infinite lifespan in comparison to human existence and is eco-friendly. It is an energy source capable of producing electricity, light and heat without adverse effects on the environment due to the absence of carbon dioxide emissions [39].

Solar energy is the largest exploitable renewable energy source capable of providing more energy in one hour to humankind than energy consumed by earth's entire populace in a year [40]. With about 165 000 terawatts of sunlight hitting earth, converting just 0.025 % of the incident solar energy is enough to solve a significant portion of human energy needs [41]. However, large scale integration and expensive initial costs hinder full scale usage of solar energy when compared to fossil fuels [42, 43]. Research is on-going to make the cost affordable and competitive to current fossil fuel electric grids [44].

Nanotechnology is technology of 1 nm to 100 nm. It is capable of solving several human challenges. It has the potential to reduce energy usage both domestically and industrially. An improved solar cell is capable of saving over $1 000 a year on electricity for homeowners that have this technology on their roof. Nanotechnology is being projected as a potential means to improve efficiency, reduce solar cell cost and develop novel applications [45, 46].

1.4.4 Renewable energy

Renewable energy derived its name from the fact that it is a source of energy that can be replaced or renewed. It is a type of energy source that provides light, electricity and heat without polluting the environment [39]. The advantage of renewable energy over fossil energy is that it is pollution free [47]. Renewable energy includes solar, wind, biomass, hydrogen and geothermal energies [48]. They are good replacements for fossil fuels and nuclear energy. The potential of renewable energy production is shown in Figure 1.1. The solar energy potential of 1 600 EJ exceeds the world annual energy consumption of 539 EJ. Figure 1.2 provides the total primary power density supply from sunlight for the world.

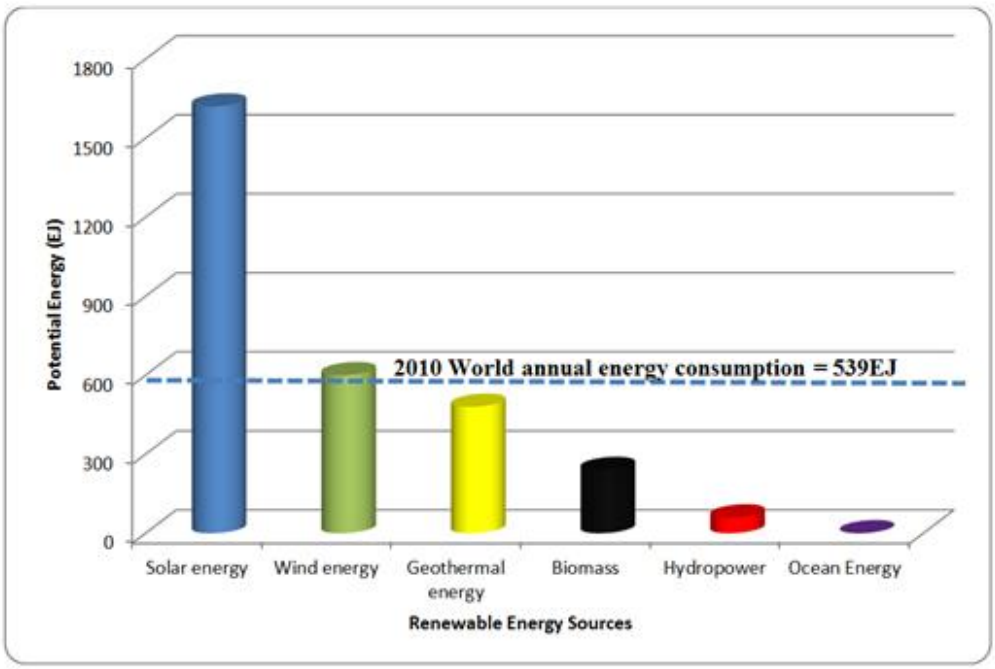

Figure 1.1. Potential energy production per year of various types of renewable energy sources [49]

Renewable energy accounts for the majority of electricity used in the European Union, generating 72 % in 2013 as opposed to 80 % for fossil fuels used a decade earlier [50].

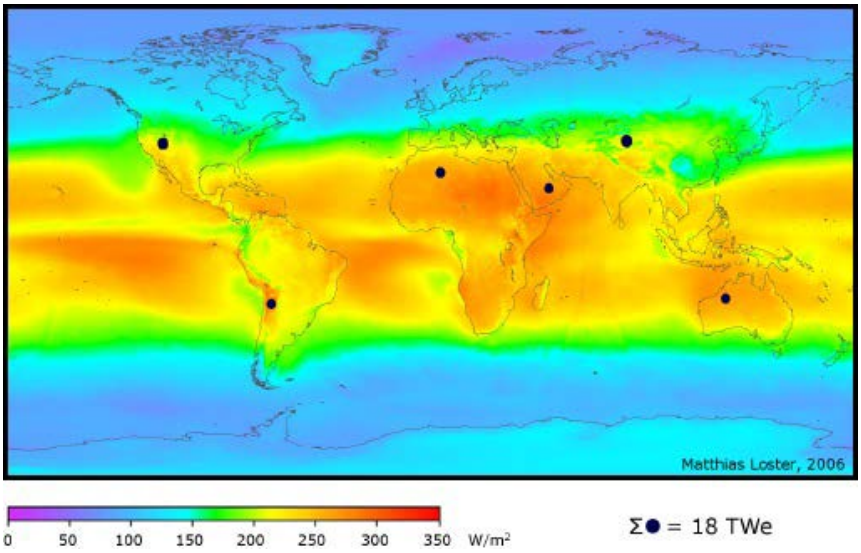

Figure 1.2. Total primary power density supplies from sunlight for the world [51]

Table 1.1 shows the total solar energy, wind, biomass and human energy consumption for the year 2005. The table shows that the total solar energy absorbed by Earth's atmosphere, oceans and land masses is approximately 3 850 000 EJ (1 EJ = 1018 J) per year [52]. The absorbed solar energy by earth in an hour is enough for world energy needs. This exceeds that of wind and biomass which is 2 250 EJ and 3 000 EJ respectively.

Table 1.1. Renewable energy forms data

Energy type	Value
Solar	3 850,000 EJ
Wind	2 250 EJ
Biomass	3 000 EJ
Primary energy use	487 EJ
Electricity	56.7 EJ

1.4.5 Barriers and issues facing renewable energy

The barriers mitigating against renewable energy are grouped as technical and non-technical [53, 54]. Technical barriers include maintenance and after-sales service, design and installation skills, training and local technical infrastructure development, quality control and warranties. Non-technical barriers include lack of awareness, institution capacity-building for micro-finance, and policy/regulatory issues [55]. Renewable energy promotion policy is now implemented in about 48 countries worldwide including 14 developing countries. The level of penetration varies according to country. Denmark had 33.2 % wind power penetration in 2013 and Spain had 20.9 %. Italy had 7.8 % solar PV penetration in their total annual electricity

demand in 2013 [50]. Table 1.2 shows the top five countries' annual investment/net capacity additions/production in 2013.

Table 1.2. Top five countries (annual investment/net capacity additions/production in 2013)[50]

	1	2	3	4	5
Investment in renewable power and fuels	China	US	Japan	UK	Germany
Share of GDP 2012 (USD) INVESTED	Uruguay	Mauritius	Costa rica	SA	Nicaragua
Geothermal power capacity	New Zealand	Turkey	Us	Kenya	Philippines
Hydropower capacity	China	Turkey	Brazil	Vietnam	India
Solar PV capacity	China	Japan	US	Germany	UK
CSP capacity	US	Spain	UAE	India	China
Wind power capacity	China	Germany	UK	India	Canada
Solar water heating capacity	China	Turkey	India	Brazil	Germany
Biodiesel production	US	Germany	Brazil	Argentina	France
Fuel ethanol production	US	Brazil	China	Canada	France

1.4.6 Solar energy

The energy emitted from the sun is referred to as solar energy. Solar energy is emitted from the sun as an electromagnetic radiation in the ultraviolet to infrared and radio spectral regions (0.2 nm to 3 nm). Solar energy can be converted to electricity using devices called solar cells through the photovoltaic effect. The energy is clean, sustainable and available in sufficient quantity with an infinite lifespan of 10 billion years [56]. The total energy from the sun in one hour (4.3×10^{20} J) is more than the total energy consumption of Earth for a year (4.1×10^{20} J) [57]. The radiation of the sun is known as insolation and about 174 petawatts (PW) of insolation is supplied to earth. Insolation is dependent on time, site, geographical location, relative position of the sun, season and reflection/diffusion/absorption by the atmosphere [58, 59]. About 70 % of this insolation is absorbed by the oceans, clouds and land masses with the absorbed solar energy being 3,850 ZJ/year and 30% is reflected back to space [60]. The incident energy from the sun on earth per second is equivalent to 4 trillion 100-watt light bulbs [61]. Despite all these, solar energy potential has not been fully utilized with global solar energy usage being 100 GW in 2012. Europe is the region in the world with the most installed capacity and Germany is the country with the highest installed capacity, with about 31% of world solar energy usage as shown in Figure 1.3 [62].

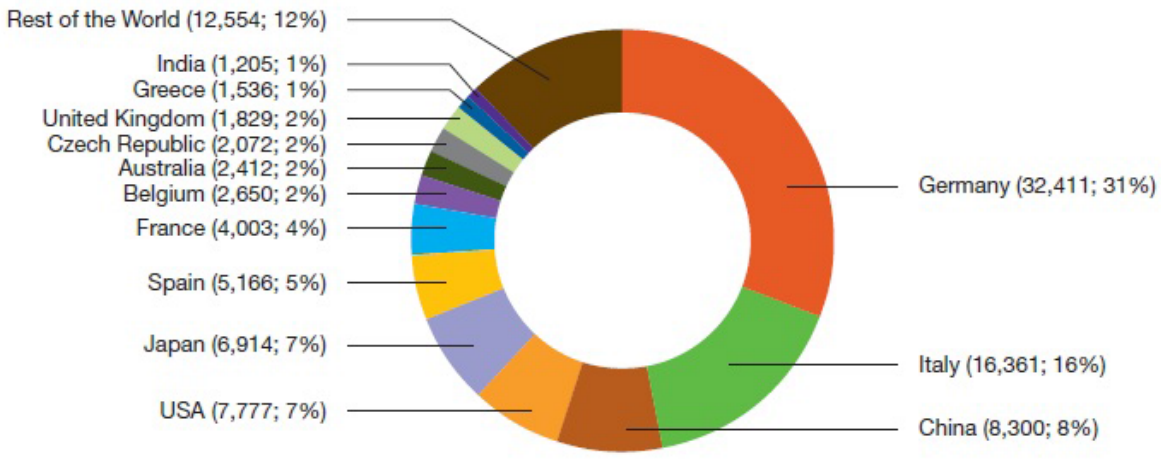

Figure 1.3. Global solar cells cumulative installed capacity in 2012 (MW)

A solar cell performs two major functions, namely, photogeneration of charge carriers in a light absorbing material, and separation of the charge carriers to a conductive contact that will transmit the electricity. This requires an electrolyte capable of transferring the charge from the photo-acceptor to the electrodes in polymer and dye sensitized solar cells. The particles need to be in close proximity to one another to be able to transfer charge directly in nanoparticle-based solar cells. Great progress has been made in improving the overall efficiencies of solar cells including the incorporation of quantum dots (QDs) and nanocrystalline materials.

Solar energy technologies are divided into solar thermal [63] and solar PV systems. Figures 1.4 and 1.5 show the solar thermal and the solar PV systems.

Figure 1.4. Schematic of a typical solar water heating system

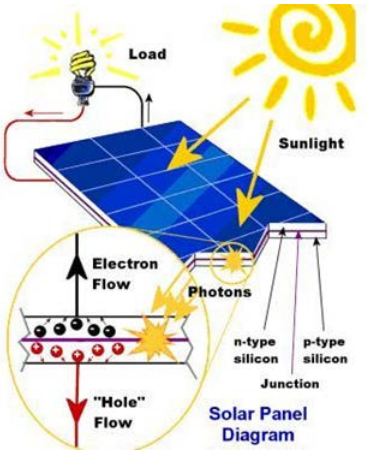

Figure 1.5. Typical PV system

Table 1.3. Examples of solar power applications and system types

Technology type (PV/solar thermal)	System	Application
PV (solar electric)	Grid connected	Supplementing mains supply
PV (solar electric)	Stand-alone	Small home systems for lighting, radio, tv, etc. Small commercial/community systems, including health care, schools, etc. Telecommunication Navigations aids Water pumping Commercial systems Remote settlements Mini-grid systems
Solar thermal	Connected to existing water and/or space heating system	Supplementing supply of hot water and/or space heating being provided by the electricity grid or gas network
Solar thermal	Stand-alone	Water heating e.g. for rural clinics Drying (e.g. grain or other agricultural products) Cooking Distillation Cooling

1.4.6.1 Solar cell efficiency

Efficiency is one of the most important figures of merit for solar cells. Figure 1.6 shows the best research-cell efficiencies from the year 1975 to present [64]. There are four categories of solar cells indicated by different colours in the plot: multijunction III-V (GaAs, Ge/GaAs/InGaP, etc.) solar cell, crystalline Si cells, thin-film technologies, and emerging PV. Table 1.4 summarizes general categories of solar cell technologies [65].

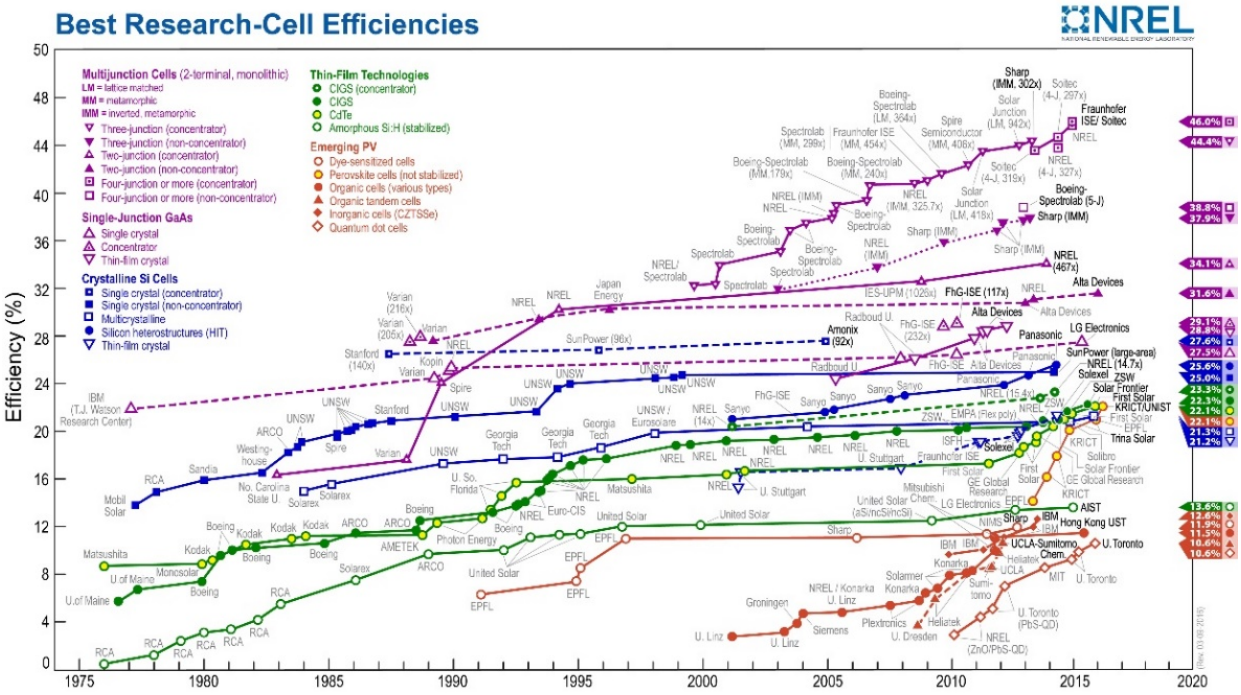

Figure 1.6. Timeline of solar cell energy conversion efficiencies

Table 1.4. General categories of solar cell technologies

Silicon	Monocrystalline or single crystalline silicon (mono-Si sc-Si); Poly- or multi-crystalline silicon (poly-Si or mc-Si): Ribbon silicon
Thin films	Amorphous Si (a-Si) CdTe (cadmium telluride) CIGS (copper-indium gallium selenide)
III –IV Solar Cell	Single-junction GaAs Multi-junction GaAs (Ge/GaAs/InGaP) Concentrating photovoltaics, CPV)
Other emerging PV	Nano-crystalline and nano-structured solar cells New concepts (MEG, multi-exciton-generation) DSSC (dye-sensitized solar cell) Organic/polymer solar cells

1.4.6.2 Cost-efficiency map and generations of solar cells

Cost is among the top barriers militating against full implementation of solar energy especially in low-income countries. Research is now tilting towards low cost yet efficient solar cells. Figure 1.7 shows the efficiency and cost mapping of different generations of solar cells.

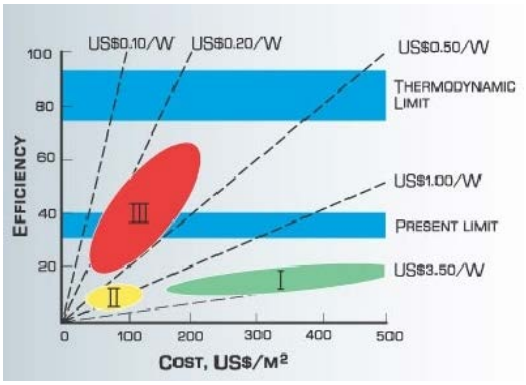

Figure 1.7. Cost-Efficiency map for different generations of solar cell

In Figure 1.7 numerals I, II and III denote Generation I, Generation II, and Generation III solar cells. The term "generations of solar cell" was coined by Green [66]. Table 1.5 summarizes the three generations of solar cells.

Table 1.5. Generations of solar cells

Generation	Features
First (1st) generation	Crystalline silicon: medium efficiency but moderately high cost
Second (2nd) generation	Thin-film: less material, cheaper substrate, less expensive manufacturing equipment; overall low cost but low efficiency.
Third (3rd) generation	Still a vibrant research effort up to now: advanced concepts and material, new physics mechanism and breakthrough. Overall high efficiency with no compromise on low cost. Still an active research area.

1.4.6.2.1 The first generation

This generation dominates the solar panel market. They are larger and silicon-based solar cells. They account for 86 % of the solar market due to their high efficiency but with high manufacturing cost. Figure 1.8 shows the first generation solar cell.

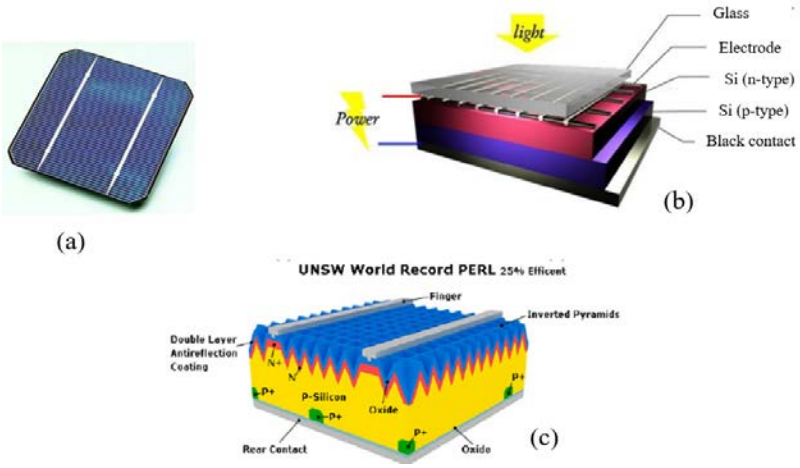

Figure 1.8. (a) silicon solar cell module. (b) schematic of a solar cell structure (c) Passivated emitter rear locally diffused (PERL) solar cell

1.4.6.2.2 The second generation

This generation consists of thin-film solar cells. Their manufacturing cost is cheaper compared with the first generation cells but with lower efficiencies. Lower cost manufacturing methods are employed and less material and less expensive substrates are used. Second generation solar cells are flexible and easy to integrate into roofing material but their lower efficiencies are a major setback. Table 1.6 is a list of typical thin film solar cells and their production and best efficiencies:

Table 1.6. **List of typical thin film solar cells**

Solar cell	Achievement
CIGS ($CuInGaSe_2$)	World record: 19.5 % Production: 9%-11%
Amorphous Si	World record: 13.2 % not completely stable Production: 6-8%
CdTe	World record: 16.5 % Production:8%-10%

1.4.6.2.3 The third generation

This is cutting edge technology in solar cells. Although still at the research phase, research has moved beyond silicon-based solar cells. This generation includes multi-exciton generation (MEG), nano-crystalline cells and polymer solar cells.

1.4.7 Photovoltaic (PV) technology

These are devices that convert the rays from the sun into electricity. The sun's intensity and the material of the PV devices determines the output. PV devises are equipped to produce output during all seasons, winter and cloudy weather inclusive, although at a reduced rate.

PV technology has three dimensions of natural cycle. There is seasonal deviation in electricity output with a maximum recorded in summer, except those PV operating in the equator region where they have constant output all year. Secondly, PV output varies daily, with the peak recorded during mid-day. Lastly, weather fluctuation affects the performance of the PV equipment, with clouds and rainfall reducing the hourly output of such equipment [67].

Solar cells are the building blocks of a PV system. Solar cell aggregation gives rise to a PV module and connection of multiple module gives rise to a PV panel. Solar cells produce about

0.5 volts to 0.6 volts of open circuit voltage and 1 amp to 8 amps DC current depending on the range of factors but mainly related to the semiconductor used [68]. About 36 to 72 solar cells are stacked together in series to produce meaningful output, forming a module.

The modular nature of PV panels account for the flexibility of PV systems. There is global inequality in pricing of PV systems with developed countries experiencing a decrease in price while the price is still unaffordable in low income countries. However, the price depends on system size, technical specifications, grid connection, and location, among other variables. The average price of a module is around $US4.5 /W [69].

A PV system produces direct current electricity when sunlight strikes a specialized semiconductor diode. Some PV cells can generate electricity from infrared or ultraviolet radiation. About 87 % of commercially available PV solar panels use silicon as their base material. However, other materials are gradually being researched and used. They are the traditional solar cells (monocrystalline and polycrystalline silicon solar cells), thin film solar cells and multiple junction solar cells [70].

1. Monocrystalline silicon cells. These are composed of silicon wafers obtained from one homogenous crystal with the atoms arranged in the same direction. They have an efficiency of 12 % to 15 %.

2. Polycrystalline silicon cells, also called multicrystals. These are made by cooling a crystal seed cast in molten silicon. They are cheaper than monocrystalline solar cells and have better efficiency than thin film solar cells. They use more roof space than monocrystalline but less space than thin film solar cells. They have efficiency of about 11 % to 14 %, although a record of 25 % has been achieved for traditional crystalline silicon solar cells [71].

3. Thin film solar cells. These are made by depositing a thin layer of PV materials on a substrate. It is much less efficient than traditional solar cells and uses more roof space. However, it performs better in low light conditions even in partial shading of the system or in extreme heat. Their efficiency is around 5 % to12 %.

4. Multiple junction solar cells. This type of solar cell combines two or more layers of different semiconductor materials to improve the efficiency of the module. Each of the materials produce electric outputs in response to wavelengths of sunlight. This helps to absorb broader wavelengths thereby producing better efficiency. However, this high

efficiency comes at a high cost and complexity. This disadvantage has reduced their role in industries such as aerospace and terrestrial applications. They have achieved a record of about 43 % under a concentrated light source and 30 % under single illumination [26, 72].

1.4.8 Thin film technology

Thin film technology uses thin film semiconducting materials with active layers a few microns thick. This reduces the high cost associated with silicon wafer based solar cells. These layers are capable of absorbing significant amounts of solar radiation owing to their strong absorption properties. Different layers can be deposited on different substrates. The layers include absorber, contact, anti-reflection, buffer. The substrates can either be flexible or rigid, metal or non-metal. Thin films have the advantage of being tailored and engineered to improve on their performance. They also have the capability of being developed into a tandem-structure called an integrated-tandem-solar-cell (ITSC) system.

1.4.9 Nanostructured materials

There is currently great interest in the study of nanostructured materials which are materials with dimensions in the nanoscale. They have a vast range of applications in various fields of human endeavour [73, 74].

The interest in nanostructured materials is due to their unique chemical and physical properties. They are capable of enhancing regular crystalline structures into becoming nanocrystalline structures. This helps to increase the amount of solar radiation absorbed by thin films or multi-layered solar cells, which helps to increase the photon capture in solar cells by increasing the surface area of the cell [75]. Nanostructured materials are capable of reducing the manufacturing cost of solar cells and improving their efficiency [76]. Figure 1.9 shows a sketch of nanostructured solar cells [77].

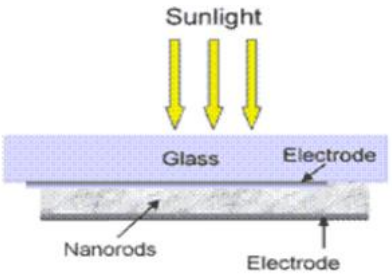

Figure 1.9. schematic of nanostructured solar cell

1.4.9.1 Merits of nanostructured solar cells

Thin film solar cells laced with nanoparticles have three vital merits, namely:

i. They have multiple reflections. The actual film thickness is smaller than the effective optical path for absorption because of multiple reflections.

ii. Recombination losses are minimized. The sunlight generated electrons and holes travel over a much shorter distance thus enabling the absorber layer thickness in nanostructured PV to be as thin as 150 nm when compared with traditional thin film solar cells which are several micrometers thick.

iii. Lastly, the various layer band gaps can be adjusted to required value by optimizing the nanoparticles. This provides more flexibility in both absorber and window layers of the solar cells [78]

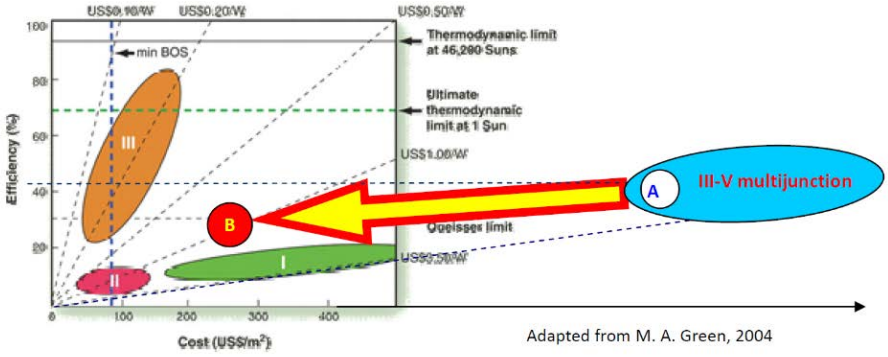

Figure 1.10. Multijunction solar cell's position in the classic cost-efficiency map

The current III-V multijunction solar cell is far out on the right of the x-axis on the cost-efficiency map shown in Figure 10 which means that it only has to be cost competitive with high solar concentration as shown in Figure 1.10. Table 1.7 sheds more light on this comparison.

Table 1.7. Comparison of conventional III-V multijunction solar cell and nanostructured III-V multijunction solar cell

Conventional III-V multijunction solar cell	**Proposed nano-structured III-V multijunction solar cell**
Manufacture cost: Reduced	
Expensive single-crystal Ge or III-V substrate	Si or flexible low-cost substrates with nano-structured templates
Expensive thick layers (absorber and buffer) of III-V compound material	Nanostructure to thin absorption layers; reduce thickness of buffer layer
Expensive multi-layer anti-reflection Coating	Light trapping to eliminate the need of anti-reflection coating
System and installation cost: Reduced	

Heavy, bulk, need concentrators and 2 axis sun-tracking systems	Light-weighted, potentially flexible, wide acceptance angle, no sun-tracking
High-efficiency: Retained	
Multiple junctions for broad spectrum absorption, but the number of junctions limited by lattice mismatch problems	New conditions for lattice mismatched material growth; III-V nano materials, favorable for multijunction configuration

Nanomaterials are classified into three main categories based on dimensionality. They are 0-dimensional, one dimensional, two and three dimensional. Nanomaterials with nanoparticles isolated from each other are known as 0-dimensional structures. They include individual molecules and quantum dots [79]. Thin nano film are a good example of one and two dimensional structures and are studied in nano device fabrication [80-82]. Powder, fibrous, multilayer and polycrystalline materials are examples of three-dimensional nanomaterials. The 0D, 1D and 2D structural elements are in close contact with each other and form interfaces.

1.4.10 Metal oxide

These materials are unique functional materials with varied structural, optical, magnetic and electronic properties. They exhibit insulating, semiconducting, and metallic behaviour at room temperature, depending on the material band gap. They are used in several applications as sensors, piezoelectric, fuel cells, solar cells and magnetic memory. The properties of metal oxides are affected by their particle sizes. They tend to have unique properties in the 'nano' domain (10^{-9} m). This is because the surface to bulk ratio of atoms increases as the particle size decreases from bulk form to tens of nanometers. This gives rise to chemically active sites and modified density. The properties of metal oxides are of interest to physics, chemistry and material science [8, 83]

1.4.10.1 Metal oxide nanomaterial

These materials can be synthesised either through physical or chemical methods [84]. They can be prepared using top-down or bottom-up techniques [85, 86]. These approaches use liquid-solid or gas-solid transformation [87, 88]. Metal oxide nanostructures are unique among semiconducting nanostructures. They are the most common, most diverse and richest class owing to their functionalities and properties. They display a wide range of fascinating properties [89]. Metal oxides are a highly sought after candidate for a variety of technological applications due to their special and tuneable properties. They are used in a wide range of applications including solar cells, superconductivity, gas sensors and so on [90-92]. Zinc oxide (ZnO), copper oxide (CuO), and nickel oxide (NiO) are some of the commonly synthesized

nanostructured metal oxides [93-95]. They can be prepared by various techniques, including thermal evaporation [96], chemical vapour deposition [97], and chemical synthesis[98], among others.

1.4.10.2 Synthesis techniques of metal oxide nanomaterial

The study of nanostructured materials comprises synthesis of the material, characterization of the properties and subsequent application in various fields of technology. There are various methods employed in synthesising of nanomaterials. These include the gas phase and the liquid phase. The gas phase is used for low-cost production of large quantities of nanopowders [99]. The liquid phase gives better flexibility in the control of the structural variation, composition and morphology of the end product material.

Over the years, nanostructured metal oxides have attracted interest owing to their novel properties and tune ability in various applications especially optoelectronic applications. Various techniques have been reported for synthesis of nanostructured metal oxides. These include evaporation [100-102], metal organic chemical vapour deposition [103, 104], and hydrothermal [105, 106], among others. These techniques are grouped into physical and chemical processes using the nature of deposition [107] as shown in Figure 1.11. Chemical methods comprise the gas-phase and the solution deposition method. This is further sub-grouped. The gas-phase methods are chemical vapour deposition (CVD) [108], atomic layer epitaxy [109], and atomic layer deposition (ALD) [110]. Solution deposition methods are: spray pyrolysis [111], sol-gel [112], spin [113] and dip-coating [114]. Physical deposition methods include: pulsed laser deposition [115], physical vapour deposition (PVD) [116], molecular beam epitaxy [117], and magnetron sputtering [118]. Other techniques include: chemical bath deposition [119], advanced reactive gas deposition [120], electron beam evaporation [121], vacuum evaporation [122], and anodic oxidation [123].

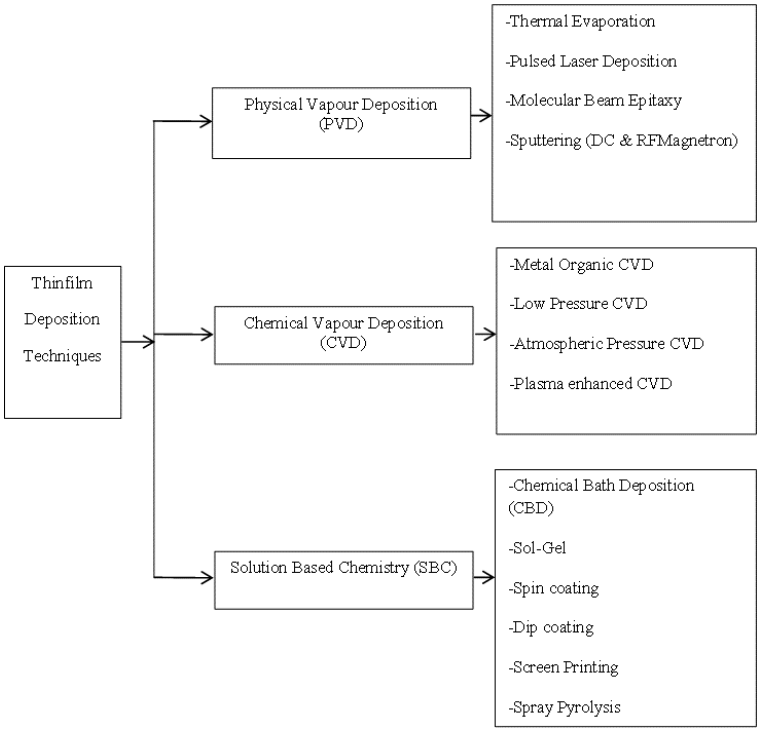

Figure 1.11. Classifications of Thin films deposition methods

1.5 Aim of the study

To fabricate and characterize a nanostructured metal oxide thin film based solar cell system for Photovoltaic and optoelectronic devices.

1.6 Objectives of the study

The objectives of the research are summarized below:

[1] Deposit nanostructured metal oxide film such as TiO_2, NiO, on both conducting indium tin oxide (ITO) and soda lime substrates suitable for solar cell fabrication using the spray pyrolysis technique;

[2] Characterize the deposited film using X-ray diffractometer, ultraviolet visible near spectroscopy, elemental and the scanning electron microscopy for possible areas of application in fabricating solar cells;

[3] Fabricate a metal oxide/metal contact thin film solar cell by depositing each of the layers on commercially available transparent conducting substrates;

[4] Characterize the solar cell fabricated using the I-V characterization technique both in dark and under illumination (100 mW/cm^2). Determine the solar cell parameters such

as short circuit current (I_{sc}), open circuit voltage (V_{oc}), series resistance (I_s), saturation current (I_o), fill factor (FF), maximum power output (P_m) and conversion efficiency (η) from the I-V measurement; and

[5] Computational modeling of the metal oxide solar cell device using the solar cell analysis program SCAPxD.

1.7 Significance of the study

Metal oxide based solar cells have hardly been studied compared to other technologies despite the fact that PV effects exist in this type of semiconductor [124]. Metal oxides' merits of being abundant, chemically stable, and easily processed make them an ideal material for affordable PV modules [125]. Studies have been conducted on the properties of NiO for thin film usage but none have used it for solar cell fabrication despite such studies pointing out its potential for solar cell usage.

1.8 Scope of the study

The scope of this work is the fabrication of nanostructured metal oxide heterojunctions for solar cell fabrication in developing and low income countries.

1.9 Main contributions to the field

The main contribution to the field arising from this thesis are here presented.

i. A complete review of NiO thin films deposited using spray pyrolysis.

ii. A new set of concentrations were optimized for NiO thin films.

iii. A new aged optimization (192 hours) was used.

iv. A new set of values were recorded for the optical band gap of NiO thin films. An optical band gap of 3.94 eV to 3.38 eV was recorded for the concentration while 3.60 eV to 3.70 eV was recorded for freshly prepared and aged (192 hours) respectively.

v. A cell efficiency of 2.3 % was achieved for NiO thin film heterojunction solar cells.

vi. This work was able to fabricate a NiO/TiO_2 P-N heterojunction solar cell for the first time.

vii. Successful modeling of NiO/TiO_2 heterojunction solar cells. This opened a new opportunity for massive research and fine tuning of the properties of the solar cells and other metal oxide solar cells.

viii. This boosts the quest to develop affordable and sustainable energy by encouraging more research in solar cells technologies in low-income countries.

1.10 Thesis layout

Chapter 1 is the introductory part of this study and provides the rationale, problem statement, and background of the study. It also presents the aim, overall objectives, significance, scope, and highlights of the study contribution. This thesis is a product of research publications and conference papers as required by the University of KwaZulu-Natal for awarding of a doctoral degree. The thesis produced a total of Seventeen (16) publications and/or conference papers.

Chapter 2 provides a comprehensive review of the need for solar energy in developing and low income countries especially Africa. Chapter 3 is a comprehensive review of nanostructured NiO thin films deposition using the spray pyrolysis method.

Chapter 4 gives the deposition and optimization of the nanostructured NiO thin films. This is divided into four parts. Part 1 discussed the optimization of the NiO under different concentration. Part 2 discussed the optimization of the NiO under different annealing condition. Part 3 looked at the effect of ageing on nanostructured NiO thin films for solar cells fabrication. Lastly, part 4 studied the combined effect of temperature and ageing on nanostructured NiO thin films for solar cell fabrication.

Chapter 5 looked at the final device fabrication of the solar cells.

Chapter 6 focused on the modeling and theoretical validation of the fabricated device of the study. It also contains the application of solar cells in global warming reduction

Chapter 7 presents the conclusions and recommendations for future work.

References

[1] You, J., et al., Improved air stability of perovskite solar cells via solution-processed metal oxide transport layers. *Nature Nanotechnology*, 2016. **11**(1): p. 75.

[2] Jeng, J.Y., et al., Nickel oxide electrode interlayer in CH3NH3PbI3 perovskite/PCBM planar ‐ heterojunction hybrid solar cells. *Advanced Mmaterials*, 2014. **26**(24): p. 4107-4113.

[3] Yin, X., et al., Highly efficient flexible perovskite solar cells using solution-derived NiO x hole contacts. *ACS nano*, 2016. **10**(3): p. 3630-3636.

[4] Baxter, J.B. and E.S. Aydil, Nanowire-based dye-sensitized solar cells. *Applied Physics Letters*, 2005. **86**(5): p. 053114.

[5] Ellabban, O., H. Abu-Rub, and F. Blaabjerg, Renewable energy resources: Current status, future prospects and their enabling technology. *Renewable and Sustainable Energy Reviews*, 2014. **39**: p. 748-764.

[6. Jia, Y., et al., Nanotube–silicon heterojunction solar cells. *Advanced Materials*, 2008. **20**(23): p. 4594-4598.

[7] Adeoye, A.E., et al., Rutherford backscattering spectrometry analysis and structural properties of thin films deposited by chemical spray pyrolysis. *Journal of Materials*, 2015. **2015**.

[8] Fierro, J.L.G., *Metal oxides: chemistry and applications*. 2005: CRC press.

[9] Pavan, M., et al., TiO2/Cu2O all-oxide heterojunction solar cells produced by spray pyrolysis. S*olar Energy Materials and Solar Cells*, 2015. **132**: p. 549-556.

[10] Fortunato, E., P. Barquinha, and R. Martins, Oxide semiconductor thin-film transistors: a review of recent advances. *Advanced Materials,* 2012. **24**(22): p. 2945-2986.

[11] Fortunato, E., et al., Transparent conducting oxides for photovoltaics. *MRS Bulletin,* 2007. **32**(3): p. 242-247.

[12] Morasch, J., et al., Reactively magnetron sputtered Bi2O3 thin films: Analysis of structure, optoelectronic, interface, and photovoltaic properties. *Physica Status Solidi* (a), 2014. **211**(1): p. 93-100.

[[13] Gerling, L.G., et al., Transition metal oxides as hole-selective contacts in silicon heterojunctions solar cells. *Solar Energy Materials and Solar Cells*, 2016. **145**: p. 109-115.

[14] Malanima, P., Energy consumption and energy crisis in Roman world. *The Ancient Mediterranean Environment between Science and History*, 2011: p. 13-36.

[15] Perlin, J., *Let it shine: the 6,000-year story of solar energy*. 2013: New World Library.

[16] Maruga, N.K., *Final year project.* 2014. University of Nairobi.

[17] Ruskin, S., *John Herschel's Cape voyage: Private science, public imagination and the ambitions of Empire*. 2017: Routledge.

[18] Kongtragool, B. and S. Wongwises, A review of solar-powered Stirling engines and low temperature differential Stirling engines. *Renewable and Sustainable Energy Reviews*, 2003. **7**(2): p. 131-154.

[19] Sufian, S.M.A., et al. Design of a Stirling engine to generate green energy in rural areas of Bangladesh. in *Green Energy and Technology (ICGET), 2014 2nd International Conference on*. 2014. IEEE.

[20] Kolin, I., P. Lista, and V. Naso, *The power formula for atmospheric stirling Engines*. 1992, SAE Technical Paper.

[21] Grätzel, M., Photoelectrochemical cells. *Nature*, 2001. **414**(6861): p. 338.

[22] Timilsina, G. and L. Kurdgelashvili, *25.* The evolution of solar energy technologies and supporting policies*. Handbook on Geographies of Technology*, 2017: p. 362-375.
[23] Ishai, M.B. and F. Patolsky, Shape-and dimension-controlled single-crystalline silicon and SiGe nanotubes: toward nanofluidic FET devices*. Journal of the American Chemical Society*, 2009. **131**(10): p. 3679-3689.
[24] Goetzberger, A. and C. Hebling, Photovoltaic materials, past, present, future. *Solar Energy Materials and Solar Cells*, 2000. **62**(1-2): p. 1-19.
[25] Hovel, H.J., Photovoltaic materials and devices for terrestrial solar energy applications*. Solar Energy Materials*, 1980. **2**(3): p. 277-312.
[26] Brown, N., Solar junction breaks concentrated solar world record with 43.5% efficiency. *CleanTechnica. com*, 2011.
[27] Wanlass, M. W., *Single-junction solar cells with the optimum band gap for terrestrial concentrator applications*. 1994, Google Patents.
[28] Hubbard, H., Photovoltaics today and tomorrow*. Science*, 1989. **244**(4902): p. 297-304.
[29] Tesla, N., *Method of utilizing radiant energy*. 1901, Google Patents.
[30] Einstein, A., Does the inertia of a body depend upon its energy-content*. Ann Phys,* 1905. **18**: p. 639-641.
[31] Hegedus, S.S. and A. Luque, Status, trends, challenges and the bright future of solar electricity from photovoltaics*. Handbook of Photovoltaic Science and Engineering,* 2003: p. 1-43.
[32] Situmbeko, S.M. and F.L. Inambao, System and component modelling of a low temperature solar thermal energy conversion cycle*. Journal of Energy in Southern Africa*, 2013. **24**(4): p. 51-62.
[33] Blanco, J., et al., Review of feasible solar energy applications to water processes. *Renewable and Sustainable Energy Reviews,* 2009. **13**(6-7): p. 1437-1445.
[34] Gray, K.A., et al., Molecular mechanisms of biocatalytic desulfurization of fossil fuels. *Nature Biotechnology*, 1996. **14**(13): p. 1705-1709.
[35] Satyanarayana, K., A. Mariano, and J. Vargas, A review on microalgae, a versatile source for sustainable energy and materials*. International Journal of Energy Research,* 2011. **35**(4): p. 291-311.
[36] Demirbas, A., Progress and recent trends in biodiesel fuels*. Energy Conversion and Management*, 2009. **50**(1): p. 14-34.
[37] Bookout, J.F., 2 Centuries of fossil-fuel enery*, Episodes*, 1989. **12**(4): p. 257-262.
[38] Ukoba, O.K., A.C. Eloka-Eboka, and F.L. Inambao, Review of nanostructured NiO thin film deposition using the spray pyrolysis technique*. Renewable and Sustainable Energy Reviews*, 2018. **82**: p. 2900-2915.
[39] Hussein, A.K., *A*pplications of nanotechnology in renewable energies—A comprehensive overview and understanding. *Renewable and Sustainable Energy Reviews*, 2015. **42**: p. 460-476.
[40] Lewis, N.S. and D.G. Nocera, Powering the planet: chemical challenges in solar energy utilization*.* P*roceedings of the National Academy of Sciences*, 2006. **103**(43): p. 15729-15735.
[41] Smil, V., *Energy: A beginner's guide (Beginner's Guides)*. 2nd ed. 2006, New York: Oxford University press. 350.
[42] Chakraborty, P., E. Baeyens, and P.P. Khargonekar, Grid Integration of renewable electricity and distributed control. In *Emerging applications of control and systems*

theory. 2018, Springer. p. 205-216.
[43] Sims, R.E., H.-H. Rogner, and K. Gregory, *Carbon emission and mitigation cost comparisons between fossil fuel, nuclear and renewable energy resources for electricity generation.* Energy policy, 2003. **31**(13): p. 1315-1326.
[44] Kumar. M.S,, S.Prabhakar, and S. Prakesh, Performance enhancing the efficiency of solar pv cells using nanotechnology*. Journal of Chemical and Pharmaceutical Sciences*, 2015(7): p. 362-364.
[45] Garnett, E. and P. Yang, *Light trapping in silicon nanowire solar cells.* Nano letters, 2010. **10**(3): p. 1082-1087.
[46] Hsu, C.-M., et al., Wafer-scale silicon nanopillars and nanocones by Langmuir–Blodgett assembly and etching*. Applied Physics Letters*, 2008. **93**(13): p. 133109.
[47] Lund, H., Renewable energy strategies for sustainable development*. Energy*, 2007. **32**(6): p. 912-919.
[48] Panwar, N., S. Kaushik, and S. Kothari, Role of renewable energy sources in environmental protection: a review. *Renewable and Sustainable Energy Reviews*, 2011. **15**(3): p. 1513-1524.
[49] Zeman, M., et al., Modelling of thin-film silicon solar cells*. Solar Energy Materials and Solar Cells,* 2013. **119**: p. 94-111.
[50] Sawin, J.L., et al., *Renewables 2014. Global status report 2014.* 2014.
[51] Bishop, J.K. and W.B. Rossow, Spatial and temporal variability of global surface solar irradiance*. J*ournal of Geophysical Research: Oceans*, 1991. **96**(C9): p. 16839-16858.
[52] Humada, M.N.A.M., et al., Exploring and assessment of effect the fast changing of the external PV parameters on the PV characteristics*. International Journal of Research Studies in Electrical and Electronics Engineering*, 2015. **1(**1): p. 29-34.
[53] Knoef, H. and J. Ahrenfeldt, *Handbook biomass gasification*. 2005: Biomass Technology Group, The Netherlands.
[54] Margolis, R. and J. Zuboy, *Nontechnical barriers to solar energy use: review of recent literature*. 2006, National Renewable Energy Laboratory (NREL), Golden, CO.
[55] Adib, R., et al., *Renewables 2016 global status report.* Global Status Report RENEWABLE ENERGY POLICY NETWORK FOR THE 21st CENTURY (REN21), 2016: p. 272.
[56] Owens, F.J. and C.P. Poole Jr, *The physics and chemistry of nanosolids*. 2008: John Wiley & Sons.
[57] Barber, J., Photosynthetic energy conversion: natural and artificial. *Chemical Society Reviews*, 2009. **38**(1): p. 185-196.
[58] Vasarevicius, D. and R. Martavicius, Solar irradiance model for solar electric panels and solar thermal collectors in Lithuania*. Elektronika ir Elektrotechnika*, 2011. **108**(2): p. 3-6.
[59] Frouin, R. and R.T. Pinker, Estimating photosynthetically active radiation (PAR) at the earth's surface from satellite observations*. Remote sensing of environment*, 1995. **51**(1): p. 98-107.
[60] Chendo, M., Factors militating against the growth of the solars-PV industry in Nigeria and their removal*. Nigerian Journal of Renewable Energy*, 2002. **10**(1&2): p. 151-158.
[61] Agbo, S. and O. Oparaku, Positive and future prospects of solar water heating in Nigeria. *The Pacific Journal of Science and Technology*, 2006. **7**(2): p. 191-198.
[62] Sahu, B.K., *A* study on global solar PV energy developments and policies with special focus on the top ten solar PV power producing countries. *Renewable and Sustainable Energy Reviews*, 2015. **43**: p. 621-634.

[63] Shukla, R., et al., Recent advances in the solar water heating systems: A review. *Renewable and Sustainable Energy Reviews*, 2013. **19**: p. 173-190.
[64] Girtan, M., *Future Solar Energy Devices*. 2018, Springer.
[65] Gu, A., et al. Design and growth of III–V nanowire solar cell arrays on low cost substrate. In *Photovoltaic Specialists Conference (PVSC), 2010 35th IEEE*. 2010. IEEE.
[66] Green, M.A., Third generation photovoltaics: Ultra-high conversion efficiency at low cost. *Progress in Photovoltaics: Research and Applications*, 2001. **9**(2): p. 123-135.
[67] Martinot, E., *Renewables 2005 global status report*. 2010: DIANE Publishing.
[68] Cutter, A., *The Electricians green handbook*. 2011: Cengage Learning.
[69] Nowak, S., *Trends in photovoltaic applications in selected IEA countries between 1992 and 2000.* IEA PVPS, 2001. 26. 2001.
[70] Xiao, W., W.G. Dunford, and A. Capel. A novel modeling method for photovoltaic cells. In *Power Electronics Specialists Conference, 2004. PESC 04. 2004 IEEE 35th Annual*. 2004. IEEE.
[71] Bagher, A.M., M.M.A. Vahid, and M. Mohsen, Types of solar cells and application. *American Journal of optics and Photonic*s, 2015. **3**(5): p. 94-113.
[72] Dimroth, F., et al., *F*our-junction wafer-bonded concentrator solar cells. *IEEE Journal of Photovoltaics*, 2016. **6**(1): p. 343-349.
[73] Ge, M., et al., A review of one-dimensional TiO 2 nanostructured materials for environmental and energy applications. *Journal of Materials Chemistry A*, 2016. **4**(18): p. 6772-6801.
[74] Li, S., et al., Flame aerosol synthesis of nanostructured materials and functional devices: Processing, modeling, and diagnostics. *Progress in Energy and Combustion Science,* 2016. **55**: p. 1-59.
[75] Shrestha, A., et al. Development of FDTD simulation tool for designing micro-nanostructured based optical devices. In *Energy Harvesting and Storage: Materials, Devices, and Applications VII*. 2016. International Society for Optics and Photonics.
[76] Nader Nabhani and M. Emami, Nanotechnology and its application in solar cells. In *International Conference on Mechanical and Industrial Engineering (ICMIE'2013)* 2013: Penang (Malaysia) p. 88-91.
[77] Nayfeh, O., et al., Thin film silicon nanoparticle UV photodetector. *IEEE Photonics Technology Letters*, 2004. **16**(8): p. 1927-1929.
[78] Singh, R., et al., Nano-structured CdTe, CdS and TiO2 for thin film solar cell applications. *Solar Energy Materials and Solar Cells,* 2004. **82**(1-2): p. 315-330.
[79] Yang, P., The chemistry and physics of semiconductor nanowires. *MRS Bulletin,* 2005. **30**(2): p. 85-91.
[80] Coffey, D.C. and D.S. Ginger, Time-resolved electrostatic force microscopy of polymer solar cells. *Nature Materials*, 2006. **5**(9): p. 735.
[81] Muccini, M., A bright future for organic field-effect transistors. *Nature Materials*, 2006. **5**(8): p. 605.
[82] Nomura, K., et al., Amorphous oxide semiconductors for high-performance flexible thin-film transistors. *Japanese Journal of Applied Physics,* 2006. **45**(5S): p. 4303.
[83] Rodríguez, J.A. et al., eds., *Synthesis, properties, and applications of oxide nanomaterials,* 2007: Wiley.
[84] Gupta, A.K. and M. Gupta, Synthesis and surface engineering of iron oxide nanoparticles for biomedical applications. *Biomaterials*, 2005. **26**(18): p. 3995-4021.
[85] Lu, W. and C.M. Lieber, Nanoelectronics from the bottom up. *Nature Materials*, 2007.

6(11): p. 841.
[86] Biswas, A., et al., Advances in top–down and bottom–up surface nanofabrication: Techniques, applications & future prospects. *Advances in Colloid and Interface Science*, 2012. **170**(1-2): p. 2-27.
[87] Bandyopadhyay, A., *Nano Materials: in Architecture, Interior Architecture and Design,* 2008: New Age International, New Delhi.
[88] Bond, G.C., C. Louis, and D.T. Thompson, *Catalysis by gold*. Vol. 6. 2006: World Scientific.
[89] Lu, J.G., P. Chang, and Z. Fan, Quasi-one-dimensional metal oxide materials—Synthesis, properties and applications. *Materials Science and Engineering Reports*, 2006. **52**(1-3): p. 49-91.
[90] Furukawa, H., et al., The chemistry and applications of metal-organic frameworks. *Science*, 2013. **341**(6149): p. 1230444.
[91] Soga, T., *Nanostructured materials for solar energy conversion*. 2006: Elsevier.
[92] Pudasaini, P.R., et al., Nanostructured solar cells. *International Journal of Photoenergy*, 2017. **2017**.
[93] Li, L., et al., Recent progress of one-dimensional ZnO nanostructured solar cells. *Nano Energy*, 2012. **1**(1): p. 91-106.
[94] Wijesundera, R., Fabrication of the CuO/Cu2O heterojunction using an electrodeposition technique for solar cell applications. *Semiconductor Science and Technology*, 2010. **25**(4): p. 045015.
[95] He, J., et al., Dye-sensitized nanostructured p-type nickel oxide film as a photocathode for a solar cell. T*he Journal of Physical Chemistry B*, 1999. **103**(42): p. 8940-8943.
[96] Xing, Y., et al., Thermal evaporation synthesis of zinc oxide nanowires. *Applied Physics A*, 2005. **80**(7): p. 1527-1530.
[97] Frohlich, K., et al., Characterization of rare earth oxides based MOSFET gate stacks prepared by metal-organic chemical vapour deposition. *Materials Science in Semiconductor Processing*, 2006. **9**(6): p. 1065-1072.
[98] Zhang, W. and J. Zhao, Synthesis, structure, and property of a uranium–potassium–organic coordination polymer containing infinite metal oxide sheets. *Journal of Molecular Structure,* 2006. **789**(1): p. 177-181.
[99] Strobel, R. and S.E. Pratsinis, Flame aerosol synthesis of smart nanostructured materials. *Journal of Materials Chemistry,* 2007. **17**(45): p. 4743-4756.
[100] Zhou, J., et al., Growth and field-emission property of tungsten oxide nanotip arrays. *Applied Physics Letters*, 2005. **87**(22): p. 223108.
[101] Umar, A. and Y. Hahn, ZnO nanosheet networks and hexagonal nanodiscs grown on silicon substrate: growth mechanism and structural and optical properties. *Nanotechnology*, 2006. **17**(9): p. 2174.
[102] Bae, S.Y., H.W. Seo, and J. Park, Vertically aligned sulfur-doped ZnO nanowires synthesized via chemical vapor deposition. T*he Journal of Physical Chemistry B*, 2004. **108**(17): p. 5206-5210.
[103] Lee, W., H. Sohn, and J.M. Myoung. Prediction of the structural performances of ZnO nanowires grown on GaAs (001) substrates by metalorganic chemical vapour deposition (MOCVD). In *Materials Science Forum*. 2004: Trans Tech Publ.
[104] Kang, T.-T., et al., InN nanoflowers grown by metal organic chemical vapor deposition. *Applied Physics Letters*, 2006. **89**(7): p. 071113.
[105] Guo, M., P. Diao, and S. Cai, Hydrothermal growth of well-aligned ZnO nanorod arrays:

Dependence of morphology and alignment ordering upon preparing conditions. *Journal of Solid State Chemistry*, 2005. **178**(6): p. 1864-1873.
[106] Zheng, D., et al., One-step preparation of single-crystalline β-MnO2 nanotubes. *The Journal of Physical Chemistry B*, 2005. **109**(34): p. 16439-16443.
[107] Freund, L.B. and S. Suresh, *Thin film materials: stress, defect formation and surface evolution*. 2004: Cambridge University Press.
[108] Morosanu, C.E., *Thin films by chemical vapour deposition*. Vol. 7. 2016: Elsevier.
[109] Leskelä, M. and M. Ritala, Atomic layer deposition (ALD): from precursors to thin film structures. T*hin Solid Films*, 2002. **409**(1): p. 138-146.
[110] Yang, T.S., et al., Atomic layer deposition of nickel oxide films using Ni (dmamp) 2 and water. J*ournal of Vacuum Science & Technology A: Vacuum, Surfaces, and Films*, 2005. **23**(4): p. 1238-1243.
[111] Rozati, S. and S. Akesteh, Characterization of ZnO: Al thin films obtained by spray pyrolysis technique. *Materials Characterization*, 2007. **58**(4): p. 319-322.
[112] Sta, I., et al., Structural, optical and electrical properties of undoped and Li-doped NiO thin films prepared by sol–gel spin coating method. *Thin Solid Films*, 2014. **555**: p. 131-137.
[113] Xu, X., et al., YSZ thin films deposited by spin-coating for IT-SOFCs. *Ceramics International,* 2005. **31**(8): p. 1061-1064.
[114] Brinker, C., et al., Fundamentals of sol-gel dip coating. T*hin Solid Films*, 1991. **201**(1): p. 97-108.
[115] Wang, H., Y. Wang, and X. Wang, Pulsed laser deposition of the porous nickel oxide thin film at room temperature for high-rate pseudocapacitive energy storage. *Electrochemistry Communications*, 2012. **18**: p. 92-95.
[116] Mahan, J.E., Physical vapor deposition of thin films. In P*hysical Vapor Deposition of Thin Films*, by John E. Mahan, pp. 336. 2000: Wiley-VCH.
[117] Herman, M.A. and H. Sitter, *Molecular beam epitaxy: fundamentals and current status*. Vol. 7. 2012: Springer Science & Business Media.
[118] Zhao, Y., et al., Structures, electrical and optical properties of nickel oxide films by radio frequency magnetron sputtering. *Vacuum*, 2014. **103**: p. 14-16.
[119] Xia, X., et al., Electrochromic properties of porous NiO thin films prepared by a chemical bath deposition. *Solar Energy Materials and Solar Cells*, 2008. **92**(6): p. 628-633.
[120] Luyo, C., et al., *G*as sensing response of NiO nanoparticle films made by reactive gas deposition. S*ensors and Actuators B: Chemical,* 2009. **138**(1): p. 14-20.
[121] Tanuševski, A. and D. Poelman, *Optical and photoconductive properties of SnS thin films prepared by electron beam evaporation. Solar Energy Materials and Solar Cells,* 2003. **80**(3): p. 297-303.
[122] Kalita, P.K., B. Sarma, and H. Das, Structural characterization of vacuum evaporated ZnSe thin films. *Bulletin of Materials Science*, 2000. **23**(4): p. 313-317.
[123] Lampert, C., T. Omstead, and P. Yu, Chemical and optical properties of electrochromic nickel oxide films. *Solar Energy Materials,* 1986. **14**(3-5): p. 161-174.
[124] Mittiga, A., et al., Heterojunction solar cell with 2% efficiency based on a Cu 2 O substrate. *Applied Physics Letters*, 2006. **88**(16): p. 163502.
[125] Wadia, C., A.P. Alivisatos, and D.M. Kammen, Materials availability expands the opportunity for large-scale photovoltaics deployment. *Environmental Science & Technology*, 2009. **43**(6): p. 2072-2077.

CHAPTER 2: REVIEW OF SOLAR ENERGY INCLUSION IN AFRICA: CASE STUDY OF NIGERIA

This chapter looks at the need for solar energy inclusion in developing and low income countries, using Nigeria as a case study.

To cite: Ukoba, O.K., Eloka-Eboka, A.C. and Inambao F.L. "Review of solar energy inclusion in Africa using Nigeria model" Proceedings of International Solar Energy Society *Solar World* 2017, pp 962 – 973, Abu Dhabi, UAE, 29th Oct – 2nd Nov., 2017.

REVIEW OF SOLAR ENERGY INCLUSION IN AFRICA USING NIGERIA MODEL

[1]Ukoba, Kingsley; [1]Eloka-Eboka, A.C and [1]Inambao, F.L

[1]University of Kwazulu-Natal, Durban, South Africa

ukobaking@yahoo.com

Abstract

This work reviews solar energy inclusion in Africa using Nigeria as a case study. It reviewed studies made on viability, challenges and solutions associated with making solar energy a viable energy option in Nigeria. The study highlighted data on current industry capacity of solar energy, installed PV capacity, and solar energy application distribution. It sheds light on solar energy initiatives and projects in Nigeria and solar energy capacity development in Nigeria. Success stories of solar energy and solar cell fabrication in Nigeria are presented. Existing government policies and legislation are discussed. The authors consider the challenges faced and the current and future prospects of solar power in Nigeria, and make recommendations regarding the speedy and seamless inclusion of solar energy in Nigeria and Africa as a whole.

KEYWORDS: solar, domestication, Nigeria, energy, Africa

1. Introduction

Sub-Sahara Africa is home to about 85 % of the 1.3 billion people in developing countries without access to electricity [1], with an estimated electrification rate of 64 % in urban and 13 % in rural areas [2]. Sub-Sahara Africa has many of the world's least electrified nations [3, 4]. A total of 70 % of such those without access to electricity reside in countries like Nigeria where the rural populace is mostly affected [5]. Nigeria is ranked seventh in world population and cannot provide electricity access to her populace both in the urban and rural areas [6, 7]. Nigeria's rural population is estimated to be about 42 % of the total population [8]. Over 60 % of the Nigerian population does not have power supply, with 40 % not on the nation's grid [9, 10]. The Nigerian grid supply of electricity is on average six hours per day rationed among inhabitants of the cities [11]. Almost all rural dwellers in Nigeria have little or no access to electricity. The majority of the electricity supply in Nigeria is generated by Kainji dam which produces about 3.2×10^8 W and 9.6×10^8 W at its peak [12, 13]. This is due to underperforming hydro dams in the country. Another factor is the high cost of distribution across the country which covers an area of 924 000 km^2 [14]. There is no uniformity in distribution of grid connection and electricity in Nigeria. About 61.2 % of households in Lagos in South-West are without access to electricity. The figure is different in Taraba in North-East where 81.3 % lack access to electricity [15]. Similarly, South-South have 61.2 % and South-East has 60 %. About 38.1 % of the rural population, 12.1% of the rural poor and 29.8% of the urban poor in Nigeria have access to electricity [16].

Erratic power supply has caused many of the inhabitants and companies in Nigeria to generate their own power. Nigeria has about 32 outages in a month with over 35 hours outage of electricity supply [17]. Figure 2.1 shows the electrical outages per month and average duration in Africa [18]. Erratic supply is due to high energy losses caused by physical deterioration of the facilities for transmission and distribution, and theft of power equipment. Other causes are vandalism, the high cost of electricity production, insufficient metering system and ease of by-passing of the metering system by the consumers, poor billing system and low available capacity (only 40 % of the installed capacity of 6 000 MW) [19].

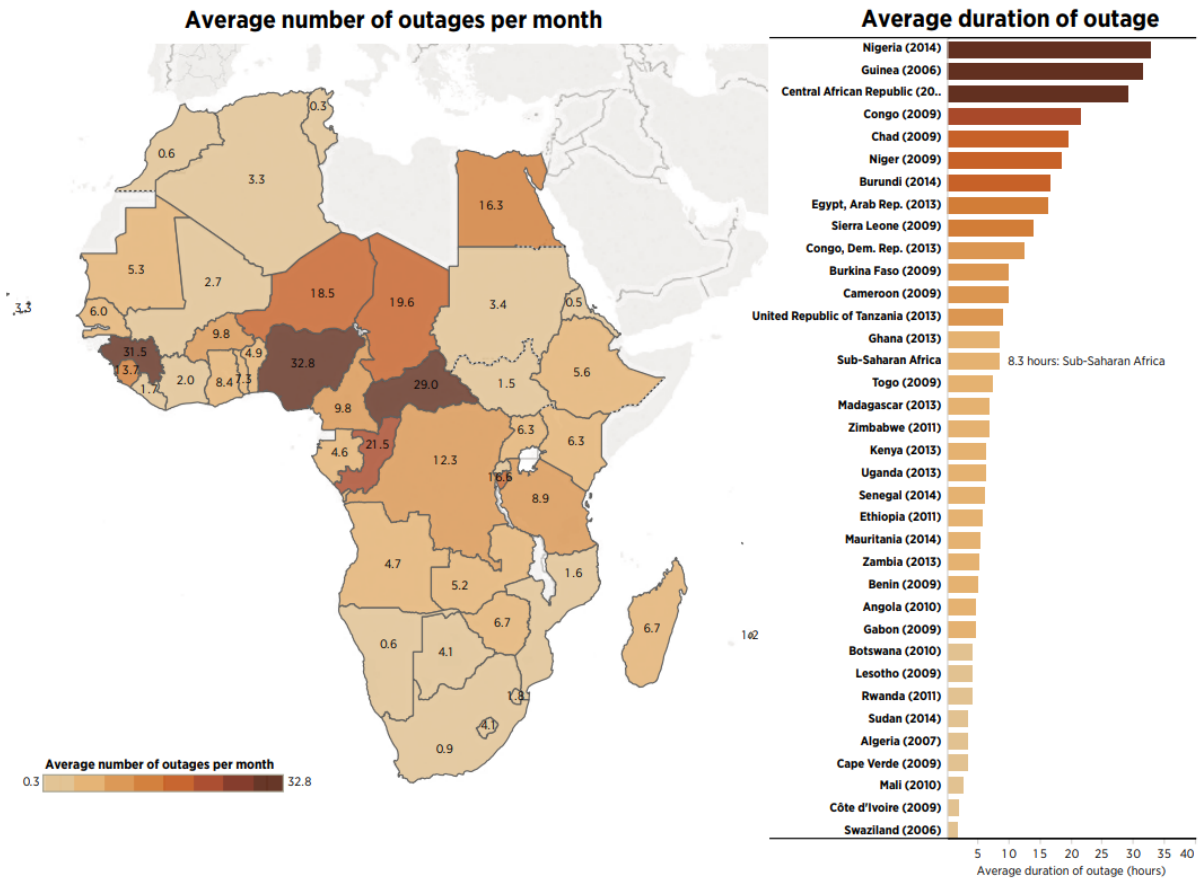

Figure 2.1. Electrical outages per month and average duration in Africa [18]

Individuals have resorted to using generators powered by petroleum fuel or diesel. This accounts for the increase in the price of petroleum products price by 70 % in 2012 [20]. The cost of generators has risen on a regular basis from 5.8 % in 2007 to 7.6 % in 2009 [21]. Generators also increase environmental pollution [22].

Electricity access has direct links to clean drinking water, good health and agricultural activities for rural dwellers [23, 24]. The lack of electricity has created, and is still responsible for, high levels of underdevelopment and poverty in the rural areas [25, 26]. Several studies attest to the fact that stable and affordable electricity contributes to higher levels of economic development [27-33].

Renewable energy is a tool that can end global electricity problems because supply exceeds world electricity demand [34]. It is an energy source that can be renewed indefinitely. Renewable energy sources include solar, ocean tides, geothermal, wind, hydro, and biomass [35-37]. They are used as electricity, thermal energy, fuels, mechanical force and hydrogen. These energy sources are obtained from non-fossil and non-nuclear sources [38]. They are sustainable and not harmful to the environment. Table 1 shows the vast potential of solar energy inclusion in Nigeria, shedding light on Nigeria's solar energy resources. From the data in Table 2.1 one can see that Nigeria only needs 0.1 % of the total solar radiation converted at 1 % efficiency to be able to meet her energy demand [39]. On average, Nigeria gets solar radiation of 20 MJ/m^2/day with minimal variation all year.

Table 2.1. Nigeria's solar energy resources [39]

Resource type	**Reserves**		**Production**	**Domestic utilization**
Natural units	**Energy units**	**Energy units (BTOE)**		
Solar Radiation	3.5 KWh/m^2/day to 7.0 KWh/m^2/day (4.2 million MWh/day using 0.1% Nigeria land area)	5.2 (40 years and 0.1% Nigeria land area)	Approximately 6 MWh/day solar Photovoltaic	Approximately 6 MWh/day solar Photovoltaic

Power generation involves the conversion of energy from an available source (sun in this case) to electrical energy in a form that is suitable for distribution, consumption and storage [40]. Solar PV is capable of powering off-grid single homes, and mini-grids incorporating from several kW to many MW [18]. Power generation using solar energy can be done in two ways, namely, solar-thermal conversion [41] and solar electric (photovoltaic) conversion [42]. Solar energy is one of the renewable energy endowments of Nigeria [43]. It can be used for powering remote villages disconnected from the nation's grid and its power can also be fed into the national grid [44]. Solar energy is used in rural clinics, powering of schools, vaccine refrigeration, street lighting, traffic lights, kiosks, among others. Solar technology is gradually being implemented in Nigeria. It is already implemented for solar crop drying, solar incubators, solar chick brooding, solar evaporative cooling and so on.

Renewable energy is capable of solving Nigeria's energy challenges [45, 46]. Several studies have looked at the viability and challenges of implementing solar energy in Nigeria. These are reviewed below.

Chilakpu [47] examined renewable energy sources benefits, potentials and challenges in Nigeria. The study stated that renewable energy improves the security of a country, and reduces greenhouse gases. The study aligned with Körbitz [48] in stating that renewable energy reduces greenhouse gases by at least 3.2 kg carbon dioxide equivalents per one kilogram of biodiesel. The study observed that the challenges working against the full-scale implementation of solar energy in Nigeria include available technology, the political climate, and the weather conditions of the country. Körbitz study dwells most on hydropower and fails to shed light on other renewable energy sources, especially solar energy.

Olaoye et al. [49] studied the energy crisis in Nigeria and suggested a renewable energy mix as a solution. Attention was given to the installed capacity and licensing of on-grid power generation companies. The study provided two tables which summarized the renewable energy potential of Nigeria. The data provided is limited to the capacity of solar PV panels in Nigeria.

Ajayi and Ajanaku [50] examined the energy challenge and power development in Nigeria and proposed a way forward. The study suggested that 80 % of hydropower in the country is untapped, and 5.5 KW-hr/m^2/day of solar radiation is not being utilized as well as unexploited wind energy resources and the gases being flared. The study believes that utilizing these resources will put an end to the energy challenge of Nigeria.

Akinboro et al. [51] studied solar energy installations in Nigeria in terms of their prospects, problems and solutions. The study set out to study the use of solar energy as an alternative energy source in Nigeria. Emphasis was on stand-alone and hybrid installations and the problems encountered during domestic and industrial solar installation. In the end, the study was only able to enumerate the challenges confronting the implementation of solar energy, its prospects and possible solutions. However, the study shed light on waste generated from gas turbines, diesel plants, solar plants, biogas plants, nuclear and small hydropower plants. There was no mention of solar installations as stated in the beginning of the study.

Ezugwu [52] discussed renewable energy in Nigeria with a focus on their sources, problems and prospects. The study was able to theoretically discuss the key renewable energy sources but lacked relevant data regarding Nigeria.

Emodi and Yusuf [53] discussed the need for standardization of renewable energy technologies in Nigeria. They opined that renewable energy technologies are imported into Nigeria and there are no existing local standards. The study recommended standardization as a solution to check the influx of renewable energy technologies into Nigeria.

Ikem et al. [54] studied integration of renewable energy sources into the Nigerian national grid as being a way out of the power crisis. It suggested a way forward for Nigeria's government to improve the current power supply of the country by investing in renewable energy. The study encouraged the government to review the power sector.

Ozoegwu et al. [43] studied the status of solar energy integration and policy in Nigeria. It did a good job in reviewing the past, the current and future status of solar integration in Nigeria. It was able to combine several data related to solar energy in Nigeria. This provided a firm basis for the case of giving solar energy a high priority in mitigating the energy problem of Nigeria. Figure 2.2 shows the relationship between electricity usage and Gross Domestic Product (GDP) while Table 2.2 grouped the different categories of solar PV applications under different headings.

Table 2.2. Categories of Solar PV applications (adapted from [18])

Item	Stand-alone			Grids		
	DC		AC	AC/DC		AC
System	Solar lighting DC Solar kits or system lanterns		AC solar system: single-facility AC systems	Nano-grid Micro-grid Pico-Mini-grid grid		National/regional grid
Application	**Off-grid**			**Off-grid or on-grid**		**On-grid**
	Lighting	Lighting and appliances	Lighting and appliances	Lighting and appliances, emergency power	All uses (including industrial)	All uses (including industrial)
Key component	Generation, storage, lighting, phone charger	Generation, storage, DC special appliances	Generation, storage, lighting, AC appliances, building wiring	Generation plus single phase distribution	Generation plus three phase distribution	Generation plus three-phase distribution plus transmission
Typical size	0.10 W	11 W to 5 kW	100 W to < 5 kW	5 kW to 1 MW		Residential (100 W to < 5 kW) Mini grid (5 kW to < 1 MW) and Utility scale (> 1 MW)

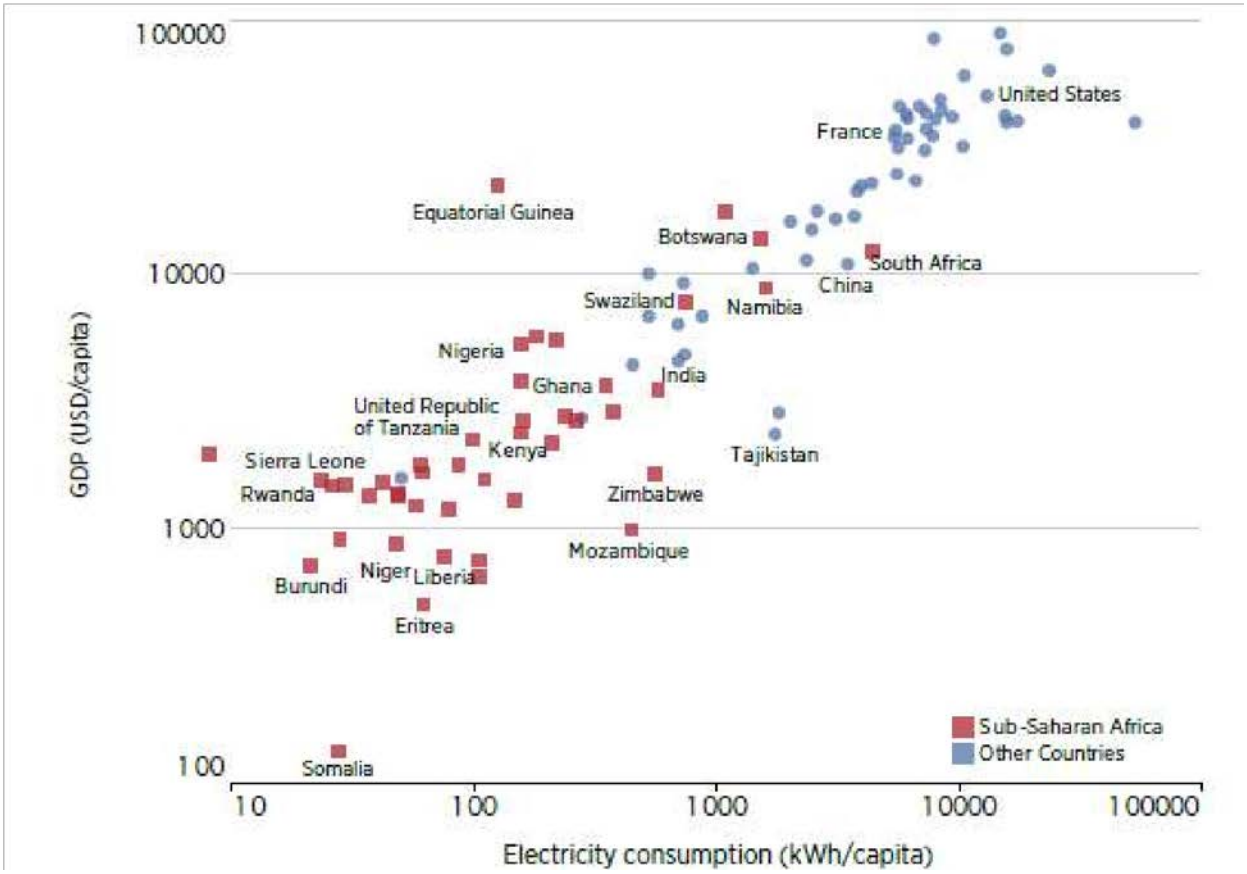

Figure 2.2. Relationship between electricity usage and Gross Domestic Product 2012 [18]

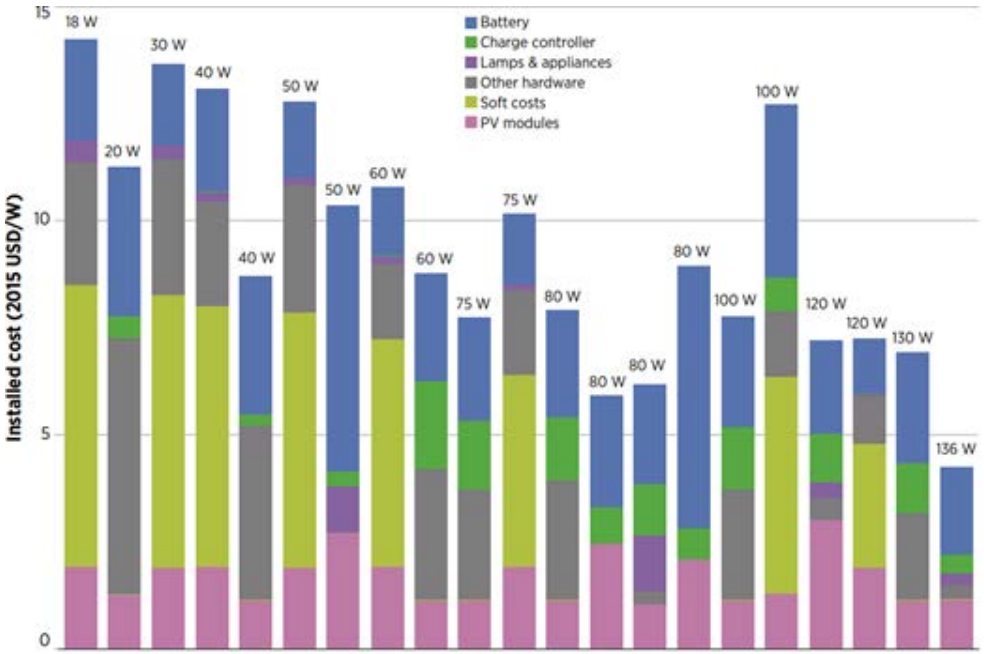

Figure 2.3. Small solar system (<1 kW) cost breakdown by cost component, 2012-2015 [18]

Figure 2.3 presents the cost breakdown for sub-1 kW where the data are available. Battery costs account for the largest single share of these Small Household Solar Supply (SHS), with a simple average of 29 % of the total costs (USD 2.7 /W). The PV modules themselves, as well as the lighting fixtures and wiring, average around 20 % (USD 2.2 /W) of the total installed costs together, soft costs 22% (USD 2 /W), other hardware 21% (USD 2 /W) and the charge controller 7% (USD 0.7 /W).

Several researchers have proposed various ways in which the technology of solar can be used in Nigeria. This includes but is not limited to the following:

Cota et al. [55] proposed the use of solar energy for street lighting and water pumping in the rural community of Igbelaba and Jigawa state.

Kumar et al. [56] presented suggestion for replacing the usage of fossil fuel energy with solar energy for street lighting of Fugar city in Edo state of Nigeria.

Ike Chinelo et al. [57] suggested the use of solar to power security lights in school hostels in Nigeria.

1.1 Data on solar energy capacity in Nigeria

The industry capacity of solar energy was a total of 33 active companies by 1999. There are no vendors or contractors for the supply and installation of solar equipment. Nigeria cannot boast of a company that manufactures the major components of solar systems, not even the basic solar cells [58]. However, NASENI assembles PV panels in Karachi, close to Abuja. Nevertheless, the country can boast about 200 installed solar PV installations with a capacity of about 3.5 kW to 7.2 kW [59]. This is insignificant when compared with the population of Nigeria and installed capacity in other Africa countries like South Africa. Figure 2.4 provides a vivid picture of installed solar PV capacity in watts per capita in Africa in 2015.

A survey was conducted in the northern part of Nigeria to show the application distribution [58]. It shows that domestic water pumping accounts for 57%, domestic lighting and rural for 8%, experimental room air conditioning for 1%, rural clinic refrigeration of clinic items like vaccines and lighting of the clinic and surrounding for 24%, and communications (TV and radio) for 10% (see Table 2.3).

In terms of installed PV in regions of Nigeria, Lagos has the highest with 23.6% closely followed by Yobe state with 16.3%. Kano and Akwa Ibom have 8.6%.

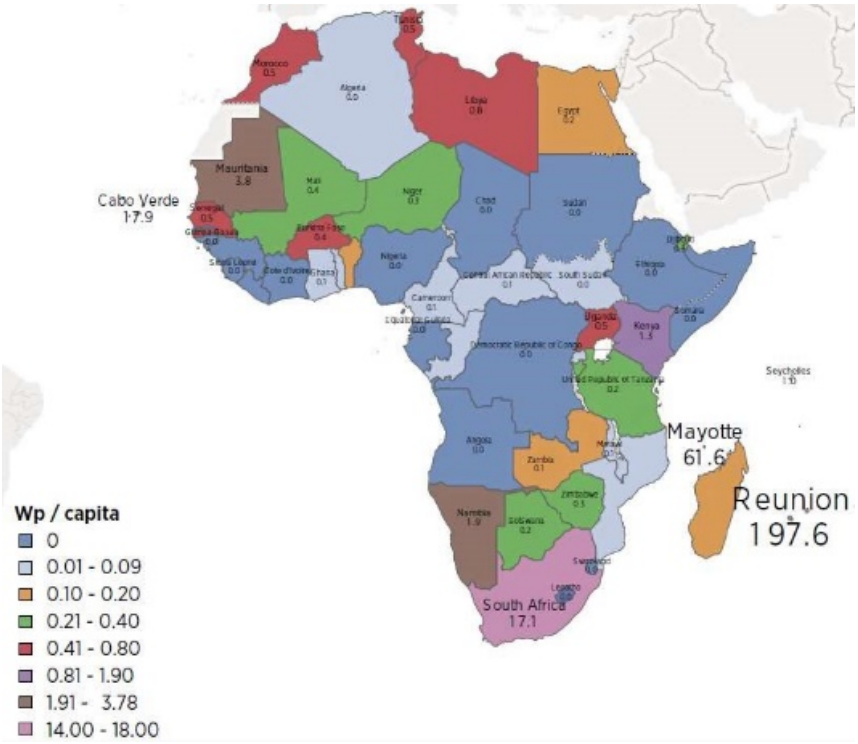

Figure 2.4. **Map of installed solar PV capacity in watts per capita, 2015**

Table 2.3. **Installed capacity of PV technology in Nigeria [59]**

S/N	APPLICATIONS	PV CAPACITY (%)
1.	Residential (mostly lighting)	6.9
2.	Rural electrification and Television	3.9
3.	Commercial lighting and equipment	3.1
4.	Street, Billboard and other lighting	1.2
5.	**All lighting**	15.1
6.	Industrial	0.4
7.	Health centre/clinic	8.7
8.	Telecom and radio	23.6
9.	Water pumping	52.2
10.	**Total**	**100**

The funding of such installations is principally by the federal government, state, local government, and international donors like the European union, Mobil and in some states like Lagos by private individuals. There are about one or two PV installations working or moribund in the 26 states out of the 36 states in Nigeria including the capital Abuja [59].

2. Solar project initiatives in Nigeria

Some striking projects on solar energy have been executed in Nigeria. The Jigawa state government embarked on a project of rural electrification of the state [60]. This was funded 60 % by the United States government through USAID and department of Energy (DOE) and 40 % by the Jigawa state government. This project demonstrated inclusive solar usage for electricity generation in rural communities. The project targeted water supply, education, health, agriculture, security, opportunities for trade and commerce [61]. Several PV water pumping, electrification, and solar thermal installations have been executed by Sokoto Energy Research Center (SERC) and the National Center for Energy Research and Development (NCERD) under the supervision of the Energy Commission of Nigeria (ECN) [62]. Some of the solar energy related pilot and demonstration projects of the ECN are shown in Table 2.4

Table 2.4. **Solar Energy pilot and demonstration projects of the ECN [14]**

S/N	TECHNOLOGY	APPLICATIONS	CAPACITY RANGE	NO
1.	Solar-PV	Village electrification Village TV Health centre power Water pumping Telecommunications	0.88 kWp to 7.2 kWp	11
2.	Solar dryer	Rice and forage drying	1.5 tonnes to 2 tonnes	4

Breakdown of the pilot projects by ECN include the 7.2 kWp solar-PV village electrification in Kwalkwalawa in Sokoto state, 1.87 kWp village electrification and TV viewing centre in Iheakpu, 1.5 kWp water pumping scheme in Nangere, Sokoto state. Solar dryer projects in Nigeria include: 2-tonnes solar rice dryer in Adani, Enugu state and 1.5 tonnes solar forage dryer in Yauri, Kebbi state.

The World Solar Programme designed for promotion of solar energy penetration worldwide has also provided about five high priority projects in Nigeria. They are:

i. The solar village.
ii. The upgrading of facilities and personnel of renewable energy R & D establishments, and development of renewable energy curricula.
iii. Training workshops and colleges in renewable energy technologies (solar-PV and solar-thermal)
iv. Rural health delivery and potable water supply using solar-PV
v. International Solar Energy Institute. The projects are threatened by inadequate funding. As a result, only projects (i) and (iv) have made significant progress.

2.1 Solar energy capacity development in Nigeria

The federal government of Nigeria has mandated the ECN with the responsibility to carry out research and development of the nation's energy needs. ECN has two centers dedicated to renewable energy spread evenly in the north and south of the country, namely, the National Centre for Energy Research and Development (NCERD) at Nsukka, in the south of Nigeria, and the Sokoto Energy Research centre (SERC) in Sokoto state, in the north of Nigeria. Apart from the research and development mandate of the centres, they are also responsible for personnel development, dissemination and promotion of renewable and alternative energy technologies. The other government agencies that have renewable energy components in their mandates are: Federal Department of Meteorological Services (FDMS), Power Holding Corporation of Nigeria (PHCN). Others are Project Development Institute (PRODA) Enugu, Nigerian Building and Road Research Institute (NBRRI), Federal and state owned Universities and Polytechnics, and the Federal Institute of Industrial Research, Oshodi (FIIRO), National Centre for Energy Research and Development (NCERD), Nsukka, Centre for Energy Research and Training (CERT), located in Ahmadu Bello University, Zaria, Centre for Energy Research and Development (CERD), located in Obafemi Awolowo University, Ile-Ife.

Some successes have been achieved in solar energy technology development in the country. These include, but are not limited to, solar crop dryers of various capacities. Worthy of note is the 2-tonne capacity rice dryer developed at the NCERD and a 2-tonne capacity forage dryer constructed by the SERC. Also, a solar manure dryer for poultry waste developed by NCERD, Nsukka. The dryer was able to reduce moisture content of manure from 71 % to 35 % in 22 hours of peak solar intensity of 600 W/m^2. Flat and concentrated solar cookers have been constructed and tested at NCERD and SERC. The flat plate cooker attained a record cooking time of 4.5 minutes at solar intensities of 850 W/m^2. Solar water heaters comprizing horizontal and vertical tanks with natural circulation have also been constructed and are available at Usman Danfodiyo University, Sokoto, and solar chick brooders at NCERD, Nsukka.

Licenses for solar energy projects in the country have been awarded by the Nigerian Electricity Regulatory Commission as shown in Figure 2.5. As at 2014, seven companies have been awarded licenses in different states of Nigeria. Bauchi has the highest capacity with 100 MW awarded to Nigeria Solar Capital Partners.

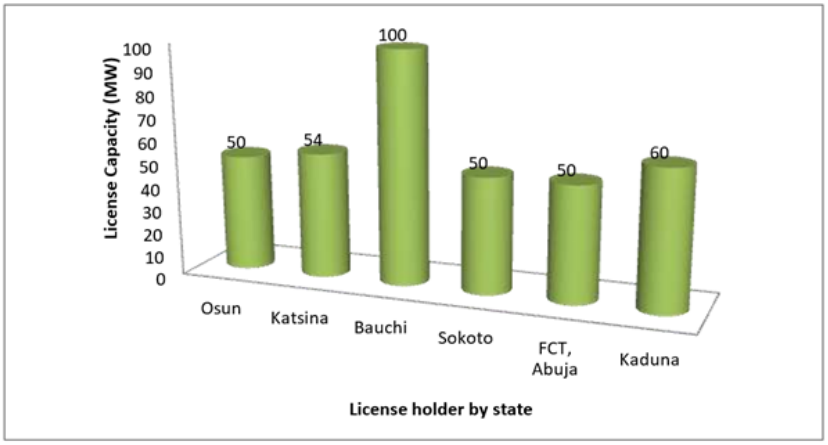

Figure 2.5. **Nigerian Electricity Regulatory Commission licensed solar power projects in Nigeria**

Kaduna have two licenses awarded to Quaint Global Nigeria Ltd and Anjeed Kafanchan Solar Ltd with a capacity of 50 MW and 10 MW respectively. Others are Lloyd and Baxter LP in Abuja, KVK Power Pvt Limited in Sokoto state, Pan African Solar in Katsina and Rock Solar Investment Company in Osun state. Due to fluctuation in generation capacity caused by water shortages in the dry season, Shiroro Hydroelectric Power Station in Niger State of Nigeria plans to construct a 300 MW PV solar power plant.

Some memorandums of understanding have been signed for solar projects in Nigeria. New Horizon Energy Resources proposed the building of a 100 MW solar plant in Nasarawa (Aniweta, 2015). Delta state government signed an MoU with Yutal Li Ltd for a 100 MW solar power plant in 2016 in addition to a 300 MW power plant signed for in 2014 with SkyPower FAS Energy (Thisday, 2016). The federal government of Nigeria also signed a 300 MW solar power with Super Solar.

2.1.1 Solar cell fabrication and research in Nigeria

Limited work has been done on materials for solar cell fabrication and thin film growth in Nigeria at Obafemi Awolowo University (OAU, Ile Ife) and NCERD, Nsukka respectively and in some laboratories in the country. Soboyejo and Kana have led some research studies at Africa University of Science and Technology (AUST, Abuja) and Sheda Science and Technology Complex (SHESTCO, Sheda), on organic solar cell materials fabrication. Fabian Ezema has worked extensively on Chemical Bath Deposition (CBD) for solar cell deposition at the University of Nigeria, Nsukka. The National Agency for Science and Engineering Infrastructure (NASENI) is also worthy of mention in terms of solar cells research and development and solar panels. NASENI, in Nigeria is leading the effort to make solar panels available at a reduced cost. It has a dedicated solar panel assembly plant in Karachi, Nigeria. Most of the solar PV studies conducted in Nigeria are on solar PV components and system testing, pilot plants and other application projects. The KwalkwalaWa 7.2 kW village electrification in Sokoto state is the largest single pilot plant established by the Energy Commission. It is used for pumping water, powering health centres and rural lighting and entertainment. Other developments include solar air heaters, solar stills for water purification, solar absorption and absorption refrigerators.

2.1.2 Solar data collection in Nigeria

Efforts are being intensified in solar energy data collection in Nigeria. Data such as solar radiation intensities (such as global, direct and diffuse), relative humidity, precipitation and ambient temperatures have been collected for over 64 towns by the Meteorological Services Department. About 33 % of these stations have been in existence for over 50 years. About twelve research institutes and centres located in and outside universities in the country are also involved in solar data collection and analysis. The Energy Commission is currently developing an Energy Data Bank for renewable energy data.

3. Existing government policies and legislation

A National Energy Policy was developed in 2003 by the Nigerian government, primarily for efficient management of the country's energy resources. It focuses on conventional and renewable energy sources for sustainable development of the country with full private sector participation.

The policy is summarized as:

- ❖ Extensive crude oil and natural gas exploration and development shall be pursued with the view to increasing their reserves base to the highest level possible.
- ❖ The nation shall continue to engage extensively in the development of electric power with the view to making reliable electricity available to 75 % of the population by 2020; as well as to broaden the energy options for generating electricity.

The Nigerian Electricity Regulatory Commission and the Rural Electrification Agency were established in 2005 with in order to liberate the electricity sector.

The Nigeria Renewable Energy Master Plan (REMP) is a policy aimed at making electricity more available through renewable energy. It envisions renewable energy providing a minimum of 10 % of total energy consumption in Nigeria by 2025 [63]. It was produced in 2006 with United Nations Development Programme support, and outlined the road map for more renewable energy usage in Nigeria's quest to meet her energy demands and improve grid reliability and security [64]. The policy hopes to meet this goal by providing an enabling platform for renewable energy, legal instruments, technical-know-how, manpower, infrastructure and the markets.

The objectives are:

- Expanding access to energy services and raising the standard of living, especially in the rural areas;
- Stimulating economic growth, employment and empowerment;
- Increasing the scope and quality of rural services, including schools, health services, water supply, information, entertainment and stemming the migration to urban areas;
- Reducing environmental degradation and health risks, particularly to vulnerable groups such as women and children;
- Improving learning, capacity-building, research and development on various renewable energy technologies in the country; and
- Providing a road map for achieving a substantial share of the national energy supply mix through renewable energy.

4. Challenges

The high cost of implementation of renewable energy technologies, particularly solar, is the major impediment militating against their widespread use [65]. High cost is not unconnected to the fact that nearly all the parts are imported from overseas at a very high cost. Most of the personnel and technologies are sourced abroad [58]. The key challenges facing the successful deployment of solar energy technologies can be grouped into cost, policy, technical, people and environment.

Some of the key challenges of solar energy in Nigeria are discussed below.

1. Cost: Cost plays a major role in the life of people and the success or failure of a technology. Nigeria is a developing country home to both rich and poor, living in rural and urban areas. Initial investment in the cost of solar energy infrastructure is one of those factors militating against penetration of solar energy in Nigeria. The lack of adequate funding for solar energy development poses a high risk to the success of solar energy in Nigeria.
2. Policy: The general absence of comprehensive national energy policy. Nigeria has never formulated a comprehensive energy policy; only sub-sectoral policies have been formulated. Since such a policy is pivotal to using energy efficiently and solar energy, the lack of such a policy has, to a large extent, contributed to the lack of attention to solar energy.
3. Technical: Lack of technological capability is an issue in penetration of solar energy in Nigeria. The bulk of the technologies for solar energy are imported thereby increasing the high investment cost of solar energy.
4. Cultural and low level of public awareness: The cultural inclination in some parts of Nigeria coupled with public awareness of renewable energy sources and technologies in Nigeria and their benefits, both economically and environmentally, are generally low. Consequently, the public is not well-equipped to influence the government to begin to take more decisive initiatives in enhancing the development, application, dissemination and diffusion of renewable energy resources and technologies in the national energy market.

5. Prospects for solar energy in Nigeria

Geographically, Nigeria lies within a high sunshine belt on longitude 3º and 14º East of Greenwich and latitude 4º and 14° north of equator [66] and thus has enormous solar energy potential [67]. The country has an annual average daily solar radiation of about 5.535 KW/m^2 /day [68]. The minimum average is about 3.55 kW/m^2/day in Katsina in January. It is 3.4 kW/m^2/day for Calabar in August. And the maximum average is 8.0 kW/m^2/day for Nguru in May [69]. This puts the solar radiation figure at an average of 19.8 MJ/m^2/day and is fairly distributed.

The country's annual average daily sunshine is 6.25 hours per day, the coastal areas are 3.5 hours and 9.0 hours at the far northern boundary [70]. Nigeria receives about 4.851 x 10^{12} KWh of energy per day from the sun [71]. This is equivalent to about 1.082 million tons of oil equivalent (mtoe) per day, and is about 4 000 times the current daily crude oil reduction, and about 13 000 times that of natural gas daily production based on energy units. This huge energy resource from the sun is available for only about 26 % of the day. This data couple with the prevailing efficiencies of commercial solar-electric generators and if solar collectors or modules were used to cover 1% of Nigeria's land area of 923 773km^2, it is possible to generate 1.804 x 10^{15} kWh of solar electricity per year. This is over one hundred times the current grid electricity consumption level in the country [72]. The annual solar energy insolation is 27 times the nation total conventional energy resources in energy units. This is over 117 000 of the electric power generated in 1998 in Nigeria [40]. Only about 3.7 % of Nigeria's land area is required for solar energy to meet the electricity demand of the country.

5.1 Future prospects

Though the bulk of the prospects for solar energy in Nigeria are in the off-grid areas and rural electrification, some areas on the grid and in urban areas also hold some prospects. Areas that provide opportunities for application include, but are not limited to: power plants, non-thermal electricity generation, large scale and family scale cooking, heating, drying of farm produce, water purification, clean water provision for humans and animals, aerospace development of the country, provision of light arms and ammunition for the Nigeria Army especially as they combat Boko haram terrorism and militants in the Niger Delta of the country. The future prospects of solar PV are shown in Figures 2.6 and 2.7.

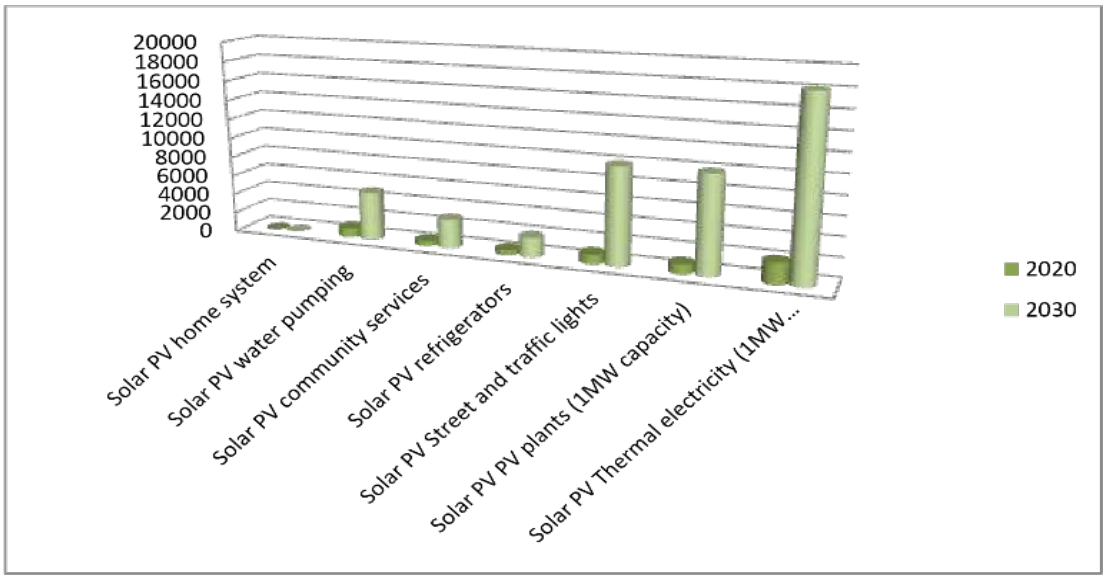

Figure 2.6. Solar PV application in Nigeria for year 2020 and 2030

The major focus on renewable energy in Nigeria is on transportation and electricity generation. Electricity generation from renewable energy in Nigeria is estimated to be 9.74 % for 2015, 18 % for 2020 and 20 % for 2030.

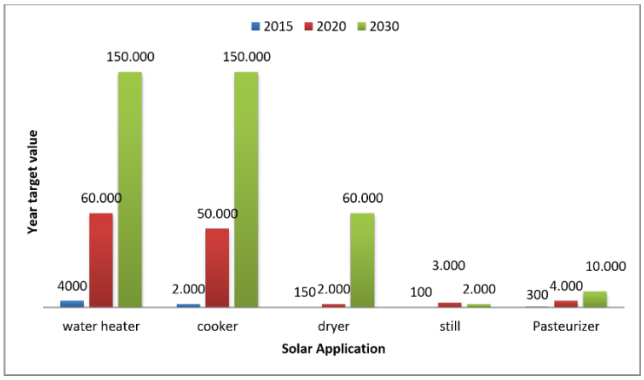

Figure 2.7. **Targets for solar thermal energy application in Nigeria for year 2015, 2020 and 2030**

However, electricity generation using solar is projected to be 1.26 % for 2015, 6.92 % for 2020 and 15.27 % for 2030. The targets of renewable electricity from solar alone is projected to be 12.96 %, 38.43 % and 76.36 % for these years. This shows that solar progressively dominates in the long-term. Figure 6 shows the targets for solar PV application in Nigeria for year 2020 and 2030. Figure 7 shows the targets for solar thermal energy application in Nigeria for year 2015, 2020 and 2030. This is too dismal to be commended even in the long-term. For example, consider the targets for solar cookers. Suppose each solar cooker is constructed to cook for five people as proposed by Saxena et al. [73]. With a population growth rate of 3.2 % per annum, the population in 2015, 2020 and 2030 population becomes 186 458 723, 218 263 539 and 299 073 660 respectively. The penetration level which represent the percentage of the population supplied with solar cooking energy becomes 0.0054 %, 0.1145 % and 0.2508 % respectively. Although this figure indicates a rising trend into the future, the penetration level is minor and does not reflect the energy crisis in Nigeria. This is because in 2014 about 80 % of the population were exposed to health issues. Many of these health issues arose from the heating and cooking used in the rural setting, using mainly biomass and waste resources. The maintenance-free and cheap nature of solar box cookers makes them well suited to developing countries.

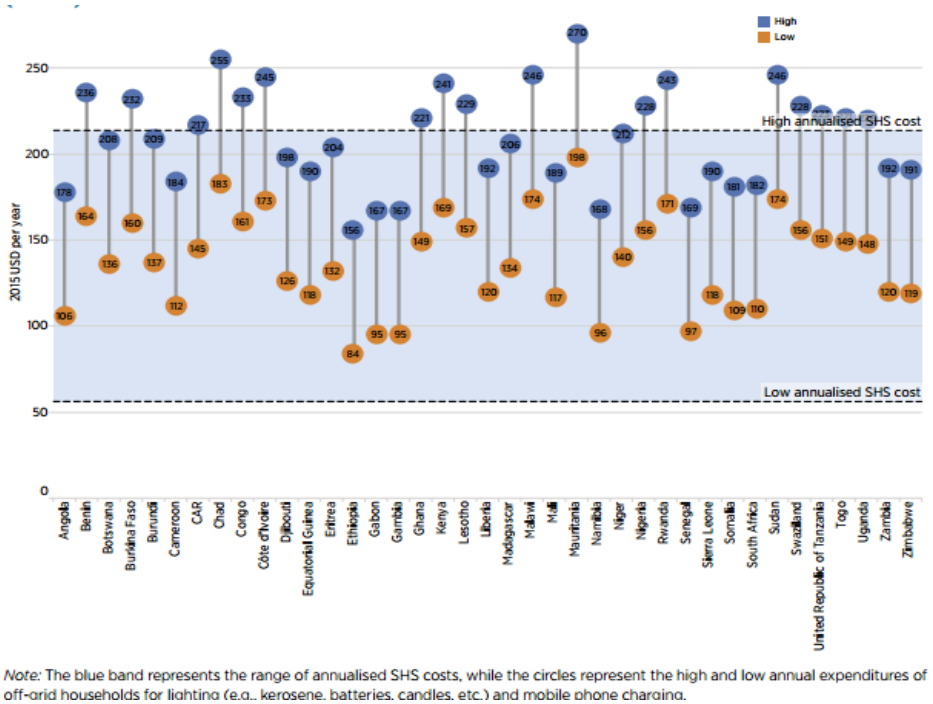

Note: The blue band represents the range of annualised SHS costs, while the circles represent the high and low annual expenditures of off-grid households for lighting (e.g., kerosene, batteries, candles, etc.) and mobile phone charging.

Figure 2.8. **Africa annual off-grid household expenditure on lighting and mobile phone charging compared to solar home system (< 1 kW) annualized costs, by country in 2015 [18]**

Figure 2.8 gives the annual expenditure for off-grid lighting and mobile phone charging in Africa in 2015. The blue band represents the range of annualized solar system costs. Circles represent the high and low annual

expenditures of off-grid households for lighting (e.g., kerosene, batteries, candles, etc.) and mobile phone charging. Expenditure in Nigeria is USD 140 per year. The lowest expenditure in Africa is in Ethiopia (USD 84) and the highest is Mauritania (USD 270). Therefore, solar systems can be a very economical solution for powering homes in Africa

6. Conclusion

Nigeria has the capacity to use solar energy to end the problem of an erratic power supply facing her. This work has been able to shed light on solar energy domestication in Nigeria, reviewing work that has been done relating to solar energy in Nigeria, and the prospects and challenges of the technology. A lot of brilliant studies have been conducted. Well-articulated policies have been made and signed with memorandums of understanding on the part of the government but well monitored implementation seems to be an issue working against the full success story of solar energy utilization in Nigeria. Research into in-country fabrication of solar cells, thin films and solar panels is highly recommended for both public and private partnership in Nigeria. The windows of opportunities for solar energy inclusion in Nigeria are enormous. These are: solar power generation, increased internally generated revenue through manufacture of solar panels, capacity building in the field of solar energy technologies, supply of renewable energy equipment and accessories, and contracts in solar energy projects. The rest of Africa can benefit from the success story of Nigeria if well implemented.

7. Recommendation

More education should be conducted to sensitize the populace on the benefits of solar energy and the government should encourage more research on solar energy, especially the setting up of and/or funding of solar cells research centres.

Acknowledgements

The financial assistance of the National Research Foundation and The World Academy of Science (NRF-TWAS) of South Africa is acknowledged.

References

[1] Kaygusuz, K., Energy for sustainable development: A case of developing countries. *Renewable and Sustainable Energy Reviews*, 2012. **16**(2): p. 1116-1126.
[2] Scarlat, N., et al., Evaluation of energy potential of municipal solid waste from African urban areas. *Renewable and Sustainable Energy Reviews*, 2015. **50**: p. 1269-1286.
[3] Karekezi, S., Poverty and energy in Africa—a brief review. *Energy Policy*, 2002. **30**(11-12): p. 915-919.
[4] Wolde-Rufael, Y., Energy demand and economic growth: the African experience. *Journal of Policy Modeling*, 2005. **27**(8): p. 891-903.
[5] Bazilian, M., et al., Energy access scenarios to 2030 for the power sector in sub-Saharan Africa. *Utilities Policy*, 2012. **20**(1): p. 1-16.
[6. Bongaarts, J., Human population growth and the demographic transition. *Philosophical Transactions of the Royal Society B: Biological Sciences*, 2009. **364**(1532): p. 2985-2990.
[7] Apulu, I., A. Latham, and R. Moreton, Factors affecting the effective utilisation and adoption of sophisticated ICT solutions: Case studies of SMEs in Lagos, Nigeria. *Journal of Systems and Information Technology*, 2011. **13**(2): p. 125-143.
[8] Oseni, M.O., An analysis of the power sector performance in Nigeria. R*enewable and Sustainable Energy Reviews*, 2011. **15**(9): p. 4765-4774.
[9] Obadote, D. Energy crisis in Nigeria: technical issues and solutions. In *Power sector prayer conference*. June 27-29, 2009.
[10] Aliyu, A.S., A.T. Ramli, and M.A. Saleh, Nigeria electricity crisis: Power generation capacity expansion and environmental ramifications. *Energy*, 2013. **61**: p. 354-367.
[11] Oyedepo, S.O., On energy for sustainable development in Nigeria. *Renewable and Sustainable Energy Reviews*, 2012. **16**(5): p. 2583-2598.
[12] Ohunakin, O.S., Energy utilization and renewable energy sources in Nigeria. J*ournal of Engineering and Applied Sciences*, 2010. **5**(2): p. 171-177.
[13] Mohammed, Y., et al., Renewable energy resources for distributed power generation in Nigeria: a review of the potential. *Renewable and Sustainable Energy Reviews*, 2013. **22**: p. 257-268.
[14] Sambo, A.S., *S*trategic developments in renewable energy in Nigeria. I*nternational Association for Energy Economics*, 2009. **16**(3): p. 15-19.
[15] Ohiare, S., Expanding electricity access to all in Nigeria: a spatial planning and cost analysis. *Energy, Sustainability and Society*, 2015. **5**(1): p. 8.

[16] Usman, Z.G. and S. Abbasoglu, An overview of power sector laws, policies and reforms in Nigeria. *Asian Transactions on Engineering*, 2014. **4**(2): p. 6-12.
[17] Oseni, M.O., Power outages and the costs of unsupplied electricity: evidence from backup generation among firms in Africa. In *Proceedings USAEE/IAEE Conference*, Austin Texas. 2012.
[18] IRENA, *Solar PV in Africa: Costs and Markets*. 2016.
[19] Sambo, A., Nigeria's long term energy demand outlook to 2030. *Journal of Energy*, 2012.
[20] Onakoya, A.B., et al., Energy consumption and Nigerian economic growth: An empirical analysis. *European Scientific Journal*, 2013. **9**(4).
[21] Ohiare, S., *Financing rural energy projects in developing countries: a case study of Nigeria*. PhD thesis, De Montfort University, Leicester, UK, 2014.
[22] Guttikunda, S.K. and R. Goel, Health impacts of particulate pollution in a megacity—Delhi, India. *Environmental Development*, 2013. **6**: p. 8-20.
[23] Zhang, J., et al., Environmental health in China: progress towards clean air and safe water. *The Lancet*, 2010. **375**(9720): p. 1110-1119.
[24] Epstein, T.S. and D. Jezeph, Development—there is another way: a rural–urban partnership development paradigm. W*orld Development*, 2001. **29**(8): p. 1443-1454.
[25] Kanagawa, M. and T. Nakata, Assessment of access to electricity and the socio-economic impacts in rural areas of developing countries. E*nergy Policy*, 2008. **36**(6): p. 2016-2029.
[26] Kaygusuz, K., Energy services and energy poverty for sustainable rural development. *Renewable and Sustainable Energy Reviews*, 2011. **15**(2): p. 936-947.
[27] Iyke, B.N., *E*lectricity consumption and economic growth in Nigeria: A revisit of the energy-growth debate. *Energy Economics*, 2015. **51**: p. 166-176.
[28] Jaunky, C.V., *I*ncome elasticities of electric power consumption: Evidence from African countries. *Regional and Sectoral Economic Studies*, 2006. **7**: p. 25-50.
[29] Akinlo, A.E., Electricity consumption and economic growth in Nigeria: evidence from cointegration and co-feature analysis. *Journal of Policy Modeling*, 2009. **31**(5): p. 681-693.
[30] Ogundipe, A.A. and A. Apata, Electricity consumption and economic growth in Nigeria. *Journal of Business Management and Applied Economics*, 2013. **11**(4).
[31] Aliero, H.M., S.S. Ibrahim, and M. Shuaibu, An empirical investigation into the relationship between financial sector development and unemployment in Nigeria. A*sian Economic and Financial Review*, 2013. **3**(10): p. 1361.
[32] Okoligwe, N. and O.A. Ihugba, Relationship between electricity consumption and economic growth: Evidence from Nigeria (1971-2012). *Academic Journal of Interdisciplinary Studies*, 2014. **3**(5): p. 137.
[33] Dantama, Y.U., Y.Z. Abdullahi, and N. Inuwa, Energy consumption-economic growth nexus in Nigeria: an empirical assessment based on ARDL bound test approach. *European Scientific Journal*, 2012. **8**(12).
[34] Ellabban, O., H. Abu-Rub, and F. Blaabjerg, Renewable energy resources: Current status, future prospects and their enabling technology. *Renewable and Sustainable Energy Reviews*, 2014. **39**: p. 748-764.
[35] Ibidapo-Obe, O., and Ajibola, Towards a renewable energy development for rural power sufficiency. In *Proceeedings International Conference on Innovations in Engineering and Technology* (IET 2011), August 8th – 10th, University of Lagos. 2011.
[36] Panwar, N., S. Kaushik, and S. Kothari, Role of renewable energy sources in environmental protection: a review. *Renewable and Sustainable Energy Reviews*, 2011. **15**(3): p. 1513-1524.
[37] Johnstone, N., I. Haščič, and D. Popp, Renewable energy policies and technological innovation: evidence based on patent counts. *Environmental and Resource Economics*, 2010. **45**(1): p. 133-155.
[38] Twidell, J. and T. Weir, *Renewable energy resources*. 2015: Routledge.
[39] Ojosu, J., *T*he iso-radiation map for Nigeria.. *Solar & Wind Technology*, 1990. **7**: p. 563-75.
[40] Emodi, N.V. and K.-J. Boo, *S*ustainable energy development in Nigeria: Overcoming energy poverty. *International Journal of Energy Economics and Policy*, 2015. **5**(2).
[41] Reif, J.H. and W. Alhalabi, Solar-thermal powered desalination: Its significant challenges and potential. *Renewable and Sustainable Energy Reviews*, 2015. **48**: p. 152-165.
[42] Archer, M.D. and M.A. Green, *Clean electricity from photovoltaics*. 2015: Imperial College Press.
[43] Ozoegwu, C., C. Mgbemene, and P. Ozor, The status of solar energy integration and policy in Nigeria. *Renewable and Sustainable Energy Reviews*, 2017. **70**: p. 457-471.
[44] Milosavljević, D.D., T.M. Pavlović, and D.S. Piršl, Performance analysis of A grid-connected solar PV plant in Niš, republic of Serbia. *Renewable and Sustainable Energy Reviews*, 2015. **44**: p. 423-435.
[45] Nwofor, O. and V. Dike. *Objective criteria ranking framework for renewable energy policy decisions in Nigeria*. in *IOP Conference Series: Earth and Environmental Science*. 2016. IOP Publishing.
[46] Sambo, A., Enhancing renewable energy access for sustainable socio-economic development in sub-Saharan Africa. *Journal of Renewable & Alternative Energy Technologies*, 2016. **1**(1).

[47] Chilapku, K.O., Renewable energy sources: its benefits, potentials and challenges in Nigeria. *Journal of Energy Technologies and Policy*, 2015. **5**: p. 21-24.
[48] Körbitz, W.,*B*iodiesel production in Europe and North America, an encouraging prospect. *Renewable Energy*, 1999. **16**: p. 1078-1083.
[49] Olaoye, T., et al., Energy crisis in Nigeria: Need for renewable energy mix. *American Journal of Electrical and Electronic Engineering*, 2016. **4**(1): p. 1-8.
[50] Ajayi, O.O. and K.O. Ajanaku, Nigeria's energy challenge and power development: the way forward. *Energy & environment*, 2009. **20**(3): p. 411-413.
[51] Akinboro, F., L. Adejumobi, and V. Makinde, Solar energy installation in Nigeria: Observations, Prospect, problems, and solution. *Transnational Journal of Science and Technology*, 2012. **2**(4): p. 73-84.
[52] Ezugwu, C., Renewable energy resources in Nigeria: Sources, Problems and prospects. *Journal of Clean Energy Technologies*, 2015. **3**(1): p. 68-71.
[53] Dike, V., et al., solar pv system utilization in Nigeria: Failures and possible solutions. *Pacific Journal of Science and Technology*, 2017. **18**(1): p. 51-61.
[54] Ikem, I., et al., Integration of Renewable Energy Sources to the Nigerian National Grid-Way out of Power Crisis. *International Journal of Engineering Research*, 2016. **5**(8): p. 694-700.
[55] Cota, O.D. and N.M. Kumar. Solar energy: a solution for street lighting and water pumping in rural areas of Nigeria. In *Proceedings of International Conference on Modelling, Simulation and Control (ICMSC-2015)*. 2015.
[56] Kumar, N.M., A.K. Singh, and K.V.K. Reddy, Fossil fuel to solar power: A sustainable technical design for street lighting in Fugar City, Nigeria. *Procedia Computer Science*, 2016. **93**: p. 956-966.
[57] Ike Chinelo, U., C.C. Okeke, and S. Okeke, Technical Report on The Design and Installation of a 1KVA Solar Energy Powered Security Light in The Dora Akunyili and Stella Okoli Female Hostels of Nnamdi Azikiwe University, Awka, Using Monocrystalline Panels. *International Refereed Journal of Engineering and Science*, 2013. **2**(8): p. 47-50.
[58] Bala, E., J. Ojosu, and I. Umar, Government policies and programmes on the development of solar-PV Sub-sector in Nigeria. *Nigerian Journal of Renewable Energy*, 2000. **8**(1&2): p. 1-6.
[59] Iloeje, O. Renewable energy development in Nigeria: status & prospects. In *Proceedings of a National workshop on energizing rural transformation in Nigeria: scaling up electricity access and renewable energy*. 2002.
[60] Oparaku, O., Photovoltaic systems for distributed power supply in Nigeria. *Renewable Energy*, 2002. **25**(1): p. 31-40.
[61] Nwofe, P., Utilization of solar and biomass energy-A panacea to energy sustainability in a developing economy. I*nternational Journal of Energy and Environmental Research*, 2014. **2**(3): p. 10-19.
[62] Charles, A., *How is 100% renewable energy possible for Nigeria.* Global Energy Network Institute (GENI), California, 2014.
[63] Scenario, N., M. East, and P. Cedex, *World energy outlook 2014 factsheet.* Paris: International Energy Agency, 2015.
[64] Akuru, U.B. and O.I. Okoro. Renewable energy investment in Nigeria: a review of the renewable energy master plan. In *Energy Conference and Exhibition (EnergyCon), 2010 IEEE International*. 2010. IEEE.
[65] Bridgwater, A.V., Renewable fuels and chemicals by thermal processing of biomass. *Chemical Engineering Journal*, 2003. **91**(2-3): p. 87-102.
[66] Simeon, P.O., H.E. Jijingi, and S.A. Ngabea, Conscientious management of soil humus and water: a major condition for purposeful mechanisation of field crop husbandry in tropical rain forest of Nigeria. *Management, Economic Engineering in Agriculture and Rural Development*, 2016. **16**(4): p. 317-326.
[67] Adeyemo, S., Estimation of direct solar radiation intensities. *Nigerian Society of Engineers (NSE) Technical Transactions*, 1997. **32**(1): p. 1-9.
[68] Fadare, D., *M*odelling of solar energy potential in Nigeria using an artificial neural network model. *Applied Energy*, 2009. **86**(9): p. 1410-1422.
[69] Medugu D.W,. and D. Yakubu, Estimation of mean monthly global solar radiation in Yola-Nigeria using angstrom model. *Advances in Applied Science Research*, 2011. **2**(2): p. 414-421.
[70] Adaramola, M.S., Estimating global solar radiation using common meteorological data in Akure, Nigeria. R*enewable Energy*, 2012. **47**: p. 38-44.
[71] Ani, V.A., Optimal sizing and application of renewable energy sources at GSM Base station site. *International Journal of Renewable Energy Research*, 2013. **3**(3): p. 579-585.
[72] Ikuponisi, F.S. Status of renewable energy in Nigeria. In *A background brief for an International Conference on Making Renewable Energy a Reality*. 2004.
[73] Saxena, A., S. Pandey, and G. Srivastav, A thermodynamic review on solar box type cookers. *Renewable and Sustainable Energy Reviews*, 2011. **15**(6): p. 3301-3318.

CHAPTER 3: REVIEW OF NANOSTRUCTURED NiO THIN FILM DEPOSITION USING THE SPRAY PYROLYSIS TECHNIQUE

This chapter critically reviews the deposition of nanostructured NiO thin film using chemical spray pyrolysis technique.

To cite this article: Ukoba, O.K., Eloka-Eboka, A.C. and Inambao F.L. (2018). "Review of nanostructured NiO thin film deposition using spray pyrolysis technique," *Renewable and Sustainable Energy Reviews*, vol 82, pp. 2900-2915. DOI: 10.1016/j.rser.2017.10.041

Renewable and Sustainable Energy Reviews 82 (2018) 2900–2915

Contents lists available at ScienceDirect

Renewable and Sustainable Energy Reviews

journal homepage: www.elsevier.com/locate/rser

Review of nanostructured NiO thin film deposition using the spray pyrolysis technique

K.O. Ukoba*, A.C. Eloka-Eboka, F.L. Inambao

Discipline of Mechanical Engineering, University of KwaZulu-Natal, Durban, South Africa

ARTICLE INFO

Keywords:
Nickel oxide
Nanostructured
Solar cells
Spray pyrolysis technique
Thin film deposition
Metal oxide

ABSTRACT

This study reviews NiO film deposition using the Spray Pyrolysis Technique (SPT). Physical and chemical methods can be used to deposit NiO film. This review looks at different precursors and their characterization methods for spray deposition of NiO thin film. The usefulness of SPT emanates from this method being simple, low cost, and viable for mass production. It gives high product purity for metallic and non-metallic material deposition. Nickel chloride, nickel acetate, nickel nitrate, nickel hydroxide, nickel sulfate, and nickel formate are the major precursors for NiO thin film deposition. Nickel chloride and nickel acetate are the most used and highly available precursors. Unlike nickel acetate, nickel chloride precursors corrode the deposition equipment (spray gun). These precursors are relatively cheap compared to current materials used for solar panels (cells). SPT equipment consumes negligible power during deposition and none after usage. Various authors have investigated the physical, chemical, optical, structural characterization and properties of nanostructured NiO thin film. NiO films are p-type semiconductors and as such possesses direct band gap suitable for various applications. The film has been categorized as an excellent material for optoelectronic applications because of its tune-ability for optimization. The wide band gap is in the range of 3.25–4.0 eV. This review will be useful to researchers exploring solar photovoltaic potentials for solving electricity problems of developing countries.

1. Introduction

About one-fourth of earth's inhabitants lack access to electricity with little or no change of outlook since over forty year now [1]. Several developing countries in Africa and elsewhere are still struggling to deliver affordable and stable electricity [2]. Renewable energy is a viable solution to ending the global electricity problem as it exceeds world electricity demand [3]. Renewable energy includes solar, wind, geothermal, oceanic, hydro, biomass and other energy sources. Solar energy can be converted to useful direct current electricity using solar cells [4]. A major breakthrough in solar cell fabrication would be large scale production at affordable cost [5]. Currently, there is difficulty in scaling up existing method of solar cell fabrication. The major obstacles are the expensive nature of materials and the complexities involved in fabricating solar cells. The Spray Pyrolysis Technique (SPT) is widely used because of its simplicity and affordability [6]. The properties of spray deposited film depend on the substrate, substrate temperatures, spray rate and droplet sizes [7]. Droplet size depends on spray rate, nozzle diameter and carrier gas / carrier gas pressure [8]. Inorganic semiconducting materials are inexpensive, environmentally friendly and viable sources for solar cell fabrication [9]. Fabrication of nanostructure metal oxide films has generated interest over the years due to their wide application [10–16]. They are used in radiation detectors, solar cells, semiconducting devices, laser materials, thermoelectric devices, and optoelectronic devices [17–20]. Nanostructured metal oxide is a promising option for thin film solar cells [21]. NiO is one such metal oxide with many suitable properties. Despite the promising properties of NiO, limited studies have been conducted on it when compared with ZnO and CuO.

1.1. NiO structural properties and applications

Nickel oxide adopts the rock salt form of NaCl, having octahedral Ni (II) and O^{2-} sites (Figs. 1 and 2). As a binary metal oxide, the ratio of Ni:O deviates from 1:1 making it non-stoichiometric most times. NiO stoichiometry is shown by the colour variation [22]. NiO can either be a black or green crystalline powder. Density of NiO is 6.67 g/cm^3 and the melting point is 1955 °C [23]. Nickel chemical composition of NiO is 78.55% while oxygen is 21.40%. It has a molar mass of 74.6928 g/mol. It has magnetic susceptibility of $+660.0{\cdot}10^{-6}$ cm^3/mol. The refractive index of NiO is 2.1818. The toxicity of nickel oxide depends on the quantity inhaled [24]. It exists in various oxidation states. The states

* Corresponding author.
E-mail address: ukobaking@yahoo.com (K.O. Ukoba).

http://dx.doi.org/10.1016/j.rser.2017.10.041
Received 29 March 2017; Received in revised form 14 July 2017; Accepted 26 October 2017
Available online 03 November 2017

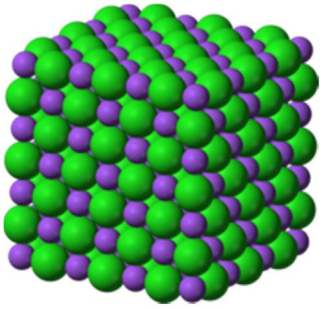

Fig. 1. Crystal structure of NiO [23].

Fig. 2. Pictorial view of NiO.

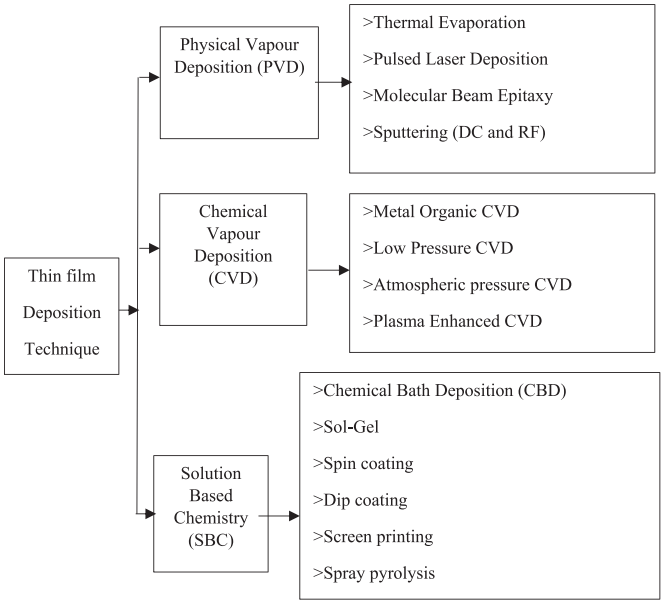

Fig. 3. Classification of thin film deposition methods.

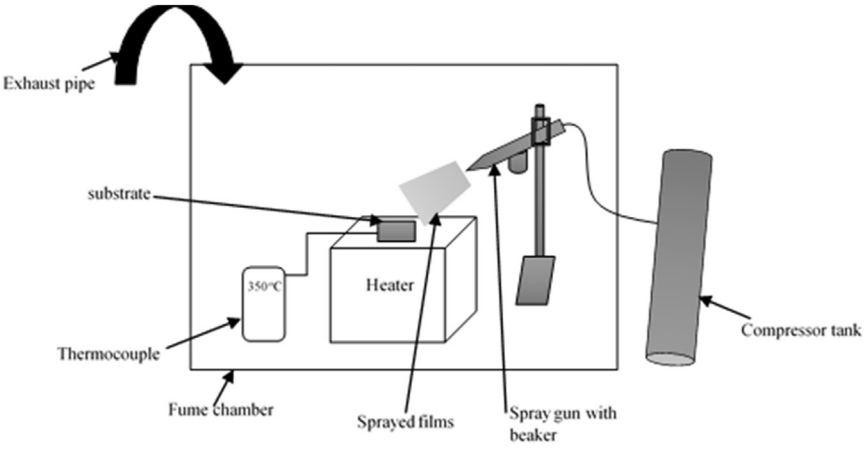

Fig. 4. Experimental set-up of spray pyrolysis technique.

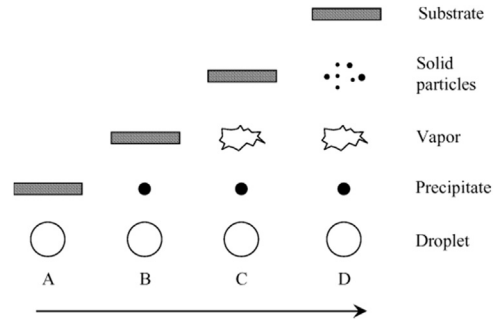

Fig. 5. Deposition processes initiated with increasing substrate temperature [67].

are nickel trioxide or sesquioxide (Ni_2O_3), nickelous oxide (NiO), nickel dioxide (NiO_2), nickelosic oxide (Ni_3O_4), and nickel peroxide (NiO_4). NiO has rhombohedral or cubic structure referred to as Bunsenite. NiO is a p-type semiconductor with a wide band gap between 3.5 and 4.0 eV [25]. NiO finds useful application in solar cells [26] and UV photodetectors [27] due to its high durability and excellent chemical stability. Other applications include electrochromic devices [28], anti-ferromagnetic layers [29], and chemical sensors [30].

Thin film deposition is divided into three groups by means of its nature of deposition as depicted in Fig. 3 [31]. However, this classification was done considering the physical or chemical processes involved. Chemical processes include gas-phase and solution deposition methods. Gas-phase methods include: chemical vapour deposition (CVD) [32], atomic layer epitaxy [33], and atomic layer deposition (ALD) [34]. Solution deposition methods include: spray pyrolysis [35], sol-gel [36], spin [37], and dip-coating [38]. Physical processes include: pulsed laser deposition [39], physical vapour deposition (PVD) [40], molecular beam epitaxy [41], and magnetron sputtering [42]. Other techniques include: chemical bath deposition [43], advanced reactive gas deposition [44], electron beam evaporation [45], vacuum evaporation [46], and anodic oxidation [47]. Different techniques have been employed to deposit nickel oxide thin films. The techniques are RF sputtering [48], electron beam evaporation [49], DC magnetron sputtering [50], and anodic electrodeposition [51]. Cathodic electrodeposition [52] and chemical vapour [53] can also be used for NiO deposition. This study will review NiO films deposited using SPT.

1.2. Spray pyrolysis technique

SPT is classified as a solution based chemistry based on the nature of the deposition. Solution based methods for films deposition are becoming more popular [54]. Solution based methods provide high purity products at low cost, starting from easily available materials. SPT is useful for depositing varieties of thin film. Using SPT, films of very thin

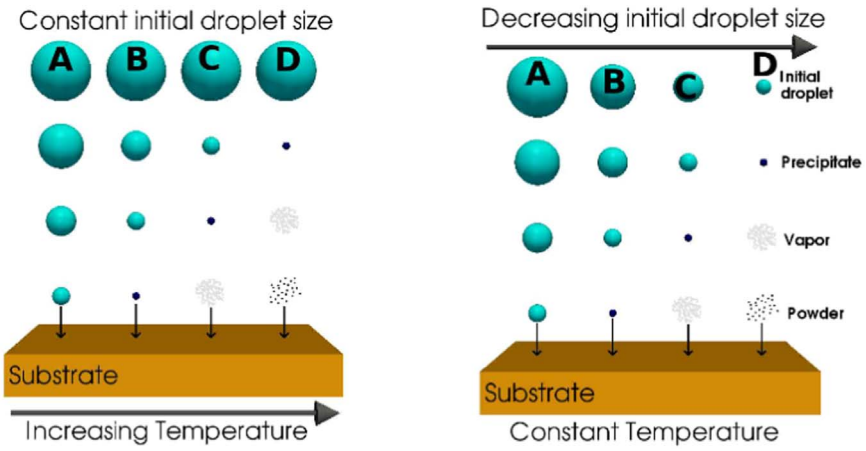

Fig. 6. Schematics of spray pyrolysis droplet modification [74].

Table 1
Effect of volume sprayed on film thickness and properties of NiO thin-films prepared by spray pyrolysis technique [82].

Serial number	Volume of sprayed solution (ml)	Thickness (μm)	Grain size (nm)	Energy Band-gap E_g (eV)	Electrical resistivity at 300k (x 10^4Ωcm)	Activation energy E_a (eV)
1	30	0.028	14	3.58	1.0	0.35
2	40	0.048	14.5	3.55	1.9	0.36
3	60	0.10	15	3.49	3.0	0.38
4	75	0.23	17	3.40	9.0	0.39

Table 2
Values of the grain size (GS) calculated from XRD and AFM investigations [84].

Molar concentration (M)	Grain Size (XRD measurement) (nm)	Average Grain Size (AFM measurement) (nm)
0.05	110.7	115.1
0.075	76	84
0.1	78	80

layers with uniform thickness can be coated on a large area [55]. It can be used to deposit thin and thick films, dense films, porous films, multilayered films, ceramic and powders [56]. It is good for preparing films of any composition [57]. It is also useful in the control of target compositions for high quality products. It allows for fewer precursor

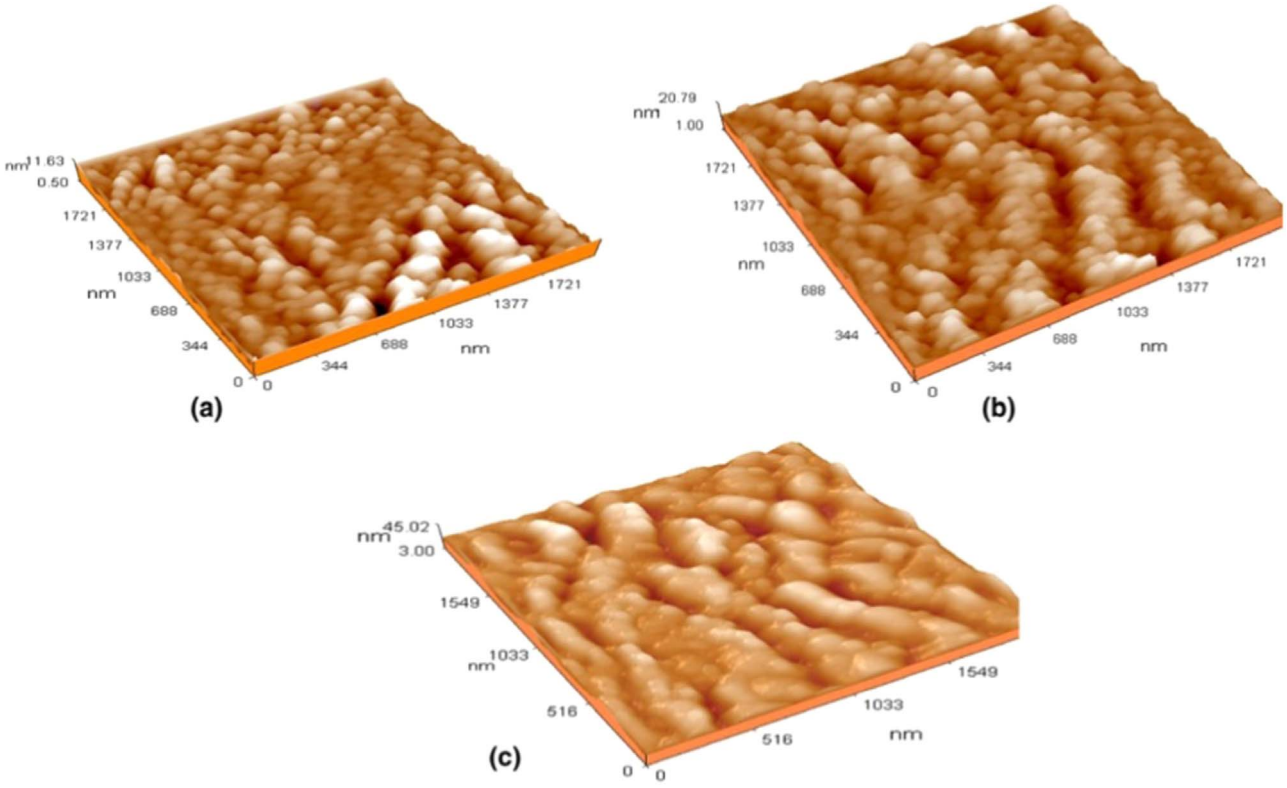

Fig. 7. AFM 3D images of nanostructured NiO thin films a = 0.1 M, b = 0.075 M and c = 0.05 M [84].

Table 3
Structural and optical parameters of NiO thin films [86].

Parameter	Value
Crystalline size (D)	51 nm
Dislocation density	0.038 × 10^{16} lines/m^2
Strain	0.0405
Thickness	161 nm
Refractive index (n) at 550 nm	1.871
Dielectric constant (Ɛ) at 550 nm	3.49
Transmittance (T) at 550 nm	83%
Reflectance (R) at 550 nm	7%
Direct band gap (E_g)	3.25 eV

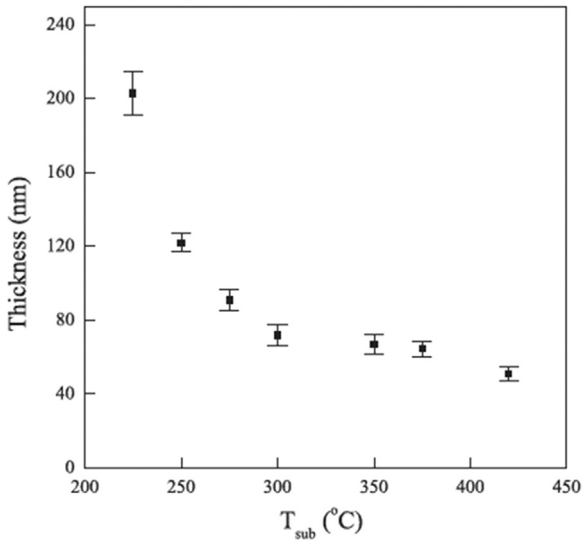

Fig. 8. Variation of film thickness versus substrate temperature [80].

usages for large surface deposition [58]. Optimization of preparative conditions is the main requirement for obtaining high quality films. Such preparatory conditions include spray rate, substrate temperature, concentration, etc. [59].

SPT involves spraying solutions of the film on a heated surface [60]. Thereafter, the film constituents react to form a chemical compound. The chemical reactants are selected so that unwanted products pyrolytically decompose at the deposition temperature [61]. The experimental set-up of a SPT is illustrated in Fig. 4. SPT equipment consists of precursor solution, an atomizer, substrate heat source, and temperature controller. The commonly used atomizers are ultrasonic [62], electrostatic [63], and air blast [64]. Ultrasonic atomizers use ultrasonic frequencies to produce a short wavelength for fine atomization. Electrostatic atomizers expose the liquid to a high electric field for atomization to take place. Air blast atomizers expose the liquid to a stream of air.

SPT is a useful method for the deposition of metal oxides because it is a simple technique with low equipment cost, and requires little maintenance. It does not consume much power compared to vacuum equipment. Also, electricity is not required after using SPT for deposition. The quality and properties of the deposited films depend largely on the process parameters. The substrate surface temperature affects the output of the films. Higher substrate temperatures produce rougher and porous film; but low temperatures give cracked film. Deposition temperature also influences the crystallinity, texture, and other physical properties of deposited film [65]. Precursor solution also affects morphology and properties of deposited film [66]. SPT is grouped into four processes by means of reaction type [67]. Process 1 involves the droplet residing on the surface as the solvent evaporates thereby making the solid react when dry. In Process 2 the solvent evaporates just before the droplet makes contact with the surface. Dry solid impinges on it allowing for decomposition. Process 3 is known as true chemical vapour deposition. Solvent vaporizes as the droplet approaches the substrate. The solid melts and vaporizes. Thereafter, the vapour diffuses to the substrate to undergo heterogeneous reaction. Process 4 occurs in the vapour state. A detailed description of all processes is shown in Figs. 5 and 6.

The droplet has four potential paths before hitting the substrate irrespective of temperature or initial droplet size [68]. This is represented as (A-D) in Figs. 5 and 6. Point (A) is the lowest temperature region. The highest is D while B and C are in-between A and D.

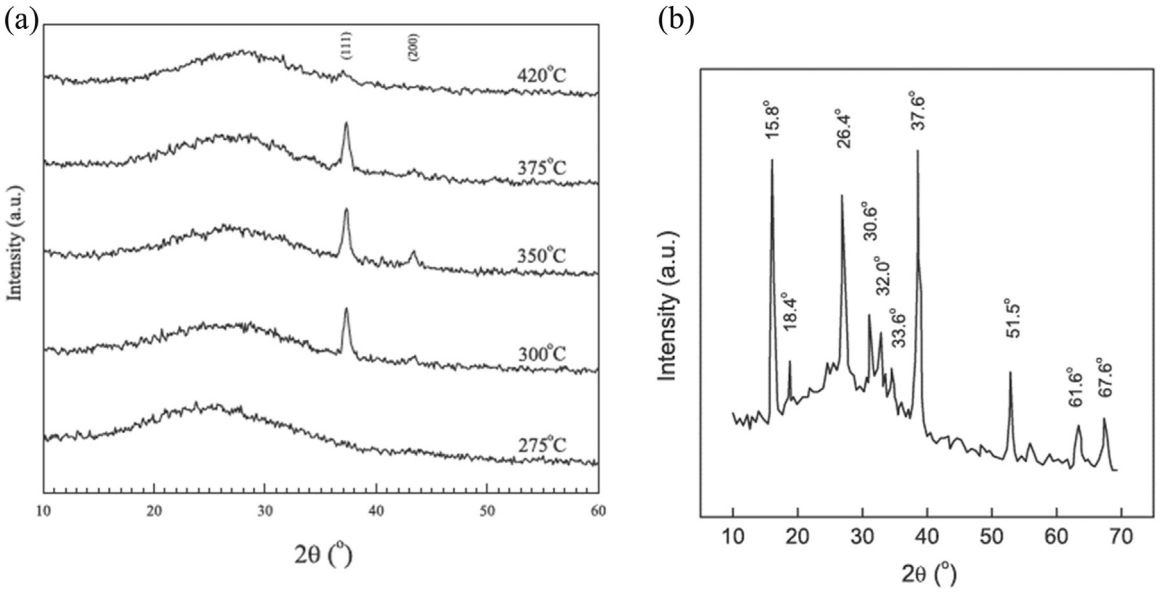

Fig. 9. X-ray diffractograms of samples prepared at: (a) 275 °C to 425 °C (b) 225 °C [80].

Table 4
Dispersion parameters of NiO films at different substrate temperature [92].

T_s°C	ε_L	ε_∞	N/m* $\times 10^{40}$(cm^{-3} g^{-1})	p(HZ) $\times$ 10^8	λ_o	S_o $\times 10^{-13}$ $(m)^{-2}$	E_o (eV)	E_d (eV)	E_g (eV)	E_o/ E_g	M_{-1}	M_{-3} (eV)
350	3.165	3.825	2.309	0.817	263	4.095	5.184	15.748	3.54	1.46	3.04	0.113
400	5.399	4.578	5.823	1.298	279	4.599	5.133	19.619	3.43	1.49	3.82	0.145
450	5.916	4.662	6.129	1.772	286	4.470	5.074	19.946	3.37	1.50	3.93	0.153

Table 5
Variation of substrate temperature with film thickness and bandgap energy [95].

Substrate temperature (°C)	Thickness (nm)	Bandgap Energy, E_g (eV)
425	280	3.25
450	350	3.04
475	310	3.16
500	275	3.28

Processes A and D give rough or non-adherent films. Adherent films are rarely obtained in process C if spray pyrolysis is used. It is caused by low deposition temperature for the precursor vaporization. It can also be caused when the precursor salt decomposes without melting and vaporization.

Chamberlin and Skarman [69] performed the first spray pyrolysis experiment involving CdS films. This paved the way for more studies on SPT [70–73]. Spray pyrolysis has the merit of cost effectiveness and high quality coating. Also, complex geometries can be coated using spray pyrolysis. SPT requires low temperatures during processing [74]. Most of the equipment used for thin film deposition is expensive [75] and is vacuum-based [76]. The equipment requires steady and high usage of power which is a major challenge in most developing countries especially Africa which are target beneficiaries/end users. This has hindered research in solar cell development, discouraging low cost production of solar devices.

SPT equipment requires low capital investment, and requires little or no maintenance. Power supply does not affect equipment storage. These advantages make SPT a good deposition method in thin film development. A comprehensive review of SPT deposition of NiO film is unavailable in the literature despite NiO's promising properties [77]. This study reviews nanostructured NiO film deposited using SPT. The different precursors used for depositing NiO films will be examined. This study will help to identify viable precursor(s) for NiO films deposition. The aim is to identify a deposition method and material suitable for solar cell research in developing countries. The emphasis is on efficiency, cost, durability and chemical stability.

2. Literature survey

Deposition of nanostructured NiO can be achieved in two major procedures. The bottom-up procedure is a chemical method. This includes sol-gel, spray pyrolysis, thermolysis, and micro emulsion. The top-down procedure is a physical method. This includes pulsed laser ablation, chemical vapour deposition, and electro-deposition [78]. NiO has been successfully deposited using various precursors which are discussed below.

2.1. Nickel chloride precursors

Nickel chloride salts are commonly used as precursors in deposition and preparation of NiO thin film [79]. The pyrolytic decomposition for NiO film formation for a chloride precursor is given in Eqs. (1)–(3):

$$Ni(Cl_2)+2NH_4OH \xrightarrow{\Delta} Ni(OH)_2+2NH_4Cl_2 \rightarrow NiO \quad (1)$$

$$NiCl_2 : 6H_2O \xrightarrow{heat} NiO+2HCl\uparrow + 5H_2O\uparrow \quad (2)$$

$$NiCl_2+2H_2O \xrightarrow{heat} 2HCl + Ni(OH)_2 \quad (3)$$

Uniform nickel oxide NiO with good adherence is formed when aqueous nickel chloride is sprayed on a preheated substrate. Formation of fine droplets occurs because of pyrolytic decomposition when droplets make contact with the hot surface. The major merit of this

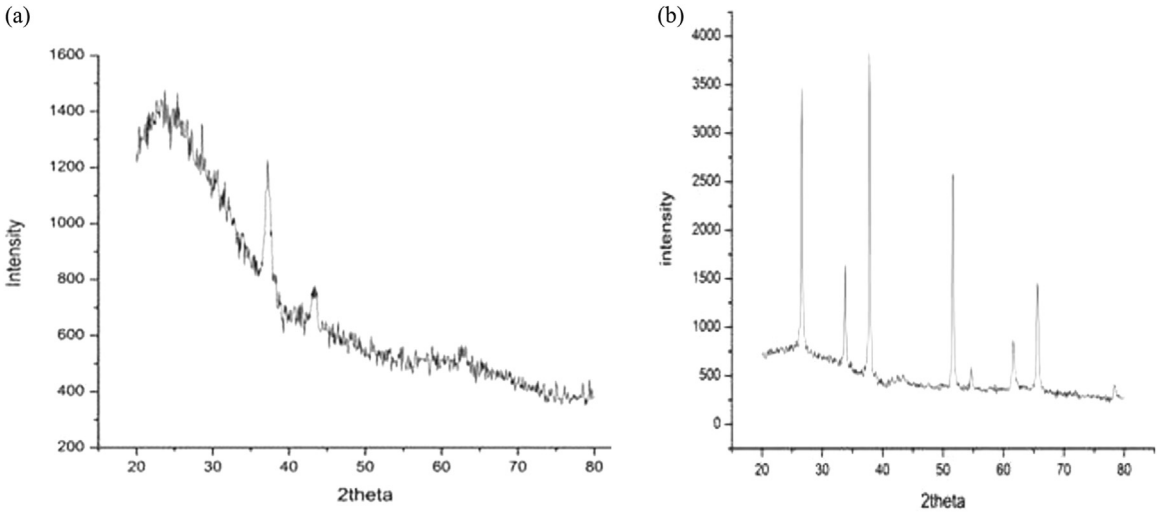

Fig. 10. X-ray diffraction pattern of nickel oxide thin film onto (a) glass substrate (b) FTO [96].

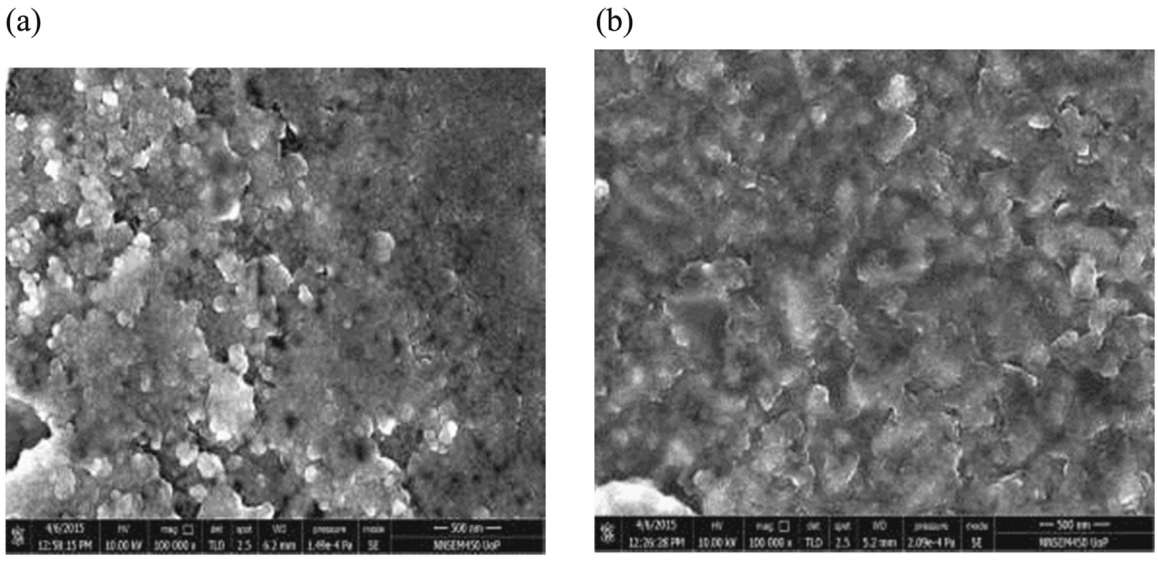

Fig. 11. Scanning electron micrographs of nickel oxide thin film using (a) glass and (b) FTO substrates [96].

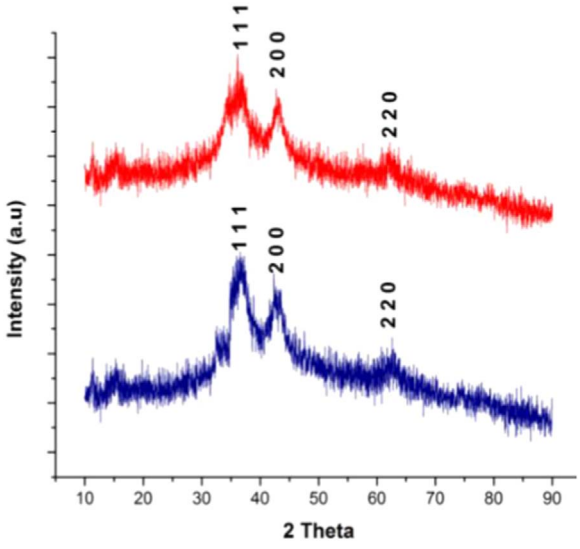

Fig. 12. X-Ray diffractograms of 24 h aged and freshly prepared NiO thin films [98].

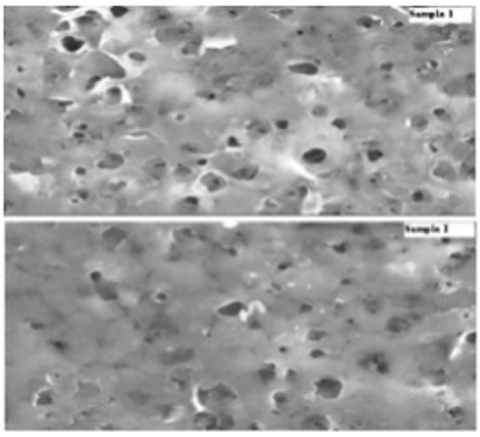

Fig. 13. SEM images of aged and freshly prepared NiO thin films [98].

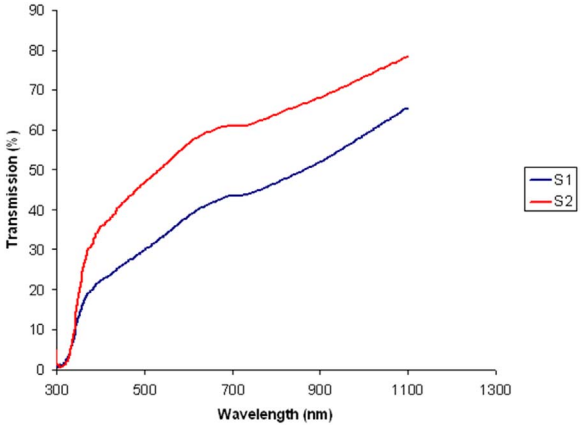

Fig. 14. Transmission spectra of aged and freshly prepared NiO thin films [98].

precursor is the availability of the precursor. The demerit is incomplete pyrolytic decomposition, producing HCl in the final product [80].

Patil and Kadam [81] studied the effect of volume of sprayed solution on the properties of NiO. This was achieved by depositing 0.05 M solution of nickel chloride precursor. An amorphous glass substrate was used at 350 °C at 8 ml/min spray rate. The sprayed volumes were 30 ml, 45 ml, 60 ml and 75 ml. The study revealed that film thickness grew from 0.028 to 0.23 μm as volume of sprayed solution increased. This was not directly proportional as a result of the variation in deposition efficiency. The study attributed this to the diminished mass transport of substrate and gas convection which pushed the droplets off the precursor. The optical band gap was found to decrease from 3.58 to 3.4 eV as film thickness increased. The grain size varied from 14 nm to 17 nm as sprayed solution volume grew from 30 ml to 75 ml. This is depicted in Table 1. The study also observed that the absorption coefficient decreased with reduction in photon energy. A sharp decrease was noticed around the band edge in the visible region as the absorption coefficient for the sample is of the order of 104 cm^{-1}. Infrared spectroscopy (IR spectroscopy) of the film indicated the presence of a NiO phase with some amount of hydration and chloride ions. The thermo-emf measurement showed that NiO films were of p-type.

Kadam and Patil [83] studied the electrochromic properties of

Table 6
Electrical properties of aged and freshly prepared NiO thin films [98].

Solution	Thickness (nm)	Mobility, μ (cm^2/Vs)	Conductivity, σ (1/Ωcm)	Resistivity, ρ (Ωcm)	Hall coefficient, R_H (cm^3/C)	Type
Non-aged	631	14.73	4.409×10^{-3}	2.271×10^{2}	3.342×10^{3}	p
Aged	676	11.715	3.669×10^{-3}	2.725×10^{2}	3.193×10^{3}	p

nickel oxide thin films prepared by SPT. A mixture of 0.05 M, 50 ml of nickel chloride in distilled water was sprayed at a rate of 10 ml/min. Fluorine-doped tin oxide (FTO) glass substrate with sheet resistance of 10 Ωcm^{-2} was deposited at a temperature of 350 °C. The study recorded a cubic NiO film with orientation of (1 1 1). The surface morphology revealed complete covering of substrate with non-uniform thin film. The study attributed micro-cracks, developed in the film, to be as a result of evaporation of water from the film. Infrared spectroscopy confirmed free hydroxyl ion and water presence in NiO thin film.

Ismail et al. [84] studied the effect of varying molarity and deposition temperature on NiO film properties. Molarity was varied from 0.025 M, 0.05 M, 0.075 M and 0.1 M while the deposition temperature was from 280 °C, 320 °C, 360 °C and 400 °C. This was achieved by depositing AR grade ($NiCl_2.6H_20$) using SPT. The substrates used were single crystal silicon and corning glass. The study attributed the uniform thin film achieved to well optimized deposition parameters. It kept the spray nozzle at a height of 35 cm, rate of spray of 15 cm^3/min and period between spray of 1 min. The study recorded a cubic crystalline peak at 400 °C. However, amorphous films were achieved at 0.025 M and a temperature of 280 °C. There was complete disappearance of the (2 0 0) plane at 350 °C. A single diffracted peak along the (1 1 1) plane was obtained at 360 °C. The substrate temperature grew from 350 °C to 400 °C with increased plane intensity (1 1 1). A weak reflection plane was noticed along the (200) plane at 2θ = 43°. The lattice constant was 0.417 nm in the (111) plane. This agrees with the data from JCPDS file #04–0835 for bulk silicon substrate. The films were polycrystalline with preferential orientation along the (2 0 0) plane. The film's thickness varied between 0.215–0.91 μm. The Atomic Force Microscope (AFM) 3D images shown in Fig. 7 gave a homogeneous and smooth morphology of the deposited NiO film. Root mean square (RMS) roughness and the crystallite size of the film decreased with increasing molarity. The study attributed this to columnar grain growth in the structure.

There is no marked difference between the results obtained for crystallite size from the AFM and the XRD. This is tabulated in Table 2.

In Ismail et al.'s [84] study, FT-IR spectrum was conducted at 400 °C and 0.075 M in the range of 400 cm^{-1} to 2000 cm^{-1}. Bands were obtained at 611.43 cm^{-1}, 875.65 cm^{-1}, 1422 cm^{-1}, 1745 cm^{-1}, 3776 cm^{-1}. Other bands revealed that the sample contains water molecules and/or hydroxide ions. Their presence in the IR spectrum was attributed to water absorption. Other molar concentrations showed the same absorption peaks but with lower intensities with the band at 1300 cm^{-1}. This was attributed to the bending vibration of water molecules caused by absorbed moisture. Transmittance showed that the films have high transparency in visible and near IR regions. There was insignificant difference in optical transparency at different molarities. The optical confinement effect was around 325 nm at 0.075 M. Molarity changed from 0.1 to 0.05 M as the optical band gap changed from 3.4 to 3.8 eV. This was attributed to a decrease in molarity of the film with increasing crystallite size. This shows dependence on the film stoichiometry [85]. The study attributed the large optical band gap value to quantum size effect. Electrical resistivity of the deposited NiO films grew as concentration increased.

Vigneshkumar et al. [86] focused on the antireflection coating of NiO thin films in solar cells. NiO films were deposited on glass substrate using a 0.5 M aqueous solution of nickel chloride at a temperature of 350 °C. Spray rate of 1 ml/min, substrate to nozzle distance of 18 cm and filtered compressed air as the carrier gas at a pressure of 1 bar were maintained. The samples were annealed at 500 °C for one hour using a muffle furnace. The XRD pattern gave two dominant peaks at 2θ = 31.74° and 37.27° assigned to the (3 1 1) and (1 1 1) crystal planes respectively. Less intense peaks were recorded at 43.32°, 62.93° and 79.45° assigned to (2 0 0), (2 2 0) and (2 2 2) crystal planes respectively. These peaks are similar to standard Bunsenite (NiO) peaks identified by JCPDS with file No. 78–0643. Strong peak intensity shows a high degree of crystallinity of the phase. Other structural and optical parameters obtained are shown in Table 3.

A reflectance of 7% was obtained at 550 nm. This low value gives an indication that it can be used as an anti-reflection coating material in solar cells. The refractive index was recorded to be 1.871 at 550 nm. Calculated optical direct band gap energy of the prepared NiO thin film was found to be 3.25 eV, which agrees with the reported band gap values of 3.15–3.80 eV for NiO films [87]. Photoluminescence (PL) spectrum was obtained at room temperature with an excitation wavelength of 325 nm. Two emission peaks were observed at 445 nm and 490 nm. The emission peaks were recorded at an energy band gap of 2.78 eV and 2.53 eV respectively. The peak of 445 nm was attributed to oxygen related defects as previously reported by Wang et al. [88]. This was observed in the visible region and also originates from the electronic transition of Ni^{2+} and O^{2-} ions. The study was able to demonstrate that p-type NiO thin film deposited using nickel chloride precursor by SPT is suitable for anti-reflection coating in solar cells.

Kamal et al. [80] focused on substrate temperature as it affects the properties of SPT deposited NiO thin films. This was achieved by depositing NiO films using 0.1 M aqueous solution of nickel chloride by SPT. A glass substrate was used. The deposition temperatures were 225 °C, 250 °C, 275 °C, 300 °C, 350 °C, 375 °C and 420 °C. The substrate to nozzle distance was 40 cm; a deposition time of 40 s, and flow rate of 15 cm^3/min were maintained to achieve uniform films. An increment in substrate temperature gave reduction in film thickness as shown in Fig. 8. This was attributed to possible re-evaporation of the film after deposition. Thermal convection of the sprayed droplets during the deposition was also thought to be responsible for this phenomenon. Film thickness reduction was attributed to water loss or interlayer removal. This resulted in formation of compact NiO film as reported by Mahmoud et al. [89].

Fig. 9 shows diffractograms for the substrate temperatures of 275 °C to 425 °C and 225 °C. There was no peak diffraction at a substrate temperature of 275 °C for the amorphous structure. The study observed that the NiO film turned white when it was in contact with air. This was attributed to absorption of moisture. The analysis of the dried samples confirmed the presence of hydrated nickel chloride $NiCl_2{\cdot}6H_2O$ which tallies with card number ICDD 25–1044. Further analysis showed that the pyrolytic reaction was not favourable at the temperature of 225 °C.

The NiO film formed crystallite at temperatures of 275 °C at 2θ = 37.5 °C. However, at a temperature above 275 °C, it was 2θ = 42.8 °C. This conforms to standard card number ICDD 78–0643 of the NiO structure. The peaks were attributed to a cubic crystalline structure with preferred orientation along the (1 1 1) plane. The study calculated lattice parameters of average a = b = c = 0.417 nm agreed with the bulk value of NiO [90]. This revealed that annealing of Ni_2O_3-like films above 300 °C gives transformation to NiO. XRD analysis of the deposited $3Ni(OH)_2{\cdot}2H_2O$ prepared by solution growth turned to nickel oxide, $NiO.xH_2O$, after annealing from 300 °C to 400 °C for 48 h [91].

Table 7
Dispersion parameters of NiO films at different substrate temperature [101].

T_s°C	ε_L (± 4× 10-3)	ε_∞(± 6× 10^{-3})	N/m*(cm^{-3} g 1) (± 3× 10-2)	ω_p(HZ) (± 4× 10^{-3})	λ_o (nm) (± 4)	S_o $(m)^{-2}$ (×10^{-13})	E_o (eV)	E_d (eV)	E_g (eV)	E_o/ E_g	M_{-1}	M_{-3} (eV)
225	3.34	3.35	6.25× 10^{40}	9.9×10^8	172	3.4 × 10^{14}	7.50	17.7	3.83	1.95	2.36	0.047
250	3.38	3.72	2.54× 10^{41}	4.03×10^9	205	3.03× 10^{14}	6.95	18.5	3.66	1.89	2.66	0.055
275	3.42	3.93	3.11× 10^{41}	4.94×10^9	222	2.92× 10^{14}	6.43	19.0	3.46	1.85	2.95	0.071
300	3.46	4.22	3.27× 10^{41}	5.20×10^9	232	3.05× 10^{14}	6.1	19.2	3.30	1.85	3.14	0.084
350	3.54	4.34	5.49× 10^{41}	8.72×10^9	245	2.96× 10^{14}	5.74	19.4	3.17	1.81	3.38	0.102

Optical constants were calculated from 300 nm to 2500 nm. Refractive index was affected slightly by the substrate temperature. The substrate temperature influenced the deducted direct and indirect energy gaps obtained in the thin films. Dark electrical resistivity ρ dropped greatly (two orders) for 250 ≤ T_s ≤ 300 °C. It also decreased (one order) in the range of 300 ≤ T_s ≤ 400 °C to attain a bulk value of 10 Ωm. This was attributed to improvement in crystallinity. Temperature of 275 °C gave excellent and reversible electrochromic behaviour at ΔTv ≈ 35% showing formation of nickel oxide. At a temperature above 275 °C lower visible modulation of ΔTv ≈ 20% was observed. The study drawback was the presence of HCl as confirmed by the infrared spectral reflectance representing incomplete pyrolytic reaction of the films.

Gowthami et al. [92] deposited a 0.3 M aqueous solution of nickel chloride on a glass slide using SPT. The aim was to evaluate the oscillator parameters (optical dispersions) of the NiO thin film. The substrate temperatures were varied from 350 °C, 400 °C and 450 °C. The emphasis was on optoelectronic devices which make use of semiconductor thin films and interference devices. Optical dispersion was considered because it reveals information useful in determining microscopic characteristics. Nozzle to substrate distance of 7 cm, volume of 0.5 ml per min and an optimized airflow of 1.2 kg/cm^2 were maintained. Optical transmittance spectra for the NiO films were recorded from 300 nm to 1100 nm wavelength. The film thickness grew as the transmittance decreased. Variation of transmittance was from 30% to 90% as the film thickness decreased. Direct band gap was found to be 3.54 eV, 3.43 eV and 3.37 eV. This agreed with the reported band gap of 3.15–3.80 eV for NiO by Sato et al. [93]. A vital factor in optical materials design is the refractive index (η*). It shows higher efficiency optical materials because of similarity with the electronic polarization of ions and the local field in the materials. This is shown in Eq. (4) [94].

$$\eta^* = \eta - ik \tag{4}$$

The complex shown in Eq. (4) can be computed using Eqs. (5) and (6)

$$\eta = \left(\frac{1+R}{1-R}\right) - \sqrt{\frac{4R}{(1-R)^2} - k^2} \tag{5}$$

$$k = \frac{\alpha\lambda}{4\pi} \tag{6}$$

Where, R is reflectance of the film and λ is the wavelength of the incident beam. All samples had maximum value of refractive index (n ≈ 2.8 at T_s = 450 °C) at very low wavelength of 300 nm (strong absorption region). The refractive index had a higher value at very low wavelength (strong absorption). This was as a result of the quality between the frequency of incident electromagnetic radiation and the plasma frequency of electrons, causing coupling of electrons in NiO films to the oscillating electric field. A better surface homogeneity of deposited NiO films was seen in the visible region. Increased substrate temperature resulted in increased refractive index (imaginary part, k). This was attributed to roughness of the film surface. This enhanced the scattering losses that resulted in reduction of the transmitting ability of the films. Optical transmittance spectra decreased as the substrate temperature grew. In general, the index of refraction is higher for shorter wavelengths of light and decreases monotonically with increasing wavelength. The crystalline material experienced a higher refractive index than the amorphous film. This was due to the lower atomic density of each element in the amorphous state caused by the higher average interatomic distance. Therefore, optical constants of NiO thin films were influenced by the substrate temperature (T_s). Optical absorption parameters, such as optical dispersion energies were calculated under the effect of substrate temperature. These optical constants correlated between obtained data and reported values. They are shown in Table 4.

Yadav and Chavan [95] studied the influence of substrate temperature on various physical and electrochemical properties of NiO thin

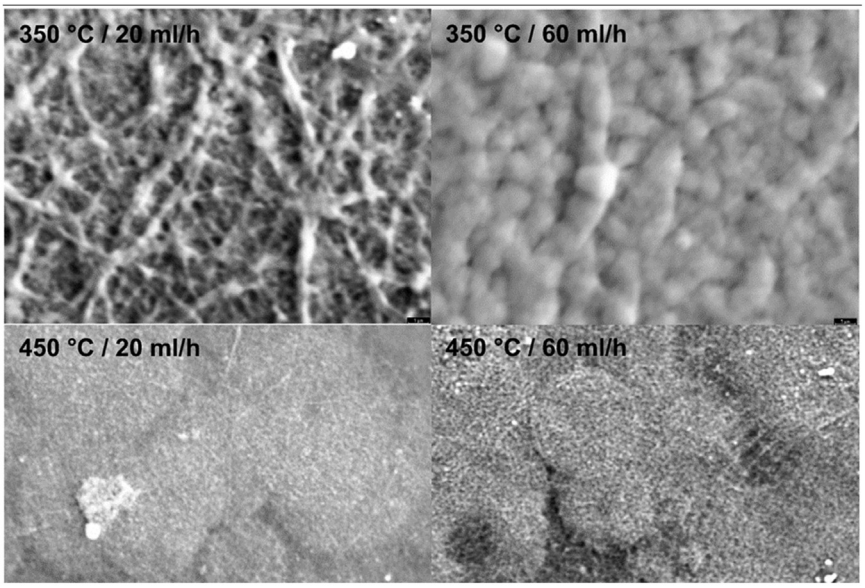

Fig. 15. SEM pictures at a magnification of 5000 of the NiO films sprayed for 30 min onto glass substrates heated to 350 °C (top) and 450 °C (bottom) for the situations of 20 ml/h (left) and 60 ml/h (right) precursor solution flux [102].

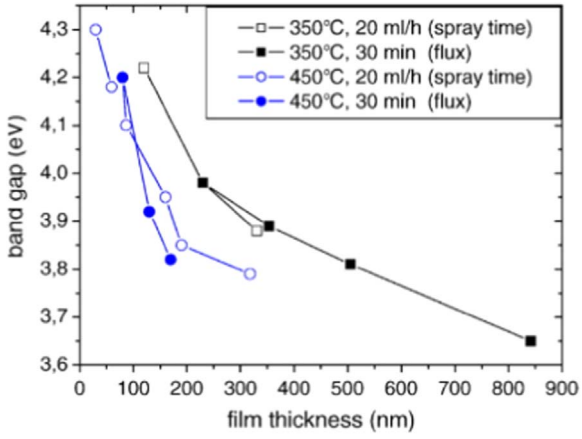

Fig. 16. NiO band gap values for both substrate temperatures versus film thickness for increasing precursor solution flux at a fixed spray time of 30 min and for increasing spray time at a fixed precursor solution flux of 20 ml/h [102].

films. This was achieved by spray depositing NiO thin films using nickel chloride precursor. The thin films were deposited at temperatures of 425 °C, 450 °C, 475 °C and 500 °C. The structural analysis confirmed cubic polycrystalline nickel oxide. The surface morphology revealed a porous surface with inhomogeneous randomly shaped heaps. Optical band gap energy was found to be in the range of 3.04–3.28 eV. The electrical resistivity confirms the semiconducting behaviour of NiO with room temperature activation energies of 0.30–0.38 eV. Other observed results are tabulated in Table 5. From the study, it was seen that substrate temperature has an effect on the physical and electrochemical properties of NiO thin film.

Devasthali and Kandalkar [96] used NiO thin film electrodes for a super capacitor. This was achieved by using two different substrates (glass and fluorine-doped Tin Oxide FTO). A nickel chloride precursor of 0.05 M was deposited at 623 K. The substrates were cleaned by first boiling in chromic acid for 10 min and then cleaned ultrasonically. The spray rate was 4 cm^3/min and nozzle to substrate distance was 28 cm. The XRD pattern is shown in Fig. 10. The film deposited on glass substrate was amorphous in nature while FTO film was polycrystalline. The

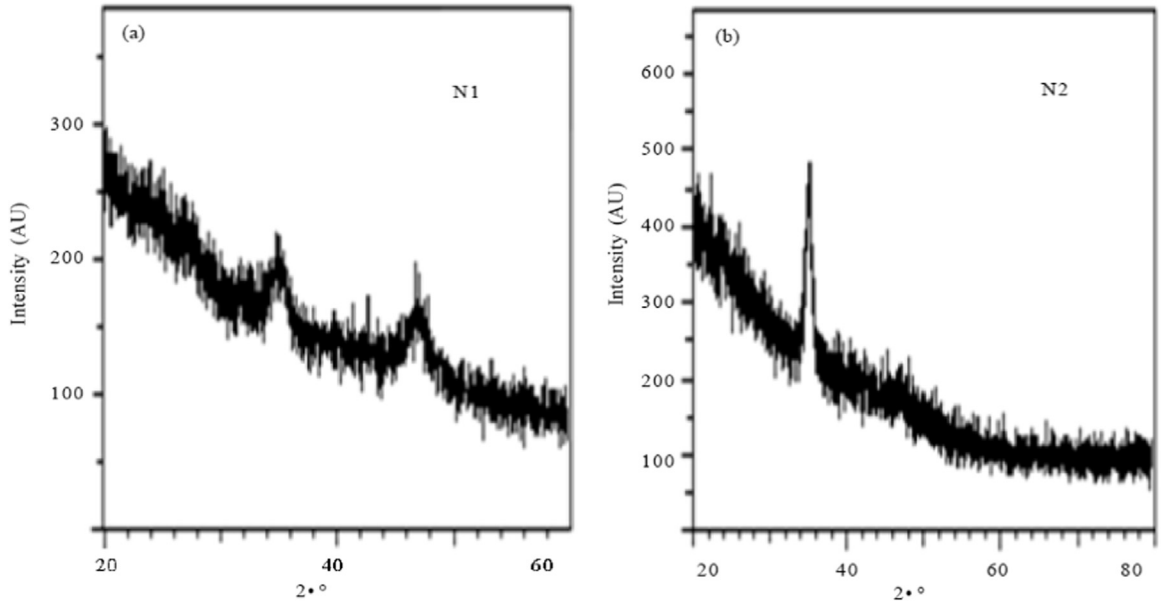

Fig. 17. XRD pattern of NiO films with (a) nickel acetate (b) nickel chloride precursor [104].

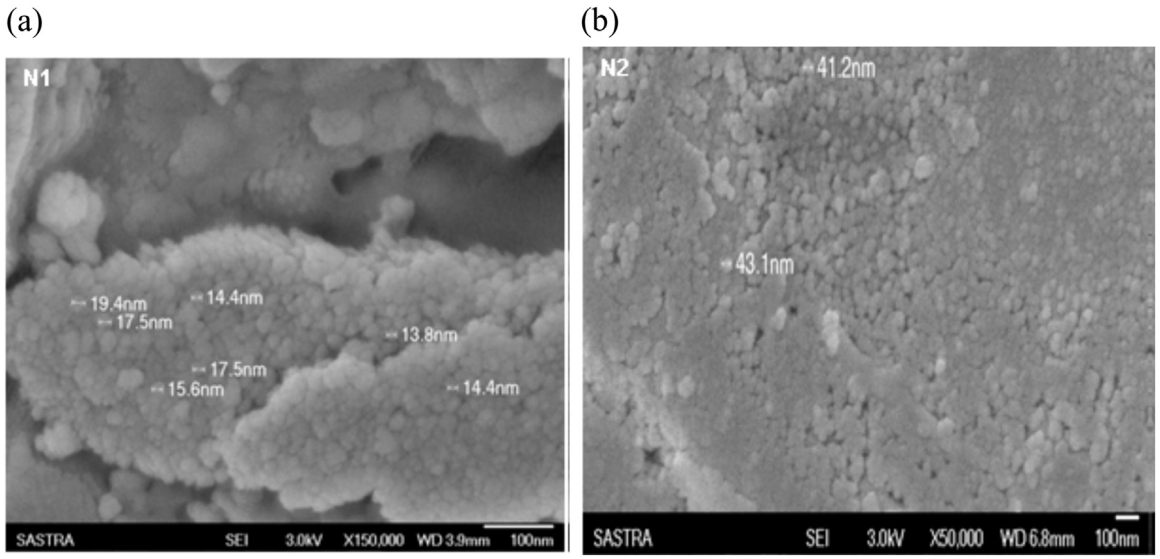

Fig. 18. SEM micrograph of NiO films (a) Nickel acetate (b) Nickel chloride precursors [104].

major XRD peak reflection was along the (1 1 1) plane and the other peak corresponding to the (2 0 0) plane was observed at lower scattering intensity.

Fig. 11 shows the SEM images of spray deposited NiO thin film on glass and FTO substrate respectively. Overgrown clusters were observed in the smaller grains. The average grain size of the NiO was found to be 120 nm from the SEM micrograph. The surface of the film was evenly covered with no cracks and pinholes.

2.2. Nickel acetate precursors

Nickel acetate tetrahydrate precursors have been reported to decompose in a two-step process [97]. The first step is by dehydration from 95 °C to 150 °C as shown in Eq. (7). Secondly, through decomposition of the acetate between 300 °C and 350 °C as shown in Eq. (8). The overall reaction process is expressed as decomposition of nickel acetate to clusters of nickel oxide in the presence of water and air oxygen.

$$Ni(C_2H_3O_2)_2.\ 4H_20 \xrightarrow{heat} Ni(C_2H_3O_2)_2 \tag{7}$$

$$Ni(C_2H_3O_2)_2 \xrightarrow{heat} NiO{+}3H_2O\uparrow + 4CO_2\uparrow \tag{8}$$

Sriram and Thayumanavan [98] studied the effect of ageing on NiO thin films. The study compared a freshly prepared NiO film with a 24 h aged thin film. The films were prepared using a 0.1 M solution of nickel acetate tetrahydrate. This was mixed in a mixture of ethanol and deionized water. The freshly prepared sample was sprayed immediately after preparation onto a glass substrate. The aged solution was left for 24 h after preparing before depositing. A volume of 50 ml was used for both films. The films were deposited at a temperature of 330 °C using air as a carrier gas. The temperature was selected since it is within the decomposition temperature of acetate. X-ray diffractograms of the freshly prepared and aged solutions of the deposited NiO thin films are shown in Fig. 12. The peaks were recorded at 2θ = 35.94, 42.67 and 62.18 for the freshly prepared solution (shown in blue). The aged solution (shown in red) were recorded at 2θ = 36.362, 43.43 and 62.58, which correspond to the (111), (200) and (220) crystal planes respectively. The XRD corresponds with the bunsenite structure of standard NiO cubic structure depicted with JCPDS card no. 89-7130.

The average particle size was 21 nm for the freshly prepared and 60.3 nm for the 24 h aged solution. The surface morphology is shown in Fig. 13. The films were well formed, adhered properly with the substrate and were devoid of cracks. The aged solution had greater grain size than the freshly prepared films.

The freshly prepared and 24 h aged absorption edge was found to be 350 nm. The transmission spectrum is shown in Fig. 14. It was observed that the freshly prepared (sample 1) transmittance is greater than the aged solution. The optical band gap for freshly prepared solution was 3.6 eV and for aged was 3.5 eV. This optical band gap decrease resulted in grain size increment. The study attributed this to ageing of the precursor solution. The calculated refractive index (η) was done using PUMA software created by Birgin et al. [99]. The freshly prepared solution had an equal refractive index in the visible region of 1.95. This value is lesser than the 2.12 obtained using the electron beam physical vapour technique [100]. However, the aged solution refractive index decreased up to 400 nm and remained constant at 1.77. Extinction coefficient varied in the UV region for both films. It was almost constant in the visible and near infrared (NIR) region for both aged and freshly prepared solutions. The electrical properties of the aged and freshly prepared NiO thin films are shown in Table 6. The NiO films were confirmed as p-type by Hall effect measurement. Therefore, ageing has an effect on NiO thin films properties.

Mahmoud et al. [101] investigated the effect of varying substrate temperatures on the structural and optical dispersion properties of NiO films. Nickel acetate of 0.05 M solution in ethanol was deposited using SPT. This was done at a substrate temperature of 225 °C to 350 °C on an ultrasonically cleaned glass substrate. The nozzle diameter was 0.7 mm, deposition time was 15 s and spraying period was 3 min. The height of the spraying nozzle was maintained at 35 cm. In addition, the rate of spraying was kept at 15 cm^3/min in order to achieve a homogeneous film. A thermocouple was used for measuring the temperature. The XRD pattern gave amorphous films at low substrate temperature of 225 °C. A cubic single phase structure was formed at above 275 °C with preferential growth along the (1 1 1) plane. The AFM 3D images gave fine surface of 45 nm thickness with mean grain size of 3.9 μm^2. Refractive index is dependent on substrate temperature and film thickness. The highest refractive index was recorded at $\lambda > 400$ nm for all the samples. The optical band gap was 3.83 eV for 225 °C and 3.14 eV for 350 °C. The film thickness reduced with increasing substrate

temperature. The film thickness was 200 nm at substrate temperature of 225 °C and at 350 °C it was 40 nm. Other dispersion parameters are shown in Table 7. The dielectric constants of ε_∞ and ε_∞, increased with increasing substrate temperature, T_s. The dispersion energy, E_o reduced with increasing substrate temperature T_s. NiO thin films properties are influenced by the substrate temperature.

Romero et al. [102] investigated the effect of substrate temperature and precursor solution flux on the properties of NiO films. The precursor solutions flux was 20 ml/h, 40 ml/h and 60 ml/h. The substrate temperatures were 350 °C and 450 °C. Nickel acetate was deposited in an open atmosphere with air as carrier gas on glass substrate. Reticular tissue-like film morphology was obtained at 350 °C. Film got thicker with increasing precursor solution flux. The surface morphology is shown in Fig. 15. The film became 4 times slower in growth at substrate temperature of 450 °C. Also, there was a highly symmetric self-ordering of the material at nanometer length scale at a temperature of 450 °C. The films consist of interconnected grains separated by pores, both of about 100 nm in size. A cubic crystallite size of 10 nm was obtained for the NiO thin films. There was a reduction in optical band gap as the film thickness increased from 4.3 to 3.65 eV. This is shown in Fig. 16.

Desai et al. [103] researched large area NiOx thin films with a focus on optimization of the preparative parameters. Preparative parameters were substrate temperature, solution concentration, spray-nozzle distance to substrate. The study used a temperature range of 330 °C to 420 °C. Nickel acetate was deposited using spray pyrolysis technique using Sn doped In_2O_3 (ITO) coated glass as substrate. The structural studies showed formation of cubic NiO. The XRD gave a bunsenite phase of NiO. The optical absorption studies gave direct band gap of

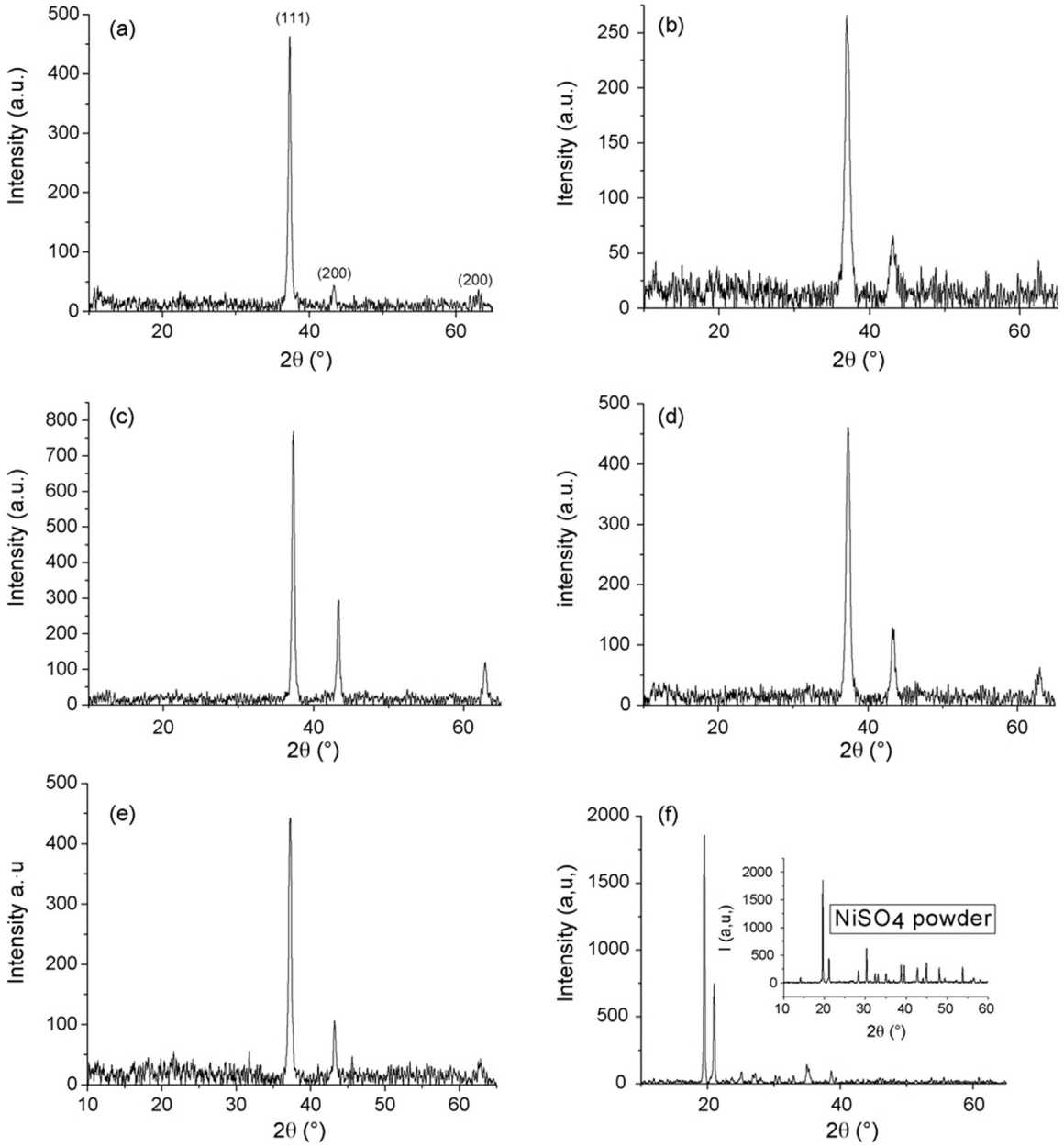

Fig. 19. XRD diffractograms of NiO films deposited with different precursors: (a) $NiCl_2{\cdot}6H_2O$ 0.1 M (b) $Ni(NO_3)_2{\cdot}6H_2O$ 0.1 M (c) $NiCl_2{\cdot}6H_2O$ 0.3 M (d) $Ni(NO_3)_2{\cdot}6H_2O$ 0.3 M (e) $Ni(OH)_2{\cdot}6H_2O$ 0.3 M (f) $NiSO_4{\cdot}4H_2O$ molarity 0.3 M (Cattin et al., 2008) [105].

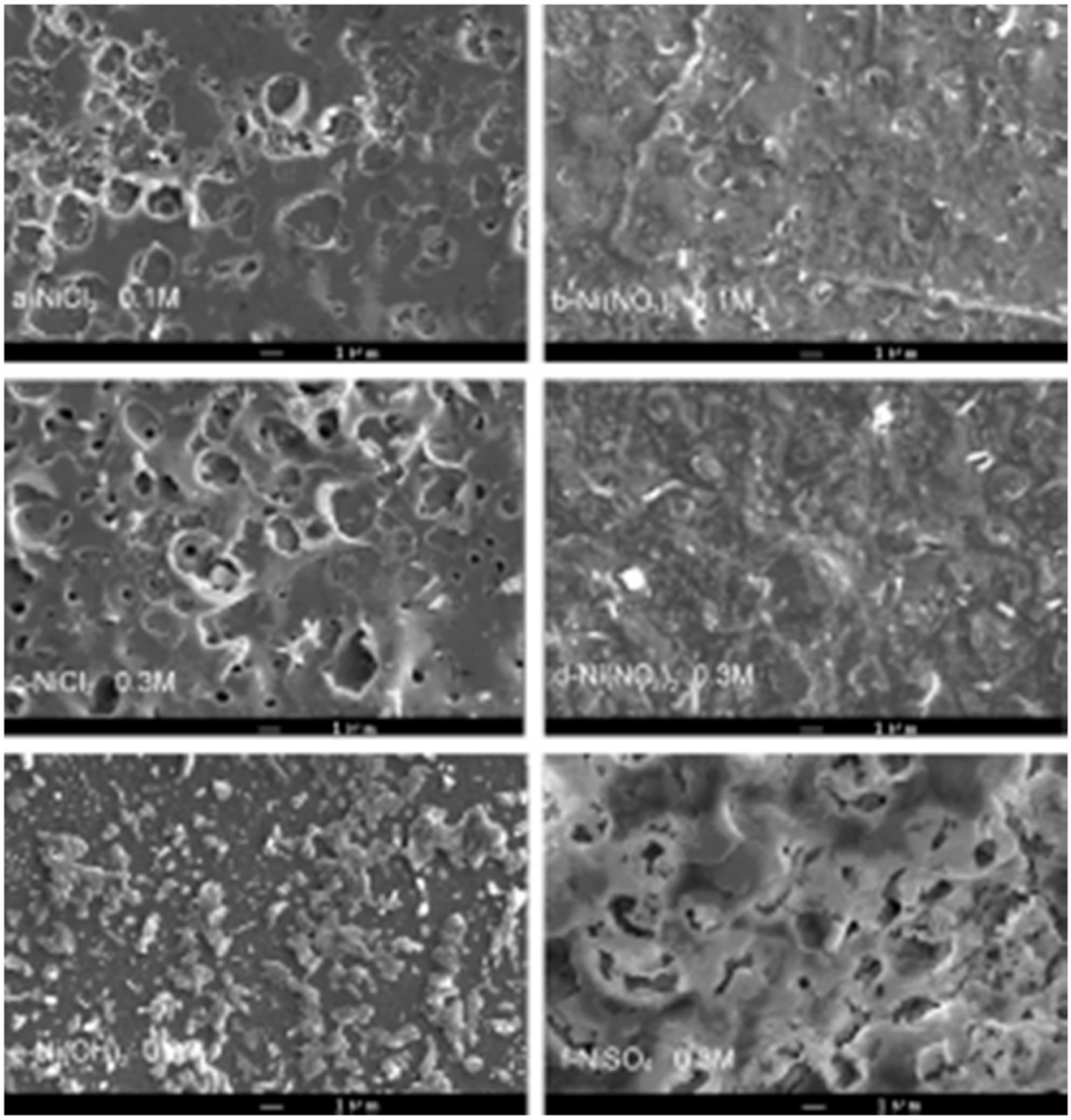

Fig. 20. SEM images of NiO films deposited with different precursors: (a) $NiCl_2{\cdot}6H_2O$ 0.1 M (b) $Ni(NO_3)_2{\cdot}6H_2O$ 0.1 M (c) $NiCl_2{\cdot}6H_2O$ 0.3 M (d) $Ni(NO_3)_2{\cdot}6H_2O$ 0.3 M (e) $Ni(OH)_2{\cdot}6H_2O$ 0.3 M (f) $NiSO_4{\cdot}4H_2O$ molarity 0.3 M (Cattin et al., 2008) [105].

3.61 eV. The compositional analysis indicated formation of non-stoichiometric nickel oxide thin films.

2.3. Other precursors

This session reviewed studies with other precursors and/or mixture of different precursors. Mathiyan et al. [104] studied effects of varying precursors and temperature on NiO thin films. Nickel acetate and nickel chloride precursors were deposited on a cleaned glass substrate. Temperatures were 473 K and 523 K. Fig. 17 shows the XRD patterns for the NiO films. Both precursors gave polycrystalline FCC structure with a strong diffraction along the (1 1 1) direction. Surface morphology indicated inhomogeneous nanostructured grains with spherical morphology. The grain size is the same for both precursors. The surface morphology of the films is represented in Fig. 18. There was an increment in grain size and size particle as spray solution increased.

A study was conducted using four different precursors of NiO films by Cattin et al. [105]. The study also varied the concentrations of the precursor between 0.2 M and 0.3 M. The four precursors were deposited using modified SPT. A perfume atomizer was used to grow the aerosol for the spray pyrolysis. The films were deposited at a substrate temperature of 350 °C. The precursors were nickel chloride hexahydrate ($NiCl_2{\cdot}6H_2O$), nickel nitrate hexahydrate ($Ni(NO_3)_2{\cdot}6H_2O$), nickel hydroxide hexahydrate ($Ni(OH)_2{\cdot}6H_2O$), and nickel sulfate tetrahydrate ($NiSO_4{\cdot}4H_2O$). Post annealing was performed on the films at 425 °C for 3 h at both room atmosphere and vacuum. All precursors gave p-type conductivity. Conductivity and optical transmittance of NiO films depended on the annealing process. The properties of films annealed at room temperature were not significantly modified. This is because the temperature and the environment of annealing were the same as the spray deposition experimental conditions. It was observed that annealing conducted in vacuum were more efficient. The conductivity and

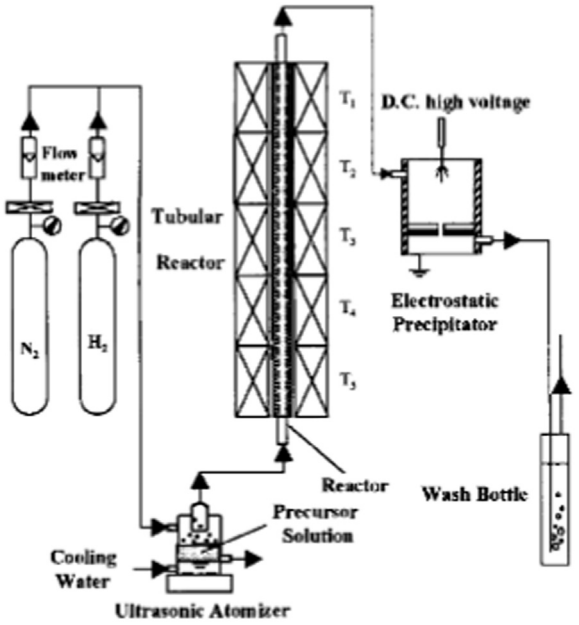

Fig. 21. Spray pyrolysis apparatus for nickel formate deposition (B. Xia et al., 2001) [106].

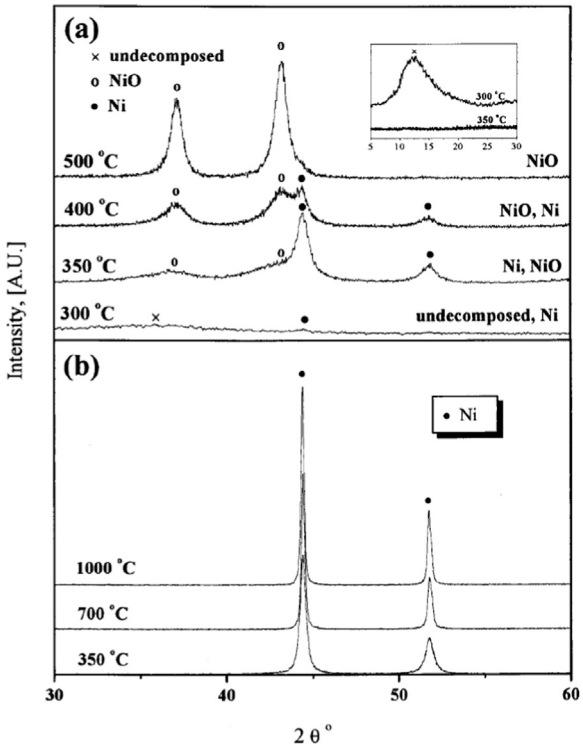

Fig. 22. XRD patterns of the powders formed in a N_2 atmosphere using 0.11 M of Ni $(HCOO)_2$ solution (a) without formic acid and (b) with formic acid 6 M of HCOOH [106].

optical transmission modifications were related to interaction between residual oxygen. The structure and morphology of the films are represented in Figs. 19 and 20 respectively. Nickel chloride and nickel nitrate precursors produced pure NiO films crystal in the cubic phase, while precursors of $Ni(OH)_2$ and $NiSO_4$ did not encourage growth of pure NiO films. However, $Ni(OH)_2$ and $NiSO_4$ precursors can be useful as original electrode in electrochromic devices and solar cells.

Xia et al. [106] worked on nickel formate as a precursor. The experimental set-up of the equipment is shown in Fig. 21. The obtained XRD patterns are shown in Fig. 22. The absence of HCOOH in the solution gives very weak nickel peaks at 300 °C. Nickel coexisted with NiO at 350 °C (and also at 400 °C), and the $Ni(HCOO)_2$ was completely decomposed.

A comparative study of NiO films prepared using two deposition methods was conducted by Chtouki et al. [107]. The study made use of spin coating and the spray pyrolysis deposition method. The structural, morphological, linear and nonlinear optical properties of NiO thin films were compared. The spray pyrolysis deposited solution was a mixture of 0.5 M and 0.75 M nickel chloride dissolved in 30 ml deionized water. The spray time was 3 min on a pre-heated glass substrate at 350 °C. The resultant films were then annealed at 350 °C for 45 mins. Also, the spin coating was deposited using a mixture of 0.5 M and 0.75 M nickel acetate dissolved in 10 ml of 2-Methoxy-ethanol ($C_3H_8O_2$). This was mixed with 0.30 ml for the 0.5 M/L and 0.45 ml for the 0.75 M/L of monoethanolamine (C_2H_7NO) (MEA). The MEA was used as a stabilizer and 2-Methoxyethanol as solvent. This was stirred at 60 °C for an hour. The filtered solution was then rotated at 3600 rpm for 30 s in a spin-coater. The films experienced reduction in band gap for both methods as precursor concentration increased. The spin coating method gave an optical band gap of 3.70–3.65 eV for 0.5 M and 0.75 M respectively. The spray pyrolysis technique gave 3.56–3.50 eV for 0.5 M and 0.75 M respectively. NiO film transmittance decreased as the concentration increased for both deposition methods. Spray pyrolysis deposited film experienced 60% transparency in visible and near infrared regions for 0.75 M and 70% for 0.5 M. Spin coated NiO films had 80% transparency in visible and near infrared regions for 0.5 M. The structural properties for both methods revealed intense manifestation of the XRD peaks as precursor concentration increased. This was attributed to growth of film thickness. NiO films had cubic structures in both methods with no unwanted phases. The spin coated method had two peaks. The major peak was at $2\theta = 43^\circ$ for the (2 0 0) plane with preferential orientation. The other is at $2\theta = 63^\circ$ for the (2 2 0) plane. The sprayed deposited NiO films had three distinct peaks: firstly, at $2\theta = 37^\circ$ for the (1 1 1) plane; secondly at $2\theta = 43^\circ$ for the (2 0 0) plane; and thirdly at $2\theta = 63^\circ$ for the (2 2 0) plane. The most intense peak was along the (1 1 1) plane. Table 8 shows the major parameters that have been reviewed.

3. Conclusion

It has been shown that both physical and chemical deposition techniques can be used to deposit NiO film on different substrates. This paper successfully reviewed different works on NiO films deposited with SPT. SPT was examined because of its simplicity, low cost, feasibility for mass production and high purity of deposited products. Nickel chloride, nickel acetate, nickel hydroxide, nickel sulfate and nickel formate have been used as precursors for spray depositing NiO thin film.

The properties of NiO thin film has been studied using XRD, SEM, AFM, FTIR and UV spectrometer respectively. Precursors of nickel nitrate, nickel chloride, and nickel acetate support growth of pure NiO thin film. However, $Ni(OH)_2$ and $NiSO_4$ precursors do not support growth of pure NiO film. Nickel chloride and nickel acetate were the most used and highly available precursors, although the end product of both precursors is different. The nickel chloride precursor contains an acid (HCl) as a final product that corrodes the spraying gun. The acid also causes reduction in the durability of the final film. However, nickel acetate precursor contains no acid making it a better option in terms of durability. The deposition parameters of NiO film have an effect on the surface texture and grain size of the film.

NiO thin film is an excellent material for optoelectronic applications. It is efficient, low cost, durable and with a wide band gap of 3.25–4.0 eV.

Table 8
Summary of major reviewed parameters for NiO thin films using spray pyrolysis technique.

Author	Precursor Used	Optical Band Gap (eV)	Molarity (M)	Substrate Temperature (°C)	Major Focus	Film Thickness	Other Parameters
[81]	Nickel chloride	3.58 for 30 ml, 3.55 for 40 ml, 3.49 for 60 ml 3.40 for 75 ml	0.05	350	Vol of sprayed (30 ml, 45 ml, 60 ml and 75 ml) on solution on NiO films	0.028 μm (30 ml) to 0.23 μm for (75 ml).	
[83]	Nickel chloride		0.05	350	Electrochromic properties of nickel oxide thin films prepared by spray pyrolysis technique.		
[84]	Nickel chloride	3.4–3.8 eV for 0.1–0.05 M respectively	0.025, 0.05, 0.075 and 0.1	280, 320, 360 and 400	Study focused on the effect of varying the concentration (0.025 M, 0.05 M, 0.075 M and 0.1 M) and the deposition temperature (280 °C, 320 °C, 360 °C and 400 °C)	0.21 μm 5–0.91 μm.	Spraying nozzle height, rate of spray and deposition time are 35 cm, 15 cm^3/min and 6 s respectively.
[86]	Nickel chloride	3.25	0.5	350 °C, annealed at a temperature of 500 °C for one hour	Focused on the antireflection coating of NiO thinfilms in solar cells	161 nm	Spray rate of 1 ml/min, substrate to nozzle distance of 18 cm.
[80]	Nickel chloride		0.1	225 to 420	study focused on substrate temperature as it affects the films properties	Decrease of the film thickness with increasing the substrate temperature (220 nm for 225 °C to 50 nm for 420 °C.	Substrate to nozzle distance of 40 cm, deposition time of 40 s, and flow rate of 15 cm^3/min.
[108]	Nickel chloride	3.54 eV, 3.43 eV and 3.37 eV for 350 °C, 400 °C and 450 °C respectively	0.3	350 °C, 400 °C and 450 °C	Evaluating the oscillator parameters (optical dispersions) of the NiO thin films	Film thickness increased as the transmittance decreased.	Nozzle to substrate distance of 7 cm, volume of 0.5 ml per min and an optimized airflow of 1.2 kg/cm^2.
[95]	Nickel chloride	3.25 eV, 3.04 eV, 3.16 eV and 3.28 eV for 425 °C, 450 °C, 475 °C and 500 °C respectively	0.5	425 °C, 450 °C, 475 °C and 500 °C	Influence of substrate temperature on electrochemical supercapacitive performance of spray deposited NiO thin films	280 nm, 350 nm, 310 nm and 275 nm for 425 °C, 450 °C, 47 °C 5 and 500 °C respectively.	Distance between spray nozzle and substrate is kept constant at 30 cm. Spray rate employed was 3 $mlmin^{-1}$.
[98]	Nickel acetate	3.6 eV for freshly prepared solution and aged 3.5 eV	0.1	330 °C	Focused on the effect of ageing on NiO thin films	631 nm for freshly prepared and 676 nm for aged.	
[101]	Nickel acetate	383 eV for 225 °C and 3.14 eV for 350 °C	0.05	225 °C to 350 °C	The work varied the substrate temperature with a view to finding the structural and optical dispersion properties of NiO thin films	The film thickness decreased with increased substrate temperature (225 °C was 200 nm while 350 °C was 40 nm).	Nozzle diameter of 0.7 mm, deposition time of 15 s, period between spraying of 3 min, spraying height of 35 cm and spraying rate was 15 cm^3/min.
[102]	Nickel acetate	The optical band gap of the films decreased with increase in film thickness from 4.3 to 3.65 eV.	0.1	350 °C and 450 °C	The study showed that the morphology of the films is principally controlled by the substrate temperature.	At 350 °C the thickness was 230 nm for 20 ml/h, 505 nm for 40 ml/h and 842 nm for 60 ml/h At 450 °C the thickness was 80 nm for 20 ml/h, 130 nm for 40 ml/h and 170 nm for 60 ml/h.	Substrate thickness of 1 mm, volume of solution varied between 20 to 60 ml/h, nozzle to substrate distance of 20 cm, spray time varied between 7.5 min and 180 min
[104]	Nickel chloride and nickel acetate.		0.05 M for both precursor.	473 K and 523 K.	To study the effect of substrate temperature on the structural and electrical properties of NiO using two precursors.		
[105]	$NiCl_2{\cdot}6H_2O$, Ni $(NO_3)_2{\cdot}6H_2O$, Ni $(OH)_2{\cdot}6H_2O$, $NiSO_4{\cdot}4H_2O$.	3.59 eV for all precursors	0.2 and 0.3	350 °C post annealed at 425 °C for 3 h.	Used four precursors of NiO films to study the properties of the film using SPT with perfume atomizer to grow the aerosol with varying molarity.		The volume of the solution for each deposition was 60 ml. 30 min was necessary for 60 ml. The substrate to nozzle distance was 30 cm.

Further studies are encouraged on nanostructured nickel oxide thin film. SPT is encouraged for depositing the film. Precursors of nickel acetate and nickel chloride are viable for pure NiO films. SPT NiO film is recommended to stakeholders interested in solving electricity problems in low income and developing countries.

Acknowledgements

The financial assistance of the National Research Foundation and Third World Academy of Science (NRF/TWAS) of South Africa under grant number 105492 towards this research is acknowledged.

References

[1] Ahuja D, Tatsutani M. Sustainable energy for developing countries. Surv Perspect Integr Environ Soc 2009;2:1.
[2] Ebhota WS, Eloka-Eboka AC, Inambao FL. Energy sustainability through domestication of energy technologies in third world countries in Africa. In: Proceedings of the 2014 International Conference on the Eleventh industrial and Commercial Use of Energy, pp. 1–7; 2014. ⟨http://ieeexplore.ieee.org/document/6904197/⟩.
[3] Ellabban O, Abu-Rub H, Blaabjerg F. Renewable energy resources: current status, future prospects and their enabling technology. Renew Sustain Energy Rev 2014;39:748–64.
[4] Islam AS, Islam M. Status of renewable energy technologies in Bangladesh. Technol 2005;5:1–5.
[5] Eslamian M. Spray-on thin film PV solar cells: advances, potentials and challenges. Coat 2014;4:60–84.
[6] Vasu V, Subrahmanyam A. Electrical and optical properties of pyrolytically sprayed SnO2 film-dependence on substrate temperature and substrate-nozzle distance. Thin Solid Films 1990;189:217–25.
[7] Sakhare YS, Thakare NR, Ubale AU. Influence of quantity of spray solution on the physical properties of spray deposited nanocrystalline MgSe thin films. St Petersburg Polytech Univ J: Phys Math 2016;2:17–26.
[8] Manifacier J, Fillard J, Bind J. Deposition of In_2O_3 SnO_2 layers on glass substrates using a spraying method. Thin Solid Films 1981;77:67–80.
[9] Joshi S, Mudigere M, Krishnamurthy L, Shekar G. Growth and morphological studies of NiO/CuO/ZnO based nanostructured thin films for photovoltaic applications. Chem Pap 2014;68:1584–92.
[10] Czapla A, Kusior E, Bucko M. Optical properties of non-stoichiometric tin oxide films obtained by reactive sputtering. Thin Solid Films 1989;182:15–22.
[11] Drevet R, Legros C, Bérardan D, Ribot P, Dragoé D, Cannizzo C, Andrieux M. Metal organic precursor effect on the properties of SnO 2 thin films deposited by MOCVD technique for electrochemical applications. Surf Coat Technol 2015;271:234–41.
[12] Jlassi M, Sta I, Hajji M, Ezzaouia H. Optical and electrical properties of nickel oxide thin films synthesized by sol–gel spin coating. Mater Sci Semicond Process 2014;21:7–13.
[13] Rahal A, Benhaoua A, Jlassi M, Benhaoua B. Structural, optical and electrical properties studies of ultrasonically deposited tin oxide (SnO_2) thin films with different substrate temperatures. Superlattices Microstruct 2015;86:403–11.
[14] Shaikh SK, Inamdar SI, Ganbavle VV, Rajpure KY. Chemical bath deposited ZnO thin film based UV photoconductive detector. J Alloy Compd 2016;664:242–9.
[15] Sharon M, Prasad B. Preparation and characterization of iron oxide thin film electrodes. Sol Energy Mater 1983;8:457–69.
[16] Zhang W, Ding S, Yang Z, Liu A, Qian Y, Tang S, Yang S. Growth of novel nanostructured copper oxide (CuO) films on copper foil. J Cryst Growth 2006;291:479–84.
[17] Farhadi S, Roostaei-Zaniyani Z. Preparation and characterization of NiO nanoparticles from thermal decomposition of the [Ni(en)3](NO3) 2 complex: a facile and low-temperature route. Polyhedron 2011;30:971–5.
[18] Salavati-Niasari M, Mir N, Davar F. A novel precursor in preparation and characterization of nickel oxide nanoparticles via thermal decomposition approach. J Alloy Compd 2010;493:163–8.
[19] Wang L, Hao Y, Zhao Y, Lai Q, Xu X. Hydrothermal synthesis and electrochemical performance of NiO microspheres with different nanoscale building blocks. J Solid State Chem 2010;183:2576–81.
[20] Wu J, Xue D. Progress of science and technology of ZnO as advanced material. Sci Adv Mater 2011;3:127–49.
[21] Pavan M, Rühle S, Ginsburg A, Keller DA, Barad H-N, Sberna PM, Fortunato E. TiO2/Cu2O all-oxide heterojunction solar cells produced by spray pyrolysis. Sol Energy Mater Sol Cells 2015;132:549–56. http://dx.doi.org/10.1016/j.solmat.2014.10.005.
[22] Kunz AB. Electronic structure of NiO. J Phys C: Solid State Phys 1981;14:L455.
[23] Hussein MAM. Effect of magnetization on ferrromagnetic and antiferromagnetic for NiO properties using quantum ESPRESSO package [Master's dissertation]. Khartoum: Sudan University of Science and Technology; 2016.
[24] Horie M, Stowe M, Tabei M, Kuroda E. Metal ion release of manufactured metal oxide nanoparticles is involved in the allergic response to inhaled ovalbumin in mice. Occup Dis Environ Med 2016;4:17.
[25] Boschloo G, Hagfeldt A. Spectroelectrochemistry of nanostructured NiO. J Phys Chem B 2001;105:3039–44.
[26] Kerli S, Alver Ü. Preparation and characterisation of ZnO/NiO nanocomposite particles for solar cell applications. J Nanotechnol 2016. http://dx.doi.org/10.1155/2016/4028062.
[27] Echresh A, Chey CO, Zargar Shoushtari M, Khranovskyy V, Nur O, Willander M. UV photo-detector based on p-NiO thin film/n-ZnO nanorods heterojunction prepared by a simple process. J Alloy Compd 2015;632:165–71. http://dx.doi.org/10.1016/j.jallcom.2015.01.155.
[28] Cai G, Darmawan P, Cui M, Lee PS Printed flexible solid state electrochromic devices based on NiO/WO3 complementary electrodes. 2015. In: Proceedings of the 227th ECS Meeting, 24-28 May 2015, Chicago.
[29] Sugiyama I, Shibata N, Wang Z, Kobayashi S, Yamamoto T, Ikuhara Y. Ferromagnetic dislocations in antiferromagnetic NiO. Nat Nanotechnol 2013;8:266–70.
[30] Kim H-J, Lee J-H. Highly sensitive and selective gas sensors using p-type oxide semiconductors: overview. Sens Actuators B: Chem 2014;192:607–27.
[31] Freund LB, Suresh S. Thin film materials: stress, defect formation and surface evolution. Cambridge: Cambridge University Press; 2004.
[32] Morosanu CE. Thin films by chemical vapour deposition 7. Amsterdam: Elsevier; 2016.
[33] Leskelä M, Ritala M. Atomic layer deposition (ALD): from precursors to thin film structures. Thin Solid Films 2002;409:138–46.
[34] Yang TS, Cho W, Kim M, An KS, Chung T-M, Kim CG, Kim Y. Atomic layer deposition of nickel oxide films using Ni (dmamp) 2 and water. J Vac Sci Technol A: Vac Surf Films 2005;23:1238–43.
[35] Rozati S, Akesteh S. Characterization of ZnO: Al thin films obtained by spray pyrolysis technique. Mater Charact 2007;58:319–22.
[36] Sta I, Jlassi M, Hajji M, Ezzaouia H. Structural, optical and electrical properties of undoped and Li-doped NiO thin films prepared by sol-gel spin coating method. Thin Solid Films 2014;555:131–7.
[37] Xu X, Xia C, Huang S, Peng D. YSZ thin films deposited by spin-coating for IT-SOFCs. Ceram Int 2005;31:1061–4.
[38] Brinker C, Frye G, Hurd A, Ashley C. Fundamentals of sol-gel dip coating. Thin Solid Films 1991;201:97–108.
[39] Wang H, Wang Y, Wang X. Pulsed laser deposition of the porous nickel oxide thin film at room temperature for high-rate pseudocapacitive energy storage. Electrochem Commun 2012;18:92–5.
[40] Mahan JE. Physical vapor deposition of thin films. New York: Wiley; 2000.
[41] Herman MA, Sitter H. Molecular beam epitaxy: fundamentals and current status 7. Berlin: Springer; 2012.
[42] Zhao Y, Wang H, Wu C, Shi Z, Gao F, Li W, Du G. Structures, electrical and optical properties of nickel oxide films by radio frequency magnetron sputtering. Vacuum 2014;103:14–6.
[43] Xia X, Tu J, Zhang J, Wang X, Zhang W, Huang H. Electrochromic properties of porous NiO thin films prepared by a chemical bath deposition. Sol Energy Mater Sol Cells 2008;92:628–33.
[44] Luyo C, Ionescu R, Reyes L, Topalian Z, Estrada W, Llobet E, Heszler P. Gas sensing response of NiO nanoparticle films made by reactive gas deposition. Sens Actuators B: Chem 2009;138:14–20.
[45] Kalita PK, Sarma B, Das H. Structural characterization of vacuum evaporated ZnSe thin films. Bull Mater Sci 2000;23:313–7.
[46] Tanuševski A, Poelman D. Optical and photoconductive properties of SnS thin films prepared by electron beam evaporation. Sol Energy Mater Sol Cells 2003;80:297–303.
[47] Lampert C, Omstead T, Yu P. Chemical and optical properties of electrochromic nickel oxide films. Sol Energy Mater 1986;14:161–74.
[48] Ferreira F, Tabacniks M, Fantini M, Faria I, Gorenstein A. Electrochromic nickel oxide thin films deposited under different sputtering conditions. Solid State Ion 1996;86:971–6.
[49] Wang Z, Zhang Z. Electron beam evaporation deposition. In: Lin Y, Chen X, editors. Advanced nano deposition methods. Weinheim, Germany: Wiley-VCH Verlag; 2016.
[50] Subramanian B, Ibrahim MM, Senthilkumar V, Murali K, Vidhya V, Sanjeeviraja C, Jayachandran M. Optoelectronic and electrochemical properties of nickel oxide (NiO) films deposited by DC reactive magnetron sputtering. Phys B: Condens Matter 2008;403:4104–10.
[51] Wu M-S, Yang C-H, Wang M-J. Morphological and structural studies of nanoporous nickel oxide films fabricated by anodic electrochemical deposition techniques. Electrochim Acta 2008;54:155–61.
[52] Hu C-C, Li W-Y, Lin J-Y. The capacitive characteristics of supercapacitors consisting of activated carbon fabric-polyaniline composites in NaNO 3. J Power Sources 2004;137:152–7.
[53] Yeh W-C, Matsumura M. Chemical vapor deposition of nickel oxide films from bis-π-cyclopentadienyl-nickel. Jpn J Appl Phys 1997;36:6884.
[54] Guo Q, Ford GM, Yang W-C, Walker BC, Stach EA, Hillhouse HW, Agrawal R. Fabrication of 7.2% efficient CZTSSe solar cells using CZTS nanocrystals. J Am Chem Soc 2010;132:17384–6.
[55] Nehru L, Umadevi M, Sanjeeviraja C. Studies on structural, optical and electrical properties of ZnO thin films prepared by the spray pyrolysis method. Int J Mater Eng 2012;2:12–7.
[56] Ilegbusi OJ, Khatami SN, Trakhtenberg LI. Spray Pyrolysis deposition of single and mixed oxide thin films. Mater Sci Appl 2017;8:153.
[57] Udayakumar R, Khanaa V, Saravanan T. Synthesis and structural characterization of thin films of SnO 2 prepared by spray pyrolysis technique. Indian J Sci Technol 2013;6:4754–7.
[58] Messing GL, Zhang SC, Jayanthi GV. Ceramic powder synthesis by spray pyrolysis. J Am Ceram Soc 1993;76:2707–26.
[59] Patil PS. Versatility of chemical spray pyrolysis technique. Mater Chem Phys

1999;59:185–98.
[60] Seeber W, Abou-Helal M, Barth S, Beil D, Höche T, Afify H, Demian S. Transparent semiconducting ZnO: Al thin films prepared by spray pyrolysis. Mater Sci Semicond Process 1999;2:45–55.
[61] Jabari-Seresht R, Jahanshahi M, Rashid A, Ghoreyshi AA. Fabrication and evaluation of non-porous graphene by a unique spray pyrolysis method. Chem Eng Technol 2013;36:1550–8.
[62] Arya SP, Hintermann H. Growth of $YB_a2C_u3_{O7-}x$ superconducting thin films by ultrasonic spray pyrolysis. Thin Solid Films 1990;193–194(Part 2):841–8466.
[63] Chen C, Kelder E, Jak M, Schoonman J. Electrostatic spray deposition of thin layers of cathode materials for lithium battery. Solid State Ion 1996;86:1301–6.
[64] Balkenende AR, Bogaerts AAMB, Scholtz JJ, Tijburg RRM, Willems HX. Thin MgO layers for effective hopping transport of electrons. Philips J Res 1996;50:365–73.
[65] Filipovic L, Selberherr S, Mutinati GC, Brunet E, Steinhauer S, Köck A, Grogger W. Modeling and analysis of spray pyrolysis deposited SnO2 films for gas sensors. In: Yang G-C, editor. Transactions on engineering technologies. Dortmund, Germany: Springer; 2014. p. 295–310.
[66] Perednis D, Gauckler LJ. Thin film deposition using spray pyrolysis. J Electroceram 2005;14:103–11.
[67] Viguie J, Spitz J. Chemical vapor deposition at low temperatures. J Electrochem Soc 1975;122:585–8.
[68] Siefert W. Properties of thin In2O3 and SnO2 films prepared by corona spray pyrolysis, and a discussion of the spray pyrolysis process. Thin Solid Films 1984;120:275–82.
[69] Chamberlin R, Skarman J. Chemical spray deposition process for inorganic films. J Electrochem Soc 1966;113:86–9.
[70] Albin D, Risbud S. Spray pyrolysis processing of optoelectronic materials. Adv Ceram Mater 1987:2.
[71] Pamplin B. Spray pyrolysis of ternary and quaternary solar cell materials. Prog Cryst Growth Charact 1979;1:395–403.
[72] Schoonman J, Riess I. Oxygen ion and mixed conductors and their technological applications 368. Dordrecht, Germany: Springer; 2000.
[73] Tomar M, Garcia F. Spray pyrolysis in solar cells and gas sensors. Prog Cryst Growth Charact 1981;4:221–48.
[74] Filipovic L, Selberherr S, Mutinati GC, Brunet E, Steinhauer S, Köck A, Schrank F. A method for simulating spray pyrolysis deposition in the level set framework. Eng Lett 2013;21:224–40.
[75] Eberspacher C, Fredric C, Pauls K, Serra J. Thin-film CIS alloy PV materials fabricated using non-vacuum, particles-based techniques. Thin Solid Films 2001;387:18–22.
[76] Wang W, Su Y-W, Chang C-H. Inkjet printed chalcopyrite CuIn x Ga 1 − x Se 2 thin film solar cells. Sol Energy Mater Sol Cells 2011;95:2616–20.
[77] Wang X, Song J, Gao L, Jin J, Zheng H, Zhang Z. Optical and electrochemical properties of nanosized NiO via thermal decomposition of nickel oxalate nanofibres. Nanotechnol 2004;16:37.
[78] Raj KP, Thangaraj V, Uthirakumar A. Synthetic routes to nickel oxide nanoparticles-an overview. Chem Sci Rev Lett 2015;4:494–501.
[79] Muecke UP, Luechinger N, Schlagenhauf L, Gauckler LJ. Initial stages of deposition and film formation during spray pyrolysis—Nickel oxide, cerium gadolinium oxide and mixtures thereof. Thin Solid Films 2009;517:1522–9.
[80] Kamal H, Elmaghraby E, Ali S, Abdel-Hady K. Characterization of nickel oxide films deposited at different substrate temperatures using spray pyrolysis. J Cryst Growth 2004;262:424–34.
[81] Patil PS, Kadam L. Preparation and characterization of spray pyrolyzed nickel oxide (NiO) thin films. Appl Surf Sci 2002;199:211–21.
[82] Varkey A, Fort A. Solution growth technique for deposition of nickel oxide thin films. Thin Solid Films 1993;235:47–50.
[83] Kadam L, Patil P. Studies on electrochromic properties of nickel oxide thin films prepared by spray pyrolysis technique. Sol Energy Mater Sol Cells 2001;69:361–9.
[84] Ismail RA, Ghafori SA, Kadhim GA. Preparation and characterization of nanostructured nickel oxide thin films by spray pyrolysis. Appl Nanosci 2013;3:509–14.
[85] Makhlouf S, Kassem M, Abedulrahim M. Crystallite size dependent optical properties of nanostructured NiO films. J Optoelectron Adv Mater 2010;4:1562.
[86] Vigneshkumar M, Muthulakshmi Suganya S, Pandiarajan J, Saranya A, Prithivikumaran N. Structural and optical properties of nanocrystalline nickel oxide thin film by spray pyrolysis technique. Int J Tech Res Appl 2016:52–6 [Special Issue 38].
[87] Puspharajah P, Radhakrishna S, Arof A. Transparent conducting lithium-doped nickel oxide thin films by spray pyrolysis technique. J Mater Sci 1997;32:3001–6.
[88] Wang Y, Ma C, Sun X, Li H. Preparation and photoluminescence properties of organic–inorganic nanocomposite with a mesolamellar nickel oxide. Microporous Mesoporous Mater 2004;71:99–102.
[89] Mahmoud S, Akl A, Kamal H, Abdel-Hady K. Opto-structural, electrical and electrochromic properties of crystalline nickel oxide thin films prepared by spray pyrolysis. Phys B: Condens Matter 2002;311:366–75.
[90] Hotový I, Buc D, Haščík Š, Nennewitz O. Characterization of NiO thin films deposited by reactive sputtering. Vacuum 1998;50:41–4.
[91] Pejova B, Kocareva T, Najdoski M, Grozdanov I. A solution growth route to nanocrystalline nickel oxide thin films. Appl Surf Sci 2000;165:271–8.
[92] Gowthami V, Perumal P, Sivakumar R, Sanjeeviraja C. Structural and optical studies on nickel oxide thin film prepared by nebulizer spray technique. Phys B: Condens Matter 2014;452:1–6.
[93] Sato H, Minami T, Takata S, Yamada T. Transparent conducting p-type NiO thin films prepared by magnetron sputtering. Thin Solid Films 1993;236:27–31.
[94] El-Ghamaz N, El-Sonbati A, Diab M, El-Bindary A, Seyam H. Optical properties of thermally evaporated 4-(4-nitrobenzalideneamino) antipyrine Schiff base thin films. Solid State Sci 2013;19:19–26.
[95] Yadav AA, Chavan U. Influence of substrate temperature on electrochemical supercapacitive performance of spray deposited nickel oxide thin films. J Electroanal Chem 2016;782:36–42.
[96] Devasthali A, Kandalkar S. Preparation and characterization of spray deposited nickel oxide (NiO) thin film electrode for supercapacitor. IOSR J Comput Eng 2015;2:47–51.
[97] Raut B, Pawar S, Chougule M, Sen S, Patil V. New process for synthesis of nickel oxide thin films and their characterization. J Alloy Compd 2011;509:9065–70.
[98] Sriram S, Thayumanavan A. Structural, optical and electrical properties of NiO thin films prepared by low cost spray pyrolysis technique. Int J Mater Sci Eng 2013;1:118–21.
[99] Birgin EG, Chambouleyron I, Martinez JM. Estimation of the optical constants and the thickness of thin films using unconstrained optimization. J Comput Phys 1999;151:862–80.
[100] Saadati F, Grayeli A, Savaloni H. Dependence of the optical properties of NiO thin films on film thickness and nano-structure. J Theor Appl Phys 2010;4:22–6.
[101] Mahmoud SA, Shereen A, Mou'ad AT. Structural and optical dispersion characterisation of sprayed nickel oxide thin films. J Mod Phys 2011;2:1178–86.
[102] Romero R, Martin F, Ramos-Barrado J, Leinen D. Synthesis and characterization of nanostructured nickel oxide thin films prepared with chemical spray pyrolysis. Thin Solid Films 2010;518:4499–502.
[103] Desai J, Min S-K, Jung K-D, Joo O-S. Spray pyrolytic synthesis of large area NiO x thin films from aqueous nickel acetate solutions. Appl Surf Sci 2006;253:1781–6.
[104] Mathiyan J, Sivalingam D, Gopalakris J, Rayappan J. Spray coated nanostructured nickel oxide thin films for ethanol sensing. J Appl Sci 2012;12:1686–90.
[105] Cattin L, Reguig B, Khelil A, Morsli M, Benchouk K, Bernede J. Properties of NiO thin films deposited by chemical spray pyrolysis using different precursor solutions. Appl Surf Sci 2008;254:5814–21.
[106] Xia B, Lenggoro IW, Okuyama K. Preparation of nickel powders by spray pyrolysis of nickel formate. J Am Ceram Soc 2001;84:1425–32.
[107] Chtouki T, Soumahoro L, Kulyk B, Bougharraf H, Kabouchi B, Erguig H, Sahraoui B. Comparison of structural, morphological, linear and nonlinear optical properties of NiO thin films elaborated by spin-coating and spray pyrolysis. Opt- Int J Light Electron Opt 2017;128:8–13.
[108] Gowthami V, Meenakshi M, Perumal P, Sivakumar R, Sanjeeviraja C. Optical dispersion characterization of NiO thin films prepared by nebulized spray technique. Int J ChemTech Res 2014;6:5196–202.

CHAPTER 4: DEPOSITION AND OPTIMIZATION OF NANOSTRUCTURED NiO THIN FILM DEPOSITION USING THE SPRAY PYROLYSIS TECHNIQUE

This chapter gives the deposition and optimization of the nanostructured NiO thin films. This is divided into four parts.

Part 1 gives the optimization of NiO using concentration and published in Energy Procedia, Elsevier publishers:

Ukoba, O.K., Eloka-Eboka, A.C. and Inambao F.L. "Influence of concentration on properties of spray deposited nickel oxide films for solar cells," ***Energy Procedia,*** **volume 142, December 2017, pp. 236–243**

Part 2 discussed the optimization from the angle of annealing and published in Energy Procedia, Elsevier publishers:

Ukoba, O.K., Inambao F. L. and Eloka-Eboka, A.C. "Influence of annealing on properties of spray deposited nickel oxide films for solar cells," ***Energy Procedia,*** **volume 142, December 2017, pp. 244–252.**

Part 3 looked at effect of ageing on nanostructured NiO thin films for solar cells fabrication published in Journal of Physical Science (JPS):

Ukoba, O.K., Eloka-Eboka, A.C. and Inambao F. L. "Optimizing Aged Nanostructured nickel oxide thin films for solar cells," ***Journal of Physical Science (JPS)*****, 2018 (Accepted)**

Lastly, part 4 studied the combine effect of temperature and ageing on nanostructured nickel oxide for solar cells published in International Journal of Renewable Energy Research (IJRER):

Ukoba, O.K., Inambao F.L. and Eloka-Eboka, A.C. "Study of deposition temperature on properties of aged nanostructured nickel oxide for solar cells," ***International Journal of Renewable Energy Research (IJRER), volume 8, No 2, June*** **2018, pp 724 - 732**

CHAPTER 4 Part 1: INFLUENCE OF CONCENTRATION ON PROPERTIES OF SPRAY DEPOSITED NICKEL OXIDE FILMS FOR SOLAR CELLS

Part 1 gives the optimization of NiO using concentration and published in Energy Procedia, Elsevier publishers:

To cite this article: Ukoba, O.K., Eloka-Eboka, A.C. and Inambao F.L. "Influence of concentration on properties of spray deposited nickel oxide films for solar cells," *Energy Procedia,* volume 142, December 2017, pp. 236–243. DOI: 10.1016/j.egypro.2017.12.038

Available online at www.sciencedirect.com

ScienceDirect

Energy Procedia 142 (2017) 236–243

Energy Procedia

www.elsevier.com/locate/procedia

9th International Conference on Applied Energy, ICAE2017, 21-24 August 2017, Cardiff, UK

Influence of concentration on properties of spray deposited nickel oxide films for solar cells

*[a]Ukoba, O.K, Eloka-Eboka, A.C[a], Inambao, F.L[a],

[a]*Discipline of Mechanical Engineering UKZN, Durban, 4041, South Africa*

Abstract

Spray pyrolysis technique was used to deposit various concentration of nickel oxide films on glass substrate. The Effect of varying precursor concentration on elemental, morphological and structural properties was investigated on the deposited NiO films. Nickel (II) acetate tetrahydrate precursor was used at substrate temperature of 350 ^{o}C. Precursor concentrations were 0.025, 0.05, 0.075 and 0.1 M. Scanning Electron Microscope (SEM) surface morphology revealed nanostructured films with particles densely distributed across substrates surface. Increased in surface grains was observed as the precursor solution increased. Elemental composition of NiO films revealed presence of Ni and O element. There was reduction in oxygen concentration as precursor solution increases. Amorphous structure was observed at concentration of 0.025 M while polycrystalline with cubic structure was observed at higher concentrations. Preferred orientation was along (1 1 1) peak with small intensity along (2 0 0) peak. XRD patterns have peak diffraction at (2θ = 37 ^{o} and 43 ^{o}) for (1 1 1) and (2 0 0) planes respectively and 64 ^{o} for (2 2 0) plane for 0.1 M. Film thickness grew with increase in precursor concentration. Film micro strain was observed to have compression for all precursor solution conspicuously revealing the effect of varied concentration on NiO films properties.

Peer-review under responsibility of the scientific committee of the 9th International Conference on Applied Energy.

Keywords: NiO; solar cells material; annealing, low income

1. Introduction

About one-fourth of earth's inhabitants lacks access to electricity with little or no changes in absolute terms since 1970s (Ahuja & Tatsutani, 2009). Most developing countries still struggle with affordable stable electricity (Ebhota,

* Corresponding author. Tel.: +27640827616; fax: +0-000-000-0000 .
E-mail address: ukobaking@yahoo.com

1876-6102
Peer-review under responsibility of the scientific committee of the 9th International Conference on Applied Energy .
10.1016/j.egypro.2017.12.038

Eloka-Eboka, & Inambao, 2014). Renewable energy especially solar energy is one of envisaged solution. Solar energy is one of the best sources of renewable energy. Hourly solar influx on earth surface surpasses annual human energy needs (Lewis, 2007). Solar energy is environmentally benign. About 40 % million tons of CO_2 emissions is saved per year when 1 % of world electricity demand is supplied by solar grid (Gardner, 2008). However, cost is militating against successful deployment of solar technology worldwide because, converting solar energy into electricity occurs at a price comparable with fossil fuel. Solar cells are integral part of solar energy (Green, 1982). Large scale production and affordable cost is still researched into in fabrications of solar cells (Eslamian, 2014). This is attributed to difficulty in scaling up existing methods or expensive nature and complexities associated with vacuum environment fabrication. However, nanostructure metal oxide offers promises. Nanostructures materials offers potential improvement on efficiency of photovoltaic (PV) solar cells, reduction in manufacturing and electricity production costs (Serrano, Rus, & Garcia-Martinez, 2009). It is achievable by increased surface area to volume ratio of nanoparticles. This enhances solar energy collection and efficiency by exposing more conducting surfaces to sunlight. Nanostructures materials have unique characteristics that cannot be obtained from conventional macroscopic materials (Hussein, 2015). Conventional materials have weaknesses in the absorption properties of the conventional fluids which can lead to reduced efficiency of solar cells devices. Inorganic semiconducting materials are economical, environmentally friendly and viable sources for solar cells (Joshi, Mudigere, Krishnamurthy, & Shekar, 2014). In recent years, fabrication of nanostructured metal oxide films is attracting interest in terms of technological applications (Drevet et al., 2015; Rahal, Benhaoua, Jlassi, & Benhaoua, 2015; Shaikh, Inamdar, Ganbavle, & Rajpure, 2016; Zhang et al., 2006). They have been studied due to their vast usage (Soonmin, 2016). They have found applications in solar cells, UV detectors, electrochromic devices, anti-ferromagnetic layers, p-type transparent conductive thin films and chemical sensors (Li & Zhao, 2010; Magaña, Acosta, Martínez, & Ortega, 2006; Nam et al., 2015; Park, Sun, Sun, Jing, & Wang, 2013; Wu & Yang, 2015; Zhu et al., 2014). Nanostructured metal oxides often express n-type conductivity with few displaying p-type. Nickel Oxide (NiO) is a p-type semiconductor with wide band gap from 3.5 to 4.0 eV (Boschloo & Hagfeldt, 2001). Nickel oxides exist in various oxidation states (Subramanian et al., 2008). NiO has rhombohedral or cubic structure and possesses pale green color. NiO have excellent durability and electrochemical stability with a large range of optical densities. It is a promising material for various applications because of its better optical, electrical and magnetic properties. Nickel oxide thin films have been deposited using different methods; sputtering (Keraudy et al., 2015), sol–gel (Jlassi, Sta, Hajji, & Ezzaouia, 2014), electron beam deposition (El-Nahass, Emam-Ismail, & El-Hagary, 2015), laser ablation (Wang, Wang, & Wang, 2012), chemical bath deposition (Vidales-Hurtado & Mendoza-Galván, 2008). Spray Pyrolysis Technique is simple, low cost and feasible for mass production (Ismail, Ghafori, & Kadhim, 2013). Spray Pyrolysis is method that allows coating on large area by films of very thin layers with uniform thickness (Gowthami, Perumal, Sivakumar, & Sanjeeviraja, 2014). This study aims to optimize the precursor concentration of NiO films with motivation for efficient and affordable application in solar cells development. The scope involves: the preparation of a nanostructured NiO thin films on a glass substrate using SPT for deposition of aqueous solution of nickel (II) acetate tetrahydrate and determine the effect of varying the concentration on different properties of NiO films.

2. Experimental Procedure

2.1. Spray Pyrolysis set up

Experimental setup for spray pyrolysis used is shown in Figure 1. The set up consists of heater, air compressor, temperature controller, exhaust fan and pipe, spray gun with attached container. The container was used to hold the precursor solution. Spray gun was connected to the air compressor using hose or pipe. Temperature of 350 ^{o}C was attained and read by thermocouple attached to the heater before commencing deposition. The carrier gas is compressed air at pressure of 1bar.

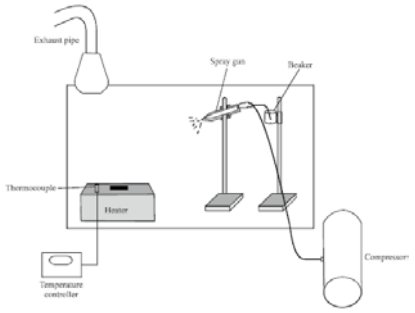

Fig 1: Experimental set-up of spray pyrolysis technique

2.2. Precursor preparation and deposition

Concentration of 0.025, 0.05, 0.075 and 0.1 M of nickel (II) acetate tetrahydrate ($\mathrm{Ni}(C_2H_3O_2)_2.4H_2O$) (Medicine, 2007) were used as precursor solution. It was dissolved in 50 mL distilled water and stirred for 10 minutes. The precursor solution was poured into spray gun container. Glass substrate was chemically and ultrasonically cleaned and thereafter heated at constant temperature of 350 ^oC on a heater. Other deposition parameters were maintained to obtain uniform film thickness. Optimum deposition parameters of spray deposited NiO films are shown in Table 1. Each droplet from the spray gun was less than micro sized particles. Sprayed solution on the preheated substrate glass undergoes evaporation. Solute precipitation and pyrolytic decomposition are as shown in Equation (1). The major end product is nickel oxide thin films.

$$\mathrm{Ni}(C_2H_3O_2)_2.4H_2O \xrightarrow{heat} NiO + 7H_2O \uparrow + 4CO_2 \uparrow \quad (1)$$

Colour of prepared thin films was observed to be gray, uniform and strongly adhered to glass substrate. Thermocouple was fixed to substrate's surface to record the temperature.

Table 1. Optimum deposition parameter of SPT NiO films

Deposition parameter	Value
Substrate temperature	350 ^oC
Height of spraying nozzle to substrate distance	20 cm
Spray rate	1 ml/min
Spray time	1 minute
Time between sprays	30 seconds
Carrier gas	Filled compressed air of 1bar

2.3. Characterization

Morphology of deposited NiO film was studied using ZEISS ULTRA PLUS Field Emission Gun Scanning Electron Microscope (FEGSEM). Elemental composition was done with Energy Dispersive X-ray Spectrometer (EDS or EDX: "AZTEC OXFORD DETECTOR"). Structural properties of deposited NiO films were investigated using EMPYREAN (PANalytical) X-ray powder diffractometer for a range of 5 º to 90 º 2θ angles.

3. Results and Discussion

3.1. Morphological studies

Figures 2 and 3 show the FEG SEM micrographs. It reveals homogeneous, smooth, well adherent films devoid of pinholes and cracks. It becomes grainier with bigger flakes as precursor concentration increased from 0.025 M to 0.1 M. This is an improvement on results observed by (Bari, Patil, & Bari, 2013; Saadati, Grayeli, & Savaloni, 2010).

This confirms that varying the concentration of the precursors affects the NiO films morphology.

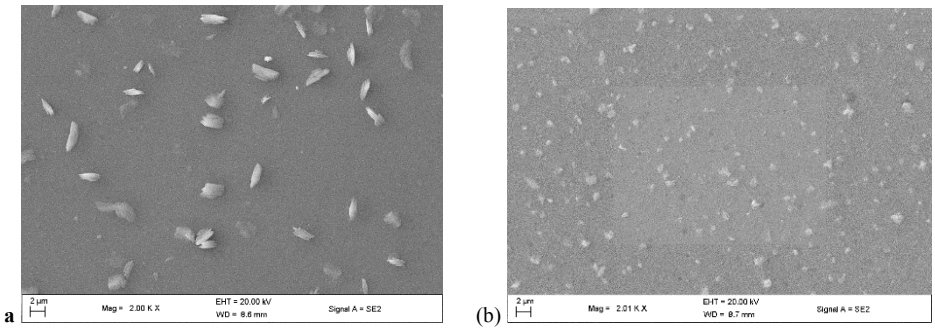

Fig 2: SEM micrographs of nickel oxide (NiO) film on glass substrate at (a) 0.025 M and (b) 0.05 M

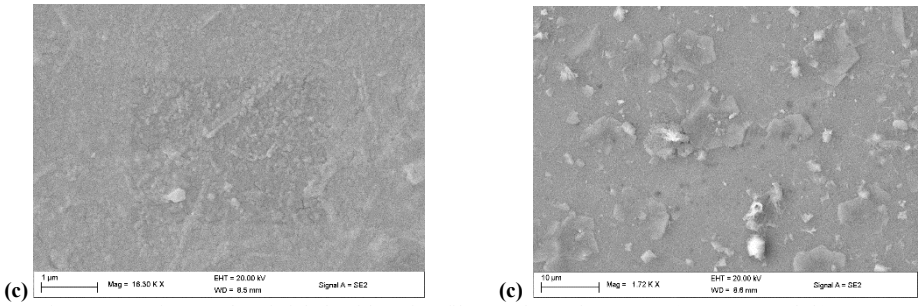

Fig 3: SEM micrographs of nickel oxide (NiO) film on glass substrate at (a) 0.075 M and (b) 0.1 M

3.2. Elemental composition Analysis

Figure 4 shows the EDX for the different concentration of the NiO thin films thereby confirming presence of Ni and O elements in NiO thin films. There was reduction in oxygen concentration in the deposited NiO films as precursor concentration increased as seen in Figure 4. This may be due to increase in film growth on the glass substrate thereby making less of the glass (oxygen) to be seen. Reguig et al. (Reguig et al., 2006) also reported presence of Ni and O elements. Additional Si element was also observed. This is because Silicon (Si) is present in soda-lime glass or soda-lime-silica glass substrate (de Jong, 1989).

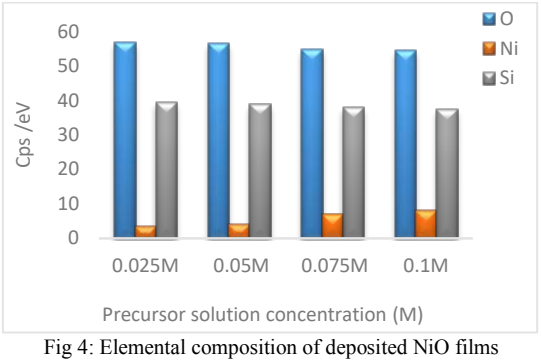

Fig 4: Elemental composition of deposited NiO films

3.3. Variation of the film thicknesses with precursor solution concentration

Films thickness was investigated as a function of the precursor concentration ranging between 0.025 M and 0.1 M. The measured data are graphically represented in Figure 5. Using the weight difference method, film thickness was calculated using the relationship in Equation (2) (Godse et al., 2011):

$$t = m/A \quad (2)$$

Where t denotes the film thickness while m is the actual mass deposited onto the substrate, A is the area of the film and ρ is the density of material.

The calculated film thickness is shown in Figure 6. From Figures 5 and 6, it was seen that the measured and calculated values are in good agreement. It was found that film thickness grew with increasing precursor concentration except for 0.025 M. This is an improvement of results by Boyraz and Urfa (Boyraz & Urfa, 2015). This is as result of accumulation of deposited NiO on substrate. This was collaborated by EDX results in Figure 4. The kinetics of the NiO forming reaction increased with precursor concentration. During the deposition, nozzle to substrate height and the deposition time were kept constant to control the thickness of NiO thin films. Average thickness range of the NiO thin films was found between 6.277 and 11.57 µm.

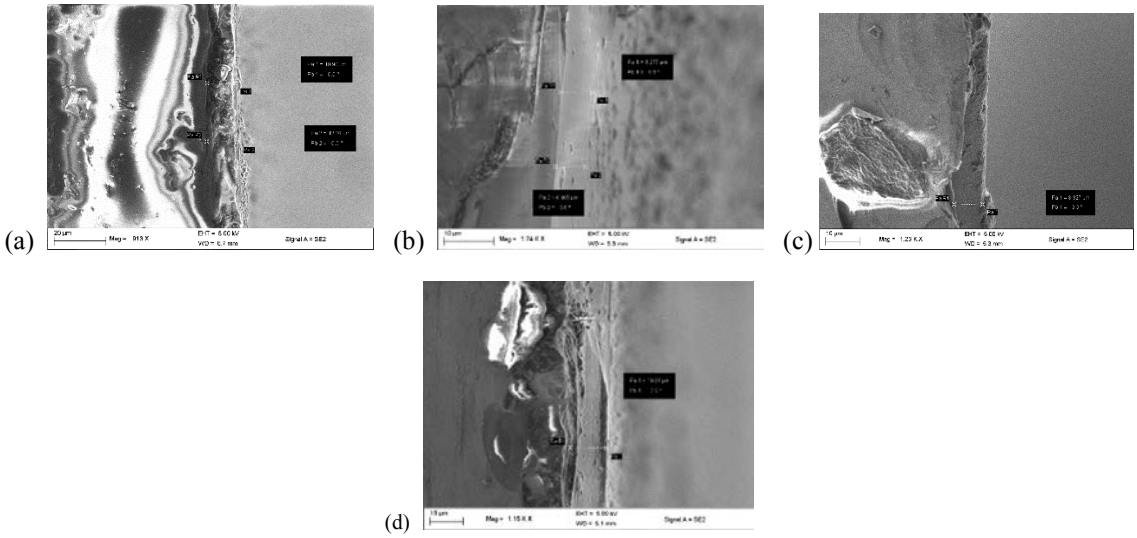

Fig. 5. Measured NiO film thickness at (a) 0.025 M; (b) 0.05 M; (c) 0.075M; (d) 0.1M

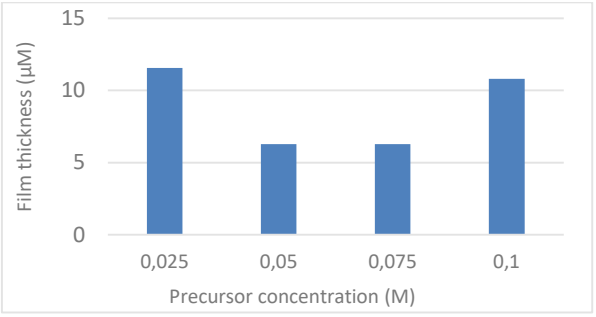

Figure 6: Calculated film thickness of NiO films

3.4. Structural studies

The phase present and preferred orientation of deposited nanostructured NiO films was determined using X-ray diffractometer (XRD). Figure 7 shows the XRD patterns of deposited nanostructured NiO films at different precursor concentration. The patterns have peak diffraction at (2θ = 37 º, and 43 º) for (1 1 1) and (2 0 0) planes respectively and 64 º for (2 2 0) plane for 0.1 M. This agrees with Joint Committee on Powder Diffraction Standards—International

Centre for Diffraction Data, JCPDS 04- 0835 for Bunsenite (NiO) (Gabal, 2003). Highest intensity was recorded for (1 1 1) having a strong peak when 2θ = 37 º for precursor solution of 0.05 M, 0.075 M and 0.1 M which is equal to (Bakr, Salman, & Shano, 2015). This maybe as a result of increase in grain growth caused by larger film thickness. It can also be due to increase in crystallinity as precursor solution concentration increases; thereby confirming polycrystalline with cubic crystalline structures of deposited NiO films similar to reported structure by Fadheela (2015). Lower intensity peak of (2 0 0) increases gradually as precursor solution increased from 0.05 M to 0.1 M with emergence of third peak (2 2 0) for 0.1 M. Average crystallite size was obtained using Debye Scherer formula (Barrett & Massalski, 1980; Scherrer & Nachr, 1918) in Equation (3) as shown in the following section.

$$D = \frac{k\lambda}{\beta \cos\theta} \quad (3)$$

Where; B denotes full width at half maximum (FWHM) intensity of the peak (in Radian), λ is wavelength, θ is Bragg's diffraction angle and k is 0.89 respectively. Grain size for (1 1 1) and (2 0 0) planes are found to be 22 nm and 63.77 nm. Lattice constant was found to be 4.1905, 4.1856, 4.1852, 4.1850 Å for 0.025 M to 0.1 M respectively. This agrees with standard lattice constant of NiO film value of 4.176 Å (Pistorius, 1963).

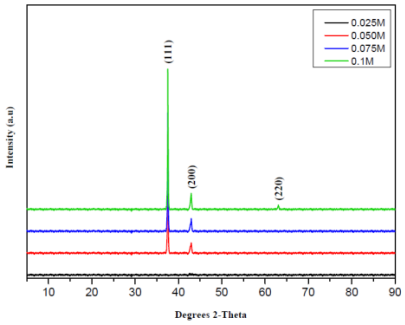

Fig 7: XRD patterns of nanostructured NiO films at different precursor concentration

Micro strain was produced through growth of thin films and was calculated using the formula in Equation (4) (AL-Jabiry, 2006).

$$\delta = (d\_(ASTM) - d\_XRD)/d\_ASTM \times 100 \quad (4)$$

Where "d" is the lattice constant and δ is micro strain.

A plot of NiO film micro strain against precursor solution is shown in Figure 8. It shows that there is an increase in micro strain as precursor concentration increases. Micro strain represents compression as seen in Table 2 which gives detail result of micro strain, lattice constants and 2θ values for deposited NiO films for precursor solution concentration of 0.025 M to 0.1 M.

Table 2: Calculated parameters from XRD data

Parameter		0.025 M	0.05 M	0.075 M	0.1 M
2θ	hkl		37	37	37
	(1 1 1)				
	(2 0 0)	x	43	43	43
	(2 2 0)	x	X	x	63
Lattice constant d (Å)	recorded XRD	4.1905	4.1855	4.1852	4.1850
	ASTM	4.1684	4.1684	4.1684	4.1684
Micro strain (δ) %		-0.5301	-0.4102	-0.4030	-0.3982

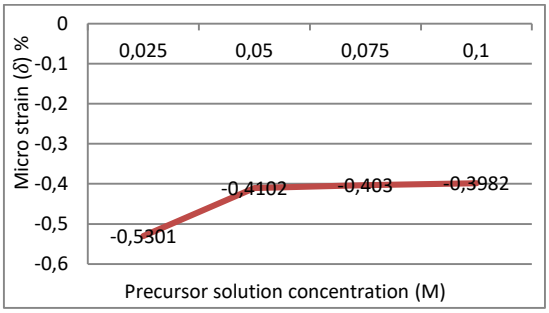

Fig. 8. Plot of Micro strain against precursor solution concentration for NiO films

4. Conclusion

In this study, nanostructured nickel oxide films were successfully deposited by spray pyrolysis of nickel (II) acetate tetrahydrate on glass substrate. The effect of varying precursor concentration of NiO films on elemental, morphological and structural properties were studied with a view to optimizing the material for solar cells application. This study contributed new results relating to surface morphology, structural, film thickness and micro strain of NiO films using SPT. The results clearly showed that varying the precursor solution concentration has effect on the morphological and elemental properties of nickel oxide thin films. The surface morphology is improved by increasing precursor solution concentration. Film thickness is improved as precursor solution concentration increases. Oxygen concentration reduces as precursor concentration decreases.

There is mark improvement on crystallinity with increasing precursor solution concentration. Leading to higher peak intensity and diffraction. New Peak diffraction was recorded at ($2\theta = 37^{o}$, and 43^{o}) for (1 1 1) and (2 0 0) planes for 0.05 M concentration and above and 64^{o} for (2 2 0) plane for 0.1 M. Lattice constant decreases from 4.1905 to 4.1850 Å for 0.025 M to 0.1 M which correlate 4.176 Å standard lattice constant of NiO. Micro strain of films shows compression and increases with precursor concentration.

Varying concentration of precursor solution has effect on overall properties of nanostructured nickel oxide thin films. Precursor solution 0.1 M outperformed others by showing good crystallinity and good film thickness. Therefore, NiO films from 0.1 M concentration can be further explored for solar cells application.

Acknowledgements

The financial assistance of the National Research Foundation (NRF/TWAS) of South Africa towards this research is hereby acknowledged.

References

Ahuja, D., & Tatsutani, M. (2009). Sustainable energy for developing countries. *SAPI EN. S. Surveys and Perspectives Integrating Environment and Society*(2.1).

AL-Jabiry, A. J. (2006). *Studying the Effect of Molarity on the Physical and Sensing Properties of Zinc Oxide Thin Films Prepared by Spray Pyrolysis Technique.* (PhD).

Bakr, N. A., Salman, S. A., & Shano, A. M. (2015). Effect of Co Doping on Structural and Optical Properties of NiO Thin Films Prepared By Chemical Spray Pyrolysis Method. *International Letters of Chemistry, Physics and Astronomy, 41*, 15--30.

Bari, R., Patil, S., & Bari, A. (2013). Effect of molarity of precursor solution on physical, structural, microstructural and electrical properties of nanocrystalline ZnO thin films. *Materials Technology, 28*(4), 214-220.

Barrett, C., & Massalski, T. (1980). Structure Metals Oxford: Pergamon.

Boschloo, G., & Hagfeldt, A. (2001). Spectroelectrochemistry of nanostructured NiO. *The Journal of Physical Chemistry B, 105*(15), 3039-3044.

Boyraz, C., & Urfa, Y. (2015). Effect of solution molarity on microstructural and optical properties of CdCr 2 S 4 thin films. *Materials Science in Semiconductor Processing, 36*, 1-6.

de Jong, B. H. W. S. (1989). *"Glass"* (5th ed. Vol. A12). Weinheim, Germany, : VCH

Drevet, R., Legros, C., Bérardan, D., Ribot, P., Dragoé, D., Cannizzo, C., . . . Andrieux, M. (2015). Metal organic precursor effect on the properties of SnO 2 thin films deposited by MOCVD technique for electrochemical applications. *Surface and Coatings Technology, 271*, 234-241.

Ebhota, W. S., Eloka-Eboka, A. C., & Inambao, F. L. (2014, 19-20 Aug. 2014). *Energy sustainability through domestication of energy technologies in third world countries in Africa.* Paper presented at the 2014 International Conference on the Eleventh industrial and Commercial Use

of Energy.
El-Nahass, M. M., Emam-Ismail, M., & El-Hagary, M. (2015). Structural, optical and dispersion energy parameters of nickel oxide nanocrystalline thin films prepared by electron beam deposition technique. *Journal of Alloys and Compounds, 646*, 937-945. doi: http://doi.org/10.1016/j.jallcom.2015.05.217
Eslamian, M. (2014). Spray-on thin film PV solar cells: advances, potentials and challenges. *Coatings, 4*(1), 60-84.
Fadheela, H. O. (2015). Structural and Optical Characterization of Nickel Oxide Thin Films Prepared by Spray Pyrolysis Technique. *Engineering and Tech Journal, 33*(part (B), No. 8), 10.
Gabal, M. (2003). Non-isothermal decomposition of NiC 2 O 4–FeC 2 O 4 mixture aiming at the production of NiFe 2 O 4. *Journal of Physics and Chemistry of Solids, 64*(8), 1375-1385.
Gardner, G. (2008). Alternative Energy and Nanotechnology. *Public Communication of Science and Technology, USA*.
Godse, P., Sakhare, R., Pawar, S., Chougule, M., Sen, S., Joshi, P., & Patil, V. P. (2011). Effect of annealing on structural, morphological, electrical and optical studies of nickel oxide thin films. *Journal of Surface Engineered Materials and Advanced Technology, 1*(02), 35.
Gowthami, V., Perumal, P., Sivakumar, R., & Sanjeeviraja, C. (2014). Structural and optical studies on nickel oxide thin film prepared by nebulizer spray technique. *Physica B: Condensed Matter, 452*, 1-6.
Green, M. A. (1982). Solar cells: operating principles, technology, and system applications.
Hussein, A. K. (2015). Applications of nanotechnology in renewable energies—A comprehensive overview and understanding. *Renewable and Sustainable Energy Reviews, 42*, 460-476.
Ismail, R. A., Ghafori, S. a., & Kadhim, G. A. (2013). Preparation and characterization of nanostructured nickel oxide thin films by spray pyrolysis. *Applied Nanoscience, 3*(6), 509-514.
Jlassi, M., Sta, I., Hajji, M., & Ezzaouia, H. (2014). Optical and electrical properties of nickel oxide thin films synthesized by sol–gel spin coating. *Materials Science in Semiconductor Processing, 21*, 7-13.
Joshi, S., Mudigere, M., Krishnamurthy, L., & Shekar, G. (2014). Growth and morphological studies of NiO/CuO/ZnO based nanostructured thin films for photovoltaic applications. *Chemical Papers, 68*(11), 1584-1592.
Keraudy, J., García Molleja, J., Ferrec, A., Corraze, B., Richard-Plouet, M., Goullet, A., & Jouan, P. Y. (2015). Structural, morphological and electrical properties of nickel oxide thin films deposited by reactive sputtering. *Applied surface science, 357, Part A*, 838-844. doi: http://doi.org/10.1016/j.apsusc.2015.08.199
Lewis, N. S. (2007). Toward cost-effective solar energy use. *Science, 315*(5813), 798-801.
Li, C., & Zhao, Z. (2010). *Preparation and characterization of nickel oxide thin films by a simple two-step method.* Paper presented at the Vacuum Electron Sources Conference and Nanocarbon (IVESC), 2010 8th International.
Magaña, C. R., Acosta, D. R., Martínez, A. I., & Ortega, J. M. (2006). Electrochemically induced electrochromic properties in nickel thin films deposited by DC magnetron sputtering. *Solar energy, 80*(2), 161-169.
Medicine, U. S. N. L. o. (2007). Nickel (II) Acetate Tetrahydrate, 98%. National Center for Biotechnology Information. PubChem Substance Database; SID=24854649. Retrieved June 6, 2017, 2017, from https://pubchem.ncbi.nlm.nih.gov/substance/24854649
Nam, W. J., Gray, Z., Stayancho, J., Plotnikov, V., Kwon, D., Waggoner, S., . . . Compaan, A. (2015). ALD NiO Thin Films As a Hole Transport-Electron Blocking Layer Material for Photo-Detector and Solar Cell Devices. *ECS Transactions, 66*(1), 275-279.
Park, N., Sun, K., Sun, Z., Jing, Y., & Wang, D. (2013). High efficiency NiO/ZnO heterojunction UV photodiode by sol–gel processing. *Journal of Materials Chemistry C, 1*(44), 7333-7338.
Pistorius, C. W. F. T. (1963). Neues Jahrb. Mineral., . *Monatsh.*, 30.
Rahal, A., Benhaoua, A., Jlassi, M., & Benhaoua, B. (2015). Structural, optical and electrical properties studies of ultrasonically deposited tin oxide (SnO 2) thin films with different substrate temperatures. *Superlattices and Microstructures, 86*, 403-411.
Reguig, B., Regragui, M., Morsli, M., Khelil, A., Addou, M., & Bernede, J. (2006). Effect of the precursor solution concentration on the NiO thin film properties deposited by spray pyrolysis. *Solar Energy Materials and Solar Cells, 90*(10), 1381-1392.
Saadati, F., Grayeli, A., & Savaloni, H. (2010). Dependence of the optical properties of NiO thin films on film thickness and nano-structure. *Journal of Theoretical and Applied Physics, 4*(1), 22-26.
Scherrer, P., & Nachr, G. (1918). Derivation of crystallite size *OH HO OH OH OH O OH*(2 (1918) 98).
Serrano, E., Rus, G., & Garcia-Martinez, J. (2009). Nanotechnology for sustainable energy. *Renewable and Sustainable Energy Reviews, 13*(9), 2373-2384.
Shaikh, S. K., Inamdar, S. I., Ganbavle, V. V., & Rajpure, K. Y. (2016). Chemical bath deposited ZnO thin film based UV photoconductive detector. *Journal of Alloys and Compounds, 664*, 242-249.
Soonmin, H. (2016). Preparation and Characterization of Nickel Oxide Thin Films: A review. . *International Journal of Applied Chemistry, 12*(2), 87-93.
Subramanian, B., Ibrahim, M. M., Senthilkumar, V., Murali, K., Vidhya, V., Sanjeeviraja, C., & Jayachandran, M. (2008). Optoelectronic and electrochemical properties of nickel oxide (NiO) films deposited by DC reactive magnetron sputtering. *Physica B: Condensed Matter, 403*(21), 4104-4110.
Vidales-Hurtado, M. A., & Mendoza-Galván, A. (2008). Electrochromism in nickel oxide-based thin films obtained by chemical bath deposition. *Solid State Ionics, 179*(35–36), 2065-2068. doi: http://doi.org/10.1016/j.ssi.2008.07.003
Wang, H., Wang, Y., & Wang, X. (2012). Pulsed laser deposition of the porous nickel oxide thin film at room temperature for high-rate pseudocapacitive energy storage. *Electrochemistry Communications, 18*, 92-95.
Wu, C.-C., & Yang, C.-F. (2015). Effect of annealing temperature on the characteristics of the modified spray deposited Li-doped NiO films and their applications in transparent heterojunction diode. *Solar Energy Materials and Solar Cells, 132*, 492-498.
Zhang, W., Ding, S., Yang, Z., Liu, A., Qian, Y., Tang, S., & Yang, S. (2006). Growth of novel nanostructured copper oxide (CuO) films on copper foil. *Journal of crystal growth, 291*(2), 479-484.
Zhu, Z., Bai, Y., Zhang, T., Liu, Z., Long, X., Wei, Z., . . . Yan, F. (2014). High‐Performance Hole‐Extraction Layer of Sol‐Gel‐Processed NiO Nanocrystals for Inverted Planar Perovskite Solar Cells. *Angewandte Chemie, 126*(46), 12779-12783.

CHAPTER 4 Part 2: INFLUENCE OF ANNEALING ON PROPERTIES OF SPRAY DEPOSITED NICKEL OXIDE FILMS FOR SOLAR CELLS

Part 2 discussed the optimization from the angle of annealing and published in Energy Procedia, Elsevier publishers:

To cite this article: Ukoba, O.K., Inambao F. L. and Eloka-Eboka, A.C. "Influence of annealing on properties of spray deposited nickel oxide films for solar cells," *Energy Procedia*, volume 142, December 2017, pp. 244–252. DOI: 10.1016/j.egypro.2017.12.039

Available online at www.sciencedirect.com

ScienceDirect

Energy Procedia 142 (2017) 244–252

Energy Procedia

www.elsevier.com/locate/procedia

9th International Conference on Applied Energy, ICAE2017, 21-24 August 2017, Cardiff, UK

Influence of annealing on properties of spray deposited nickel oxide films for solar cells

*[a]Ukoba, O.K., Inambao, F.L[a] and Eloka-Eboka, A.C[a]

[a]*Discipline of Mechanical Engineering, University of KwaZulu-Natal, Durban, 4041, South Africa*

Abstract

Nickel oxide thin films were deposited on soda lime glass substrates by spray pyrolysis technique (SPT). Post-deposition annealing was carried out at 450 ºC. Effects of annealing on the structural, elemental and surface morphological properties of the thin NiO films were investigated. XRD confirms polycrystalline with cubic crystalline structures of deposited and annealed NiO films. Preferred orientation was along (1 1 1) peak with intensity along (2 0 0) peak improved by annealing. The annealing process improved on formation of crystalline phases. XRD patterns have peak diffraction at (2θ = 37 º, and 43 º) for (1 1 1) for deposited and annealed. Peak diffraction at (2θ = 64 º, and 79 º) for (2 0 0) planes for 0.1 M and annealed respectively. Annealing improved on the film thickness by over 10 %. Surface morphology of deposited and annealed NiO films reveals nanocrystalline grains with uniform coverage of the substrate surface with randomly oriented morphology. Larger flakes are formed as a result of the annealing process. EDX elemental NiO films composition revealed presence of Ni and O elements in NiO films. A decrease in oxygen concentration was also observed confirming positive effect of annealing as an optimization process. Optimization of nickel oxide deposition process parameters offers opportunities for efficient and affordable solar cells.

Peer-review under responsibility of the scientific committee of the 9th International Conference on Applied Energy.

Keywords: NiO; solar cells material; annealing, spray pyrolysis technique

1. Introduction

Population growth geometrically increases the need for more demand for energy [1]. Solar energy is a viable source of sustainable energy. Present solar panels are still not affordable to low income earners. This is caused by the expensive nature of silicon. Current solar photovoltaics market is dominated by silicon. Silicon is an abundant element

* Corresponding author. Tel.: +27640827616 and +2348035431913; fax: +0-000-000-0000 .
E-mail address: ukobaking@yahoo.com

1876-6102
Peer-review under responsibility of the scientific committee of the 9th International Conference on Applied Energy .
10.1016/j.egypro.2017.12.039

but large production of it for photovoltaic is expensive. Key Materials selection for future solar cells are abundance and inexpensive elements for large scale production [2]. Nanostructured metal oxides fit this description. Metal Oxide thin films have promising technological potentials in solar cells. They require both vast area electrical contact and optical access in visible region of light spectrum [3]. Fabrication of nanostructure metal oxide films has generated interests over the years [4-8]. There are wide range of applications in radiation detector, solar cells, semiconducting devices, laser materials and thermoelectric devices optoelectronic devices [9-12].

Nanostructured metal oxides with p-type conductivity are rare. Nickel Oxide (NiO) is a one of few p-type semiconductors [13] with wide band gap from 3.5 eV to 4.0 eV [14]. It offers great prospect for large scale production of efficient low cost solar energy. NiO has rhombohedral or cubic structure and possesses pale green color. It has excellent durability and electrochemical stability [15]. It possesses large range of optical densities due to better optical, electrical and magnetic properties. It is a promising material for various applications which includes: solar cells, UV detectors, electrochromic devices, anti-ferromagnetic layers, p-type transparent conductive thin films, chemical sensors [16-20].

Nickel oxide thin films have been deposited using different methods; laser ablation [21], sputtering [22], sol–gel [23], chemical bath deposition [24] among others. Spray pyrolysis has the advantages of easy, quick, economic and large area deposition [25]. Spray pyrolysis is a process for depositing films. Solutions are sprayed on a heated surface and constituents react to form chemical compounds [26]. Chemical reactants are chosen to enable unwanted product to be decompose at the deposition temperature [27].

Optimization of NiO deposition process parameters offers opportunities for its usage in varied applications especially solar cells [28]. This study is on the influence of annealing temperature on resultant properties of spray pyrolysis deposited nickel oxide thin films for possible solar cells application.

Several studies have used Nickel chloride over nickel acetate as precursor [29, 30]. Nickel acetate precursor is used in this study. It does not react with the spraying gun unlike the Nickel chloride which also leaves traces of chlorine [31]. This study is an improvement to existing approach of depositing NiO films for solar cells application.

2. Experimental Procedure

2.1. Substrate selection and Cleaning

Soda lime glass was used as substrate. It was first washed with detergent and cotton wool. Thereafter it was cleaned chemically using acetone, methanol and isopropanol for 15 minutes each in ultrasonic bath. It was finally washed with deionized water and dried by flow of nitrogen gas.

2.2. Preparation of the solution for spray pyrolysis

Analytical grade nickel (II) acetate tetrahydrate was used. Precursor solutions were sprayed on glass substrates with air as carrier gas by spray pyrolysis technique (SPT). Pure nickel oxide thin films were deposited with concentrations of 0.05 M and 0.1 M using nickel (II) acetate $Ni(C_2H_3O_2)_2.4H_2O$ as precursor. Each precursor concentration was dissolved in 50 ml of distilled water. Solution mixtures were stirred thoroughly with a magnetic stirrer for 15 minutes leading to the formation of a pale green solution. Solution was sprayed manually on the pre-heated glass substrate kept at 350 ^oC. The sprayed 0.1 M films was annealed for 60 minutes at 450 ^oC in a furnace. This became the annealed samples. Sprayed solution on the preheated substrate glass undergoes evaporation, solute precipitation and pyrolytic decomposition according to Equations (1) [32]. The end product is nickel oxide thin films.

$$\mathrm{Ni}(C_2H_3O_2)_2.4H_2O \xrightarrow{heat} NiO + 7H_2O \uparrow + 4CO_2 \uparrow \qquad (1)$$

Optimum deposition parameters of the spray deposited NiO films are shown in table 1. Thermocouple was fixed to substrate's surface to record substrate temperature. Prepared NiO films were observed to be gray in colour, uniform and strongly adhered to the glass substrate.

Table 1. Optimum deposition parameter of SPT NiO films

Deposition parameter	Value
Substrate temperature	350 ºC
Height of spraying nozzle to substrate distance	20 cm
Spray rate	1 ml/min
Spray time	1 minute
Time between sprays	30 seconds
Carrier gas	Filled compressed air of 1 bar

2.3. Characterization

Morphological property of deposited and annealed NiO film was studied using ZEISS ULTRA PLUS Field Emission Gun Scanning Electron Microscope (FEGSEM). Elemental composition was done with Energy Dispersive X-ray Spectrometer (EDS or EDX: "AZTEC OXFORD DETECTOR"). Structural properties of deposited NiO film were investigated using EMPYREAN (PANalytical) X-ray powder diffractometer for a range of 5 º to 90 º 2θ angles. Results of characterized annealed and un-annealed samples are hereby compared.

3. Results and Discussion

3.1. Morphological studies

Figure 1 shows the SEM micrographs for both annealed and not annealed deposited NiO films. The SEM micrographs reveal homogeneous, smooth, well adherent films devoid of pinholes and cracks. Bigger flakes of grain were observed as a result of annealing. It is as a result of accelerated inter-diffusion between the deposited atoms and the glass substrates. The annealed samples show more concentration of particles, closely parked and bigger flakes compared with the un-annealed. This is due to the rearrangement and alignment caused by application of heat to the films. This agrees with previous report of Godse, et al. [33]. This confirms that annealing affects NiO films morphology.

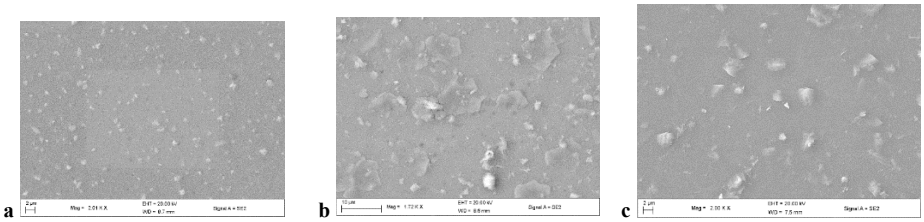

Fig. 1. SEM micrographs of nickel oxide (NiO) film on glass substrate at (a) 0.05M un-annealed; (b) 0.1M un-annealed (c) 0.1M annealed

3.2. Elemental composition analysis

EDX spectra in Figure 2 confirm presence of Ni and O elements in deposited and annealed NiO thin films. This is in agreement with previous report of Hakim, et al. [34]. Additional Si element was also observed. This is because Silicon (Si) is present in soda-lime glass or soda-lime-silica glass substrate [35]. A decrease was observed for Si peak intensity due to increase surface roughness from annealing process.

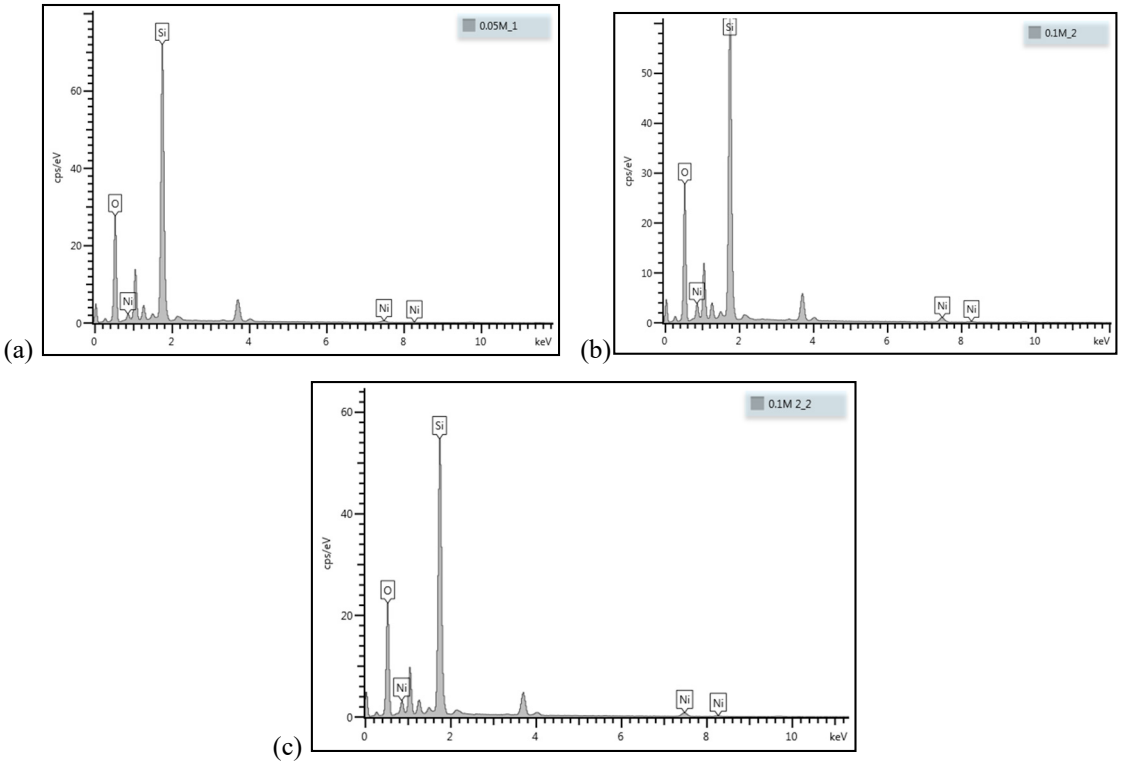

Fig. 2. EDX spectra of deposited and annealed NiO thin films (a) 0.05M (b) 0.1M (c) Annealed

3.3. Variation of the Film Thicknesses with precursor solution concentration

Films thickness was investigated as a function of deposited and annealed NiO films. Measured data are graphically represented in Figure 3.

Using the weight difference method, film thickness was calculated using the relationship in Equation (2) [33]:

$$t = \frac{m}{A\rho} \qquad (2)$$

Where t is the thickness of the film while m is the actual mass deposited onto the substrate, A is the area of the film and ρ is the density of material. This is represented in Figure 4.

It was observed that measured and calculated values are in good agreement. It was found that film thickness was improved with annealing and agrees with previous report of Madhavi, et al. [36]. This is as a result of accumulation of deposited NiO on substrate. This was collaborated by EDX results in Figure 2. During deposition, nozzle to substrate height and deposition time were kept constant to control thickness of NiO thin films. Average thickness range of NiO thin films was found between 6.277 and 11.85 µm.

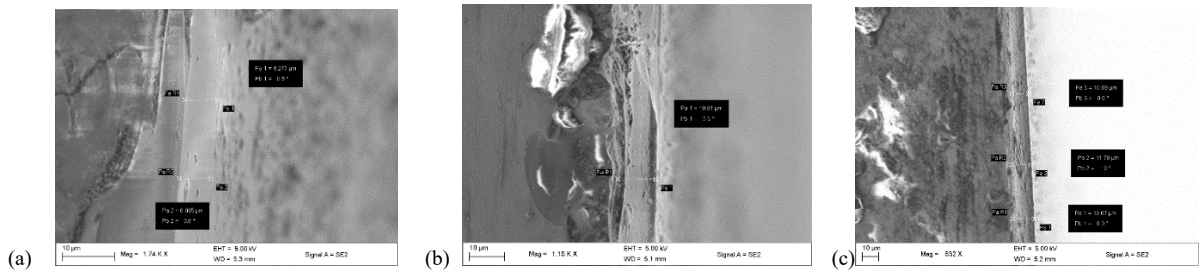

Fig. 3. Measured NiO film thickness at (a) 0.05 M; (b) 0.1 M; (c) annealed

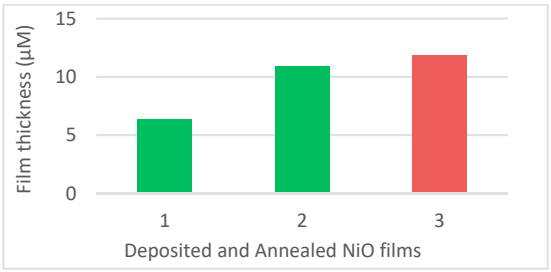

Fig. 4. Calculated film thickness of NiO films with green for deposited and red for annealed films

3.4. Structural studies

Structural properties of the NiO sprayed films were examined by X-Ray diffraction technique. Figure 5 shows XRD of the thin films with concentrations of 0.05 M, 0.1 M and annealed pattern. XRD patterns have peak diffraction at (2θ = 37 º, and 43 º) for (1 1 1) and (2 0 0) planes for all samples. Peak diffraction occurs at (2θ = 64 º, and 79 º) for (2 2 0) plane for 0.1 M and annealed respectively. Annealed samples have higher intensity for all planes compared with the un-annealed. This corresponds to JCPDS 04- 0835 for Bunsenite which is NiO [37]. Highest intensity was recorded for (1 1 1) having a strong peak when 2θ = 37 º for precursor solution of anneal and the un-annealed samples which agrees with previous report of Gomaa, et al. [38]. This is as result of increase in grain growth caused by larger thicknesses. It can also be due to the increase in crystallinity caused by thermal treatment. It is a confirmation of the polycrystalline with cubic crystalline structures of deposited NiO films which is in agreement with previous report [39, 40]. There was increase at intensity peak of (2 0 0) for all samples with emergence of third peak (2 2 0) for 0.1 M and the annealed samples.

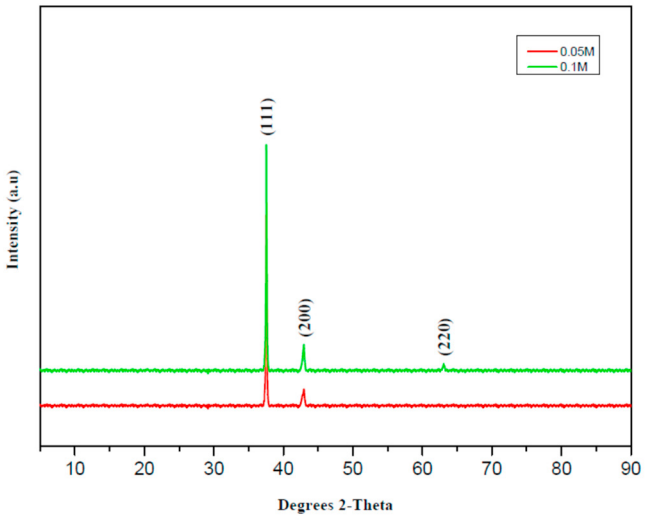

(a)

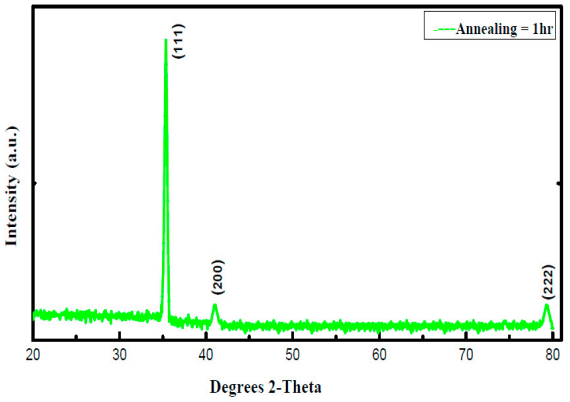

(b)

Fig. 5. XRD patterns of nanostructured NiO films (a) un-annealed; (b) un-annealed at one hour

The average crystallite size was obtained using Debye Scherer formula [41, 42] in Equation (3).

$$D = \frac{k\lambda}{\beta \cos\theta} \quad (3)$$

Where; B is full width at half maximum (FWHM) intensity of the peak (in Radian), λ is wavelength, θ is Bragg's diffraction angle and k is 0.89 respectively.

Lattice constant was found to be 4.1855, 4.1850 Å and 4.19 Å for 0.05 M, 0.1 M and annealed respectively. This is an improvement on standard lattice constant of NiO film value of 4.176 Å reported by Pistorius [43].

Micro strain was produced through growth of thin films and was calculated using the formula in equation (4) [44]

$$\delta = \frac{d_{ASTM} - d_{XRD}}{d_{ASTM}} \times 100 \quad (4)$$

Where "d" is the lattice constant and δ is micro strain.

A plot of NiO film micro strain against deposited and annealed NiO films is shown in Figure 6. It shows that annealing process affects micro strain. Micro strain represents compression as seen in Table 2 which gives detail result of micro strain, lattice constants and 2θ values for deposited and annealed NiO films.

Table 2: Calculated parameters from XRD data

Parameter		0.05 M	0.1 M	Annealed
	hkl	37	37	37
2θ	(1 1 1)			
	(2 0 0)	43	43	43
	(2 2 0)	X	63	79
Lattice constant d (Å)	recorded XRD	4.1855	4.1850	4.190
	ASTM	4.1684	4.1684	4.1684
Micro strain (δ) %		-0.4102	-0.3982	-0.5280

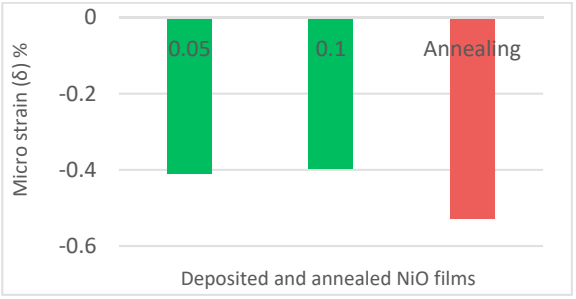

Fig. 6. Plot of micro strain against deposited and annealed NiO films.

4. Conclusion

In this study, nanostructured nickel oxide films were successfully deposited by spray pyrolysis of nickel acetate on glass substrate. The effect of annealing of NiO films on elemental, morphological and structural properties were studied with a view to optimizing it for solar cells application.

Annealing helps to improve on surface morphology of NiO films and also improves the film thickness of nickel oxide films from 6.277 to 11.851 µm.

Crystalline structure of NiO films are improved by application of thermal conditioning (annealing). Intensity of NiO films increased with annealing. Peak diffraction obtained at (2θ = 37 º and 43 º) for (1 1 1) and (2 0 0) planes respectively. Peak diffraction at (2θ = 64 º and 79 º) for (2 2 0) plane for 0.1 M and annealed sample. Lattice constant decreased with annealing. Film strain was improved upon by annealing. Micro strain of films shows compression and increased with annealing.

Annealing of deposited NiO films has effect on overall properties of nanostructured nickel oxide thin films. Therefore, annealed NiO films can be further explored for solar cells application.

Acknowledgements

The financial assistance of the National Research Foundation (NRF/TWAS) of South Africa towards this research is hereby acknowledged.

References

[1] A. M. Omer, "Energy, environment and sustainable development," *Renewable and sustainable energy reviews,* vol. 12, pp. 2265-2300, 2008.

[2] M. Inpasalini, R. G. Devi, D. Balamurugan, B. Ieyaprakash, and J. B. B. Rayappan, "Solar Cell Application," *Journal of Applied Sciences,* vol. 12, pp. 1742-1745, 2012.

[3] A. Balu, V. Nagarethinam, M. Suganya, N. Arunkumar, and G. Selvan, "Effect of solution concentration on the structural, optical and electrical properties of SILAR deposited CdO thin films," *J. Electron Devices,* vol. 12, pp. 739-749, 2012.

[4] A. Czapla, E. Kusior, and M. Bucko, "Optical properties of non-stoichiometric tin oxide films obtained by reactive sputtering," *Thin Solid Films,* vol. 182, pp. 15-22, 1989.

[5] R. Drevet, C. Legros, D. Bérardan, P. Ribot, D. Dragoé, C. Cannizzo*, et al.*, "Metal organic precursor effect on the properties of SnO 2 thin films deposited by MOCVD technique for electrochemical applications," *Surface and Coatings Technology,* vol. 271, pp. 234-241, 2015.

[6] M. Jlassi, I. Sta, M. Hajji, and H. Ezzaouia, "Optical and electrical properties of nickel oxide thin films synthesized by sol–gel spin coating," *Materials Science in Semiconductor Processing,* vol. 21, pp. 7-13, 2014.

[7] A. Rahal, A. Benhaoua, M. Jlassi, and B. Benhaoua, "Structural, optical and electrical properties studies of ultrasonically deposited tin oxide (SnO 2) thin films with different substrate temperatures," *Superlattices and*

Microstructures, vol. 86, pp. 403-411, 2015.
[8] S. K. Shaikh, S. I. Inamdar, V. V. Ganbavle, and K. Y. Rajpure, "Chemical bath deposited ZnO thin film based UV photoconductive detector," *Journal of Alloys and Compounds,* vol. 664, pp. 242-249, 2016.
[9] S. Farhadi and Z. Roostaei-Zaniyani, "Preparation and characterization of NiO nanoparticles from thermal decomposition of the [Ni (en) 3](NO 3) 2 complex: a facile and low-temperature route," *Polyhedron,* vol. 30, pp. 971-975, 2011.
[10] M. Salavati-Niasari, N. Mir, and F. Davar, "A novel precursor in preparation and characterization of nickel oxide nanoparticles via thermal decomposition approach," *Journal of Alloys and Compounds,* vol. 493, pp. 163-168, 2010.
[11] L. Wang, Y. Hao, Y. Zhao, Q. Lai, and X. Xu, "Hydrothermal synthesis and electrochemical performance of NiO microspheres with different nanoscale building blocks," *Journal of Solid State Chemistry,* vol. 183, pp. 2576-2581, 2010.
[12] J. Wu and D. Xue, "Progress of science and technology of ZnO as advanced material," *Science of Advanced Materials,* vol. 3, pp. 127-149, 2011.
[13] M. Guziewicz, J. Grochowski, M. Borysiewicz, E. Kaminska, J. Z. Domagala, W. Rzodkiewicz*, et al.*, "Electrical and optical properties of NiO films deposited by magnetron sputtering," *Opt. Appl,* vol. 41, pp. 431-440, 2011.
[14] G. Boschloo and A. Hagfeldt, "Spectroelectrochemistry of nanostructured NiO," *The Journal of Physical Chemistry B,* vol. 105, pp. 3039-3044, 2001.
[15] B. Subramanian, M. M. Ibrahim, V. Senthilkumar, K. Murali, V. Vidhya, C. Sanjeeviraja*, et al.*, "Optoelectronic and electrochemical properties of nickel oxide (NiO) films deposited by DC reactive magnetron sputtering," *Physica B: Condensed Matter,* vol. 403, pp. 4104-4110, 2008.
[16] C. Li and Z. Zhao, "Preparation and characterization of nickel oxide thin films by a simple two-step method," in *Vacuum Electron Sources Conference and Nanocarbon (IVESC), 2010 8th International*, 2010, pp. 648-649.
[17] W. J. Nam, Z. Gray, J. Stayancho, V. Plotnikov, D. Kwon, S. Waggoner*, et al.*, "ALD NiO Thin Films As a Hole Transport-Electron Blocking Layer Material for Photo-Detector and Solar Cell Devices," *ECS Transactions,* vol. 66, pp. 275-279, 2015.
[18] N. Park, K. Sun, Z. Sun, Y. Jing, and D. Wang, "High efficiency NiO/ZnO heterojunction UV photodiode by sol–gel processing," *Journal of Materials Chemistry C,* vol. 1, pp. 7333-7338, 2013.
[19] C.-C. Wu and C.-F. Yang, "Effect of annealing temperature on the characteristics of the modified spray deposited Li-doped NiO films and their applications in transparent heterojunction diode," *Solar Energy Materials and Solar Cells,* vol. 132, pp. 492-498, 2015.
[20] Z. Zhu, Y. Bai, T. Zhang, Z. Liu, X. Long, Z. Wei*, et al.*, "High‐Performance Hole‐Extraction Layer of Sol‐Gel‐Processed NiO Nanocrystals for Inverted Planar Perovskite Solar Cells," *Angewandte Chemie,* vol. 126, pp. 12779-12783, 2014.
[21] I. Fasaki, M. Kandyla, M. Tsoutsouva, and M. Kompitsas, "Optimized hydrogen sensing properties of nanocomposite NiO: Au thin films grown by dual pulsed laser deposition," *Sensors and Actuators B: Chemical,* vol. 176, pp. 103-109, 2013.
[22] H.-L. Chen and Y.-S. Yang, "Effect of crystallographic orientations on electrical properties of sputter-deposited nickel oxide thin films," *Thin Solid Films,* vol. 516, pp. 5590-5596, 2008.
[23] D. S. Dalavi, R. S. Devan, R. S. Patil, Y.-R. Ma, and P. S. Patil, "Electrochromic performance of sol–gel deposited NiO thin film," *Materials Letters,* vol. 90, pp. 60-63, 2013.
[24] M. Z. Sialvi, R. J. Mortimer, G. D. Wilcox, A. M. Teridi, T. S. Varley, K. U. Wijayantha*, et al.*, "Electrochromic and colorimetric properties of Nickel (II) oxide Thin films prepared by aerosol-assisted chemical vapor deposition," *ACS applied materials & interfaces,* vol. 5, pp. 5675-5682, 2013.
[25] R. Krishnakumar, V. Subramanian, Y. Ramprakash, and A. Lakshmanan, "Thin film preparation by spray pyrolysis for solar cells," *Materials chemistry and physics,* vol. 16, pp. 385-395, 1987.
[26] L. Filipovic, S. Selberherr, G. C. Mutinati, E. Brunet, S. Steinhauer, A. Köck*, et al.*, "A method for simulating spray pyrolysis deposition in the level set framework," *Eng. Lett,* vol. 21, pp. 224-240, 2013.
[27] J. B. Mooney and S. B. Radding, "Spray pyrolysis processing," *Annual Review of Materials Science,* vol. 12, pp. 81-101, 1982.
[28] P. S. Patil, "Versatility of chemical spray pyrolysis technique," *Materials Chemistry and physics,* vol. 59, pp.

185-198, 1999.
[29] R. A. Ismail, S. a. Ghafori, and G. A. Kadhim, "Preparation and characterization of nanostructured nickel oxide thin films by spray pyrolysis," *Applied Nanoscience,* vol. 3, pp. 509-514, 2013.
[30] M. Vigneshkumar, S. Muthulakshmi Suganya, J. Pandiarajan, A. Saranya, and N. Prithivikumaran, "Structural and Optical Properties of Nanocrystalline Nickel Oxide Thin Film by Spray Pyrolysis Technique," *International Journal of Technical Research and Applications,* pp. 52-56, 2016.
[31] H. Kamal, E. Elmaghraby, S. Ali, and K. Abdel-Hady, "Characterization of nickel oxide films deposited at different substrate temperatures using spray pyrolysis," *Journal of crystal growth,* vol. 262, pp. 424-434, 2004.
[32] J. C. De Jesus, I. González, A. Quevedo, and T. Puerta, "Thermal decomposition of nickel acetate tetrahydrate: an integrated study by TGA, QMS and XPS techniques," *Journal of Molecular Catalysis A: Chemical,* vol. 228, pp. 283-291, 2005.
[33] P. Godse, R. Sakhare, S. Pawar, M. Chougule, S. Sen, P. Joshi*, et al.*, "Effect of annealing on structural, morphological, electrical and optical studies of nickel oxide thin films," *Journal of Surface Engineered Materials and Advanced Technology,* vol. 1, p. 35, 2011.
[34] A. Hakim, J. Hossain, and K. Khan, "Temperature effect on the electrical properties of undoped NiO thin films," *Renewable Energy,* vol. 34, pp. 2625-2629, 2009.
[35] B. H. W. S. de Jong, *"Glass"*, 5th ed. vol. A12. Weinheim, Germany, : VCH 1989.
[36] A. Madhavi, G. Harish, and P. S. Reddy, "Effect of Annealing Temperature on Optical and Electrical Properties of Electron Beam Evaporated NiO Thin Films," 2016.
[37] M. Gabal, "Non-isothermal decomposition of NiC 2 O 4–FeC 2 O 4 mixture aiming at the production of NiFe 2 O 4," *Journal of Physics and Chemistry of Solids,* vol. 64, pp. 1375-1385, 2003.
[38] M. Gomaa, M. Boshta, B. Farag, and M. Osman, "Structural and optical properties of nickel oxide thin films prepared by chemical bath deposition and by spray pyrolysis techniques," *Journal of Materials Science: Materials in Electronics,* vol. 27, pp. 711-717, 2016.
[39] A. Balu, V. Nagarethinam, N. Arunkumar, and M. Suganya, "Nanocrystalline NiO thin films prepared by a low cost simplified spray technique using perfume atomizer," *J. Electron Devices,* vol. 13, pp. 920-930, 2012.
[40] H. O. Fadheela, "Structural and Optical Characterization of Nickel Oxide Thin Films Prepared by Spray Pyrolysis Technique," *Engineering and Tech Journal,* vol. 33, p. 10, 2015.
[41] P. Scherrer and G. Nachr, "Derivation of crystallite size " *OH HO OH OH OH O OH,* 1918.
[42] C. Barrett and T. Massalski, "Structure Metals Oxford," ed: Pergamon, 1980.
[43] C. W. F. T. Pistorius, " Neues Jahrb. Mineral., ," *Monatsh.,* p. 30., 1963.
[44] A. J. AL-Jabiry, "Studying the Effect of Molarity on the Physical and Sensing Properties of Zinc Oxide Thin Films Prepared by Spray Pyrolysis Technique," PhD, Applied Science Dep. University of Technology,, 2006.

Chapter 4 Part 3

This part is on the effect of ageing on nanostructured NiO thin films for solar cells fabrication published in Journal of Physical Science (JPS):

Ukoba, O.K., Eloka-Eboka, A.C. and Inambao F.L. "Optimizing Aged Nanostructured nickel oxide thin films for solar cells" ***Journal of Physical Science (JPS),*** **2018 (Accepted)**

OPTIMIZING AGED NANOSTRUCTURED NICKEL OXIDE THIN FILMS FOR SOLAR CELLS FABRICATION

Ukoba, O.K; Inambao, FL and Eloka-Eboka, A.C

Discipline of Mechanical Engineering, University of Kwazulu-Natal,

Durban, South Africa.

*Corresponding Author: ukobaking@yahoo.com

Abstract

The effect of ageing on properties of nickel oxide thin films deposited using spray pyrolysis technique was the focus of this study. Freshly prepared and aged nickel oxide films were successfully deposited by spray pyrolysis technique on glass substrate at 350 °C. The morphological, elemental, structural and optical properties of two different films were studied. The surface morphology was studied using Field Emission Gun Scanning Electron Microscope. The X-ray diffraction shows that both freshly prepared and aged films have a polycrystalline cubic structure with preferred orientation along the (1 1 1) and (2 0 0) planes. Optical studies show a high transparency in the visible and NIR regions. The band gap grew with ageing from 3.60 eV to 3.70 eV. The optical constant including the refractive index and extinction coefficient reduced with ageing. Based on the result obtained, the prepared sample can be used as the absorber layer of a solar cells. The findings may open new frontiers in affordable and efficient solar cell fabrication in developing countries.

Keywords: Aged; NiO; Spray Pyrolysis Technique; optical properties; solar cells

1. Introduction

Over 20 % of world population still struggles with access to electricity,[1] with the majority of those affected being from sub-Sahara Africa and south Asia.[2] The solution to such electricity woes may be found in nanostructured metal oxide.[3] This is due to the low cost of processing and the simplicity of deposition of metal oxides. Nickel oxide (NiO) holds great promise being a p-type metal oxide with vast range of applications.[4-6] Several methods have been used to deposit NiO with a view to optimizing it for various applications. The deposition methods are hydrothermal growth,[7] laser ablation,[8] sol-gel,[9] sputtering,[10] and atomic layer deposition,[11] among others. However, Spray Pyrolysis Technique (SPT) is preferred for films because it allows coatings on large areas in thin layers with uniform thickness.[12] SPT's simplicity, affordability and the possibilities for mass production[13, 14] singled it out for this study.

The optical properties of a metal oxide play a vital role in its usage in the fabrication of optoelectronic devices.[15] The optical properties reveal information relating to the microscopic behavior of the material. Very few works have studied the effect of ageing on NiO films despite the promise it holds.[16] The objectives of this study were to prepare and deposit nanostructured NiO thin films on a glass substrate using SPT, then to determine the effect of ageing on the properties of the NiO films.

2. Methodology

Soda lime glass substrate was chemically and ultrasonically cleaned before usage for deposition. The precursor was a mixture of analytical grade nickel acetate tetrahydrate $Ni(CH_3COO)_2.4H_2O$ of 0.05 M mixed and stirred in 50 ml distilled water. The freshly prepared sample was spray deposited immediately after preparation. The aged sample was left for 192 hours (one week and one day) after mixing to age before deposition. The samples were spray deposited using the set-up[17] in Figure 4.15.

The sprayed solution on the preheated substrate glass undergoes evaporation, solute precipitation and pyrolytic decomposition according to Equation (1).[18] The end product is a nickel oxide thin film.

$$Ni(CH_3COO)_2.4H_2O \xrightarrow{heat} NiO + 7H_2O \uparrow + 4CO_2 \uparrow \quad (1)$$

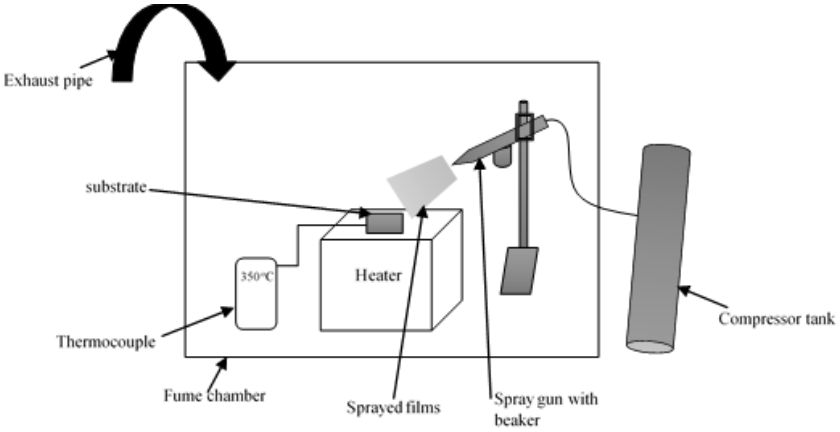

Figure 4.1. experimental set-up of Spray Pyrolysis Technique

The pictorial representation of the experimental set up is shown in Figure 4.16. It shows the various component of the equipment

Figure 4.2. Experimental set up of the spray pyrolysis

Optimum deposition parameters of the spray deposited NiO films are shown in Table 4.5. A thermocouple was fixed to the substrate's surface to record substrate temperature.

Table 4.1. Optimum deposition parameter of SPT NiO films

Deposition parameter	Value
Substrate temperature	350 ºC
Height of spraying nozzle to substrate distance	20 cm
Spray rate	1 ml/min
Spray time	1 min
Time between sprays	30 sec
Carrier gas	Filled compressed air of 1 bar

The prepared NiO films were observed to be gray in colour, uniform and strongly adherent to the glass substrate.

3. Characterization

The morphology of deposited NiO film was studied using a Scanning Electron Microscope (ZEISS EVO MA15VP). An Energy Dispersive X-ray Spectrometer (EDS or EDX: "GENESIS XM2") was used for assessing elemental composition. An Empyrean (PANalytical) X-ray powder diffractometer was used for structural properties of deposited NiO films from 5º to 90º 2Ɵ angles. The absorption of the film was conducted using a

Perkin Elmer Spectrum 100 Fourier Transform Infrared Spectrometer (FTIR). The measured film thickness was compared with the weight difference method. Optical properties were studied in wavelength range of 300 nm to 1000 nm with a SHIMADZU UV-3600UV-VIS Spectrometer. The results of characterized freshly prepared and aged samples were compared and are reported on below.

4. Results and discussion

4.1 Morphological studies

The surface morphology of the freshly prepared and the aged NiO films are represented in Figure 4.17. The freshly prepared micrograph reveals scattered distribution of the tiny particles across the surface of the film. The aged films however reveal broader flake-like particles across the surface of the film. Both films have even distribution, are adherent to the film surface, and are devoid of cracks. This may be attributed to proper optimization of the deposition parameters. This is an improvement on the 24-hour aged NiO films reported by Sriram and Thayumanavan.[16]

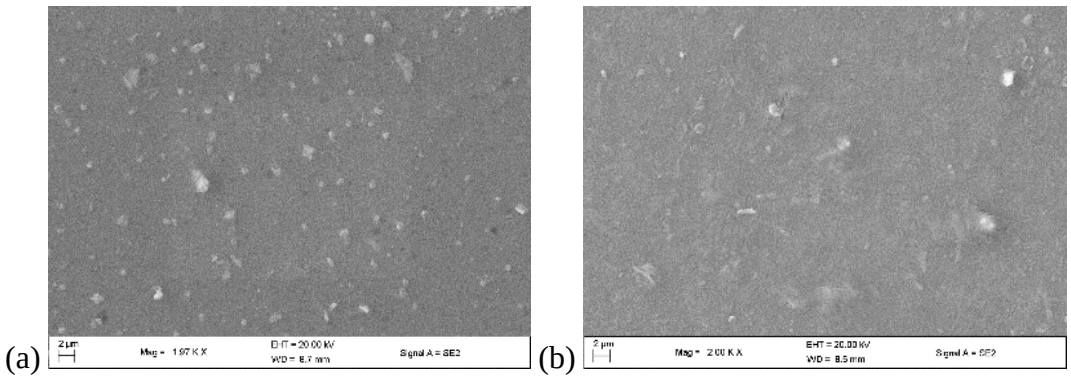

Figure 4.3. SEM micrographs of (NiO) film on glass substrate (a) freshly prepared (b) aged for one week and one day

4.2 Elemental composition analysis

The elemental composition analysis of freshly prepared and aged NiO thin films are presented in Figure 4.18. Both spectra confirm the presence of Ni and O elements in the NiO thin films. Oxygen concentration decreased with ageing. Similarly, nickel weight percent grew for the aged sample in comparison with the freshly prepared film. This may be due to increment in film grown on the glass substrate causing reduction in oxygen concentration of the aged films. This observation was also reported by Lu and Hwang.[19] Apart from the nickel and oxygen, silicon (SI) was also observed. The existence of the Si is as a result of the elemental composition of the soda-lime glass used as substrate[20] and the EDX of the empty soda-lime glass is shown in the Figure 4.18c.

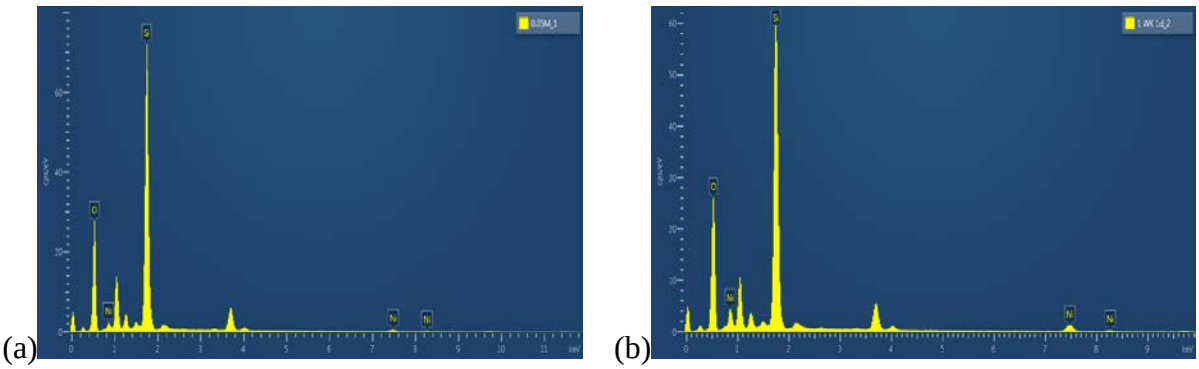

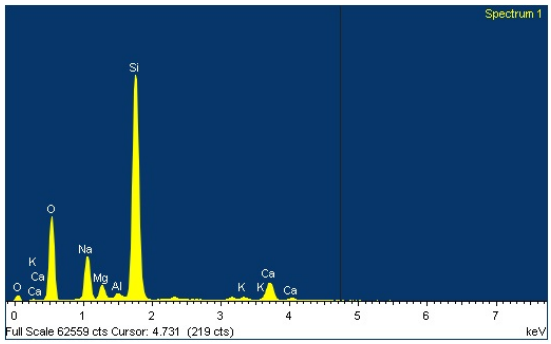

(c)

Figure 4.4. EDX spectra of (NiO) film on glass substrate (a) Freshly prepared (b) Aged for one week and one day (c) EDX of empty glass

4.3 Structural studies

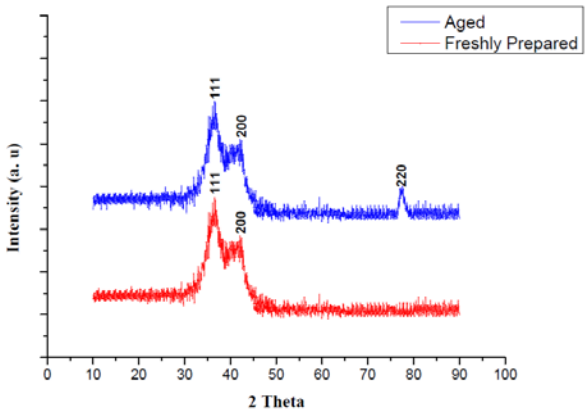

Figure 4.5. XRD of aged and freshly prepared NiO films

The phase present and the preferred orientation of deposited nanostructured NiO films was determined using an x-ray diffractometer. The XRD patterns of the aged and freshly deposited films are shown in Figure 4.19. The films were observed to be polycrystalline with cubic structures. The peaks for the freshly prepared films were observed at 2Θ values of 37º and 43º for (1 1 1) and (2 0 0) planes respectively. However, the aged films were observed at 2Θ values of 36.38º, 43.47º and 62.01º for (1 1 1), (2 0 0) and (2 2 0) respectively. The XRD analysis confirms Bunsenite which corresponds to JCPDS card number 89-7130 for NiO films. The slight difference in the diffraction angle (2Θ) of the freshly prepared and aged sample may be attributed to the ageing effect of the precursor. The diffraction angle (2Θ) for the aged obtained for this study gives an improvement on earlier reported value of on 2Θ = 36.362º, 2Θ = 43.43º and 2Θ = 62.58º obtained for 24-hour aged NiO films earlier reported by Sriram and Thayumanavan.[16]

The films' average particle size was obtained from the Scherrer expression[21, 22] in Equation (2)

$$D = \frac{k\lambda}{\beta \cos\theta} \qquad (2)$$

Where: B is full width at half maximum (FWHM), λ is wavelength, θ represent Bragg's diffraction angle and k is 0.89 respectively. The values are 22 nm and 60.4 nm.

4.4 NiO films absorption (FTIR)

Figure 4.20 gives the FT-IR spectra used to identify molecular components and the structure of the NiO films. It is done in the range of 400 cm^{-1} and 4000 cm^{-1}. The Ni-O stretching vibration mode was recorded in the broad absorption band region of 432 cm^{-1} to 698 cm^{-1}. This was also earlier reported as the range of absorption for NiO films.[23] The broadness confirms that the NiO are nanocrystalline. The NiO film FTIR absorption is blue-shifted due to their nanostructure size. Other significant absorption bands were also recorded. There is no band indicating

the presence of other groups. This confirms that there is no impurity in the film and that the sample was washed and well cleaned. This result agrees with standard FTIR data for NiO films as reported by Qiao et al.[24]

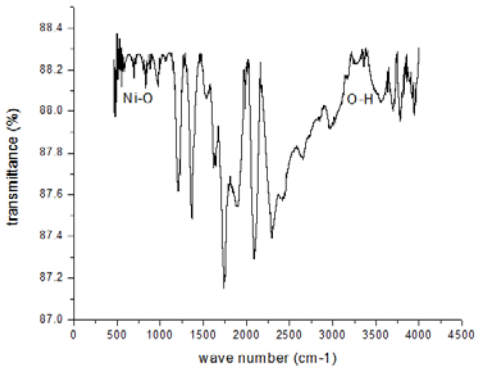

Figure 4.6. FTIR spectrum of of aged and freshly prepared NiO films

4.5 Optical properties

4.5.1 Film thickness

The film thickness was considered for both freshly prepared and aged films. The film thickness was obtained using SEM cross sectional profiling as shown in Figure 4.21 and also using the weight difference method expressed in Equation (3)[25] and shown in Figure 4.22. There is no marked difference between both values.

$$t = \frac{m}{A\rho} \qquad (3)$$

Where: *t* denotes film thickness, *m* represents the actual mass deposited, *A* denotes thin film area while ρ represents the density of material. The film thickness grew with ageing. The thickness of the films was controlled by keeping deposition parameters constant. The NiO thin films average thickness was between 6.277 µm and 8.627 µm for freshly prepared and aged respectively.

(a)

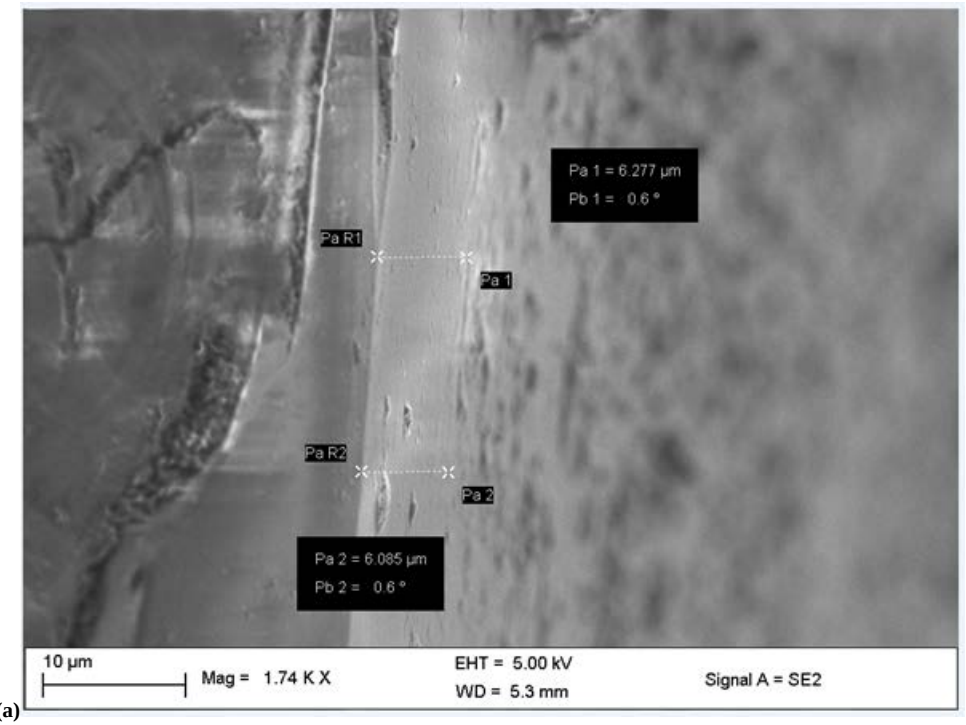

(b)

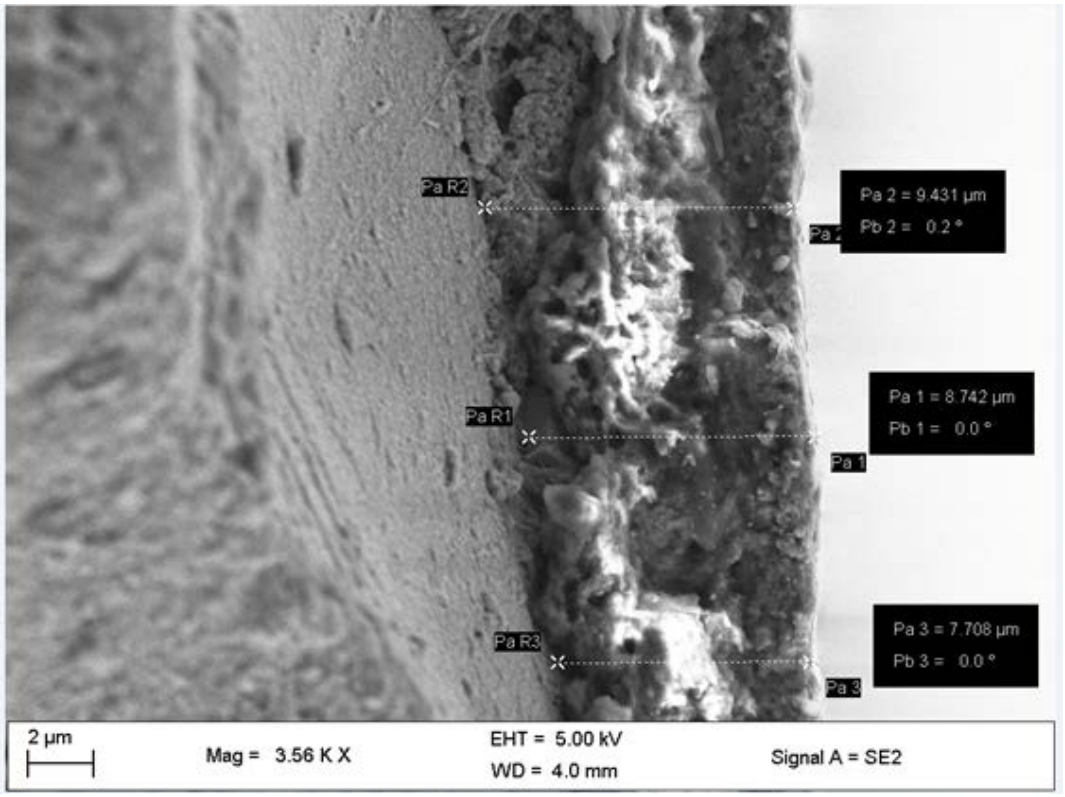

Figure 4.7. Film thickness of (NiO) film on soda lime glass substrate (a) freshly prepared (b) aged for one week and one day using SEM

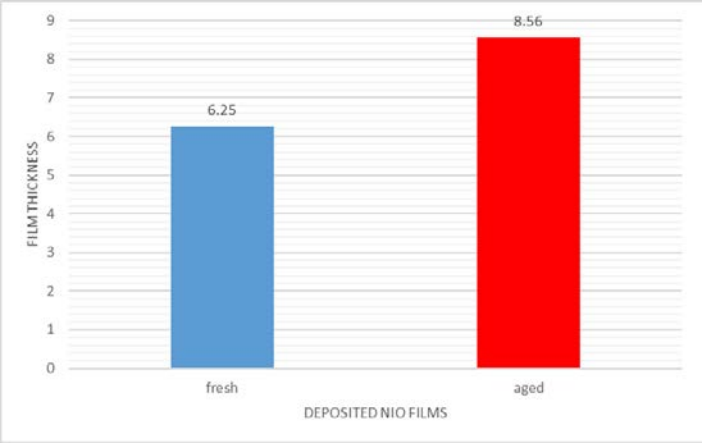

Figure 4.8. Calculated Film thickness of of freshly prepared and aged NiO films

4.5.2 Transmittance

The transmission spectra of the freshly prepared and aged NiO films is shown in Figure 4.23. The absorption edge occurred for both samples at 360 nm which compares favorably with 350 nm obtained by Sriram and Thayumanavan.[16] The aged film has more transparency than the freshly prepared films occurring at approximately 83 % and 78 % respectively. The aged films showed high transparency in both visible and NIR regions.

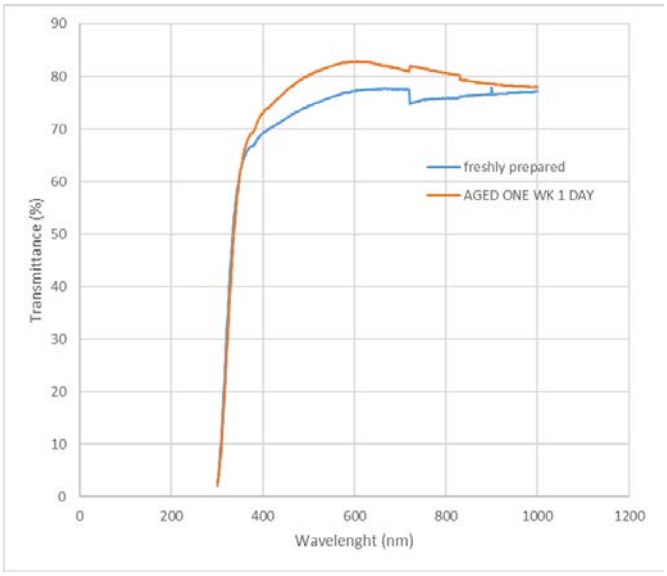

Figure 4.9. Transmission spectra of freshly prepared and aged NiO films

4.5.8 Optical band gap

Figure 4.24 shows a graph of $(\alpha h\upsilon)^2$ against $h\upsilon$ for aged and freshly prepared spray deposited NiO films. The optical band gap is obtained from extrapolation of Figure 4.24 to the $h\upsilon$ axis when $(\alpha h\upsilon)^2 = 0$. The optical band gap grew with the aged NiO films. A shift towards lower energy was observed for the value of the optical band gap. This may be attributed to the Moss-Burstein shift.[26, 27] The recorded optical energy band gaps are 3.60 eV for freshly prepared and 3.70 eV for aged NiO films. This gives a better optical band gap compared to the existing reported value of 3.50 eV by Boschloo and Hagfeldt.[28] This may be ascribed to crystallite size increment.[29] Quantum size effect may be responsible for the large value of the band gap of NiO films.[30] Careful and well optimized deposition parameters also helped in obtaining better optical band gap values.

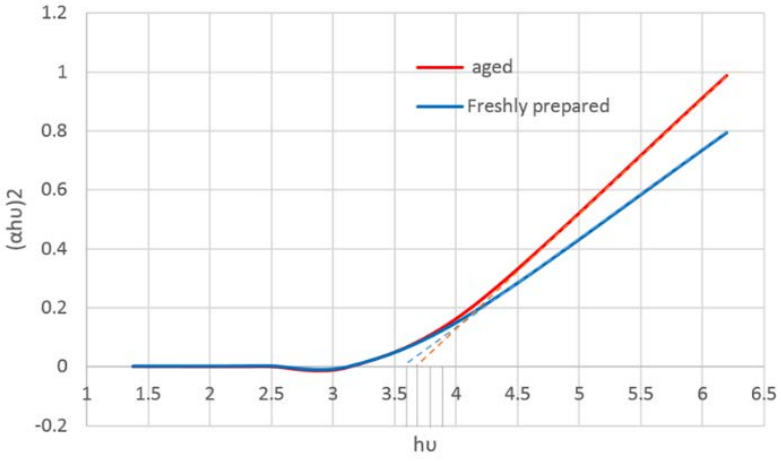

Figure 4.10. Graph of $(\alpha h\upsilon)^2$ against $h\upsilon$ of freshly prepared and aged NiO films

4.5.3 Optical constant

The optical constant can be termed as the “fingerprint of an optical material”. The optical constant alongside the thickness of the film are useful for allowing repeatable manufacturing. Refractive index and extinction coefficients are jointly termed optical constants. They are actually not a constant because their values are influenced by photon energy. They both describe how photons of different energies interact with the films.[31] The interface between a

film and incident ray which is associated with refraction and absorption gives the refractive index (η) and the extinction coefficient (k) respectively.[32]

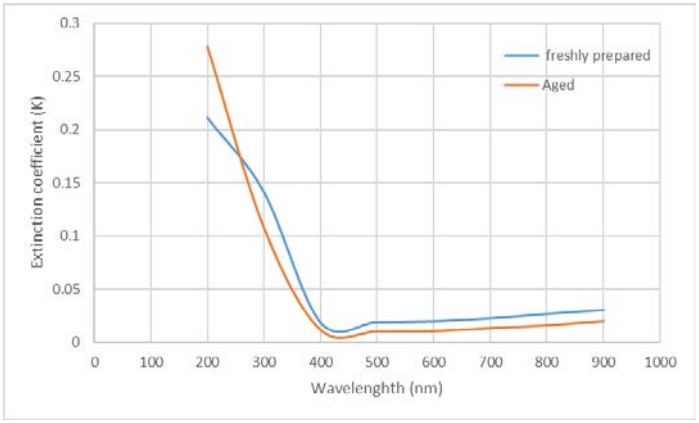

Figure 4.11. Extinction coefficient of freshly prepared and aged NiO films

The films extinction coefficients were computed over the visible and near infrared wavelength from the absorption coefficient using Equation (4) by Lee and Lai.[33]

$$k = \frac{\alpha\lambda}{4\pi} \qquad (4)$$

Where: k denotes the extinction coefficient, α represent the absorption coefficient while λ is wavelength. Figure 4.25 gives the extinction coefficient for the freshly prepared and aged NiO films. It shows that the extinction coefficients of both films varies within the UV region and are almost constant for both visible and near infrared regions.

Figure 4.12. Refractive index of freshly prepared and aged NiO films

Figure 4.26 shows the refractive index of for both samples. Refractive index is a major property of an optical material which gives the electronic polarization of ions and the local field inside the material.[34] The refractive index of deposited films was calculated using the refractive index and optical band gap expression shown in Equation (5) by Reddy et al.[35]

$$\eta = \sqrt{(12.417 \,/\, (Eg - 0.365))} \qquad (5)$$

Where: η denotes refractive index while E_g represents optical band gap. The refractive indices were found to be 1.9592 and 1.9295 for freshly prepared and aged respectively. This is an improvement on reported values of 1.95 and 1.99 by Sriram and Thayumanavan.[16]

5. Conclusion

This study was able to advance research on NiO films for solar cells fabrication by spray depositing freshly and 192 hours aged NiO films. The surface morphology of the deposited NiO films showed broader flakes with ageing. Nickel weight percent grew for the aged sample in comparison with the freshly prepared film. Film thickness grew with ageing. An improved absorption edge was recorded for both freshly prepared and 192 hours aged NiO films at 360 nm. The aged film had more transparency than the freshly prepared films, with aged film having approximately 83 % and freshly prepared 78 % transparency. An improved value for optical band gaps for NiO films were recorded at 3.60 eV and 3.70 eV for freshly prepared and aged NiO films respectively. The "fingerprint of an optical material" for NiO films was reduced for the aged film. The extinction coefficients of both films varied within the UV region and were almost constant for both visible and near infrared regions. The refractive indices were found to be 1.9592 and 1.9295 for freshly prepared and aged films respectively. Based on the result obtained, the prepared sample can be used as the absorber layer of a solar cell. These improved results were as a result of careful and well optimized deposition parameters.

Acknowledgement

The authors acknowledge the National Research Foundation and The World Academy of Science (NRF-TWAS) grants towards this research with grant number 105492.

References

1 Shyu, C-W (2014). Ensuring access to electricity and minimum basic electricity needs as a goal for the post-MDG development agenda after 2015. Energy Sustainable Dev 19:29-38.
2 Adib, R (2015). Renewables global status report. REN21, Paris.
3 Serrano, E., Garcia-Martinez, J., Rus, G (2009). Nanotechnology for sustainable energy. Renewable Sustainable Energy Rev 13:2373-2384.
4 Nam, W. J, Gray, Z., Kwon, D., Plotnikov, V., Stayancho, J., Waggoner, S., et al. (2015). ALD NiO Thin films as a hole transport-electron blocking layer material for photo-detector and solar cell devices. ECS Trans 66:275-9.
5 Wu, C-C. & Yang, C-F (2015). Effect of annealing temperature on the characteristics of the modified spray deposited Li-doped NiO films and their applications in transparent heterojunction diode. Sol Energy Mater Sol Cells 132:492-8.
6 Zhu, Z., Bai, Y., Liu, Z., Long, X., Wei, Z., Zhang, T., et al. (2014). High-performance holeextraction layer of sol–gel-processed NiO nanocrystals for inverted planar perovskite solar cells. Angewandte Chemie 126:12779-83.
7 Kerli, S., Alver, Ü (2016). Preparation and characterisation of ZnO/NiO nanocomposite particles for solar cell applications. J Nanotechnol 2016. http://dx.doi.org/10.1155/2016/4028062.
8 Sasi, B., Gopchandran, K. G (2007). Preparation and characterization of nanostructured NiO thin films by reactive-pulsed laser ablation technique. Sol Energy Mater Sol Cells 91:1505-9.
9 Kim, K. H., Abe Y, Kawamura, M., Takahashi C (2014). Effects of Cu doping on nickel oxide thin film prepared by sol–gel solution process. Optik- Int J Light Electron Optics 125:2899-2901.
10 Wang, K. C., Chen, P., Chen, S., Li, M. H., Lin, M. W., Shen PS, et al. (2014). Low temperature sputtered nickel oxide compact thin film as effective electron blocking layer for mesoscopic NiO/CH3NH3PbI3 perovskite heterojunction solar cells. ACS Appl Mater Interfaces 6:11851-8.
11 Hsu, C-C., Hou, C-H., Shyue, J-J., Su, H-W., Tsai F-Y (2015). Atomic layer deposition of NiO hole-transporting layers for polymer solar cells. Nanotechnol 26:385201.
12 Gowthami, V., Perumal, P., Sanjeeviraja, C., Sivakumar R (2014). Structural and optical studies on nickel oxide thin film prepared by nebulizer spray technique. Physica B: Condens Matter 452:1-6.
13 Patil, P. S (1999) Versatility of chemical spray pyrolysis technique. Mater Chem Phys 59:185-198.
14 Faraj, M. G (2015). Effect of aqueous solution molarity on the structural and electrical properties of spray pyrolysed Lead sulfide (PbS) Thin Films. Int Lett Chem Phys Astron 57:122.
15 Gowthami, V., Meenakshi, M., Perumal, P., Sanjeeviraja, C., Sivakumar, R (2014). Optical dispersion characterization of NiO thin films prepared by nebulized spray technique. Int J ChemTech Res 6:5196-202.
16 Sriram, S., Thayumanavan, A (2013). Structural, optical and electrical properties of NiO thin films prepared by low cost spray pyrolysis technique. Int J Mater Sci Eng 1:118-21.

17 Ukoba, K. O., Eloka-Eboka, A. C., Inambao, F. L (2017). Review of nanostructured NiO thin film deposition using the spray pyrolysis technique. Renewable and Sustainable Energy Reviews 82:2900-2915
18 De Jesus J. C. C., González, I., Puerta, T., Quevedo, A (2005). Thermal decomposition of nickel acetate tetrahydrate: an integrated study by TGA, QMS and XPS techniques. J Mol Catal A: Chem 228:283-91.
19 Lu, Y., Hwang, W-S., Yang, J (2002) Effects of substrate temperature on the resistivity of non-stoichiometric sputtered NiO x films. Surf Coat Technol 155:231-235.
20 De Jong BHWS (1989) Glass. 5th ed. VCH, Weinheim, Germany.
21 Scherrer, P (1918) Derivation of crystallite size OH HO OH OH OH O OH. Gottingen Nachr, 2:98.
22 Das, M. R., Mitra, P. (2017). Microstructural, optical and ethanol sensing characteristics of CBD-synthesised AgO thin film: Influence of bath temperature. J. Phys. Sci., 28(2):127-141, https://doi.org/10.21315/jps2017.28.2.9
23 Anandan K., Rajendran, V (2011). Morphological and size effects of NiO nanoparticles via solvothermal process and their optical properties. Mater Sci Semicond Process 14:43-7.
24 Qiao, H., Wei, Z., Yan, X., Yang, H., Zhu, L (2009). Preparation and characterization of NiO nanoparticles by anodic arc plasma method. J Nanomater 2009:5.
25 Godse, P., Chougule, M., Joshi, P., Pawar, S., Sakhare, R., Sen, S., et al. (2011). Effect of annealing on structural, morphological, electrical and optical studies of nickel oxide thin films. J Surf Eng Mater Adv Technol 1:35.
26 Burstein, E (1954) Anomalous optical absorption limit in InSb. Phys Rev 93:632.
27 Moss, T (1954) The interpretation of the properties of indium antimonide. Proc Phys Soc Section B 67:775.
28 Boschloo, G., Hagfeldt, A (2001). Spectroelectrochemistry of nanostructured NiO. J Phys Chem B 105:3039-44.
29 Makhlouf, S., Abedulrahim, M., Kassem, M (2010). Crystallite size dependent optical properties of nanostructured NiO films. J Optoelectron Adv Mater 4:1562.
30 Romero, R., Leinen, D., Martin, F., Ramos-Barrado, J (2010) Synthesis and characterization of nanostructured nickel oxide thin films prepared with chemical spray pyrolysis. Thin Solid Films 518:4499-502.
31 Forouhi, A., Bloomer, I (1991) Calculation of optical constants, n and k, in the interband region. In: Palik ED (ed) Handbook of optical constants of solids, Vol II. College Park, Maryland, pp 151-76.
32 Tan, W., Koughia, K., Kasap, S., Singh, J (2006) Fundamental optical properties of materials I. Opt Prop Condens Matter Appl 6:1.
33 Lee, M-K., Lai, Y-T (2013). Characterization of transparent conducting p-type nickel oxide films grown by liquid phase deposition on glass. J Phys D: Appl Phys 46:055109.
34 Ahmad, S., Haq, MM-u (2014). A study of energy gap, refractive index and electronic polarizability of ternary chalcopyrite semiconductors. Iran J Phys Res 14:89-93.
35 Reddy, R., Aharnmed, Y. N., Azeem, P. A., Devi, B. S., Gopal, K. R., Rao, T. (2003) Dependence of physical parameters of compound semiconductors on refractive index. Defence Sci J 53:239.

Chapter 4 Part 4

This part studied the combined effect of temperature and ageing on nanostructured nickel oxide for solar cells published in International Journal of Renewable Energy Research (IJRER):

To cite this article: Ukoba, O.K., Inambao F.L. and Eloka-Eboka, A.C. "Study of deposition temperature on properties of aged nanostructured nickel oxide for solar cells" ***International Journal of Renewable Energy Research,*** **vol 8,** ***No 2,*** **June 2018, pp 724 – 732.**

Study of Deposition Temperature on Properties of Aged Nanostructured Nickel Oxide for Solar Cells

Ukoba, O. Kingsley*‡, Inambao, L. Freddie**, Eloka-Eboka, C. Andrew***

*‡Department of Mechanical Engineering, University of KwaZulu-Natal, Durban, 4041, South Africa.

** Department of Mechanical Engineering, University of KwaZulu-Natal, Durban, 4041, South Africa.

*** Department of Mechanical Engineering, University of KwaZulu-Natal, Durban, 4041, South Africa.

(ukobaking@yahoo.com, inambaof@ukzn.ac.za, fatherfounder@yahoo.com)

‡
Corresponding Author; Tel: +27640827616, +2348035431913

Received: 16.10.2017 Accepted:27.02.2018

Abstract- Nanostructured nickel oxide (NiO) films were deposited on preheated glass substrate using spray pyrolysis technique. This study examined the influence of deposition temperature on properties of aged nickel oxide thin films. A preferred orientation along the (1 1 1) plane was observed with a polycrystalline cubic structure. Films were formed with a stoichiometric ratio at higher deposition temperatures. It was revealed that the surface morphology and elemental composition of NiO films can be optimized by deposition temperature. The optical band gap grew as deposition temperature increased. Refractive index decreased with increasing deposition temperature. Optical band gap varied from 3.31 eV to 3.69 eV as deposition temperature increased. The deposition temperature has an influence on properties of aged NiO films. These results may be of interest in the development of affordable and efficient solar cell fabrication especially in developing countries.

Keywords- NiO; solar cell material; deposition temperature, developing countries, aged.

1. Introduction

Provision of affordable and efficient energy is a major human challenge [1]. Electricity is nonexistent for 20 % of the world's population with developing countries comprising 99.8 % of that figure [2]. Several developing countries lack access to electricity [3] while many others have highly disrupted supply with less than four hours of power supply per day [4]. Optimized techniques and materials are being researched to solve this energy problem. Interest is on development of renewable energy due to their vast advantage [5-7]. Energy from the sun has been proposed as a viable solution for power supply [8-9]. Photovoltaic is one way of using the solar energy [10-14]. Solar energy can be converted to useful direct current electricity using solar cells [15]. The focus of current solar cell research is on affordability and efficiency. Most of the equipment used for thin film deposition is expensive [16] and vacuum-based [17]. This has caused researchers in developing countries look for in-country resources, resulting in research on inexpensive materials and methods requiring only a small power supply.

Nanostructure metal oxides are reported to offer improvement for solar cells [18]. Nickel oxide (NiO) is a unique metal oxide with several uses [19-24]. It is a p-type metal oxide and is an inexpensive material. It can be manufactured by several techniques such as sputtering [25], sol-gel [26], laser ablation [27], electron beam deposition [28] and chemical bath deposition [29]. Studies have been conducted on the effect of ageing and the effect of deposition temperature on NiO films [30-32], showing that ageing and deposition temperature improved NiO film properties. However, most of the studies focused on the influence of substrate temperature on sensing properties, electrochromic properties [33] and photovoltaic cells [34]. There is little or no systematic study of the influence of deposition temperature on aged NiO film properties. Therefore, there is a need to study their combined effect on NiO films.

This research will help to ascertain if deposition of nickel oxide at either low temperatures or temperatures above 350 ^{o}C give the same optimal properties. This temperature was reported to be the optimal range for pyrotic decomposition of NiO [35]. Therefore, this research will study the influence of deposition temperature below 350 ^{o}C and above 350 ^{o}C on properties of aged NiO films. Morphological, structural, elemental, and optical properties will be examined with a view to optimizing NiO film for efficient and affordable solar cells application.

2. Experimental Procedure

2.1 Deposition

Pure nickel (II) acetate tetrahydrate $Ni(CH_3CO_2)_2.4H_2O$ of 0.05 M was mixed and stirred in 50 mL distilled water. The solution was left for one week after mixing to age before deposition. This was spray deposited using the set-up in Fig. 1. Thereafter, it was deposited at different temperatures T_d (< 350 ºC and ≥ 350 ºC). The samples were sprayed from 270 ºC to 325 ºC for Td< 350 ºC samples and done at 350 ºC to 400 ºC for Td ≥ 350 ºC. The glass substrate was chemically and ultrasonically cleaned before usage for deposition of the solution. Other deposition parameters were maintained to obtain uniform film thickness.

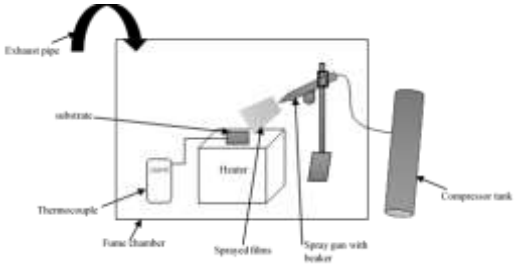

Fig. 1. Experimental set-up of Spray pyrolysis technique.

The optimum deposition parameters of spray deposited NiO films are shown in Table 1. Each droplet was found to be smaller than micro sized particles. The sprayed solution on the preheated substrate glass experiences evaporation and solute precipitation before pyrolytic decomposition as shown in equation (1). Nickel oxide was obtained as a final product [36].

$$Ni(CH_3COO)_2.4H_2O \xrightarrow{heat} NiO + 7H_2O \uparrow + 4CO_2 \uparrow \quad (1)$$

The colour of prepared thin films was observed to be gray, uniform and strongly adherent to the glass.

Table 1. Optimum deposition parameter of SPT NiO film.

Deposition parameter	Value
Height of spraying nozzle to substrate distance	20 cm
Spray rate	1 ml/min
Spray time	1 min
Time between sprays	30 sec
Carrier gas	Filled compressed air of 1 bar

2.2 Characterization

The morphology of deposited NiO film was studied using Scanning Electron Microscope ZEISS EVO MA15VP. An Energy Dispersive X-ray Spectrometer (EDS or EDX: "GENESIS XM2") was used for elemental composition. An EMPYREAN (PANalytical) X-ray powder diffractometer model was used for structural properties of deposited NiO films from 5 º to 90 º 2θ angles. The absorption of the film was measured with a Perkin Elmer Spectrum 100 Fourier Transform Infrared Spectrometer (FTIR). The measured film thickness was compared with the calculated values obtained using the weight difference method. Optical properties were studied in wavelengths of 300 nm to 1000 nm with a SHIMADZU UV-3600UV-VIS Spectrometer.

3. Results and Discussion

3.1 Morphological studies

SEM micrographs are represented in Fig. 2. These micrographs reveal homogeneous, smooth, well adherent films devoid of pinholes and cracks. The film of $T_d \geq 350$ ºC has better distribution of grains than $T_d < 350$ ºC, although it has almost the same particle size and shape as $T_d < 350$ºC. This may be ascribed to the ageing of the films and optimized deposition parameters. This shows that deposition temperature influences structural properties of aged NiO films by increasing grain on the film. These micrographs are an improvement on earlier results reported by Chen et al. [37] using radio-frequency (RF) magnetron sputtering.

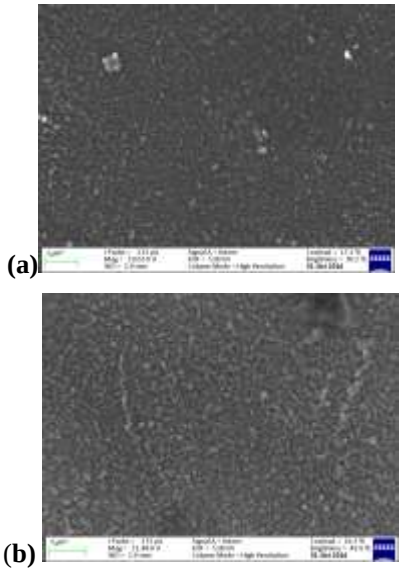

Fig. 2. SEM micrographs of aged (one week) nickel oxide (NiO) film on glass substrate at (a) Td < 350 ºC and (b) Td ≥ 350 ºC

3.2 Elemental composition analysis

Fig. 3 shows the EDX for the different deposition temperatures for NiO thin films. Both spectra confirm presence of Ni and O elements in NiO thin films. Oxygen concentration in deposited NiO films decreases as deposition temperature increases. This may be due to increased film growth on the glass substrate as seen from Fig. 2 thereby making less of the glass (oxygen) visible.

Related results were reported by Lu et al. [38]. An additional Si element was also observed from the EDX. This is because Silicon (Si) is a major material in the soda-lime glass substrate used [39].

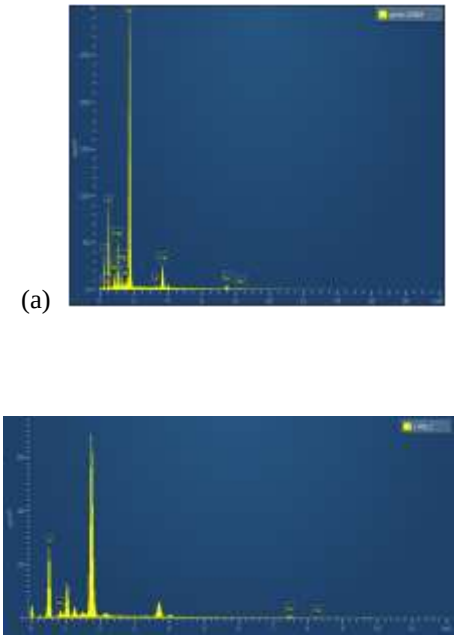

Fig. 3. EDX spectra for one week aged nickel oxide (NiO) film on glass substrate at (a) Td < 350 ºC and (b) Td ≥ 350 ºC

3.3 Structural studies

The phase and preferred orientation of deposited nanostructured NiO films was determined using an x-ray diffractometer. Fig. 4 gives XRD patterns of deposited nanostructured NiO films at Td < 350 ºC and Td ≥3 50 ºC.

The peak diffraction for Td < 350 ºC is at (2θ = 43.36º and 50.54º) for the (1 1 1) and (2 0 0) planes respectively. At Td ≥ 350 ºC, peak diffraction is (2θ = 36.96º and 43.14º) for the (1 1 1) and (2 0 0) planes respectively. The XRD analysis confirms Bunsenite which correspond to JCPDS card: 04- 0835 for NiO [40]. A high intensity was recorded for $T_d \geq 350$ ºC in both planes, which may be due to better alignment of the grains. This led to increased grain growth at higher deposition temperature. It can also be ascribed to increased crystallinity as deposition temperature increased. This is related to the reported value of 37.3º for the (1 1 1) plane by Sharma et al. [30].

The XRD spectra shows that films prepared at T_d < 350 ºC have weak and broadened (1 1 1) diffraction peaks, which implies poor crystallinity. However, those at $T_d \geq 350$ ºC have good crystallinity and the (1 1 1) preferred orientation. These are pointers that the microstructure of NiO films are influenced by deposition temperature as evidence from the grain growth at higher deposition temperature. NiO films with either a (1 1 1) or (2 0 0) preferred orientation are recommended for optoelectronic applications [41].

There is separate colliding of Ni^{2+} and O^{2-} on the growing aged NiO films surface at lower deposition temperature, thereby making it difficult for Ni^{2+} and O^{2-} to recombine due to insufficient energy or oxygen. There is a tendency for non-stoichiometric ratio films to be formed which are electrostatically polar. Ni^{2+} and O^{2-} strike, simultaneously, on the growing aged NiO films at higher deposition temperature, producing film formation with stoichiometric ratios that are electrostatically neutral [42]. This is corroborated with a higher intensity for the (1 1 1) preferential orientation for low deposition temperature [43].

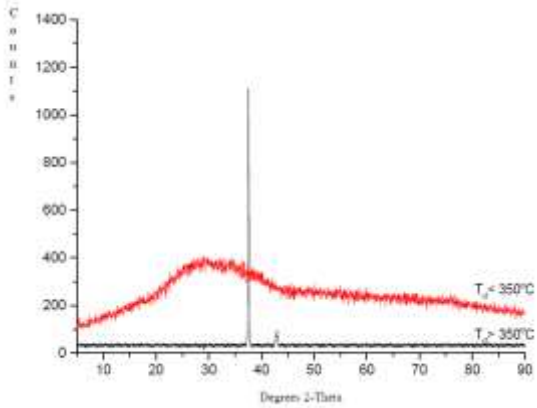

Fig. 4. XRD patterns of one week aged nanostructured NiO films at different deposition temperature

The Debye-Scherer relationship [44]; [45] in equation (2) was used to obtain the average crystallite size.

$$D = \frac{k\lambda}{\beta \cos \theta} \quad (2)$$

Where B represents the Full Width at Half Maximum (FWHM) peak intensity (in Radian), λ denotes wavelength, θ represent Bragg's diffraction angle and k is 0.89.

Other structural parameters are shown in Table 2.

Table 2. Parameters from XRD data

Deposition Temperature	hkl	Diffraction angle 2theta	FWHM	Relative intensity	d-spacing
T_d < 350 ºC	(1 1 1)	43.3641	0.5038	100	2.42290
	(2 0 0)	50.5425	0.7557	81.78	2.09685
$T_d \geq 350$ ºC	(1 1 1)	36.9621	0.5510	62.14	2.43190
	(2 0 0)	43.1404	0.3149	100	2.09688

The average crystallite size of NiO film index for the (1 1

1) and (2 0 0) planes for $T_d \geq 350$ °C as observed from XRD are 26 nm and 47 nm respectively. Those of $T_d < 350$ °C are 34 nm and 23 nm for the (1 1 1) and (2 0 0) planes respectively.

3.4 Optical properties

The film thickness was considered for the NiO films at deposition temperatures below ($T_d < 350$ °C) and above ($T_d \geq 350$ °C). The measured data is depicted in Fig. 6. This was compared with the calculated value. The calculated value was obtained using the weight difference method expressed in Equation (3) [46]:

$$t = \frac{m}{A\rho} \tag{3}$$

Where t denotes film thickness, m represents the actual mass deposited, A denotes thin film area while ρ represents the density of material.

Fig. 7 shows the calculated values. Both measured and calculated values are in good agreement. Film thickness grew as deposition temperature increased. The NiO film thickness was controlled by keeping deposition parameters constant. NiO thin film average thickness was between 11.85 µm and 12.55 µm.

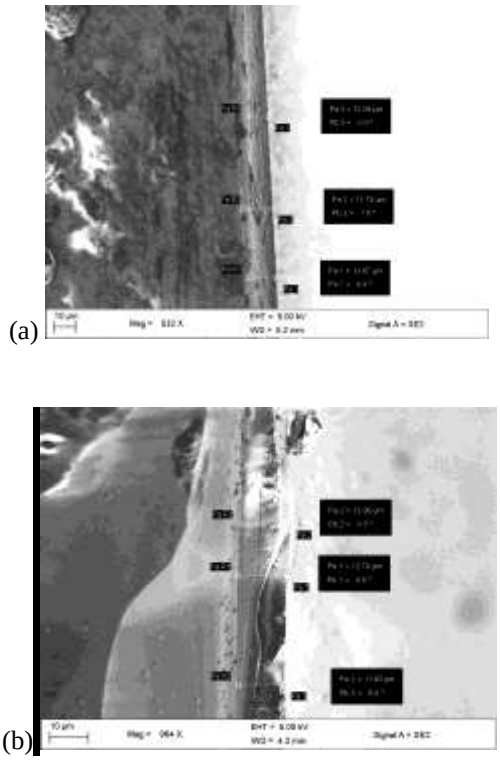

Fig. 6. Measured film thickness for aged (one week) nickel oxide (NiO) film on glass substrate at (a) $T_d < 350$ °C and (b) $Td \geq 350$ °C

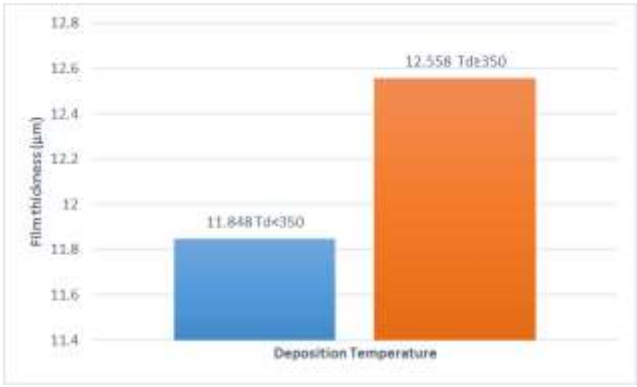

Fig. 7. Calculated film thickness of the aged (one week) NiO films at different deposition temperature.

Fig. 8 gives FTIR spectra used to identify molecular components and the structure of NiO films. It gives the spectrum of aged (one week) 0.05 M NiO films at $T_d \geq 350$ °C alone, in the range of 400 cm^{-1} and 4000 cm^{-1}. The NiO stretching vibration mode was recorded in the broad absorption band region of 432 cm^{-1} to 698 cm^{-1}. This is similar to the earlier reported NiO absorption range [47]. The broadness confirms that the NiO are nanocrystalline. The NiO film FTIR absorption is blue-shifted due to their nanostructure size. Other significant absorption bands were also recorded. The band at 3475 cm^{-1} reveals an O-H (hydroxyl group or hydroxide ion) stretching vibration. This is the natural portion of water due to a self-ionization reaction [48]. An H-O-H bending vibration mode was observed at 1630 cm^{-1}. This shows that there is a negligible quantity of water in the NiO film. This may be attributed to adsorption of water from the air since the experiment was conducted in open air [49]. This is corroborated by the EDX result in Fig 3. The region between 1000 cm^{-1} to 1500 cm^{-1} with band centre at 1210 is assigned O-C=O symmetric and non-symmetric stretching vibration. This accounts for the traces of H_2O and CO_2 in the reaction of Equation (1) which were burnt off. There is no band indicating the presence of other groups, confirming that there is no impurity in the film and that the sample was washed and well cleaned. This result agrees with the standard FTIR data for NiO films as reported by [50]. The NiO film deposited at $T_d < 350$ °C did not give FTIR. This may be due to non-absorption of the film.

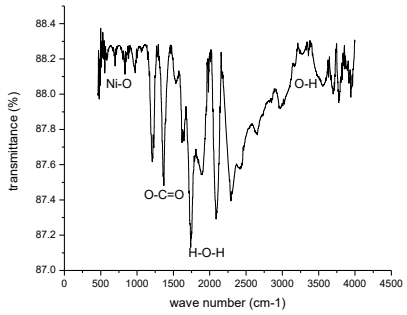

Fig. 8. FTIR spectrum of aged (one week) 0.05 M NiO films at $T_d \geq 350$ °C.

Fig. 9 represents measurement of transmittance and wavelength for deposited NiO films at the deposition temperatures. Transmittance grew from 70.70 % to 76.41 % as deposition temperature increased. However, both films exhibited high transparency in visible and near IR regions. This occurred at wavelengths of 1000 nm and 611 nm respectively. This may be due to an increase in film thickness and absorbance (shown in Fig. 10) as deposition temperature increases, making the scattered radiation more pronounced because of surface roughness [51]. These results exceed previously reported values of less than 70 % by Ismail et al. [52].

Absorption coefficient, α was obtained using Equation (4) [53]:

$$\alpha = (2.303 \times A) / t \quad (4)$$

Where t is film thickness and A is absorbance. The relationship between optical absorption and optical energy band gap is expressed in Equation (5) [54]; [55]:

$$\alpha^2 = C(h\upsilon - E_g) \quad (5)$$

Where C has constant value, h denotes Planck's constant, υ represent incidence light frequency, and E_g denotes optical energy band gap.

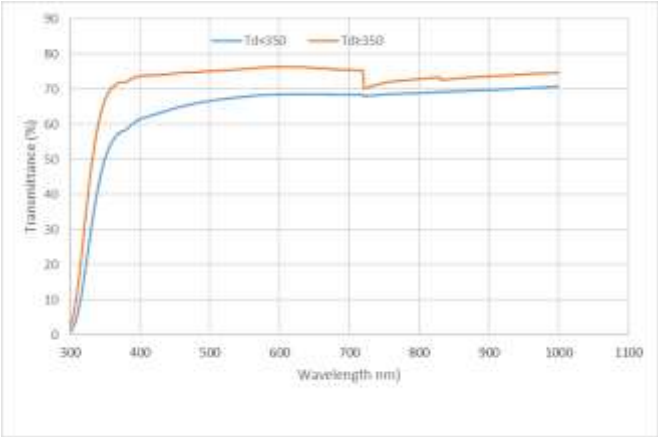

Fig. 9. Plot of transmittance against wavelength of deposition temperature of NiO films

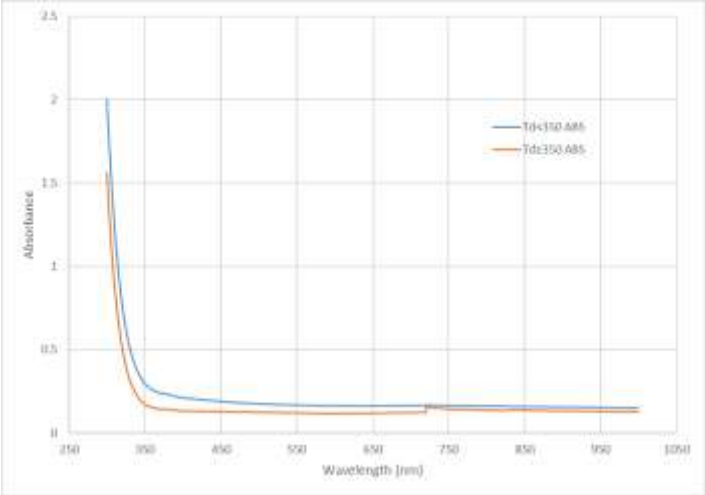

Fig. 10. Plot of absorbance against wavelength of deposition temperature of NiO films

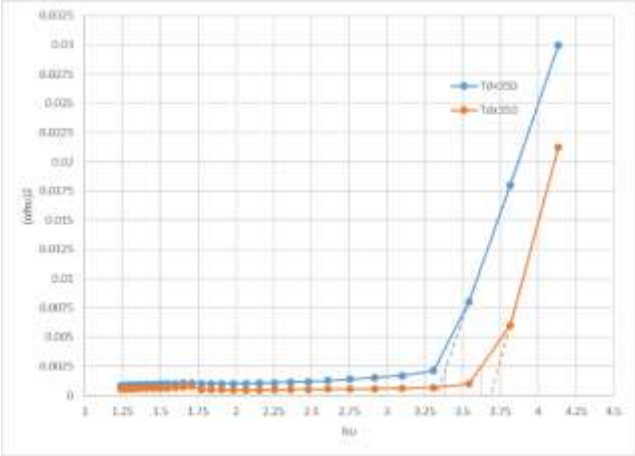

Fig. 11. Graph of $(\alpha h\upsilon)^2$ against hυ for NiO films

Fig. 11 shows a graph of $(\alpha h\upsilon)^2$ against hυ for aged NiO films spray deposited at both deposition temperatures. Extrapolation of Fig. 11 to hυ axis for $(\alpha h\upsilon)^2 = 0$ gives the optical band gap. A decrease in slope of the plot is observed as deposition temperature increases. A shift towards lower energy is observed for value optical band gap. The reduction is attributed to the Moss-Burstein shift [56, 57]. Optical energy band gaps are 3.31 eV and 3.69 eV for T_d <350 ºC and $T_d \geq 350$ ºC respectively. This gives a better optical band gap compared to the existing reported value of 3.5 eV [58]. This may be ascribed to crystallite size increment [59]. The quantum size effect may be responsible for the large value of the band gap of NiO films [60]. Careful and well optimized deposition parameters also help in obtaining a better optical band gap.

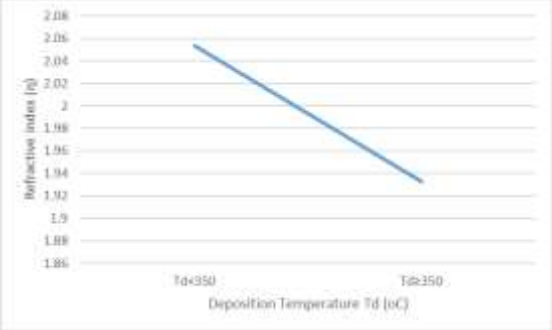

Fig. 12. Refractive index plot against deposition temperature of aged NiO films

Fig. 12 shows the refractive index of the NiO films. The refractive index of deposited films was calculated using refractive index and optical band gap expression as shown in Equation 6 [61]:

$$\eta = \sqrt{(12.417 \,/\, (Eg - 0.365))} \quad (6)$$

Where η denotes refractive index while E_g represents optical band gap.

Refractive indices were found to be 2.0533 and 1.9324 for T_d < 350 ºC and T_d≥350 ºC respectively. This is an improvement on reported values of 1.99 by Sriram and Thayumanavan [32].

4. Conclusion

This study reported spray pyrolysis deposition of aged nanostructured NiO films on glass substrate. The influence of deposition temperature on aged NiO films on elemental, morphological, structural and optical properties was studied with a view to optimizing deposition temperature for solar cell application.

This study contributed new results relating to surface morphology, structural, film thickness and optical of NiO films using spray pyrolysis.

Deposition temperature only affected the surface morphology of aged NiO films by producing a grainier surface. It does not affect the shape and size. Elemental composition using EDX confirmed the presence of Ni and O elements in NiO films. It was observed that the film thickness grew as deposition temperature increased.

NiO films are formed with a non-stoichiometric ratio at lower deposition temperatures, but are electrostatically neutral at higher deposition temperatures.

Transmittance grew from 70.70 % to 76.41 % as deposition temperature increased. This resulted in a reduction in the refractive index of the aged NiO films as deposition temperatures increased. Optical band gap varied from 3.31 eV to 3.69 eV as deposition temperature increased. This study produced better optical band gaps than existing reported values. The new findings were a result of well optimized deposition parameters. Therefore, deposition temperature does affect the properties of aged nanostructured NiO thin films. This optimized result may be explored further for affordable, durable and efficient solar cell fabrication and research in developing countries by ageing the precursor for longer period and at different concentrations, it can also be doped with another material or this result used directly to fabricate a solar device using a pn heterojunction technology. This optimized results will help in affordable and sustainable solar cells fabrication as it will be useful as p-type material in a pn heterojunction solar cells

Acknowledgements

The authors acknowledge the National Research Foundation (NRF) and the World Academy of Science (NRF/TWAS) under grant number 105492 towards this research.

References

[1] M. Grätzel, Mesoscopic solar cells for electricity and hydrogen production from sunlight, Chem. Lett. 34 (2004) 8-13.

[2] C-W. Shyu, Ensuring access to electricity and minimum basic electricity needs as a goal for the post-MDG development agenda after 2015, Energy Sustainable Dev. 19 (2014) 29-38.

[3] R. Adib, Renewables 2015 Global Status Report, Paris: REN21 Secretariat, 2015.

[4] N. Emodi, S. Yusuf, Improving electricity access in Nigeria: obstacles and the way forward, Int. J. Energy Econ. Policy, 5 (2015) 335-351.

[5] O. Henni, M. Belarbi, K. Haddouche, K., & E.H. Belarbi, Design and Implementation of a Low-Cost Characterization System for Photovoltaic Solar Panels, Int. J. of Renew Energy Res, Vol. 7, No. 4, pp. 1586-1594, 2017

[6] C. Chukwuka, K.A. Folly, "Technical and economic modeling of the 2.5kW grid-tie residential photovoltaic system". Int J Renew Energy Res, Vol. 3, No. 2, pp. 412–419, 2013

[7] J. Liu, R. Hou, "Solar cell simulation model for photovoltaic power generation system". Int J Renew Energy Res, Vol. 4, No. 1, pp. 49–53, 2014.

[8] M. Eslamian, Spray-on thin film PV solar cells: advances, potentials and challenges, Coatings, 4 (2014) 60-84.

[9] A.K. Hussein, Applications of nanotechnology in renewable energies: a comprehensive overview and understanding, Renewable Sustainable Energy Rev. 42 (2015) 460-476.

[10] M.T. Ahmed, T. Gonçalves and M. Tlemcani, "Single diode model parameters analysis of photovoltaic cell", ICRERA'2016 5th International Conference on Renewable Energy Research and Applications, Birmingham, UK, pp. 396–400, 20–23 November 2016. (Conference Paper)

[11] M.R. Rashel, A. Albino, M. Tlemcani, T Gonçalves and J. Rifath, "MATLAB Simulink modeling of photovoltaic cells for understanding shadow effect", ICRERA'2016 5th International Conference on Renewable Energy Research and Applications, Birmingham, UK, pp. 747–750, 20–23 November 2016. (Conference Paper)

[12] A. Cordeiro, D. Foito and V. Fernão Pires, "A PV panel simulator based on a two quadrant DC/DC power converter with a sliding mode controller", ICRERA'2015 4th International Conference on Renewable Energy Research and Applications, Palermo, Italy, pp. 928–932, 22–25 November 2015. (Conference Paper)

[13] J. Cubas, S. Pindado and A. Farrahi, "New method for analytical photovoltaic parameter extraction", ICRERA'2013 2nd International Conference on Renewable Energy Research and Applications, Madrid, Spain, pp. 873–877, 20–23 October 2013. (Conference Paper)

[14] A. Parisi, L. Curcio, V. Rocca, S. Stivala and A.C. Cino et al., "Photovoltaic module characteristics from CIGS solar cell modelling", ICRERA'2013 2nd International Conference on Renewable Energy Research and Applications, Madrid, Spain, pp. 1139–1144, 20–23 October 2013. (Conference Paper)

[15] A.S. Islam, M. Islam, Status of renewable energy technologies in Bangladesh, Technol. 5 (2005) 1-5.

[16] C. Eberspacher, C. Fredric, K. Pauls, J. Serra, Thin-film CIS alloy PV materials fabricated using non-vacuum, particles-based techniques, Thin Solid Films, 387 (2001) 18-22.

[17] W. Wang, Y-W. Su, C-H. Chang. Inkjet printed chalcopyrite CuIn x Ga 1− x Se 2 thin film solar cells, Sol. Energy Mater. Sol. Cells, 95 (2011) 2616-2620.

[18] E. Serrano, G. Rus, J. Garcia-Martinez, Nanotechnology for sustainable energy, Renewable Sustainable Energy Rev. 13 (2009) 2373-2384.

[19] W.J. Nam, Z. Gray, J. Stayancho, V. Plotnikov, D. Kwon, S. Waggoner, et al., ALD NiO Thin films as a hole transport-electron blocking layer material for photo-detector and solar cell devices, ECS Transac. 66 (2015) 275-279.

[20] N. Park, K. Sun, Z. Sun, Y. Jing, D. Wang, High efficiency NiO/ZnO heterojunction UV photodiode by sol-gel processing, J. Mater. Chem. C, 1 (2013) 7333-7338.

[21] C. Li, Z. Zhao, Preparation and characterization of nickel oxide thin films by a simple two-step method, Vacuum Electron Sources Conference and Nanocarbon (IVESC), 2010 8th International: IEEE, (2010) 648-649.

[22] C-C. Wu, C-F. Yang, Effect of annealing temperature on the characteristics of the modified spray deposited Li-doped NiO films and their applications in transparent heterojunction diode, Sol. Energy Mater. Sol. Cells, 132 (2015) 492-498.

[23] Z. Zhu, Y. Bai, T. Zhang, Z. Liu, X. Long, Z. Wei, et al., High-Performance hole-extraction layer of sol-gel-processed NiO nanocrystals for inverted planar perovskite solar cells, Angewandte Chemie, 126 (2014) 12779-12783.

[24] C.R. Magaña, D.R. Acosta, A.I. Martínez, J.M. Ortega, Electrochemically induced electrochromic properties in nickel thin films deposited by DC magnetron sputtering, Sol. Energy, 161 (2006) 161-169.

[25] J. Keraudy, J. García Molleja, A. Ferrec, B. Corraze, M. Richard-Plouet, A. Goullet, et al., Structural, morphological and electrical properties of nickel oxide thin films deposited by reactive sputtering, Appl. Surf. Sci. 357 (2015) Part A 838-844.

[26] M. Jlassi, I. Sta, M. Hajji, H. Ezzaouia, Optical and electrical properties of nickel oxide thin films synthesized by sol-gel spin coating, Mater. Sci. Semicon. Processing, 21 (2014) 7-13.

[27] H. Wang, Y. Wang, X. Wang, Pulsed laser deposition of the porous nickel oxide thin film at room temperature for high- rate pseudocapacitive energy storage, Electrochem. Commun. 18 (2012) 92-95.

[28] M.M. El-Nahass, M. Emam-Ismail, M. El-Hagary, Structural, optical and dispersion energy parameters of nickel oxide nanocrystalline thin films prepared by electron beam deposition technique, J. Alloys Compd. 646 (2015) 937-945.

[29] M.A. Vidales-Hurtado, A. Mendoza-Galván, Electrochromism in nickel oxide-based thin films obtained by chemical bath deposition, Solid State Ionics, 179 (2008) 2065-2068.

[30] R. Sharma, A. Acharya, S. Moghe, S. Shrivastava, V. Ganesan, S. Bhardwaj, et al., Effect of deposition temperature on structural and optical properties of sprayed nickel oxide thin films, AIP Conference Proceedings: AIP, (2013) 507-508.

[31] I Fasaki, A. Koutoulaki, M. Kompitsas, C. Charitidis, Structural, electrical and mechanical properties of NiO thin films grown by pulsed laser deposition, Appl. Surf. Sci. 257 (2010) 429-433.

[32] S. Sriram, A. Thayumanavan, Structural, optical and electrical properties of NiO thin films prepared by low cost spray pyrolysis technique, Int. J. Mater. Sci. Eng. 1 (2013) 118-121.

[33] D-M. Na, L. Satyanarayana, G-P. Choi, Y-J. Shin, J.S. Park, Surface morphology and sensing property of NiO-WO3 thin films prepared by thermal evaporation, Sensors, 5 (2005) 519-528.

[34] M.D. Irwin, D.B. Buchholz, A.W. Hains, R.P. Chang, T.J. Marks, p-Type semiconducting nickel oxide as an efficiency-enhancing anode interfacial layer in polymer bulk-heterojunction solar cells, Proc. Natl. Acad. Sci. 105 (2008) 2783-2787.

[35] M. El-Kemary, N. Nagy, I. El-Mehasseb, Nickel oxide nanoparticles: synthesis and spectral studies of interactions with glucose, Mater. Sci. Semicon, Processing, 16 (2013) 1747-1452.

[36] J.C. De Jesus, I. González, A. Quevedo, T Puerta, Thermal decomposition of nickel acetate tetrahydrate: an integrated study by TGA, QMS and XPS techniques, J. Mol. Catal. A: Chem. 228 (2005) 283-291.

[37] H-L. Chen, Y-M. Lu, J-Y. Wu, W-S. Hwang, Effects of substrate temperature and oxygen pressure on crystallographic orientations of sputtered nickel oxide films, Mater. Transac. 46 (2005) 2530-2535.

[38] Y. Lu, W-S. Hwang, J. Yang, Effects of substrate temperature on the resistivity of non-stoichiometric sputtered NiO x films, Surf. Coat. Technol. 155 (2002) 231-235.

[39] B.H.W.S. de Jong, Glass, fifth ed., Weinheim, Germany, VCH, 1989.

[40] M. Gabal, Non-isothermal decomposition of NiC 2 O 4–FeC 2 O 4 mixture aiming at the production of NiFe 2 O 4, J. Phys. Chem. Solids, 64 (2003) 1375-1385.

[41] E. Fujii, A. Tomozawa, H. Torii, R. Takayama, Preferred orientations of NiO films prepared by plasma-enhanced metalorganic chemical vapor deposition, Jpn. J. Appl. Phys. 35 (1996) L328.

[42] H.L. Chen, Y.S. Yang, Effect of crystallographic orientations on electrical properties of sputter-deposited nickel oxide thin films, Thin Solid Films, 516 (2008) 5590-5596.

[43] C.A. Fisher, Molecular dynamics simulations of reconstructed NiO surfaces, Scripta Materialia, 50 (2004) 1045-1049.

[44] P. Scherrer, G. Nachr, Derivation of crystallite size OH HO OH OH OH O OH. 1918.

[45] C. Barrett, T. Massalski, Structure of metals, Oxford, Pergamon Press, 1980.

[46] P. Godse, R. Sakhare, S. Pawar, M. Chougule, S. Sen, P. Joshi, et al., Effect of annealing on structural, morphological, electrical and optical studies of nickel oxide thin films, J. Surf. Eng. Mater. Adv. Technol. 1 (2011) 35.

[47] K. Anandan, V. Rajendran, Morphological and size effects of NiO nanoparticles via solvothermal process and their optical properties, Mater. Sci. Semicon. Processing, 14 (2011) 43-47.

[48] P.L. Geissler, C. Dellago, D. Chandler, J. Hutter, M. Parrinello, Autoionization in liquid water, Science, 291 (2001) 2121-2124.

[49] T. Theivasanthi, M. Alagar, Chemical capping synthesis of nickel oxide nanoparticles and their characterizations studies, arXiv preprint arXiv, (2012) 12124595

[50] H. Qiao, Z. Wei, H. Yang, L. Zhu, X. Yan, Preparation and characterization of NiO nanoparticles by anodic arc plasma method, J. Nanomater. (2009) 5.

[51] A. Balu, V. Nagarethinam, N. Arunkumar, M. Suganya, Nanocrystalline NiO thin films prepared by a low cost simplified spray technique using perfume atomizer, J. Electron. Devices, 13 (2012) 920-930.

[52] R.A. Ismail, S.A. Ghafori, G.A. Kadhim, Preparation and characterization of nanostructured nickel oxide

thin films by spray pyrolysis, Appl. Nanosci. 3 (2013) 509-514.

[53] J. Barman, K. Sarma, M. Sarma, K. Sarma, Structural and optical studies of chemically prepared CdS nanocrystalline thin films, Indian J. Pure Appl. Phys. 46 (2008) 339-343.

[54] F. Ezema, A.. Ekwealor, R Osuji, Effect of thermal annealing on the band GAP and optical properties of chemical bath deposited ZnSe thin films, Turk. J. Phys. 30,pp 157-163, 2006.

[55] V. Estrella, M. Nair, P. Nair, Semiconducting Cu3BiS3 thin films formed by the solid-state reaction of CuS and bismuth thin films, Semicon. Sci. Technol. 18 (2003) 190.

[56] E. Burstein, Anomalous optical absorption limit in InSb, Phys. Rev. 93 (1954) 632.

[57] T. Moss, The interpretation of the properties of indium antimonide, Proc.Phys. Soc. Sect. B, 67 (1954) 775.

[58] G. Boschloo, A. Hagfeldt, Spectroelectrochemistry of nanostructured NiO, J. Phys. Chem. B, 105 (2001) 3039-3044.

[59] S. Makhlouf, M. Kassem, M. Abedulrahim, Crystallite size dependent optical properties of nanostructured NiO films, J. Optoelectron Adv. Mater. 4 (2010) 1562.

[60] R. Romero, F. Martin, J. Ramos-Barrado, D. Leinen, Synthesis and characterization of nanostructured nickel oxide thin films prepared with chemical spray pyrolysis, Thin Solid Films, 518 (2010) 4499-4502.

[61] R. Reddy, Y.N. Aharnmed, P.A. Azeem, K.R. Gopal, B.S. Devi, T. Rao, Dependence of physical parameters of compound semiconductors on refractive index, Defence Sci. J. 53 (2003) 239.

CHAPTER 5: DEVICE FABRICATION

Chapter 5 looks at the final device fabrication of the solar cells using TiO_2/NiO metal oxides heterojunctions. It is divided into two parts.

Part 1: **Ukoba, O.K.,** Inambao F.L. and Eloka-Eboka, A.C. (2018) "Experimental optimization of nanostructured nickel oxide deposited by spray pyrolysis for solar cells application" International Journal of Applied Engineering Research, vol. 13, No. 6, pp. 3165-3173

Link to the article: https://www.ripublication.com/ijaer18/ijaerv13n6_05.pdf

Part 2: Ukoba, K. O., Inambao, F. L., & Eloka-Eboka, A. C. (2018) "Fabrication of affordable and sustainable solar cells using NiO/TiO2 PN heterojunction" *International Journal of Photoenergy*, vol. 2018, pp 1-7, Hindawi publishers. DOI: 10.1155/2018/6062390

Link to the article: https://www.hindawi.com/journals/ijp/2018/6062390/

CHAPTER 5 Part 1: EXPERIMENTAL OPTIMIZATION OF NANOSTRUCTURED NICKEL OXIDE DEPOSITED BY SPRAY PYROLYSIS FOR SOLAR CELLS APPLICATION

To cite the article: Ukoba, O.K., Inambao F.L. and Eloka-Eboka, A.C. (2018) "Experimental optimization of nanostructured nickel oxide deposited by spray pyrolysis for solar cells application" International Journal of Applied Engineering Research, vol 13(6), pp. 3165-3173

Link to the article: https://www.ripublication.com/ijaer18/ijaerv13n6_05.pdf

International Journal of Applied Engineering Research ISSN 0973-4562 Volume 13, Number 6 (2018) pp. 3165-3173

Experimental Optimization of Nanostructured Nickel Oxide Deposited by Spray Pyrolysis for Solar Cells Application

[1a]Ukoba, O.K, [a]Inambao, F.L. and [a]Eloka-Eboka, A.C.

[a]Discipline of Mechanical Engineering University of KwaZulu-Natal, Durban, 4041, South Africa.

Abstract

This study focused on the experimental optimization of nanostructured nickel oxide (NiO) for solar cell applications. The optimization procedure involved the variation of the precursor concentrations of nickel acetate with attendant measurement of the properties of nickel oxide films. The films were spray deposited on glass substrate. Nickel acetate precursor was used at a substrate temperature of 350 ºC. Precursor concentrations were: 0.025 M, 0.05 M, 0.075 M and 0.1 M respectively. The surface morphology revealed nanostructured film with particles densely distributed across the substrate's surface. The films are homogeneous, smooth, well adherent and devoid of pinholes and cracks. The morphology became grainier as the precursor solution increased. Elemental composition exposes the presence of Ni and O elements in NiO film. Oxygen concentration decreases as precursor solution increases. The film structural property reveals that deposited NiO film has an amorphous structure at 0.025 M while the other concentrations are polycrystalline in nature with cubic structure. X-ray diffractometry (XRD) further reveals that the intensity of NiO films increases with increased molarity. Preferred orientation was along the (1 1 1) peak with minor intensity along the (2 0 0) peak. XRD patterns have peak diffraction at ($2\theta = 37^{o}$ and 43^{o}) for the (1 1 1) and (2 0 0) planes respectively, and 64^{o} for the (2 2 0) plane for 0.1 M. Crystallite size was obtained at 63.77 nm maximum. Film thickness increased with increasing precursor concentration from 6.277 μm to 11.57 μm. Film micro strain was observed to have compression for all precursor solutions. Optical studies showed that transmittance decreased with increasing concentration from 80 % to 71 %. Optical band gap energy was between 3.94 eV to 3.38 eV as precursor concentration increased, revealing the effect of varied concentrations on NiO film properties. Optimized results obtained are precursors in the development of low cost, efficient, durable solar cell fabrication for developing countries.

Keywords: NiO; solar cell material; annealing, low income

INTRODUCTION

The provision of affordable and efficient energy is among the top 50 grand challenges facing humankind in the 21st century [1-2]. Electricity is non-existent for over 20 % of the world's population with developing countries comprising 99.8 % of that number [3]. Sub-Sahara Africa is home to nearly 85 % of the 1.3 billion people living in developing countries without access to electricity [4], with an estimated electrification rate of around 32 % [5]. Several countries in Africa and south Asia lack access to electricity [6], while many countries on those continents have a high degree of electricity supply disruption with an average of less than four hours of power supply daily [7]. However, developed countries like in Europe, America and Asia have turned their fortunes around in terms of electricity generation by harnessing power from renewable energy sources.

Apart from the stable supply of electricity, other attendant challenges still loom in such regions. They include the relatively high cost of electricity, underdeveloped infrastructure especially in remote areas, uneven billing of electricity, high tariffs, and unfavorable policies to mention but a few. This has caused many citizens to resort to alternate sources of electricity supply. Renewable energy has been confirmed as a viable solution to ending global electricity problems as it exceeds world energy demand [8]. Renewable energy is sustainable and not harmful to the environment. Solar energy is a good source of renewable energy [9]. The hourly solar influx on the surface of the earth surpasses annual human energy needs [10]. Solar energy is environmentally benign [11-12]. About 40 % of CO_2 emissions is saved per year for each 1 % of world electricity demand supplied by solar grid [13]. However, high costs are militating against the successful deployment of solar technology worldwide. Solar cells are an integral aspect of solar energy [14].

Large scale production at affordable cost is being studied for the purpose of fabrication of solar cells [15]. Existing methods are not suitable for scaling up due to the expensive nature and complexities associated with the vacuum environment required for fabrication. Nanostructured metal oxide, however, is promising. Nanostructured materials offer potential improvement in solar cells efficiency and reduction in manufacturing and electricity production costs [16] due to the increased surface area to volume ratio of nanoparticles. This makes nanostructured materials more efficient and better energy collectors [17]. Nanostructured materials have unique characteristics that cannot be obtained from conventional macroscopic materials [9]. The drawback of conventional materials is low absorption properties resulting in low efficiency in solar cell devices. Inorganic semiconducting materials are economical, environmentally friendly and viable sources for solar cells [18].

Fabrication of nanostructured metal oxide films is attracting interest in terms of technological applications [19-22]. They have been studied due to their vast range of use [23], including in applications such as solar cells, UV detectors,

*Corresponding author's email id: ukobaking@yahoo.com

electrochromic devices, anti-ferromagnetic layers, p-type transparent conductive thin films, and chemical sensors [24-29]. The properties of metal oxides can be experimentally optimized for better results in a specific application. The properties of the metal oxides are affected by the control of the desired morphology, structure, size and other properties of the material for specific applications [30- 31]. Metal oxides often show n-type conductivity with a few displaying p-type. NiO has p-type conductivity [32]. NiO exists in various oxidation states [33]. It is pale green with a cubic structure. It is durable with stable chemical properties and optical densities. NiO has been prepared using sputtering [34], sol-gel [35], electron beam deposition [36], laser ablation [37], and chemical bath deposition [38]. The spray pyrolysis technique (SPT) allows coating of large areas by films of very thin layers with uniform thickness [39]. SPT has low material cost, is easy to set up and economical for mass production [40-41]. These features informed the application of SPT in this study. Some of the relevant literature has highlighted the potential of SPT in NiO fabrication of solar cells.

A recent review by Ukoba et al. [42] presented the different precursors and their characterization methods for spray deposition of NiO thin film and concluded that the usefulness of SPT as a simple but efficient method cannot be over-emphasized for mass production of solar cells. The review advocated for the exploration of different optimization approaches [42]. The present study is therefore tilted towards the optimization of the precursor concentrations of NiO films and the properties of NiO films as an alternate solar energy material with emphasis on efficiency and affordability. The objectives include: preparing a nanostructured NiO thin film on glass substrate using SPT to deposit an aqueous solution of nickel acetate, and subsequently determining the effects of varying the concentrations of nickel acetate on the properties of NiO films.

EXPERIMENTAL PROCEDURE

Spray Pyrolysis Setup

The experimental configuration used is shown in Fig. 1, comprising air compressor, temperature controller, heater, exhaust fan and pipe, and spray gun with attached container. The container houses the precursor solution. A hose connects the air compressor to the spray gun. A temperature of 350 ^{o}C was attained and read by a thermocouple attached to the heater before commencing deposition.

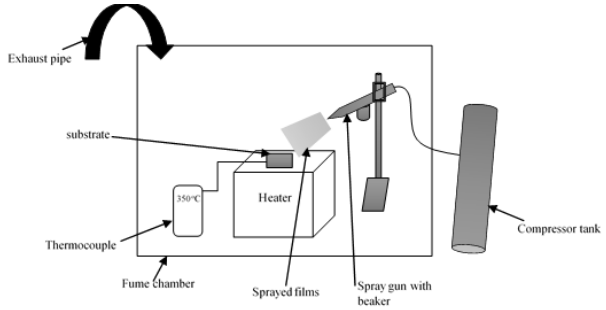

Figure 1: Experimental set-up of Spray pyrolysis technique

Precursor Preparation and Deposition

Precursor solution was nickel acetate tetrahydrate of concentration 0.025 M, 0.05 M, 0.075 M and 0.1 M. This was mixed and stirred in 50 mL distilled water for 10 min. Thereafter the solution was poured into the spray gun container. The glass substrate was chemically and ultrasonically cleaned before usage. The glass substrate was heated at a constant temperature of 350 ^{o}C on a heater. Other deposition parameters were maintained to obtain uniform film thickness. The optimum deposition parameters of spray deposited NiO film are shown in Table 1. Each droplet is found to be smaller than micro-sized particles. The sprayed solution on the preheated substrate glass experiences evaporation and solute precipitation before pyrolytic decomposition as shown in Equation (1). Nickel oxide is given off as a final product.

$$\mathrm{Ni}(CH_3COO)_2.4H_2O \xrightarrow{heat} NiO + 7H_2O \uparrow + 4CO_2 \uparrow \quad (1)$$

The color of prepared thin film was observed to be gray, uniform and strongly adherent to the glass.

Table 1. Optimum deposition parameter of SPT NiO film

Deposition parameter	Value
Substrate temperature	350 ^{o}C
Distance of spray nozzle to substrate distance	20 cm
Spray rate	1 ml/min
Spray time	1 min
Time between sprays	30 s
Carrier gas	Filled compressed air of 1 bar

Characterization

The morphology of deposited NiO film was studied using a ZEISS ULTRA PLUS Field Emission Gun Scanning Electron Microscope (FEGSEM). Elemental analysis was performed using an Energy Dispersive X-ray Spectrometer (EDX: "AZTEC OXFORD DETECTOR"). Structural properties of the deposited NiO films were investigated using an EMPYREAN (PANalytical) X-ray powder diffractometer for a range of 5 º to 90 º 2θ angles. Measured film thickness was compared with calculated film thickness obtained using the weight difference method. Optical properties were studied in wavelengths of 300 nm to 1000 nm with a SHIMADZU UV-3600UV-VIS Spectrometer model.

RESULTS AND DISCUSSION

Morphological Studies

FEGSEM micrographs are represented in Fig. 2. These micrographs reveal homogeneous, smooth, well adherent film devoid of pinholes and cracks. The morphology becomes grainier with bigger flakes with increasing concentration. This is an improvement on results observed by Bari et al. [43] and Sadaati et al.[44]. This confirms that varying the concentration of the precursors affects NiO film morphology.

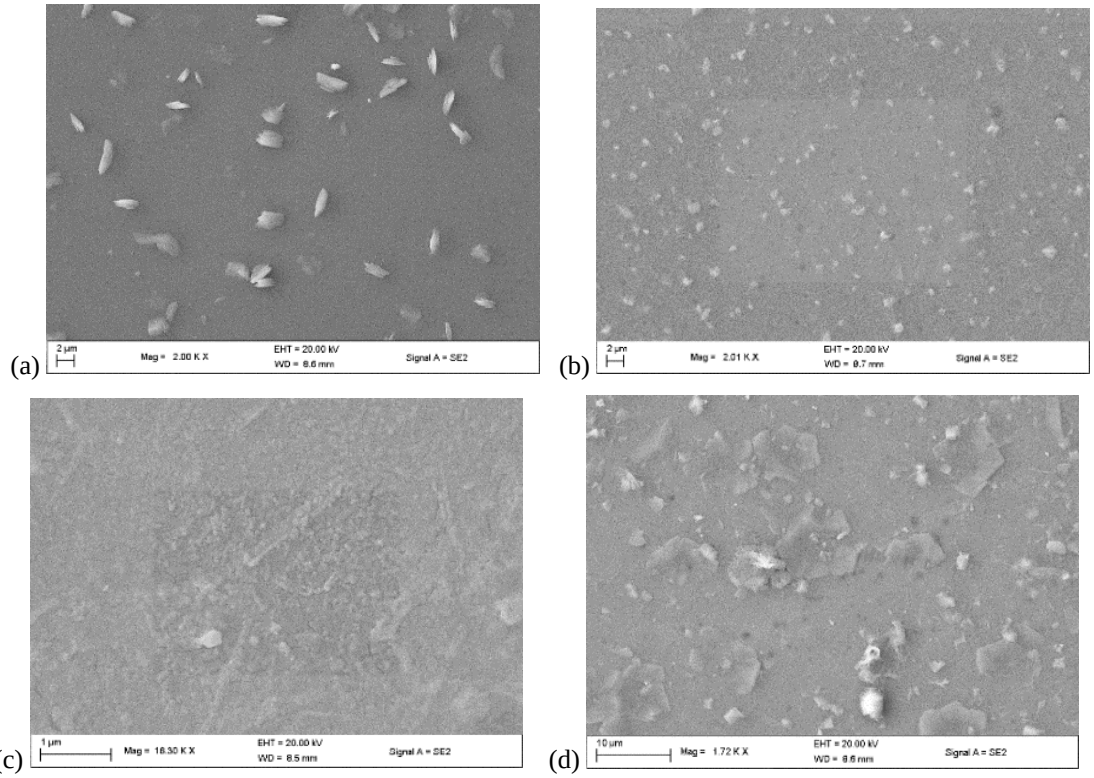

Figure 2: SEM micrographs of nickel oxide (NiO) film on glass substrate at (a) 0.025M and (b) 0.05Mgreen (c) 0.075M and (d) 0.1M

Elemental Composition Analysis

Figure 3 shows the EDX for the different concentrations for the NiO thin films thereby confirming the presence of Ni and O elements in the NiO thin films. Oxygen concentration in deposited NiO films decreases as the precursor concentration increases as seen in the EDX result. This may be due to increased film growth on the glass substrate thereby making less of the glass (oxygen) visible. This gives better distribution of Ni and O compared with a previous reported distribution [45]. An additional silicon (Si) element was also observed. This is because Si is present in soda-lime glass or soda-lime-silica glass substrate [46].

Film Thicknesses and Precursor Solution Concentration

Film thicknesses were considered with precursors of concentration 0.025 M and 0.1 M. The film thickness was obtained using SEM cross sectional profiling as shown in Fig. 4 and the weight difference method expressed in Equation (2) [47] and plotted in Fig. 5.

$$t = \frac{m}{A\rho} \qquad (2)$$

Where t is film thickness, m is actual mass deposited, A is thin film area and ρ is density of material.

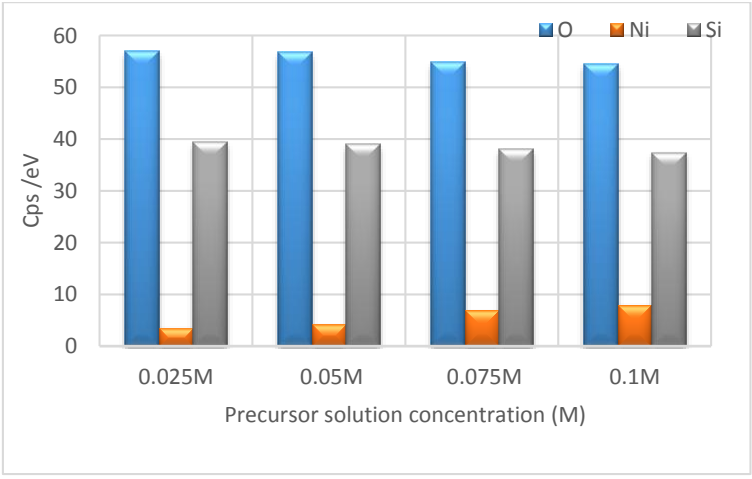

Figure 3: Elemental composition of deposited NiO films

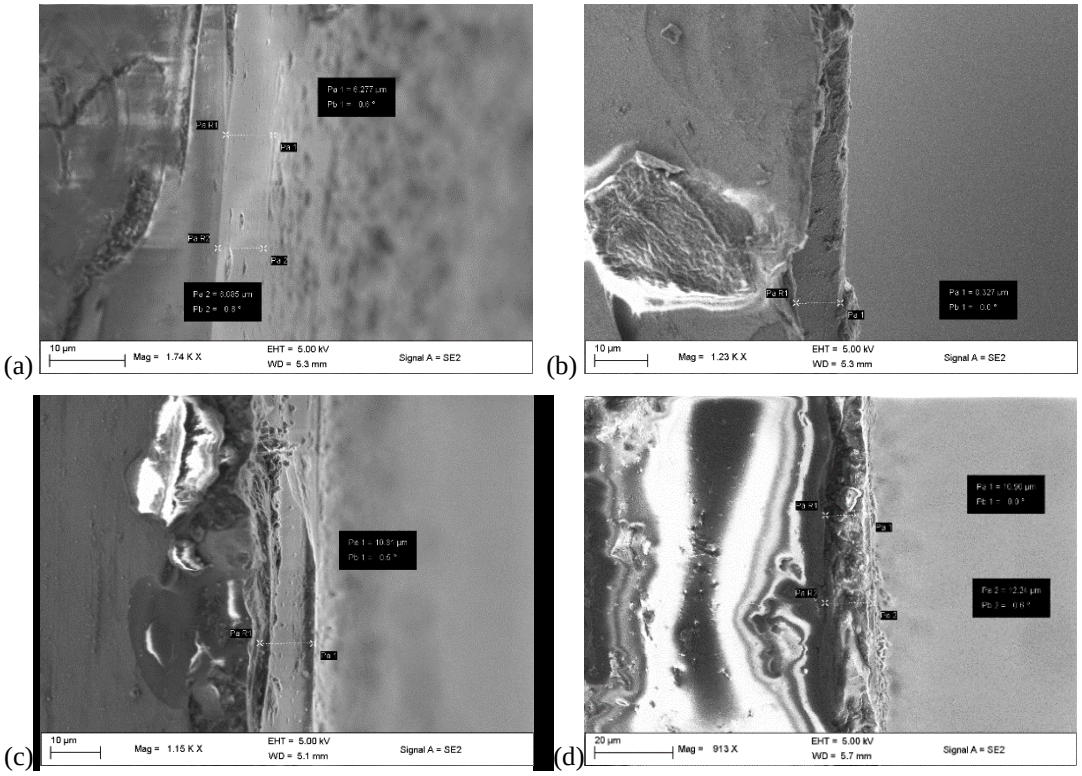

Figure 4. Film thickness obtained from SEM cross-sectional profiling for (a) 0.025M; (b) 0.05M; (c) 0.075M; (d) 0.1M

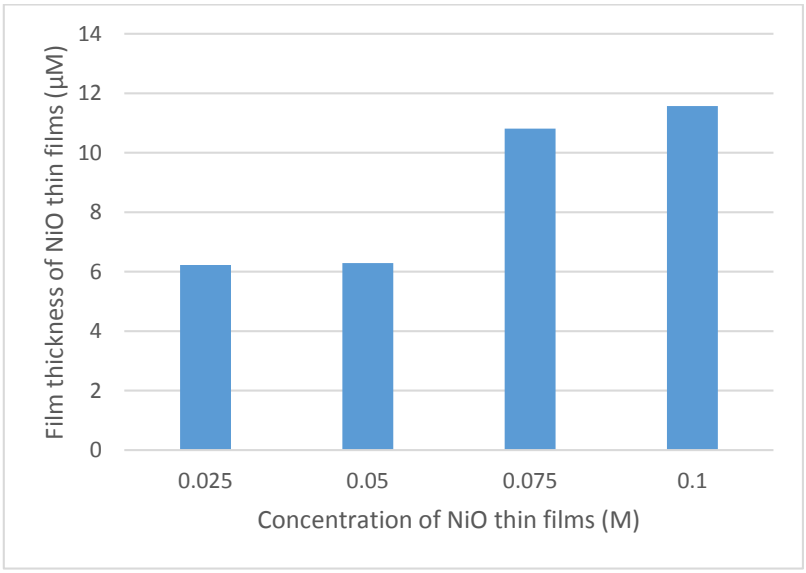

Figure 5. Film thickness of NiO thin films using weight difference method

There was no disparity between the SEM cross sectional profiling and the film thickness obtained using the weight difference. Film thickness increases as precursor concentration increases. This is an improvement on previous study results [48]. This improvement may be as a result of accumulation of deposited NiO on the substrate. This was collaborated by the EDX results. The thickness of the NiO film was controlled by keeping the deposition parameters constant. The NiO thin film average thickness was between 6.277 µm and 11.57 µm.

Structural Studies

The phase and the preferred orientation of the deposited nanostructured NiO films were determined using an x-ray diffractometer. Figure 6 gives the XRD patterns of the deposited nanostructured NiO films at different precursor concentrations. The patterns have peak diffractions at (2θ = 37 º and 43 º) for the (1 1 1) and (2 0 0) planes respectively and 64 º for the (2 2 0) plane for 0.1 M. The XRD analysis confirms Bunsenite which corresponds to the JCPDS card: 04- 0835 for

Nickel oxide [49]. The highest intensity was recorded for the (1 1 1) plane with a strong peak of 2θ = 37 º for precursor solutions of 0.05 M, 0.075 M and 0.1 M which is an improvement on Bakr et al. [50]. This could be due to an increase in grain growth caused by greater thickness. It can also be due to an increase in crystallinity as the concentration of the precursor solution increases. These results confirm the polycrystalline with cubic crystalline structures of deposited NiO film. Balu et al. [51] also observed polycrystalline with cubic structures when they varied concentrations of NiO films using SPT with a perfume atomizer but this seemed to have more intensity. The lower intensity peak of (2 0 0) increased gradually as the precursor solution increased from 0.05 M to 0.1 M with emergence of a third peak of (2 2 0) for 0.1 M. The average crystallite size was obtained using the Debye-Scherrer formula [52-53] in Equation (3).

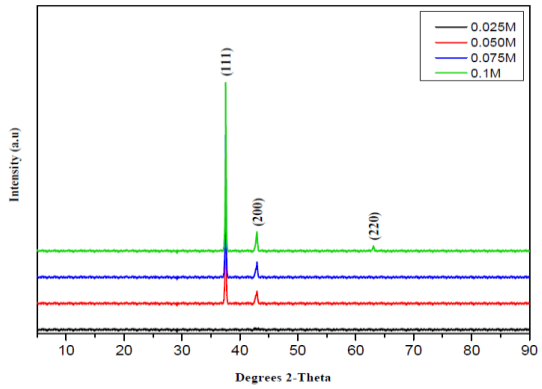

Figure 6. XRD patterns of nanostructured NiO films for various precursor concentrations

$$D = \frac{k\lambda}{\beta \cos\theta} \quad (3)$$

Where B is full width at half maximum (FWHM) peak intensity (in Radian), λ is wavelength, θ represent Bragg's diffraction angle and k is 0.89 respectively.

The lattice constant was found to be 4.1905 Å, 4.1856 Å, 4.1852 Å, 4.1850 Å for 0.025 M to 0.1 M respectively. This agrees with the standard lattice constant of NiO film value of 4.176 Å [54].

Micro strain was produced through growth of thin film and was calculated using the formula in Equation (4) [55].

$$\delta = \frac{d_{ASTM} - d_{XRD}}{d_{ASTM}} \times 100 \quad (4)$$

Where d is the lattice constant and δ is the micro strain.

A plot of NiO film micro strain against precursor solution is shown in Fig. 7. It shows that there is an increase in micro strain as precursor concentration increases. Micro strain represents compression as seen in Table 2 which gives detailed results of micro strain, lattice constants and 2θ values for deposited NiO films for precursor solution concentrations of 0.025 M to 0.1 M.

Table 2. Calculated parameters from XRD data

Parameter		0.025	0.05M	0.075	0.1M
2θ	hkl		37	37	37
	(1 1 1)				
	(2 0 0)	x	43	43	43
	(2 2 0)	x	X	X	63
Lattice constant d (Å)	recorded XRD	4.1905	4.1855	4.1852	4.1850
	ASTM	4.1684	4.1684	4.1684	4.1684
Micro strain (δ) %		-0.5301	-0.4102	-0.4030	-0.3982

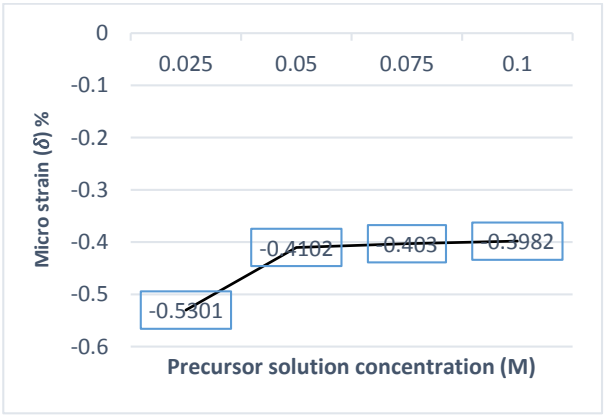

Figure 7. Graph of micro strain against precursor solution concentration for NiO films

Optical properties

Figure 8 represents measurements of transmittance and wavelength for deposited NiO films at various precursor solution concentrations. Transmittance decreases from 80 % to 71 % as precursor solution concentration increases (0.025 M to 0.1 M). This may be ascribed to the increased value of NiO thickness and absorbance. The absorption edge in thicker films was less sharp. This occurred because as precursor concentration increases there is bigger cluster of deposited films causing the scattered radiation to be more pronounced because of surface roughness [56]. These results exceeded previous reported values [57-58].

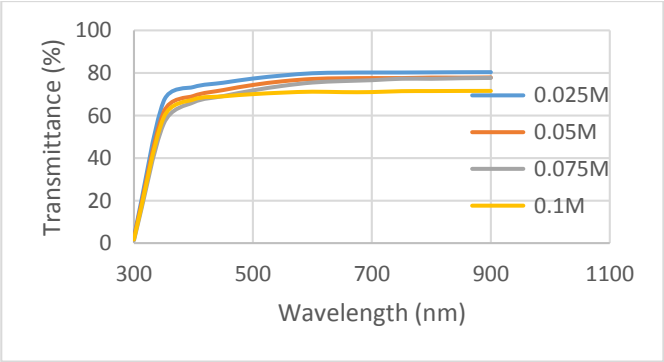

Figure 8. Plot of transmittance against wavelength of varied NiO film molarity

Absorption coefficient, α was obtained using Equation (5) [59].

$$\alpha = (2.303 \times A) / t \quad (5)$$

Where t is film thickness and A is absorbance. Optical absorption is related with optical energy band gap as expressed in Equation (6) [60-61].

$$\alpha^2 = C\left(h\upsilon - E_g\right) \quad (6)$$

Where C has constant value, h denotes Planck's constant, υ represent incidence light frequency, and E_g denotes optical energy band gap.

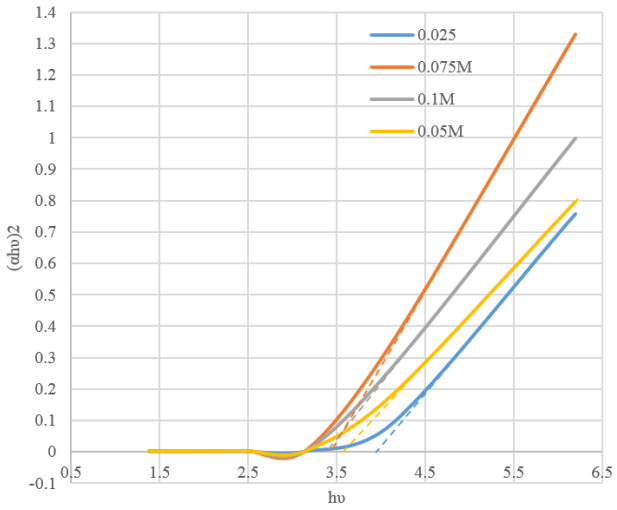

Figure 9. Graph of $(\alpha h\upsilon)^2$ against hυ for NiO films

Figure 9 shows a graph of $(\alpha h\upsilon)^2$ against hυ for NiO film spray deposited at different precursor concentrations. Extrapolation of the linear line of the graph to hυ axis for $(\alpha h\upsilon)^2 = 0$ gives the optical band gap. A decrease in slope of the plot is also observed as precursor concentration increases. A shift towards lower energy is observed according to the value of the optical band gap. This reduction is attributed to the Moss-Burstein shift [62-63]. Optical energy band gaps are: 3.94 eV, 3.56 eV, 3.44 eV and 3.38 eV for 0.025 M, 0.05 M, 0.075 M and 0.1 M respectively. This gives a better optical band gap than existing reported values [64]. This may be ascribed to crystallite size increment as precursor concentration decreases [65]. A quantum size effect may be responsible for the large value of the band gap of NiO film [66]. Careful and well optimized deposition parameters also helped in obtaining better optical band gaps.

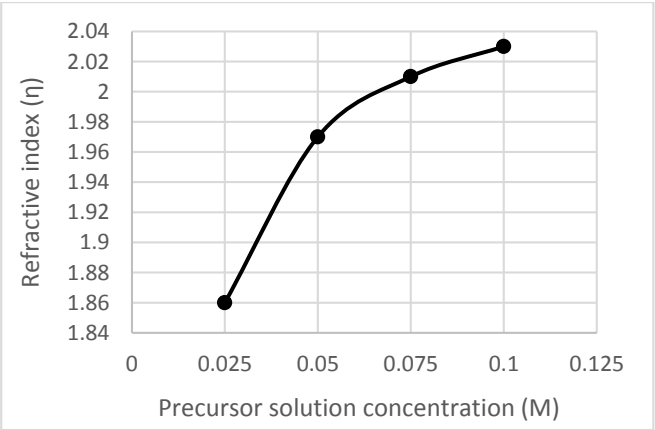

Figure 10. Variation of refractive index with precursor solution concentration of NiO films

The refractive index of deposited films, shown in Fig. 10, was calculated using the relation between the refractive index and the optical band gap as shown in Equation 7 [67].

$$\eta = \sqrt{(12.417 / (E_g - 0.365)} \quad (7)$$

Where η is refractive index and E_g is optical band gap. The refractive indices were found to be 1.86, 1.97, 2.01 and 2.03 for precursor solutions of 0.025 M, 0.05 M, 0.075 M and 0.1 M respectively. This is an improvement on reported values by Sriram and Thayumanavan [68].

CONCLUSION

This study showed successful spray deposition of nanostructured NiO films using nickel acetate on glass substrate. The effect of varying precursor concentrations of NiO films in terms of elemental, morphological and structural properties were studied. In terms of Elemental and morphology properties, surface morphology showed an increasingly grainier surface as the molarity increased. Elemental composition confirmed the presence of the Ni and O elements in NiO films. Oxygen concentration decreased as precursor concentration increased. It was observed that the film thickness increased as the precursor solution increased from 0.025 M to 0.1 M with an average thickness range of 10 µm and 21µm respectively.

XRD patterns showed that the 0.025 M concentration has an amorphous structure while the 0.05 M to 0.1 M concentrations have a polycrystalline cubic structure. Intensity of NiO films increased with increased molarity. Preferred orientation was along the (1 1 1) peak. The patterns had peak diffraction at (2θ = 37 º, and 43 º) for the (1 1 1) and (2 0 0) planes respectively and 64 º for the (2 2 0) plane for 0.1 M. The lattice constant decreased from 4.1905 Å to 4.1850 Å for 0.025 M to 0.1 M which correlated with the 4.176 Å standard lattice constant of NiO. Micro strain of films showed compression and increases with precursor concentration.

Transmittance reduced as precursor concentration increased. Transmittance decreased from about 80 % to 71 % as concentration increased. Optical band gap varied from 3.94 eV

to 3.38 eV as concentration increased. This study produced better optical band gaps than existing literature. These new results were as a result of optimization of the deposition parameters. Therefore, varying precursor solution concentration has an effect on properties of nanostructured NiO thin film. Based on the result obtained, the prepared NiO thin film sample can be used as an absorber layer of a solar cell. This optimized result may be the answer to low cost, durable yet efficient solar cell fabrication and research in developing countries.

ACKNOWLEDGEMENTS

This work was supported by National Research Foundation and The World Academy of Science and (NRF/TWAS) of South Africa [grant number 105492].

REFERENCES

[1] Grätzel, M., 2004, "Mesoscopic Solar Cells for Electricity and Hydrogen Production from Sunlight," Chem. Lett., 34(1), pp. 8-13.

[2] Lubega, W. N., and Farid. A. M., 2014, "Quantitative Engineering Systems Modeling and Analysis of the Energy-Water Nexus," Appl. Energy,135, pp. 142-157.

[3] Shyu, C.-W., 2014, "Ensuring Access to Electricity and Minimum Basic Electricity Needs as a Goal for the Post-MDG Development Agenda after 2015," Energy Sustainable Dev., 19, 29-38.

[4] International Energy Agency, United Nations Development Programme and United Nations Industrial Development Organisation, 2010, "Energy Poverty: How to make Modern Energy Access Universal? Special Early Excerpt of the World Energy Outlook 2010 for the UN General Assembly on the Millennium Development Goals. Paris: Organization for Economic Co-Operation and Development/International Energy Agency. Energy Modern Energy Services in Brazil, 269.

[5] International Energy Agency, 2013, World Energy Outlook Special Report. Paris:). Retrieved from: https://www.iea.org/publications/freepublications/publication/SoutheastAsiaEnergyOutlook_ WEO2013SpecialReport. pdf.

[6] REN21., 2015, Renewables 2015 Global Status Report. Paris: REN21 Secretariat.

[7] Ellabban, O., Abu-Rub, H., and Blaabjerg, F., 2014, "Renewable Energy Resources: Current Status, Future Prospects and their Enabling Technology," Renewable Sustainable Energy Rev., 39, pp.748-764.

[8] Emodi, N., and Yusuf, S., 2015, Improving Electricity Access in Nigeria: Obstacles and the Way Forward. Int. J. Energy Economics Policy, 5(1), pp. 335-351.

[9] Hussein, A. K., 2015, "Applications of Nanotechnology in Renewable Energies—A Comprehensive Overview and Understanding," Renewable Sustainable Energy Rev., 42, pp. 460-476.

[10] Lewis, N. S., 2007, "Toward Cost-Effective Solar Energy Use," Science, 315, pp. 798-801.

[11] Bustamante, M. L., and Gaustad. G., 2014, "Challenges in Assessment of Clean Energy Supply-Chains Based on Byproduct Minerals: A Case Study of Tellurium use in Thin Film Photovoltaics," Appl. Energy, 123, pp. 397-414.

[12] Menoufi, K., Chemisana D., and Rosell. J. I., 2013, "Life Cycle Assessment of a Building Integrated Concentrated Photovoltaic Scheme" Appl. Energy, 111, pp. 505-514.

[13] Gardner, G., 2008, Alternative Energy and Nanotechnology. Publ. Commun. Sci. Technol.

[14] Green, M. A., 1982, Solar Cells: Operating Principles, Technology, and System Applications. Prentice-Hall, Englewood Cliffs, NJ.

[15] Eslamian, M., 2014, "Spray-On Thin Film PV Solar Cells: Advances, Potentials and Challenges," Coat., 4, pp. 60-84.

[16] Serrano, E., Rus, G., and Garcia-Martinez J., 2009, "Nanotechnology for Sustainable Energy," Renewable Sustainable Energy Rev., 13, pp. 2373-2384.

[17] Bankole, M., Tijani, J. O., Mohammed, I., and Abdulkareem, A., 2014, "A Review on Nanotechnology as a Tool of Change in Nigeria," Sci. Res. Essays, 9, 213-223.

[18] Joshi, S., Mudigere, M., Krishnamurthy, L., Shekar, G., 2014, "Growth and Morphological Studies of NiO/CuO/ZnO Based Nanostructured Thin Films for Photovoltaic Applications," Chem. Pap., 68:1584-1592.

[19] Rahal, A., Benhaoua, A., Jlassi, M., and Benhaoua, B., 2015, "Structural, Optical and Electrical Properties Studies of Ultrasonically Deposited Tin oxide (SnO_2) Thin Films with Different Substrate Temperatures," Superlattices Microstruct., 86, pp. 403-411.

[20] Zhang, W., Ding, S., Yang, Z., Liu, A., Qian ,Y., Tang, S., and Yang, S., 2006, "Growth of novel Nanostructured Copper Oxide (CuO) Films on Copper Foil," J. Cryst. Growth, 291, pp. 479-484.

[21] Shaikh, S. K., Inamdar, S. I., Ganbavle, V. V., and Rajpure, K. Y., 2016," Chemical Bath Deposited ZnO Thin Film Based UV Photoconductive Detector," J. Alloys Compd., 664, pp. 242-249.

[22] Drevet, R, Legros C, Bérardan D, Ribot P, Dragoé D, Cannizzo C., and Andrieux M., 2015, "Metal Organic Precursor Effect on the Properties of SnO 2 Thin Films Deposited by MOCVD Technique for Electrochemical Applications," Surf. Coat. Technol.,

271, pp. 234-241.

[23] Soonmin, H., 2016 "Preparation and Characterization of Nickel Oxide Thin Films: A Review," Int. J. Appl. Chem., 12, pp. 87-93.

[24] Nam, W. J., Gray, Z., Stayancho, J., Plotnikov, V., Kwon, D., Waggoner, S., et al., 2015, "ALD NiO Thin Films as a Hole Transport-Electron Blocking Layer Material for Photo-Detector and Solar Cell Devices," ECS Meeting Abstracts, 66, pp. 275-279.

[25] Park, N., Sun, K., Sun, Z., Jing, Y., and Wang, D., 2013, "High Efficiency NiO/ZnO Heterojunction UV Photodiode by Sol-Gel Processing," J. Mater. Chem. C, 1, pp. 7333-7338.

[26] Li, C., and Zhao Z., 2010, "Preparation and Characterization of Nickel Oxide Thin Films by a Simple Two-Step Method," In Vacuum Electron Sources Conference and Nanocarbon (IVESC), 2010 8th International, pp. 648-649.

[27] Wu, C-C., and Yang, C-F., 2015, "Effect of Annealing Temperature on the Characteristics of the Modified Spray Deposited Li-Doped NiO Films and their Applications in Transparent Heterojunction Diode," Sol. Energy. Mater. Sol. Cells, 132, pp. 492-498.

[28] Zhu, Z., Bai, Y., Zhang, T., Liu, Z., Long, X., Wei, Z, et al., 2014, "High-Performance Hole-Extraction Layer of Sol-Gel-Processed NiO Nanocrystals for Inverted Planar Perovskite Solar Cells," Angewandte Chemie, 126, pp. 12779-12783.

[29] Magaña, C. R., Acosta, D. R., Martínez, A. I., Ortega, J. M., 2006, "Electrochemically Induced Electrochromic Properties in Nickel Thin Films Deposited by DC Magnetron Sputtering," Sol. Energy, 80, pp. 161-169.

[30] Su, S. Liu, T., Wang, Y., Chen, X., Wang, J., and Chen, J,. 2014, "Performance Optimization Analyses and Parametric Design Criteria of a Dye-Sensitized Solar Cell Thermoelectric Hybrid Device," Appl. Energy, 120, pp. 16-22.

[31] Wang, X., Li, H., Liu, Y., Zhao, W., Liang, C., Huang, H., Mo, D., Liu, Z., Yu, X. and Deng, Y., 2012, "Hydrothermal Synthesis of Well-Aligned Hierarchical Tio_2 Tubular Macrochannel Arrays with Large Surface Area for High Performance Dye-Sensitized Solar Cells," Appl. Energy, 99, pp. 198-205.

[32] Kim, H-J, and Lee, J-H., 2014, "Highly Sensitive and Selective Gas Sensors Using P-Type Oxide Semiconductors: Overview," Sens. Actuators B: Chem., 192, pp. 607-627.

[33] Subramanian, B., Ibrahim, M. M., Senthilkumar, V., Murali, K., Vidhya, V., Sanjeeviraja, C., and Jayachandran, M., 2008, "Optoelectronic and Electrochemical Properties of Nickel Oxide (Nio) Films Deposited by DC Reactive Magnetron Sputtering," Physica B: Condens. Matter, 403, pp. 4104-4110.

[34] Keraudy, J., García Molleja, J., Ferrec, A., Corraze, B., Richard-Plouet, M., Goullet, A., et al., 2015, "Structural, Morphological and Electrical Properties of Nickel Oxide Thin Films Deposited by Reactive Sputtering," Appl. Surf. Sci, 357, Part A, pp. 838-844.

[35] Jlassi, M., Sta, I., Hajji, M., and Ezzaouia, H., 2014, "Optical and Electrical Properties of Nickel Oxide Thin Films Synthesized by Sol-Gel Spin Coating," Mater. Sci. Semicond. Process, 21, pp. 7-13.

[36] El-Nahass, M. M., Emam-Ismail, M., and El-Hagary, M., 2015, "Structural, Optical and Dispersion Energy Parameters of Nickel Oxide Nanocrystalline Thin Films Prepared by Electron Beam Deposition Technique," J. Alloys Compd., 646, pp. 937-945.

[37] Wang, H., Wang, Y., and Wang, X., 2012, "Pulsed Laser Deposition of the Porous Nickel Oxide Thin Film at Room Temperature for High-Rate Pseudocapacitive Energy Storage," Electrochem. Commun., 18, pp. 92-95.

[38] Vidales-Hurtado, M. A., and Mendoza-Galván, A., 2008, "Electrochromism in Nickel Oxide-Based Thin Films Obtained by Chemical Bath Deposition," Solid State Ionics, 179, pp. 2065-2068.

[39] Gowthami, V., Perumal, P., Sivakumar, R., and Sanjeeviraja, C., 2014, "Structural and Optical Studies on Nickel Oxide Thin Film Prepared by Nebulizer Spray Technique," Physica B: Condens. Matter, 452, pp. 1-6.

[40] Patil, P. S., 1999, "Versatility of Chemical Spray Pyrolysis Technique," Mater. Chem. Phys., 59, pp. 185-198.

[41] Faraj, M. G., 2015, "Effect of Aqueous Solution Molarity on the Structural and Electrical Properties of Spray Pyrolysed Lead Sulfide (PbS) Thin Films," Int. Lett. Chem. Phys. Astron., 57, pp. 122.

[42] Ukoba, K. O, Eloka-Eboka, A. C., and Inambao, F. L., 2017, "Review of Nanostructured Nio Thin Film Deposition Using the Spray Pyrolysis Technique," Renewable Sustainable Energy Rev. In Press., http://dx.doi.org/10.1016/j.rser.2017.10.041

[43] Bari, R., Patil, S., and Bari, A., 2013, "Effect of Molarity of Precursor Solution on Physical, Structural, Microstructural and Electrical Properties of Nanocrystalline Zno Thin Films," Mater. Technol., 28, pp. 214-220.

[44] Saadati, F., Grayeli, A., and Savaloni, H., 2010, "Dependence of the Optical Properties of Nio Thin Films on Film Thickness and Nano-Structure," J. Theor. Appl. Phy., 4, pp. 22-26.

[45] Reguig, B., Regragui, M., Morsli, M., Khelil, A., Addou, M., and Bernede, J., 2006, "Effect of the Precursor Solution Concentration on the Nio Thin

Film Properties Deposited by Spray Pyrolysis," Sol. Energy Mater. Sol. Cells, 90, pp. 1381-1392.

[46] de Jong, B. H. W. S., 1989, Glass in Ullman's Encyclopedia of Industrial Chemistry, 5th ed. vol. A12, VCH Publishers, Weinheim, Germany, pp. 365-432.

[47] Godse, P., Sakhare, R., Pawar, S., Chougule, M., Sen, S., Joshi, P., et al., 2011, "Effect of Annealing on Structural, Morphological, Electrical and Optical Studies of Nickel Oxide Thin Films," J. Surf. Eng. Mater. Adv. Technol., 1, pp. 35.

[48] Boyraz, C., and Urfa, Y., 2015, "Effect of Solution Molarity on Microstructural and Optical Properties of CdCr 2 S 4 thin films," Mater. Sci. Semicond. Process., 36, pp. 1-6.

[49] Gabal, M., 2003, "Non-Isothermal Decomposition of NiC_2O_4–FeC_2O_4 Mixture Aiming at the Production of NiFe 2 O 4," J. Phys. Chem. Solids, 64, pp. 1375-1385.

[50] Bakr, N. A., Salman, S. A., and Shano, A. M., 2015, "Effect of Co Doping on Structural and Optical Properties of NiO Thin Films Prepared By Chemical Spray Pyrolysis Method," Int. Lett. Chem. Phys. Astron., 41, pp. 15-30.

[51] Balu, A., Nagarethinam, V., Suganya, M., Arunkumar, N., and Selvan, G., 2012, "Effect of Solution Concentration on the Structural, Optical and Electrical Properties of SILAR Deposited CdO thin films," J. Electron. Devices, 2, pp. 739-749.

[52] Scherrer, P., Nachr, G., 1918, "Derivation of Crystallite Size," OH HO OH OH OH O OH.

[53] Barrett, C., and Massalski, T., 1980, Structure of Metals, Pergamon Press, Oxford.

[54] Pistorius, C. W. F. T., 1963, "Some Phase Relations in the System COO-SiOerO. NiO-SiOz-Hzo and ZnO-SiOrHiO to High Pressures and Temperatures," Neues Jahrb Mineral Monatsh, pp. 30-57.

[55] Mohammad, A. J., 2006, "Studying the Effect of Molarity on the Physical and Sensing Properties of Zinc Oxide Thin Films Prepared by Spray Pyrolysis Technique," PhD thesis, Applied Science Dep. University of Technology, Baghdad.

[56] Balu, A., Nagarethinam, V., Arunkumar, N., and Suganya, M., 2012, "Nanocrystalline NiO Thin Films Prepared by A Low Cost Simplified Spray Technique Using Perfume Atomizer," J. Electron. Devices, 13, pp. 920-930.

[57] Ismail, R. A., Ghafori, S. A., and Kadhim, G. A., 2013, "Preparation and Characterization of Nanostructured Nickel Oxide Thin Films By Spray Pyrolysis," Appl. Nanosci. 3, pp. 509-514.

[58] Fadheela, H. O., 2015, "Structural and Optical Characterization of Nickel Oxide Thin Films Prepared by Spray Pyrolysis Technique," Eng. Tech. J., 33, pp. 10.

[59] Barman, J., Sarma, K., Sarma, M., and Sarma, K., 2008, "Structural and Optical Studies of chemically Prepared Cds Nanocrystalline Thin Films," Indian J. Pure Appl. Phys., 46, pp. 339-343.

[60] Ezema, F., Ekwealor, A., and Osuji, R., 2006, "Effect of Thermal Annealing on the Band GAP and Optical Properties of Chemical Bath Deposited Znse Thin Films," Turk. J. Phys., 30, pp. 157-163.

[61] Estrella, V., Nair, M., and Nair, P., 2003, "Semiconducting Cu3BiS3 Thin Films Formed by the Solid-State Reaction of CuS and Bismuth Thin Films," Semicond. Sci. Technol., 18, pp. 190.

[62] Burstein, E., 1954, "Anomalous Optical Absorption Limit in InSb," Phys. Rev., 93, pp. 632.

[63] Moss, T., 1954, "The Interpretation of the Properties of Indium Antimonide," Proc. Phys. Soc. Section B., 67, pp. 775.

[64] Boschloo, G., and Hagfeldt, A., 2001, "Spectroelectrochemistry of Nanostructured NiO," J. Phys. Chem. B., 105, pp. 3039-3044.

[65] Makhlouf, S., Kassem, M., and Abedulrahim, M., 2010, "Crystallite Size Dependent Optical Properties of Nanostructured Nio Films," J. Optoelectron. Adv. Mater., 4, pp. 1562.

[66] Romero, R., Martin, F., Ramos-Barrado, J., and Leinen, D., 2010, "Synthesis and Characterization of Nanostructured Nickel Oxide Thin Films Prepared with Chemical Spray Pyrolysis," Thin Solid Films, 518, pp. 4499-4502.

[67] Reddy, R., Aharnmed, Y. N., Azeem, P. A., Gopal, K. R., Devi, B. S., and Rao, T., 2003, "Dependence of Physical Parameters of Compound Semiconductors on Refractive Index," Defence Sci. J., 53, pp. 239.

[68] Sriram, S., and Thayumanavan, A., 2013, "Structural, Optical and Electrical Properties of NiO Thin Films Prepared by Low Cost Spray Pyrolysis Technique," Int. J. Mater. Sci. Eng., 1, pp. 118-21.

[69] Chen, Z., Zhang, X.-d. Fang, J. Liang, J.-h. Liang, X.-j. Sun, J. Zhang, D.-k. Wang, N. Zhao H.-x. and Chen, X.-l., 2014, "Enhancement in Electrical Performance of Thin-Film Silicon Solar Cells Based on a Micro- and Nano-Textured Zinc Oxide Electrode," Applied Energy; 135, pp. 158-164.

CHAPTER 5 Part 2: FABRICATION OF AFFORDABLE AND SUSTAINABLE SOLAR CELLS USING NiO/TiO2 PN HETEROJUNCTION

To cite the article: Ukoba, K. O., Inambao, F. L., & Eloka-Eboka, A. C. (2018) "Fabrication of affordable and sustainable solar cells using NiO/TiO2 PN heterojunction" *International Journal of Photoenergy,* vol. 2018, pp 1-7, Hindawi publishers. DOI: 10.1155/2018/6062390

Link to the article: https://www.hindawi.com/journals/ijp/2018/6062390/

Hindawi
International Journal of Photoenergy
Volume 2018, Article ID 6062390, 7 pages
https://doi.org/10.1155/2018/6062390

Research Article

Fabrication of Affordable and Sustainable Solar Cells Using NiO/TiO_2 *P-N* Heterojunction

Kingsley O. Ukoba, Freddie L. Inambao, and Andrew C. Eloka-Eboka

Mechanical Engineering, University of KwaZulu-Natal, Durban, South Africa

Correspondence should be addressed to Kingsley O. Ukoba; ukobaking@yahoo.com

Received 7 December 2017; Revised 22 January 2018; Accepted 28 January 2018; Published 29 March 2018

Academic Editor: Ahmad Umar

The need for affordable, clean, efficient, and sustainable solar cells informed this study. Metal oxide TiO_2/NiO heterojunction solar cells were fabricated using the spray pyrolysis technique. The optoelectronic properties of the heterojunction were determined. The fabricated solar cells exhibit a short-circuit current of 16.8 mA, open-circuit voltage of 350 mV, fill factor of 0.39, and conversion efficiency of 2.30% under 100 mW/cm^2 illumination. This study will help advance the course for the development of low-cost, environmentally friendly, and sustainable solar cell materials from metal oxides.

1. Introduction

The need for affordable and sustainable electricity in developing nations has been an issue of concern to all stakeholders. Renewable energy has been identified as a viable solution to ending global electricity problems as its availability exceeds world energy demand [1]. Solar energy is a good source of renewable energy [2]. The hourly solar influx on the surface of the earth surpasses annual human energy needs [3]. Photovoltaic energy has received increasing interest caused by a decrease in module prices in countries like China [4]. Interest in these devices is due to improved reliability, efficiency, and costs in generating electricity [5]. Solar cells of high efficiency have been achieved with inorganic materials [6], but they require expensive materials of high purity and a technique that is energy intensive. There is, therefore, a need to explore ways of manufacturing solar cells that can scale-up to large volumes at low cost.

Metal oxide solar cells offer a good replacement for conventional silicon solar cells. This is because metal oxides are low-cost materials, have flexible optical properties, can be deposited using low-cost techniques, and are simple to scale-up to large volume production. They also display quantum confinement effects in two dimensions [7]. Nanostructured metal oxides are used in a wide range of device applications because of their broad composition and band structures [8–14]. The widely used oxides are ZnO [15], CuO [16], In_2O_3 [17], and TiO_2 [18], to mention but a few. They are widely applied in optoelectronic devices such as humidity sensors [19], photodiodes [20], solar cells [21], and photocatalysts [22].

NiO is a *P*-type semiconductor with a wide bandgap between 3.5 eV and 4.0 eV [23]. The excellent properties of NiO make it a promising material for solar cells [24]. Similarly, TiO_2 is a desirable material for harvesting solar energy because of its optoelectronic properties, high resistance to photocorrosion, affordability, stability in a wide range of pH, and nonpoisonous nature [25]. Various techniques are available for depositing metal oxides [26–31]. Low cost of equipment, ease of control of deposited film structure, and the ability to coat large areas in thin layers with uniform thickness [32–35] influenced the choice of the technique used in this study.

Heterojunctions are known to be the most competitive method of solar cell fabrication on account of being the simplest [36]. A *P-N* junction is created when *P*-type (NiO) and *N*-type (TiO_2) semiconductor materials are placed in contact with one another. A solar cell is basically a *P-N* junction with

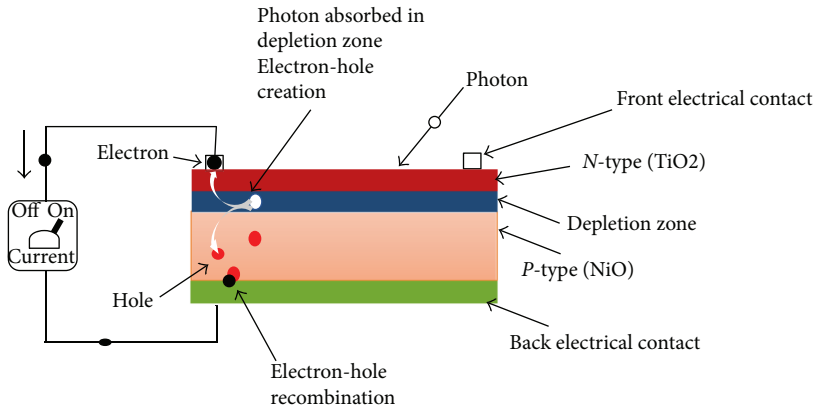

Figure 1: Solar cell generation of electricity using a *P-N* junction.

a large surface area. Figure 1 depicts generation of electricity by a solar cell using a *P-N* junction.

The overall aim of this research is the provision of affordable and sustainable solar panels for developing and low-income countries. This was achieved by fabricating nanostructured TiO_2/NiO heterojunction thin-film solar cells using the spray pyrolysis technique.

2. Methodology

2.1. Deposition. The chemicals used are of analytical reagent grade and were used without further purification. Distilled and deionized pure water were used during the course of the experiment.

The solar cell was fabricated using a modified spray pyrolysis technique (SPT) as reported by Ukoba et al. [37] and represented pictorially in Figure 2. Prior to sample preparation, the indium tin oxide- (ITO-) coated glass and soda lime glass used as substrate were clean ultrasonically as reported by Adeoye Abiodun and Salau [38]. The precursor for the window layer titanium oxide (TiO_2) nanostructure thin film was prepared by mixing 3 ml of titanium ethoxide with 30 ml of distilled water and ethanol mixture, and three droplets of acetic acid. This was stirred for one hour before spraying on cleaned indium tin oxide- (ITO-) coated glass substrates and soda lime glass substrates maintained at about 350°C. Also, deposition parameters such as substrate temperature, carrier gas flow rate, and pressure were optimized to obtain quality films.

The nanostructured nickel oxide (NiO) absorber layer was deposited on the prepared ITO/TiO_2 layers and empty soda lime glass using SPT, as shown in Figure 3. The precursor for NiO was obtained by preparing 0.05 M nickel acetate tetrahydrate in double distilled water.

The precursors were thoroughly stirred for several minutes prior to spraying onto preheated substrates maintained at about 350°C. Other deposition parameters were maintained to obtain good quality thin films. The optimized parameters used in the deposition of the NiO films are tabulated in Table 1. To complete the TiO_2/NiO heterojunction solar cell illustrated in Figure 4, gold (Au) metal contact was deposited as a back contact using DC magnetron sputtering.

Figure 2: Pictorial representation of the experimental set-up of the spray pyrolysis technique.

2.2. Testing. The TiO_2 and NiO prepared on soda lime glass were used to study the elemental, morphological, and structural characteristics of TiO_2 and NiO using energy dispersive X-ray spectrometer (EDS or EDX: "AZtec Oxford Detector"), a ZEISS Ultra Plus field emission gun scanning electron microscope (FEGSEM), and Bruker AXS D8 Advance X-ray diffractometer (XRD) with Cu-Kα radiation, respectively. The *J-V* characteristics of the fabricated TiO_2/NiO heterojunction cell in dark and under illumination were done using the Keithley SourceMeter 2400, coupled with a two-point probe. Newport solar simulator of intensity (100 mW/cm^2) was used as the source of illumination.

3. Results and Discussion

3.1. Morphological Studies. Figures 5(a) and 5(b) show the scanning electron micrograph of the NiO thin film at lower and higher magnification, respectively. The micrograph reveals scattered distribution of the NiO particles across the surface of the film. The film has even distribution, is adherent to the film surface, and has no cracks. This represents a better surface morphology compared to that of NiO films reported by Sriram and Thayumanavan

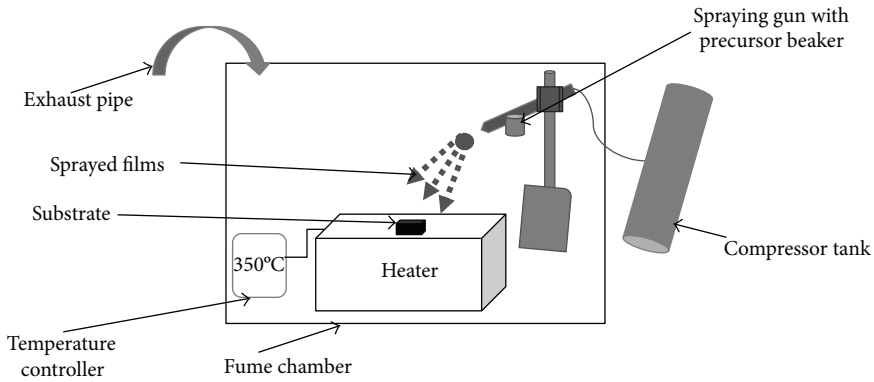

Figure 3: Experimental set-up of spray pyrolysis technique.

Table 1: Optimum deposition parameters of SPT NiO film.

Deposition parameter	Value
Substrate to nozzle height	20 cm
Rate of spray	1 ml/min
Spray time	1 min
Sprays interval	30 sec
Carrier gas	1 bar of filled compressed air

[39]. The SEM shows the potential of NiO as an absorber layer in solar cell fabrication. Figures 5(c) and 5(d) show the scanning electron micrograph of the heterojunction of NiO/TiO_2. This micrograph was obtained by the SEM at the junction or point of interaction between the TiO_2 and NiO. It shows a polycrystalline structure. The micrograph shows the *P*-type NiO and *N*-type TiO_2 of the thin film with their polycrystalline structures. It shows complete penetration at the heterojunction.

3.2. Elemental Composition. Figure 6 shows the elemental composition of the NiO/TiO_2 heterojunction solar cell deposited on the ITO-coated glass substrate. Figure 6 shows the presence of Ti, O, and Ni for the TiO_2 and NiO, respectively, and the indium (In) representing the ITO-coated glass substrate. This confirms the presence of the metal oxides in the heterojunction.

3.3. Structural Analysis. Figure 7 shows the X-ray diffraction patterns of the fabricated ITO/TiO_2/NiO heterojunction solar cell. The peaks corresponding to NiO and TiO_2 were determined with JCPDS patterns. The XRD spectrum indicates strong NiO peaks with (1 1 1), (2 0 0), and (2 2 0) preferential orientation. The patterns of the NiO thin film have peak diffractions at ($2\theta = 37^\circ$, 43°, and 64°) for the (1 1 1), (2 0 0), and (2 2 0) plane. The XRD analysis confirms Bunsenite, which corresponds to the JCPDS card: 04-0835 for nickel oxide [40] confirming it as a good absorber layer of solar cells [41]. The TiO_2 spectrum also shows strong spectrum and polycrystalline structures typical of *N*-type in heterojunction solar cells. The structure of the heterojunction indicates that the film is polycrystalline and chemically pure.

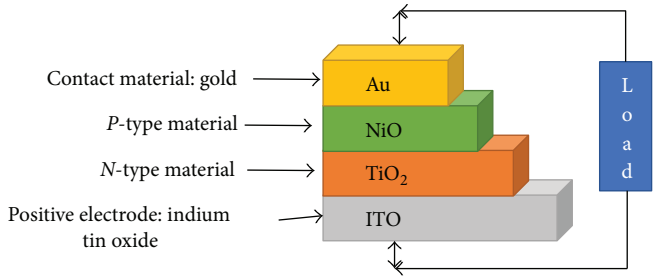

Figure 4: Schematic of the fabricated NiO/TiO_2 heterojunction solar cells.

3.4. Current Density-Voltage (J-V) Characterization. The *J-V* characteristic curve of the prepared TiO_2/NiO heterojunction thin-film solar cell under illumination and in the dark is depicted in Figure 8. The *J-V* characteristic at room temperature in the dark shows that the forward current of the cells increases slowly with increasing voltage. The solar cell has rectification properties since the dark *J-V* plots were similar to the Shockley diode characteristics, which can be expressed by the standard diode equation

$$J = J_O\left[\exp\left(\frac{qV}{AkT}\right) - 1\right], \quad (1)$$

where q is the electronic charge, A is the diode quality factor (ideality factor), k is Boltzmann's constant, T is the absolute temperature, and J_o is the reverse saturation current.

The solar cell parameters evaluated from the *J-V* curve are presented in Table 2. The fabricated solar cell exhibits the short-circuit current (J_{sc}) of 16.8 mA, the open-circuit voltage (V_{oc}) of 350 mV, the fill factor (FF) of 0.39, and the conversion efficiency (η) of 2.30%. This is a marked improvement on the values of 0.33 V and 0.29 recorded by Georgieva and Tanusevski [42] for the open-circuit voltage and fill factor, respectively. It also showed improvement in the fill factor of 0.28 reported by Noda et al. [43].

4. Solar Cell Parameters

The primary parameters that describe the performance of a photovoltaic device are discussed below.

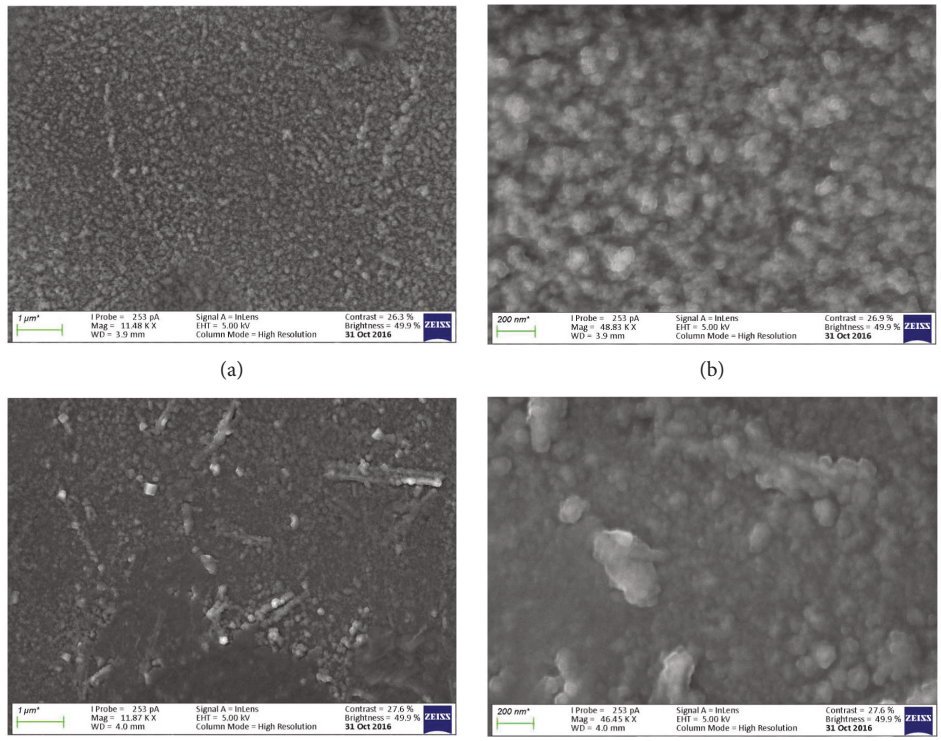

Figure 5: SEM of (a) NiO thin film at lower magnification, (b) NiO thin film at higher magnification, (c) fabricated NiO/TiO_2 heterojunction solar cell at lower magnification, and (d) fabricated NiO/TiO_2 heterojunction solar cell at higher magnification.

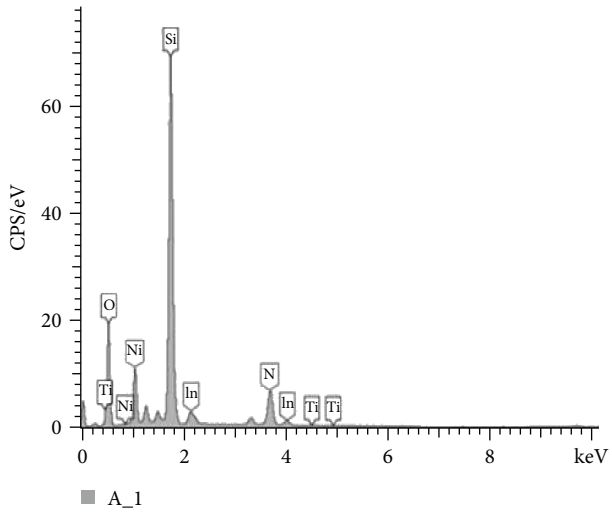

Figure 6: EDX of fabricated ITO/TiO_2/NiO heterojunction solar cell.

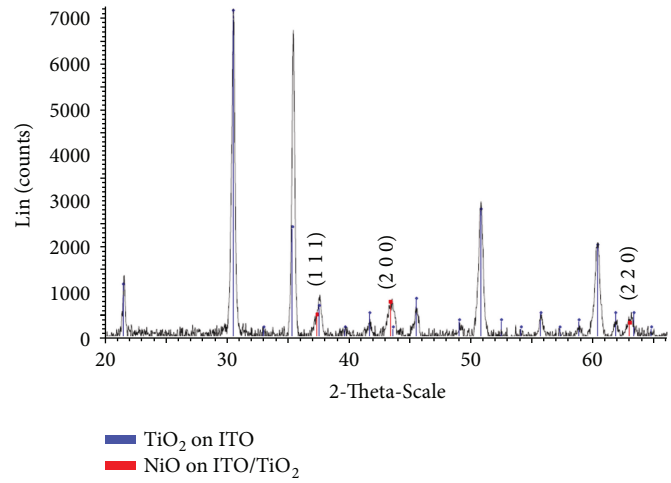

Figure 7: XRD of fabricated ITO/TiO_2/NiO heterojunction solar cell.

4.1. Open-Circuit Voltage (V_{oc}). Open-circuit voltage is the applied voltage relative to an open circuit where no current flows through the device (i.e., the voltage across the device at zero current). V_{oc} is obtained at the point of intersection of the *I-V* curve under illumination at the voltage axis. Under open-circuit conditions, the structure has to bias itself to some voltage V_{oc} in order to counter the light-beam-induced current. The open-circuit voltage V_{oc} arises as a result of the built-in electric field present in the materials system and can be expressed as

$$V_{OC} = \frac{AkT}{q} \ln\left(\frac{J_L}{J_o} + 1\right). \quad (2)$$

This quantity is left unaffected by series resistance losses in the cell but is sensitive to shunt losses.

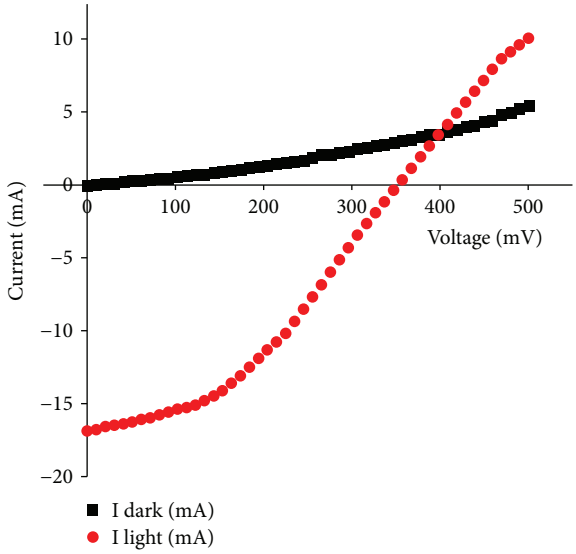

Figure 8: Typical *I-V* curve for the prepared TiO_2/NiO heterojunction thin-film solar cell under illumination and in the dark.

Table 2: Solar cell parameters of the fabricated solar cell.

Sample	J_{sc} (mA)	V_{oc} (mV)	J_{max} (mV)	V_{max} (mV)	FF (%)	η (%)
TiO_2/NiO	16.8	350.0	13.10	173.57	39	2.30

4.2. Short-Circuit Current Density (J_{sc}). J_{sc} is the current that flows through the junction under illumination at zero applied voltage, that is, $J_{sc} = J(V = 0)$. In the ideal case, it equals the photogenerated current density (J_L) and is proportional to the incident number of photons or alternatively the intensity of illumination.

J_{sc} is represented as the intersection of the *J-V* curve under illumination at the current axis. For an ideal solar cell ($R_S = 0$ and $R_{SH} = \infty$), the short-circuit current is given by

$$J_{sc} = J_o\left[\exp\left(\frac{q(0)}{AkT}\right) - 1\right] - J_L, \quad V = 0. \tag{3}$$

4.3. Fill Factor (FF). The fill factor is defined as the inverse of the ratio of the ideal power to the maximum power in operating conditions. It can be defined also as the area of the maximum power rectangle to the product of the short-circuit current and the open-circuit voltage. This is shown as

$$FF = \frac{V_{max}J_{max}}{V_{oc}J_{sc}}. \tag{4}$$

4.4. Efficiency (η). The most important parameter of a solar cell in terms of its ultimate function is the photovoltaic conversion efficiency. This is defined as the ratio of the output power (electricity) to the input power (light) and can be calculated as

$$\eta = \frac{P_{max}}{P_{in}} = \frac{FF\,(V_{oc}J_{sc})}{P_{in}}. \tag{5}$$

5. Conclusion

In this study, TiO_2 and NiO thin films were used to fabricate ITO/TiO_2/NiO heterojunction solar cells. It shows that NiO can be used in thin-film solar cells. The conversion efficiency, open-circuit voltage, short-circuit current, and fill factor were 2.30%, 350 mV, 16.8 mA, and 0.39 under 100 mW/cm^2 illumination, respectively. This is an improvement on existing values. This will open up frontiers in affordable and sustainable solar cell fabrication in developing and low-income countries.

Nomenclature

NiO: Nickel oxide
Ni: Nickel
Ti: Titanium
O: Oxygen
TiO_2: Titanium oxide
ZnO: Zinc oxide
CuO: Copper oxide
In_2O_3: Indium oxide
ITO: Indium tin oxide
Au: Gold
SPT: Spray pyrolysis technique
FEGSEM: Field emission gun scanning electron microscope
EDX: Energy dispersive X-ray spectrometer
XRD: X-ray diffractometer
J-V: Current density-voltage
I-V: Current-voltage
V_{oc}: Open-circuit voltage
J_{sc}: Short-circuit current density
FF: Fill factor
P_{in}: Power in
P_{max}: Maximum power.

Conflicts of Interest

The authors declare that there are no conflicts of interest regarding the publication of this paper.

Acknowledgments

The financial assistance of the National Research Foundation and The World Academy of Science (NRF/TWAS) of South Africa under Grant number 105492 towards this research is acknowledged. The first author also wishes to thank EMDI Akure, Adeoye Eyitayo, and Remy Bucher of iThemba Lab for their assistance in the experiment analysis.

References

[1] O. Ellabban, H. Abu-Rub, and F. Blaabjerg, "Renewable energy resources: current status, future prospects and their enabling technology," *Renewable and Sustainable Energy Reviews*, vol. 39, pp. 748–764, 2014.

[2] A. K. Hussein, "Applications of nanotechnology in renewable energies—a comprehensive overview and understanding," *Renewable and Sustainable Energy Reviews*, vol. 42, pp. 460–476, 2015.

[3] N. S. Lewis, "Research opportunities to advance solar energy utilization," *Science*, vol. 351, no. 6271, article aad1920, 2016.

[4] G.-N. Lee, M. P. Machaiah, W.-H. Park, and J. Kim, "Enhanced optical and electrical properties of ITO/Ag/AZO transparent conductors for photoelectric applications," *International Journal of Photoenergy*, vol. 2017, Article ID 8315802, 9 pages, 2017.

[5] S.-H. Hong, J.-H. Yun, H.-H. Park, and J. Kim, "Nanodome-patterned transparent conductor for highly responsive photoelectric device," *Applied Physics Letters*, vol. 103, no. 15, article 153504, 2013.

[6] M. A. Green, "Third generation photovoltaics: ultra-high conversion efficiency at low cost," *Progress in Photovoltaics: Research and Applications*, vol. 9, no. 2, pp. 123–135, 2001.

[7] S. Joshi, M. Mudigere, L. Krishnamurthy, and G. Shekar, "Growth and morphological studies of NiO/CuO/ZnO based nanostructured thin films for photovoltaic applications," *Chemical Papers*, vol. 68, no. 11, pp. 1584–1592, 2014.

[8] A. Czapla, E. Kusior, and M. Bucko, "Optical properties of non-stoichiometric tin oxide films obtained by reactive sputtering," *Thin Solid Films*, vol. 182, no. 1-2, pp. 15–22, 1989.

[9] A. Rahal, A. Benhaoua, M. Jlassi, and B. Benhaoua, "Structural, optical and electrical properties studies of ultrasonically deposited tin oxide (SnO_2) thin films with different substrate temperatures," *Superlattices and Microstructures*, vol. 86, pp. 403–411, 2015.

[10] W. Zhang, S. Ding, Z. Yang et al., "Growth of novel nanostructured copper oxide (CuO) films on copper foil," *Journal of Crystal Growth*, vol. 291, no. 2, pp. 479–484, 2006.

[11] M. Sharon and B. Prasad, "Preparation and characterization of iron oxide thin film electrodes," *Solar Energy Materials*, vol. 8, no. 4, pp. 457–469, 1983.

[12] S. K. Shaikh, S. I. Inamdar, V. V. Ganbavle, and K. Y. Rajpure, "Chemical bath deposited ZnO thin film based UV photoconductive detector," *Journal of Alloys and Compounds*, vol. 664, pp. 242–249, 2016.

[13] M. Jlassi, I. Sta, M. Hajji, and H. Ezzaouia, "Optical and electrical properties of nickel oxide thin films synthesized by sol–gel spin coating," *Materials Science in Semiconductor Processing*, vol. 21, pp. 7–13, 2014.

[14] R. Drevet, C. Legros, D. Bérardan et al., "Metal organic precursor effect on the properties of SnO_2 thin films deposited by MOCVD technique for electrochemical applications," *Surface and Coatings Technology*, vol. 271, pp. 234–241, 2015.

[15] B. Siwach, S. Sharma, and D. Mohan, "Structural, optical and morphological properties of ZnO/MWCNTs nanocomposite photoanodes for dye sensitized solar cells (DSSCs) application," *Journal of Integrated Science and Technology*, vol. 5, no. 1, pp. 1–4, 2017.

[16] O. Langmar, C. R. Ganivet, G. de la Torre, T. Torres, R. D. Costa, and D. M. Guldi, "Optimizing CuO p-type dye-sensitized solar cells by using a comprehensive electrochemical impedance spectroscopic study," *Nanoscale*, vol. 8, no. 41, pp. 17963–17975, 2016.

[17] Z. Yu, I. R. Perera, T. Daeneke et al., "Indium tin oxide as a semiconductor material in efficient p-type dye-sensitized solar cells," *NPG Asia Materials*, vol. 8, no. 9, article e305, 2016.

[18] M. Rokhmat, E. Wibowo, and M. Abdullah, "Performance improvement of TiO_2/CuO solar cell by growing copper particle using fix current electroplating method," *Procedia Engineering*, vol. 170, pp. 72–77, 2017.

[19] Z. Yuan, H. Tai, X. Bao, C. Liu, Z. Ye, and Y. Jiang, "Enhanced humidity-sensing properties of novel graphene oxide/zinc oxide nanoparticles layered thin film QCM sensor," *Materials Letters*, vol. 174, pp. 28–31, 2016.

[20] A. Kathalingam, D. Vikraman, H.-S. Kim, and H. J. Park, "Facile fabrication of n-ZnO nanorods/p-Cu_2O heterojunction and its photodiode property," *Optical Materials*, vol. 66, pp. 122–130, 2017.

[21] T. Shinagawa, M. Chigane, J. Tani, and M. Izaki, "Effect of oxide intermediate layers on pyramidally textured Cu2O/ZnO solar cells prepared by electrodeposition," *ECS Meeting Abstracts*, vol. 2, no. 21, p. 1636, 2016.

[22] A. Samad, M. Furukawa, H. Katsumata, T. Suzuki, and S. Kaneco, "Photocatalytic oxidation and simultaneous removal of arsenite with CuO/ZnO photocatalyst," *Journal of Photochemistry and Photobiology A: Chemistry*, vol. 325, pp. 97–103, 2016.

[23] G. Boschloo and A. Hagfeldt, "Spectroelectrochemistry of nanostructured NiO," *The Journal of Physical Chemistry B*, vol. 105, no. 15, pp. 3039–3044, 2001.

[24] S. Kerli and Ü. Alver, "Preparation and characterisation of ZnO/NiO nanocomposite particles for solar cell applications," *Journal of Nanotechnology*, vol. 2016, Article ID 4028062, 5 pages, 2016.

[25] S. A. Rawool, M. R. Pai, A. M. Banerjee et al., "*pn* Heterojunctions in NiO:TiO_2 composites with type-II band alignment assisting sunlight driven photocatalytic H_2 generation," *Applied Catalysis B: Environmental*, vol. 221, pp. 443–458, 2018.

[26] A. Chrissanthopoulos, S. Baskoutas, N. Bouropoulos, V. Dracopoulos, P. Poulopoulos, and S. N. Yannopoulos, "Synthesis and characterization of ZnO/NiO p–n heterojunctions: ZnO nanorods grown on NiO thin film by thermal evaporation," *Photonics and Nanostructures - Fundamentals and Applications*, vol. 9, no. 2, pp. 132–139, 2011.

[27] M. Boroujerdnia and A. Obeydavi, "Synthesis and characterization of NiO/$MgAl_2O_4$ nanocrystals with high surface area by modified sol-gel method," *Microporous and Mesoporous Materials*, vol. 228, pp. 289–296, 2016.

[28] M. El-Nahass, M. Emam-Ismail, and M. El-Hagary, "Structural, optical and dispersion energy parameters of nickel oxide nanocrystalline thin films prepared by electron beam deposition technique," *Journal of Alloys and Compounds*, vol. 646, pp. 937–945, 2015.

[29] H. Wang, Y. Wang, and X. Wang, "Pulsed laser deposition of the porous nickel oxide thin film at room temperature for high-rate pseudocapacitive energy storage," *Electrochemistry Communications*, vol. 18, pp. 92–95, 2012.

[30] C. E. Morosanu and G. Siddall, *Thin Films by Chemical Vapour Deposition*, Elsevier, Amsterdam, 2016.

[31] I. Sta, M. Jlassi, M. Hajji, and H. Ezzaouia, "Structural, optical and electrical properties of undoped and Li-doped NiO thin films prepared by sol–gel spin coating method," *Thin Solid Films*, vol. 555, pp. 131–137, 2014.

[32] F. Garcés, N. Budini, J. Schmidt, and R. Arce, "Highly doped ZnO films deposited by spray-pyrolysis. Design parameters for optoelectronic applications," *Thin Solid Films*, vol. 605, pp. 149–156, 2016.

[33] M. G. Faraj, "Effect of aqueous solution molarity on the structural and electrical properties of spray pyrolysed lead sulfide (PbS) thin films," *International Letters of Chemistry, Physics and Astronomy*, vol. 57, pp. 122–125, 2015.

[34] A. Enigochitra, P. Perumal, C. Sanjeeviraja, D. Deivamani, and M. Boomashri, "Influence of substrate temperature on structural and optical properties of ZnO thin films prepared by cost-effective chemical spray pyrolysis technique," *Superlattices and Microstructures*, vol. 90, pp. 313–320, 2016.

[35] A. E. Adeoye, E. Ajenifuja, B. A. Taleatu, and A. Fasasi, "Rutherford backscattering spectrometry analysis and structural properties $Zn_xPb_{1-x}S$ of thin films deposited by chemical spray pyrolysis," *Journal of Materials*, vol. 2015, Article ID 215210, 8 pages, 2015.

[36] D. Chen, X. Zou, H. Yang et al., "Effect of annealing process on $CH_3NH_3PbI_{3-X}Cl_X$ film morphology of planar heterojunction perovskite solar cells with optimal compact TiO_2 layer," *International Journal of Photoenergy*, vol. 2017, Article ID 7190801, 9 pages, 2017.

[37] O. K. Ukoba, A. C. Eloka-Eboka, and F. L. Inambao, "Review of nanostructured NiO thin film deposition using the spray pyrolysis technique," *Renewable and Sustainable Energy Reviews*, vol. 82, pp. 2900–2915, 2018.

[38] E. Adeoye Abiodun and A. Salau, "Effect of annealing on the structural and photovoltaic properties of cadmium sulphide: copper sulphide (Cds:Cuxs) heterojunction," *International Journal of Scientific and Research Publications*, vol. 5, no. 8, pp. 1–5, 2015.

[39] S. Sriram and A. Thayumanavan, "Structural, optical and electrical properties of NiO thin films prepared by low cost spray pyrolysis technique," *International Journal of Material Science Engineering*, vol. 1, pp. 118–121, 2013.

[40] M. Gabal, "Non-isothermal decomposition of NiC_2O_4–FeC_2O_4 mixture aiming at the production of $NiFe_2O_4$," *Journal of Physics and Chemistry of Solids*, vol. 64, no. 8, pp. 1375–1385, 2003.

[41] N. A. Bakr, S. A. Salman, and A. M. Shano, "Effect of co doping on structural and optical properties of NiO thin films prepared by chemical spray pyrolysis method," *International Letters of Chemistry, Physics and Astronomy*, vol. 41, pp. 15–30, 2015.

[42] V. Georgieva and A. Tanusevski, "Characterization of p-Cu_2O/n-ZnO heterojunction solar cells," *AIP Conference Proceedings*, vol. 1203, pp. 1074–1078, 2010.

[43] S. Noda, H. Shima, and H. Akinaga, "Cu_2O/ZnO heterojunction solar cells fabricated by magnetron-sputter deposition method films using sintered ceramics targets," *Journal of Physics: Conference Series*, vol. 433, pp. 1–10, 2013.

CHAPTER 6: MODELING OF THE FABRICATED NiO/TiO_2 P-N HETEROJUNCTION SOLAR CELLS

Chapter 6 focused on the modeling and theoretical validation of the developed solar cells. This is divided into three parts. Part 1 did an overview of modeling tools used for solar cells and part 2 modelled the fabricated solar cells of this study. Part 3 studied the application of solar cells in combating global warming.

Part 1: Ukoba**, O.K; Inambao, F. L and Adeoye A. E. "Modeling and Simulation of Metal Oxide Solar Cells: An Overview" ICUE 2018.**

Part 2: **Ukoba, O.K., and Inambao F.L. (2018) "Modeling of properties of fabricated NiO/TiO_2 heterojunction solar cells," *International Journal of Applied Engineering Research*, vol. 13, No 11, pp. 9701 - 9705**

Part 3: **Ukoba, O.K., and Inambao F.L. (2018). "Solar cells and global warming reduction," *International Journal of Applied Engineering*, ISSN 09734562 Volume 13, Number 10, pp. 8303-8310**

Chapter 6 Part 1: Modeling and Simulation of Metal Oxide Solar Cells: An Overview

Ukoba**, O.K; Inambao, F. L and Adeoye A. E. "Modeling and Simulation of Metal Oxide Solar Cells: An Overview"** ***ICUE, 2018.***

MODELING AND SIMULATION OF METAL OXIDE SOLAR CELLS: AN OVERVIEW

[1]Ukoba, O.K; Inambao, F. L[1] and Adeoye A. E[2]

[1]**Mechanical Engineering, University of Kwazulu-Natal, Durban**

[2]**Physical Sciences Dept., The Technical University, Ibadan. Oyo state**

ukobaking@yahoo.com

Abstract

This study provides a brief overview of device modeling and simulation of metal oxide thin film solar cells. Modeling tools have been used for solar cells but mainly traditional solar cells. Modeling tools are used to study and predict fabrication of devices. This is done with a view to improving on solar cell properties and gaining a better understanding of the device data. This study examined different tools used for modeling and simulation of metal oxide solar cells and some studies where they were used. It also highlights the steps for solar cell modeling, and the classification of modeling tools.

KEYWORDS Metal oxide; modeling; simulation; solar cells; overview

1. Introduction

Solar technologies still lack full implementation globally despite the well-known potential of solar energy. This is caused by the challenge of device performance and costs associated with solar technologies [1, 2]. Thinner solar cells are envisaged to be capable of cutting costs while retaining optimum performance. Nano-structuring of metal oxide thin film is one such approach. Despite the increase in experimental fabrication of metal oxide solar cells [3-5], insufficient consideration is being given to understanding the device principles by means of modeling.

Nanostructured metal oxide thin film solar cells are attracting wide interest due to their potential for affordable and sustainable optoelectronic applications [6-11]. These materials offer a number of significant advantages compared to traditional solar cells that are large and costly to fabricate [12-18]. However, their efficiencies are still far from those of traditional silicon solar cells [19]. A different approach has been developed to improve on their efficiency with low-cost and sustainability kept in view.

Modeling is an effective way of tuning the properties of solar cells in order to achieve better efficiency at a reduced cost with reduced resources. Modeling of solar has become a vital tool for development of effective solar cells. Modeling tools help to demystify solar cell operation and are needed in the improvement of the efficiency of solar cells [20, 21]. Solar modeling is also capable of producing new types of brightly colored and transparent solar cells. These colored solar cells can be used in integrated photovoltaics systems. However, the photovoltaic industry, compared to the electronic industry, has not leveraged the merits of solar cell modeling.

Before the advent of solar cell modeling, understanding of solar cells was by intuition and empirical studies without quantitative analysis. This was due to the fact that the solar cell industry, before 2008, was more interested in scaling up device over performance improvement [22, 23]. Since 2008, solar cell modeling has garnered more attention mainly due to interest in the better efficiency of solar cells [24]. The major reason for the increase in demand for solar cell modeling is that better device performance can be achieved when the whole solar cell device is included in the optimization process.

This study provides a brief overview of metal oxide solar cell modeling and simulation. It highlights the steps for device modeling and simulation, classification of the modeling and simulation tools, and examples of modelled and simulated metal oxides.

2. Principle of metal oxide solar cells simulations

Metal oxide thin film solar cells are basically P-N heterojunctions as seen in the equivalent circuit model of the cells shown in Figure 6.1. They exhibit nonlinear I-V characteristics that vary with the temperature of the solar cells and the radiant intensity.

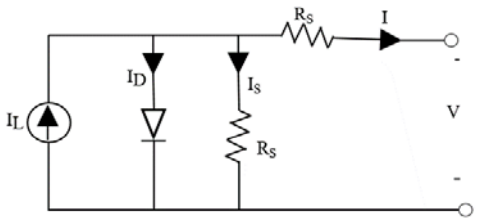

Figure 6.1. Solar cells model equivalent circuit

Under ideal conditions, a solar cell can be theoretically modelled as a current source under a diode. The I-V characteristic equation of a solar cell can be expressed in Equation (1):

$$I = I_{ph} - I_s\left[e^{\left(\frac{q(V+R_S I_{pv})}{AkT_C}\right)} - 1\right] - \frac{V+R_S I_{pv}}{R_{sh}} \quad (1)$$

where; I_{ph} is photocurrent, I_s is reverse saturation current, R_S and R_{sh} are inherent resistances in series and parallel associated with the cell, q is the electron charge, K is Boltzmann's constant and A, the modified ideality factor.

Three special parameters influence the performance of solar cells, namely, fill factor, open-circuit voltage, and short circuit current. Short circuit current and open circuit voltage are the major determinant factors of solar cell efficiency because the fill factor is a function of both parameters. Electron flow in the external circuit when the energy of incident photons is greater than the band gap of cells.

Figure 6.2 shows typical characteristics of solar cells. It shows the behavior of the voltage and current with irradiation and temperature of solar cells.

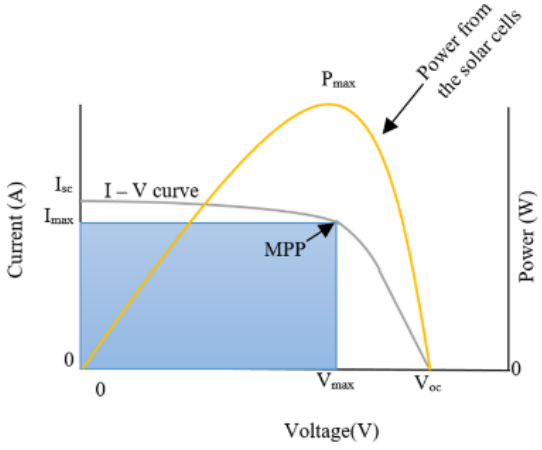

Figure 6.2. Typical characteristics of a solar cells

Most solar cells comprise different layers of semiconductor materials stacked to form a one-dimensional sequence. Most metal oxide thin film solar cells can be modeled as one-dimensional cells because of the one direction of flow of the electron/hole current [25]. Most silicon wafer solar cells can also be modelled in a similar manner. This is feasible provided the series connection is not clearly modelled. Two dimensional modeling is applied in solar cells which have metal contacts embedded in a passivation layer that helps reduce recombination. In such two-dimensional modeling, the internal electron and hole current flows in two dimensions, or three dimensions in some cases.

2.1 Steps for device modeling

The steps for modeling and simulating metal oxide solar cells involve derivation of the basic equations. This is followed by normalization of the derived equations. Thereafter, the equations are linearized. Finally, a solution of the linearized equation is obtained. A partial understanding of device input parameters is needed for successful device modeling and simulation. A starting baseline is needed for all types of metal oxide solar cell modeling.

2.2 History of solar cell modeling

A lot of materials and methods have been studied with a view to developing improved solar cells with regard to cost and efficiency. Experimental and modeling/simulation have also been employed for the purpose of device fabrication and tuning. Numerical analysis gives a better understanding of the operation of metal oxide solar cell devices. The pioneer solar cell modeling tool was developed in 1980 by a PhD student named Mark S. Lundstrom [26]. Gray [27] in 1989 developed the Thin-Film Semiconductor Simulation Program (TFSSP). Lundstrom also worked on the Solar Cell Analysis Program (SCAP) in 1985 [28]. SCAP is said to have been developed at Ghent University, Belgium [29, 30]. In 1989 a PhD student used the SCAP in one-dimension and two-dimensions for a doctoral dissertation in an engineering faculty [31]. Purdue University also developed one- and two-dimensional modeling tools called PUSH [32, 33].

3. Classifications of solar cell device modeling

Solar cell device modeling/simulation can be used to calculate current densities and the carrier. This is achieved by solving the transport and Poisson's equation [34]. The general solution to the current densities and carrier is derived by applying the essential boundary conditions at the junctions (P-N). However, the non-linear recombination makes it difficult to solve the current densities and carrier with ease. Device modeling of metal oxide solar cells can be classified into three broad categories, based on: the solver approach; the modeling tool used; and the dimension (one-dimensional, two-dimensional or three-dimensional).

3.1 The solver approach

This is divided into the analytical and numerical solver approach as shown in Figure 6.3.

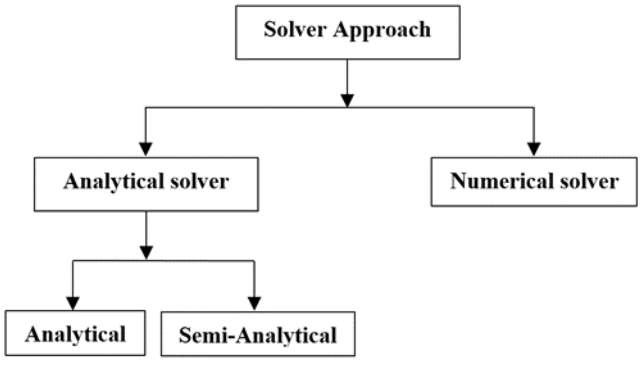

Figure 6.3. Schematic representation of the analytical and numerical approach to solar cell modeling

3.1.1 Analytical solver approach

This involves analytical modeling of the solar cell device. It is sub-grouped into analytical and semi-analytical.

The analytical approach solves the semiconductor equations. The equations include the diffusion-drift current, equation of carriers' continuity, and Poisson's equations. This approach is capable of calculating the key parameters of solar cell efficiency. It is not sufficient to give the cell's detailed parameters but it can give the fill factor, short circuit current and the open circuit voltage. It is capable of modeling and simulating the effects of diameter and length on the optical absorption of the cell. It allows for comparison of the planar cell geometry and the solar cell performance in relation to the material properties. A good example is the work of Kayes and Atwater [35]. That study was able to achieve 11% efficiency from an initial efficiency of 1.5 %. It employed the analytical model to solve diffusion-drift equations for minority carriers, the continuity equations, and Poisson's equation. The study compared analytically the performance of (c-Si) and gallium arsenide (GaAs), using a 100 mW/cm^2 Air Mass 1.5 spectrum. Petrosyan, Yesayan and Neryesayan [36] solved the semiconductor equations using the analytical approach. Ali et al. [37] used the analytical model but employed the Green's function method. Green's function method eliminates the uniform generation assumption made by other models. This method gained prominence in 2014. It calculates the current density, fill factor, open circuit and conversion efficiency.

The semi-analytical approach is used to optimize the device absorption. It does not involve massive calculations yet is efficient. This method permits the assessment of the ideal design parameters for optimum charge generation over a shorter time and material thickness [38]. This approach depends only on the refractive indices of the device parent materials. The theoretical framework links the reflection, transmission and absorption of solar cells to geometric parameters. It focuses on abridged parameters that enable the device to achieve optimum short circuit currents. This reduces the time and resources associated with comprehensive study of the geometry yet gives a better and faster optimized device.

Although analytical models are not voluminous in simulation results they are easier to implement compared to numerical models. They also give a better view of the variables that influence the model.

3.1.2 Numerical solver approach

This involves numerical simulation techniques of modeling solar cell devices. Poisson's equation connects the hole density and the electron. The complex nature of Poisson's equation makes it difficult for mathematical tools to be used to solve it but it can be solved with the numerical approach. The merit of this approach is that it permits inclusion of key physical effects which ordinarily may not be considered. These include such parameters as band-gaps, lifetime, doping, among others. This helps to prevent closed form solutions. The key numerical tools used for solving the differential equations are the finite element [39], finite difference [40], and finite volume methods [41]. Others include transfer matrix method, rigorous couple wave analysis, and finite difference time domain. The finite element is the most flexible of the three methods in solving complex geometry involving complicated boundary conditions. This is because it makes room for arbitrary geometries and consists of several physics parameters of the solar cells. It is more effective when the incident light is absorbed along the axis. This method has attracted several studies that employ Technology Computer-Aided Design (TCAD) [42] and COMSOL multiphysics [43]. The Transfer Matrix Method is the most effective in devices involving small diameters and periodic structures [44]. In such a case, one side of the unit cell is represented by the end of a transfer matrix.

3.2 The modeling tool used

The second classification of solar cells modeling is based on the modeling tool used, mainly software tools. Almost all modeling tools base their design on basic solar cell equations (Poisson and continuity equations for electron and holes) [45]. Any modeling tool that is able to solve basic semiconductor equations can be used for modeling/simulation of metal oxide solar cells. The continuity equation is non-linear due to the presence of recombination terms.

A standard thin film tool, and by extension metal oxide solar cell modeling/simulation tool, should be able to satisfy the conditions enumerated in Table 6.1 for it to be considered for usage.

Table 6.1. Criteria for metal oxide thin film modeling tools

S/N	CRITERIA	VALUE
1.	LAYERS	Multiple layers (5 layers minimum)
2.	BAND GAP E_g	$E_g > 2 – 3.7$ eV
3.	BAND DISCONTINUITY	E_C & E_V: ΔE_C & ΔE_V
4.	INTERFACE (GUI)	SIMPLE, FAST AND FRIENDLY
5.	NON-ROUTINE MEASUREMENTS (current-density, capacitance, surface photo voltage, kelvin probe, transient measurement of current, voltage and capacitance)	ABLE TO SIMULATE: J-V, C-V, C-f, QE(λ), as a function of ambient Temperature (T)
6.	GRADED BAND GAPS	E_g, χ(x), N_C(X), N_V(X), α(x),
7.	RECOMBINATION ABILITY	RECOMBINATION EVEN IN DEEP INTERFACE STATES
8.	RECOMBINATION IN BULK STATE	RECOMBINATION EVEN IN BULK STATE

3.2.1 Solar Cells Analysis Program (SCAPS)

SCAPS stands for Solar Cell Analysis Program in one and two dimensions (SCAP1D and SCAP2D) developed at Ghent University. Its solar cell simulation program is used for opto-electrical simulation of the 1-D or 2-D structures of semiconductor layers [46-49]. SCAPS was originally developed for cell structures of the $CuInSe_2$ and the CdTe family. However, there has been improvement thereby making room for other types of solar cells. SCAPS uses finite difference methods to solve the differential equations which, along with several relations from the physics of semiconductors, describe mathematically the performance of a solar cell. SCAPS performs a complete simultaneous numerical solution of the two continuity equations and Poisson's equation conditional on the boundary conditions appropriate to one and two-dimensional cells [28]. The equations are expressed as shown in Equations (2) to (4).

$$\nabla^2 v = -\frac{q}{\epsilon}(p - n + N_D - N_A) \quad (2)$$

$$\nabla . J_p = q(G - R) \quad (3)$$

$$\nabla . J_n = q(R - G) \quad (4)$$

The general terms of 3 and 4 can be represented as:

$$G(x) = \int_0^\infty \phi a e^{-ax} d\lambda \quad (5)$$

The hole and electron current densities which appear in Equations 3 and 4 are given by:

$$J_p = -q\mu_p p \nabla V_p - kT\mu_p \nabla_p \quad (6)$$

$$J_n = -q\mu_n n \nabla V_n + kT\mu_n \nabla_n \quad (7)$$

$$V_p = V - (1 - \gamma)\frac{\Delta_G}{q} \quad (8)$$

$$V_n = V + \gamma\frac{\Delta_G}{q} \quad (9)$$

where v_p and v_n represent the effective potentials expressed in Equations (8) and (9). Δ_G and γ account for variations in the band structure, such as density of states and band gap, and account for Fermi-Dirac statistics.

Figure 6.4 depicts the structure of the SCAPS programme, summarizing its work. The operator inputs the information about the materials parameters, a description of the device to be analyzed, the type of analysis to be performed and the spectrum (optional). The results are printed in summary form and the detailed results of the calculation are stored. A separate plotting routine is used to access the information and to display the appropriate parameters. The plotting capability is one of the most valuable features of the code because it allows one to effectively have a microscopic view of most of the parameters of interest in the interior of the cell under operating conditions.

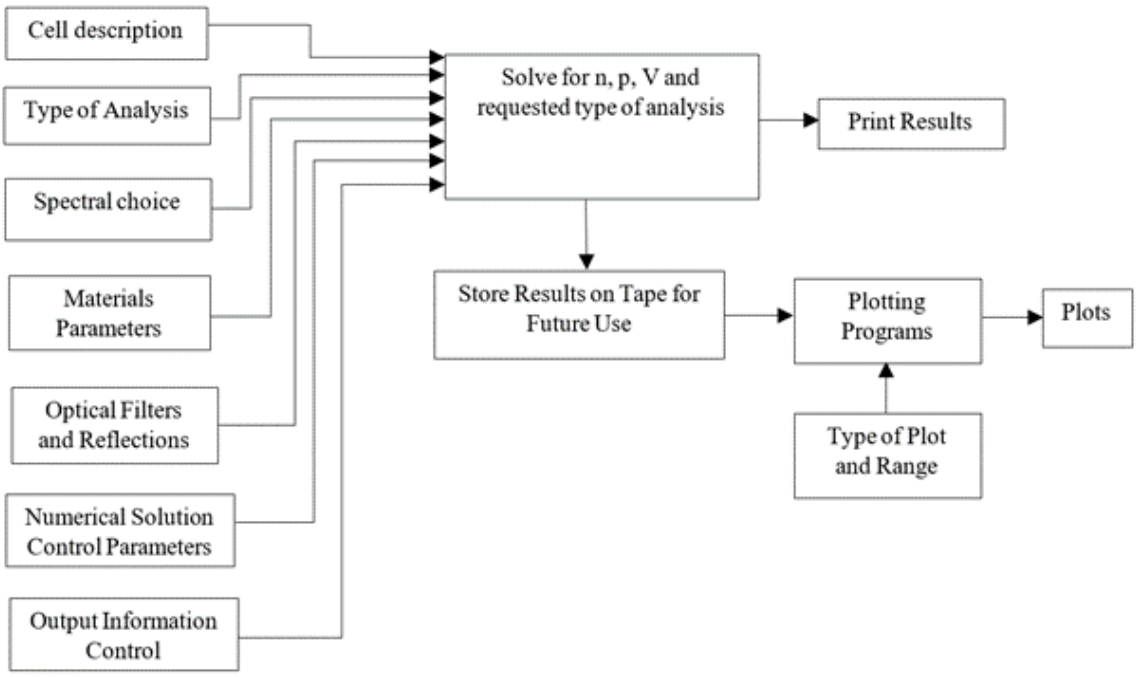

Figure 6.4. Block diagram of the structure of SCAP1D and SCAP2D

Figure 6.5 shows the SCAP interface with the major input parameters used for solar cell modeling. Some studies have successfully used it for modeling thin film solar cells [50-55].

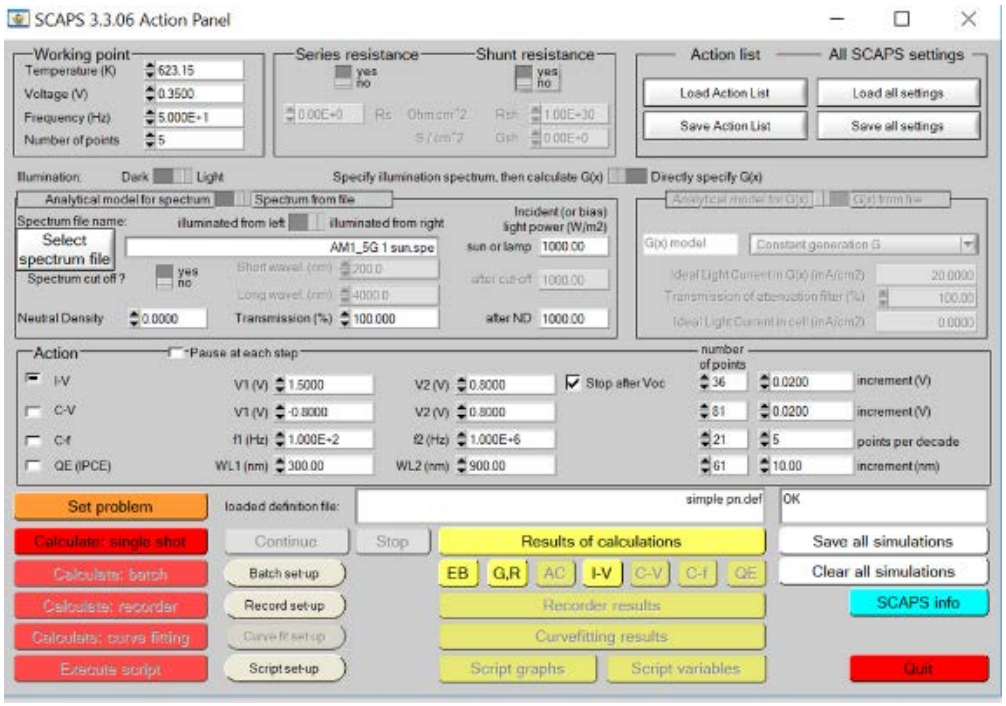

Figure 6.5. Defined parameters used for the modeling the solar cells

3.2.2 PC1D

This was written for personal computers to solve non-linear equations of one-dimensional electron and hole transport in semiconductor devices with a focus on photovoltaic devices. It was written by a team at Sandia National Laboratory led by Basore. It was later improved at the University of New South Wales, Australia. PC1D is generally used for interpreting experimental data to define the structure of a device. It is used to determine several device parameters by matching an experimental curve to a simulated Internal Quantum Efficiency (IQE) curve as shown in Figure 6.6. The latest version (ver. 5) provides the ability to display experimental data and simulation results on the same graph within PC1D, enabling rapid comparison.

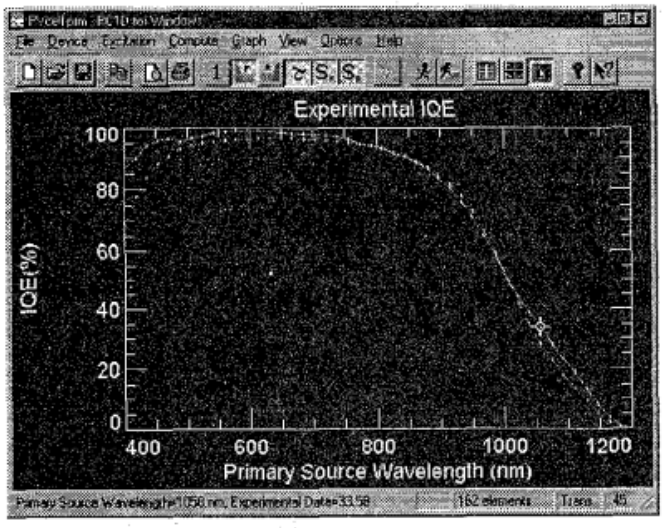

Figure 6.6. PC1D schematic display and output display

The schematic display of common parameters in PC1D is shown in Figure 6.7. The displayed parameters include dopant, front-surface charge, contacts, texturing, shunt and series element.

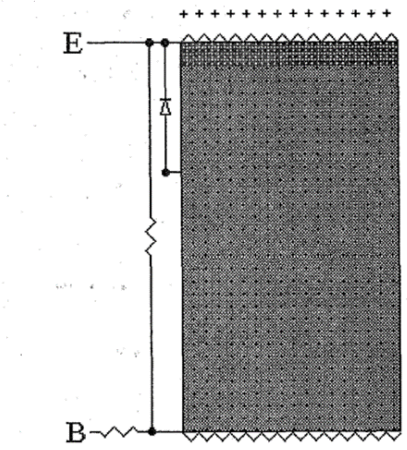

Figure 6.7. PC1D Schematic display of common parameters

This modeling tool has a user-friendly interface. The layer and contact can easily be adjusted by a click on the graphic user interface. The parameters can also be changed by a menu system. Five layers are permitted per device. These layers are sufficient for certain devices that have little or no doping. It implements the most common recombination mechanisms. Band to band, Auger, and trap assisted tunneling are all implemented [56].

PC1D is capable of simulating spectral response measurements, transients and the J-V characteristics of solar cells [57, 58]. The output of the simulation can be manipulated in other programs (including spreadsheets). Although, it has been heavily used in traditional types of solar cell modeling and simulation [59], it can be deployed in metal oxide solar cell modeling as well [60-67]. These resources shed more light on PC1D [68-71].

3.2.3 MatLab/Simulink

Some works have used Simulink for device modeling and simulation. Tsai, Tu and Su [72] developed a generalized photovoltaic model using Simulink. The model enabled the dynamic of a photovoltaic power system to be simulated, analyzed and optimized. Simulink is a versatile modeling and simulation tool. It has been deployed in modeling and simulating photovoltaic system including solar cells [73-77].

3.2.4 Analysis of Microelectronic and Photonic Structures (AMPS)

This model was developed for modeling and simulation for the purpose of understanding solar cell device physics and design. It was developed by a team from Pennsylvania State University led by Fonash [78]. It is a one-dimensional modeling tool that uses finite difference and the Newton-Raphson method to solve the Poisson and continuity equations of solar cells. It has the ability to work on several models simultaneously. It refers to device as *case*. The clean and user-friendly interface makes it easy to describe the model. Each *case* or device is capable of being assigned about 30 layers with each having separate defined parameters. These layers can be assigned about 50 deep donor and acceptor levels capable of creating arbitrary density of states distribution. And the deep levels can be distributed in the uniform, discrete and Gaussian. Electron/hole mobility, bandgap and other parameters are independent of temperature. It can simulate a graded junction because of the ability to add different layers with varying parameters, and is capable of simulating both in illumination and dark. Figure 6.8 gives the major parameters defined for modeling of devices in AMPS [79].

Parameter and units e, h for electrons and holes, respectively	a-Si:H(p+)	a-Si:H(i)	a-Si:H(n+)	a-Si:H/c-Si interface	c-Si(n)
Thickness (nm)	10	10	10	3	300,000
Electron affinity (eV)	3.8	3.8	3.8		4.05
Band gap (eV)	1.72	1.72	1.72		1.12
Effective conduction band density (cm^{-3})	2.50×10^{20}	2.50×10^{20}	2.50×10^{20}		2.80×10^{19}
Effective valence band density (cm^{-3})	2.50×10^{20}	2.50×10^{20}	2.50×10^{20}		1.04×10^{19}
Electron mobility ($cm^2 V^{-1} s^{-1}$)	10	20	10		1350
Hole mobility ($cm^2 V^{-1} s^{-1}$)	1	2	1		450
Acceptor concentration (cm^{-3})	3×1019	0	0		0
Donor concentration (cm^{-3})	0	0	1×10^{19}		3×10^{15}
Band tail density of states ($cm^{-3} eV^{-1}$)	2×10^{21}	2×10^{21}	2×10^{21}		1×10^{14}
Characteristic energy (eV) for donors, acceptors	0.06, 0.03	0.06, 0.03	0.06, 0.03		0.01, 0.01
Capture cross-section for donor states, e, h (cm^2)	1×10^{-15}, 1×10^{-17}	1×10^{-15}, 1×10^{-17}	1×10^{-15}, 1×10^{-17}		1×10^{-15}, 1×10^{-17}
Capture cross-section for acceptor states, e, h (cm^2)	1×10^{-17}, 1×10^{-15}	1×10^{-17}, 1×10^{-15}	1×10^{-17}, 1×10^{-15}		1×10^{-17}, 1×10^{-15}
Gaussian density of states N_{DB} (cm^{-3})	8×10^{17}–5×10^{20}	8×10^{15}–8×10^{17}	8×10^{17}–5×10^{20}		
Gaussian peak energy (eV) donors, acceptors	1.22, 0.70	1.22, 0.70	1.22, 0.70		
Standard deviation (eV)	0.23	0.23	0.23		
Capture cross section for donor states, e, h (cm^2)	1×10^{-14}, 1×10^{-15}	1×10^{-14}, 1×10^{-15}	1×10^{-14}, 1×10^{-15}		
Capture cross-section for acceptor states, e, h (cm^2)	1×10^{-15}, 1×10^{-14}	1×10^{-15}, 1×10^{-14}	1×10^{-15}, 1×10^{-14}		
Total interface density of states D_{it} (cm^{-2})				5×10^{9}–5×10^{13}	
Midgap density of states in c-Si ($cm^{-3} eV^{-1}$)					1×10^{11}
Switch-over energy (eV)					0.56
Capture cross-section for donor states, e, h (cm^2)				1×10^{-15}, 1×10^{-17}	1×10^{-15}, 1×10^{-17}
Capture cross-section for acceptor states, e, h (cm^2)				1×10^{-17}, 1×10^{-15}	1×10^{-17}, 1×10^{-15}

Figure 6.8. AMPS-1D parameter definition for simulating heterojunction solar cells

Figure 6.9 shows the graphic user interface of the AMPS with an open model known as *case.*

The disadvantages of AMPS include the limited number of discretization nodes with the latest version capable of handling 3 000 nodes. Another disadvantage is manual input of the wavelength, spectrum intensity and absorption coefficients into AMPs. Also, there is difficulty in explicit definition of interface recombination. It encourages batch mode processing due to the slow pace of processing compared to other modeling tools. It however has an excellent plotting facility for analyzing and designing of two terminal structures results. AMPS is capable of modeling p–n, single or heterojunction p–i–n, Schottky barrier devices and the likes. It can simulate several optoelectronic devices including solar cells and diodes due to the ability to function both under illumination and dark.

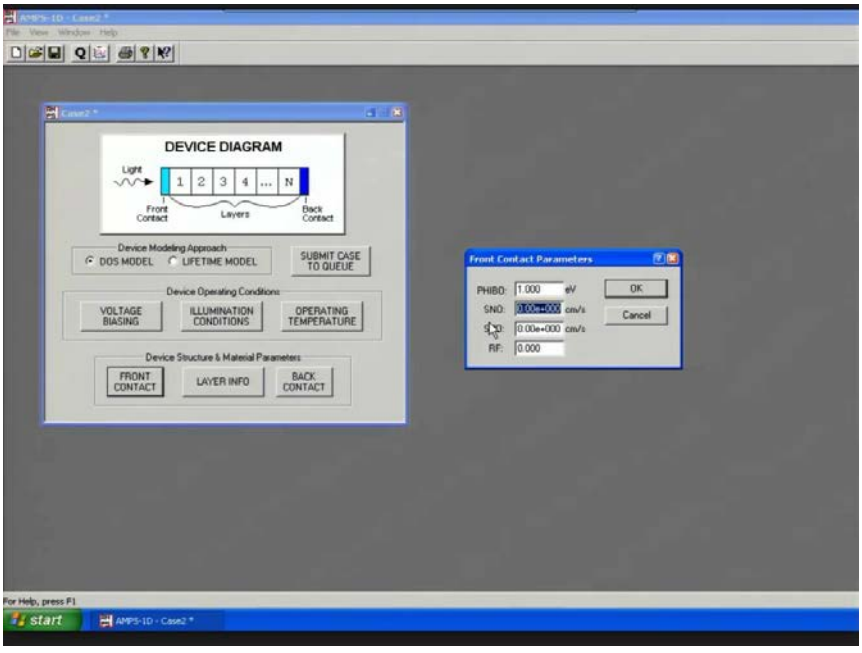

Figure 6.9. The graphic user interface of AMPS showing *case*

3.2.5 wxAMPS

This is an improvement on AMPS and is very stable. The improvements are tunneling currents, improved visualization, better speed and convergence [80]. This is due to the improved algorithm solved by the Newton and Gummel technique. It was developed by a team from University of Illinois and Nankai University [81]. The user interface of wxAMPS deploys a cross-platform library. It also provides better data entry [82]. It is an open source program, comparing favorably with SCAP and other tools. However, it offers better modeling capability for materials with high defect densities and band tails. It can be used for tandem and graded solar cells. The WIKI feature enables device parameters sharing. Figure 6.10 shows the interface. Some studies have deployed it in modeling of solar cell devices [83, 84].

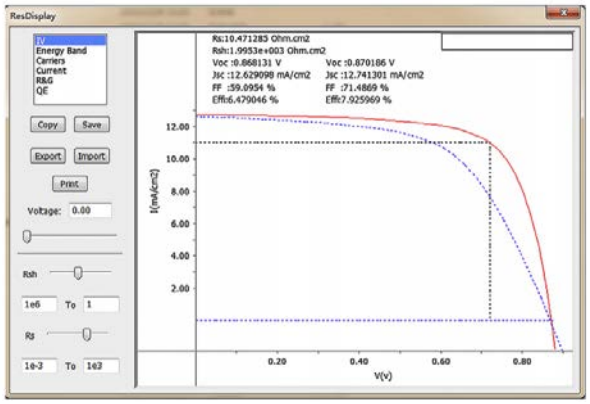

Figure 6.10. Interface of wxAMPS

3.2.6 TCAD

The drift-diffusion equation, Poisson equation, Klassen's low field mobility model, Auger model, and Klaassen's concentration dependent SHR model were used in the development of this tool. The absorption of light, transmission, reflection and refraction at the interface are modelled using a photo-generation model. It uses AM 1.5 G solar spectrum, incident power density of 100 mW/cm^2. The commonly used optoelectronic device parameters are shown in Figure 6.11 [85].

Parameters	p-a-Si:H	i1-a-Si:H	i2-μc-Si:H	n-μc-Si:H
Layer thickness (nm)	5-20	250-500	1500-2500	10-20
Mobility gap (eV)	1.9	1.86	1.4	1.8
Donor doping density(cm^{-3})	8×10^{18}			
Acceptor doping density(cm^{-3})				2×10^{18}
Electron mobility(cm^2/Vs)[4]	20	20	32	32
Hole mobility(cm^2/Vs)[4]	4	4	8	8
Electron life time(μs)[4]	0.01	0.01	0.01	0.01
Hole life time(μs)[4]	0.1	0.1	0.1	0.1
Effective DOS in the valance and conduction bands (cm^{-3})[4]	2×10^{20}	2×10^{20}	2×10^{20}	2×10^{20}
Exponential tail prefactors NTD,NTA ($cm^{-3}eV^{-1}$) [4]	4×10^{21}	4×10^{21}	4×10^{21}	4×10^{21}
Characteristic energy for Gaussian distribution WGD (donor like state) (eV)[4]	0.2	0.2	0.2	0.2
Characteristic energy for Gaussian distribution WGA (acceptor like state) (eV)[4]	0.2	0.2	0.2	0.2
Characteristic energy WTD (VB tail) [4]	0.05	0.08	0.05	0.05
Characteristic energy WTA (CB tail)[4]	0.03	0.05	0.03	0.03
Gaussian distribution density NGD , NGA ($cm^{-3}eV^{-1}$)[4]	5×10^{18}	5×10^{17}	4×10^{16}	9×10^{18}
Correlation energy U (eV)[4]	0.2	0.2	0.2	0.2
Surface recombination velocity	1×10^{17}			1×10^{17}

Figure 6.11. TCAD optoelectronic device parameters

3.3 Based on dimension

This is divided into one-, two- and three-dimensional. Solar cells with conventional geometry and low solar intensities can be modelled using the one-dimension (1D) modeling tool. However, at high intensity, the two-dimension (2D) effect is considered even in some conventional geometry devices. For a high efficiency solar cell design, a two-dimension or three-dimension (3D) modeling tool is required.

The interdigitated back contact solar cell is an example of 2D geometry and the point contact solar cell is an example of an inherently 3D geometry. Although the basic modeling approach is the same for all solar cell devices, a unique algorithm has been developed for each class of solar cells. Most of the modeling tools distinguish the capability of the tool with 1D, 2D and 3D. Examples are SCAP1D, SCAP2D, PUSH1D, PUSH2D, among others.

The Numerical Solar Cell Simulation Program (NSSP) is a 1-D modeling program for solar cells. Amin, Sopianand Konagai [19] used this program for modeling CdTe solar cell structures from different perspectives. It focused on reduction of CdTe absorber thickness using theoretical analysis.

Other modeling tools that have gained usage include Silvaco [86-90], AFORS-HET (Automat For Simulation of Hetero-structures) [25, 91-94], Crosslight [95, 96], Sunshine [97], Synopsis [98], and Advanced Semiconductor Analysis (ASA) [99], among others. Silvaco uses a sophisticated technology called TFT for simulation. This uses both physical models and numerical methods for simulation of thin film solar cells and transistors. Crosslight uses a technology called Advanced Physical Models of Semiconductor Devices (APSYS). This employs the finite element technique for modeling optoelectronic properties of two-dimension thin film solar cells devices. AFORS-HET exists

as 1D and 2D. The ASA is used widely to study the effect of a nano-textured interface on solar cell performance [100]. Figure 6.12 gives an overview of commonly used modeling/simulation tools [45].

	AMPS	SCAPS	ASA	PC1D
Maximum number of layers	30	7	Unlimited	5
Band discontinuities ΔE_C, ΔE_V	All programs use the Anderson model: $\Delta E_C = \Delta\chi$ and $\Delta E_V = \Delta\chi + \Delta E_g$			
Graded bandgaps	No	No	Yes	No
Deep bulk states	50	3	4	No charge
Deep interface states	No	Yes	No	No
Charge in deep states	Yes	Yes	Yes	No
Simulation of non-routine measurements	No	C–V C–f	C–V	Transients
Numerical robustness (convergence)	++	OK	++	OK
Speed	–	+	++	++
User friendliness, interactivity	+	++	–	++

Figure 6.12. Some modeling tools used for thin film solar cells

Conclusion

This study was able to give an overview of modeling and simulation tools used for metal oxide thin film solar cells. A mathematical modeling and theoretical validation of solar cells can help a great deal to encourage research and development of solar technology in developing countries. There are numerous solar cell modeling tools which have been developed and are used commercially and at laboratory scale worldwide today. The fundamental challenge is to find a balance and adapt the tool that satisfies the required criteria.

Acknowledgements

The financial assistance of the National Research Foundation and The World Academy of Science (NRF-TWAS) of South Africa under grant number 105492 towards this research is acknowledged.

References

[1] Ukoba, O. K, Inambao, F. L. and Eloka-Eboka, A. C., 2017, “Influence of Annealing on Properties of Spray Deposited Nickel Oxide Films for Solar Cells,” Energy Procedia, 142, pp. 244-252.

[2] Ukoba, O. K., Inambao, F. L. and Eloka-Eboka, A. C., 2018, “Experimental Optimization of Nanostructured Nickel Oxide Deposited by Spray Pyrolysis for Solar Cells Application,” Int. J. Appl. Eng. Res., 13(6), pp. 3165-3173.

[3] Ty, J. T. D. and Yanagi, H., 2015, “Electrochemical Deposition of Zinc Oxide Nanorods for Hybrid Solar Cells,” Jpn J. Appl. Phys., 54(4S), p. 04DK05.

[4] Ukoba, O. K., Inambao, F. L. and Eloka-Eboka, A. C., 2018, “Fabrication of Affordable and Sustainable Solar Cells Using NiO/TiO2 PN Heterojunction,” Int. J. Photoenergy, Hindawi.

[5] Liyanage, W.P., et al., 2015, “Fabrication of CdTe Nanorod Arrays over Large Area Through Patterned Electrodeposition for Efficient Solar Energy Conversion,” Sol. Energy Mater. Sol. Cells, 133, pp. 260-267.

[6] Czapla, A., Kusior, E. and Bucko, M. 1989, “Optical Properties of Non-Stoichiometric Tin Oxide Films Obtained by Reactive Sputtering,” Thin Solid Films, 182(1-2), pp. 15-22.

[7] Drevet, R., et al., 2015, “Metal Organic Precursor Effect on the Properties of SnO2 Thin Films Deposited by MOCVD Technique for Electrochemical Applications,” Surf. Coat. Technol., 271, pp. 234-241.

[8] Jlassi, M., et al., 2014, “Optical and Electrical Properties of Nickel Oxide Thin Films Synthesized by Sol–Gel Spin Coating,” Mater. Sci. Semicond. Process., 21, pp. 7-13.

[9] Rahal, A., et al., 2015, “Structural, Optical and Electrical Properties Studies of Ultrasonically Deposited Tin Oxide (SnO2) Thin Films with Different Substrate Temperatures,” Superlattices Microstruct., 86, pp. 403-411.
[10] Shaikh, S.K., et al., 2016, “Chemical Bath Deposited ZnO Thin Film Based UV Photoconductive Detector,” J. Alloys Compd., 664, pp. 242-249.
[11] Sharon, M. and Prasad, B., 1983, “Preparation and Characterization of Iron Oxide Thin Film Electrodes,” Solar Energy Mater., 8(4), pp. 457-469.
[12] Chopra, K., Paulson, P. and Dutta, V., 2004, “Thin-film Solar Cells: an Overview. Prog. Photovoltaics Res. Appl., 12(2-3), pp. 69-92.
[13] Poortmans, J. and Arkhipov, V., 2006, Thin Film Solar Cells: Fabrication, Characterization and Applications. Vol. 5, John Wiley & Sons, New York, New York, USA.
[14] Kodigala, S., 2010, Thin Films and Nanostructures, vol. 35.: Academic, New York, New York, USA.
[15] Aberle, A.G., 2009, “Thin-Film Solar Cells.” Thin solid films, 517(17), pp. 4706-4710.
[16] Movla, H., Salami, D. and Sadreddini, S.V. 2012, “Simulation Analysis of the Effects of Defect Density on the Performance of Pin InGaN Solar Cell.” Appl. Phys. A., 109(2), pp. 497-502.
[17] Gorji, N. E. et al., 2010, “The Effects of Recombination Lifetime on Efficiency and J–V characteristics of InxGa1− xN/GaN Quantum Dot Intermediate Band Solar Cell,” Physica E: Low-dimensional Syst. Nanostruct., 42(9), pp. 2353-2357.
[18] Jackson, P., et al., 2011, “New World Record Efficiency for Cu (In, Ga) Se2 Thin-Film Solar Cells beyond 20%,” Prog. Photovoltaics Res. Appl., 19(7), pp. 894-897.
[19] Amin, N., Sopian, K. and Konagai, M., 2007, “Numerical Modeling of CdS/CdTe and CdS/CdTe/ZnTe Solar Cells as a Function of CdTe Thickness,” Sol. Energy Mater. Sol. Cells, 91(13), pp. 1202-1208.
[20] Aramoto, T., et al., 1997, “16.0% Efficient Thin-Film CdS/CdTe Solar Cells,” Jpn J. Appl. Phys., 36(10R), pp. 6304.
[21] Britt, J. and Ferekides, C., 1993, “Thin-film CdS/CdTe Solar Cell with 15.8% Efficiency,” Appl. Phys. Lett., 62(22), pp. 2851-2852.
[22] Van Sark, W., et al., 2008, “Accuracy of Progress Ratios Determined from Experience Curves: the Case of Crystalline Silicon Photovoltaic Module Technology Development,” Prog. Photovoltaics Res. Appl., 16(5), pp. 441-453.
[23] Hossain, T.M., 2011, “Diffusion and Experience Curve Pricing of New Products in the Consumer Electronics Industry,” J. Management Marketing Res., 6, p. 1.
[24] Altermatt, P.P., 2011, “Models for Numerical Device Simulations of Crystalline Silicon Solar Cells—a Review,” J. Comput. Electron., 10(3), pp. 314.
[25] Stangl, R. and Leendertz, C., 2012, “General Principles of Solar Cell Simulation and Introduction to AFORS-HET,” Physics and Technology of Amorphous-Crystalline Heterostructure Silicon Solar Cells, W. G. J. H. M. van Sark, L. Korte, F. Roca eds, Springer-Verlag, Berlin, pp. 445-458.
[26] Lundstrom, M. S., 1980, Numerical Analysis of Silicon Solar Cells, PhD thesis, Purdue University, West Lafayette, Indiana, USA.
[27] Gray, J. L., 1989, “A Computer Model for the Simulation of Thin-Film Silicon-Hydrogen Alloy Solar Cells” IEEE Transactions on Electron Devices, 36(5), pp. 906-912.
[28] Schwartz, R., Gray, J. and Lundstrom, M., 1985, “Current Status of One- and Two-Dimensional Numerical Models: Successes and Limitations.” Proc. Flat-Plate Solar Array Project Research Forum on High-Efficiency Crystalline Silicon Solar Cells, Jet Propulsion Laboratory California Institute of Technology Pasadena, California, May 15.
[29] Niemegeers, A. and Burgelman, M. 1996, “Numerical Modelling of AC-Characteristics of CdTe and CIS Solar Cells,” Conference Record of the 25th Photovoltaic Specialists Conference, IEEE.
[30] Niemegeers, A., Gillis, S. and Burgelman, M., 1998, “A User Program for realistic Simulation of Polycrystalline Heterojunction Solar Cells: SCAPS-1D,” Proc. of the 2nd World Conference on Photovoltaic Energy Conversion, JRC, European Commission.
[31] Banghart, E. K., 1989, Physical Mechanisms Contributing to Nonlinear Responsivity in Silicon Concentrator Solar Cells, PhD thesis, Purdue University, West Lafayette, Indiana, USA.
[32] DeMoulin, P. D. and Lundstrom, M. S., 1989, “Projections of GaAs Solar-Cell Performance Limits Based on Two-Dimensional Numerical Simulation,” IEEE Transactions on Electron. Devices, 36(5), pp. 897-905.

[33] DeMoulin, P., Lundstrom, M. and Schwartz, R., 1987, "Back-Surface Field Design for n+ p GaAs Cells," Solar Cells, 20(3), pp. 229-236.
[34] Singh, S., 2017, Mathematical Modeling of a PN Junction Solar Cell using the Transport Equations, Master's thesis, Wright State University, Dayton, Ohio, USA.
[35] Kayes, B. M., Atwater, H. A. and Lewis, N. S., 2005, "Comparison of the Device Physics Principles of Planar and Radial P-N Junction Nanorod Solar Cells," J. App. Phys., 97(11), p. 114302.
[36] Petrosyan, S., Yesayan, A. and Nersesyan, S., 2012, "Theory of Nanowire Radial P-N-Junction," Proc. World Acad. Sci., Eng. Technol., 71, pp. 1065-1070.
[37] Ali, N.M., et al., 2014, "Analytical Modeling of the Radial Pn Junction Nanowire Solar Cells," J. App. Phys., 116(2), pp. 024308.
[38] Sturmberg, B. C., et al., 2014, "Optimizing Photovoltaic Charge Generation of Nanowire Arrays: a Simple Semi-Analytic Approach," ACS Photonics, 1(8), pp. 683-689.
[39] Strang, G. and Fix, G. J., 1973, An Analysis of the Finite Element Method. Vol. 212, Prentice-Hall, Englewood Cliffs, New Jersey, USA.
[40] Smith, G.D., 1985, Numerical Solution of Partial Differential Equations: Finite Difference Methods, Oxford University Press, Oxford, UK.
[41] Eymard, R., Gallouët, T. and Herbin, R., 2000, "Finite Volume Methods," Handbook of Numerical Analysis Vol 7, P. Ciarlet and J. L. Lions, eds, North Holland, Amsterdam, Netherlands, pp. 713-1018.
[42] Wen, L., et al., 2011, "Theoretical Analysis and Modeling of Light Trapping in High Efficiency GaAs Nanowire Array Solar Cells," Appl. Phys. Lett., 99(14), p. 143116.
[43] LaPierre, R., 2011, "Numerical Model of Current-Voltage Characteristics and Efficiency of GaAs Nanowire Solar Cells," J. Appl. Phys., 109(3), p. 034311.
[44] Born, M. and Wolf, E., 2013, Principles of Optics: Electromagnetic Theory of Propagation, Interference and Diffraction of Light, Cambridge University Press, Cambridge, UK.
[45] Burgelman, M., et al., 2004, "Modeling Thin-Film PV Devices," Prog. Photovoltaics Res. Appl., 12(2-3), pp. 143-153.
[46] Burgelman, M. and Marlein, J., 2008, "Analysis of Graded Band Gap Solar Cells with SCAPS," Proc. 23rd European Photovoltaic Solar Energy Conference, Valencia.
[47] Burgelman, M., Nollet, P. and Degrave, S., 2000, "Modelling Polycrystalline Semiconductor Solar Cells," Thin Solid Films, 361, pp. 527-532.
[48] Decock, K., Khelifi, S. and Burgelman, M., 2011, "Modelling Multivalent Defects in Thin Film Solar Cells," Thin Solid Films, 519(21), pp. 7481-7484.
[49] Verschraegen, J. and Burgelman, M., 2007, "Numerical Modeling of Intra-Band Tunneling for Heterojunction Solar Cells in SCAPS," Thin Solid Films, 515(15), pp. 6276-6279.
[50] Lin, P.-J., et al., 2014, "Numerical Simulation of Cu_2ZnSnS_4 Based Solar Cells with In_2S_3 Buffer Layers by SCAPS-1D," 淡江理工學刊, 17(4), pp. 383-390.
[51] Simya, O., Mahaboobbatcha, A. and Balachander, K., 2015, "A Comparative Study on the Performance of Kesterite Based Thin Film Solar Cells using SCAPS Simulation Program," Superlattices Microstruc., 82, pp. 248-261.
[52] Khoshsirat, N. and Yunus, N. A. M., 2013, "Numerical Simulation of CIGS Thin Film Solar Cells Using SCAPS-1D," Sustainable Utilization and Development in Engineering and Technology (CSUDET), IEEE Conference.
[53] Sibiński, M., et al., 2011, "Carbon Nanotube Transparent Conductive Layers for Solar Cells Applications," Optica Applicata, 41(2).
[54] Zerfaoui, H., et al., 2016, "Study by Simulation of the SnO2 and ZnO Anti-Reflection Layers in n-SiC/p-SiC Solar Cells," AIP Conference Proceedings, 1758(1).
[55] Pogrebnyak, A.D., Jamil, N. and Muhammed, A., 2011, "Simulation Study of n-ZnO/p-Si Heterojunction Solar Cell," Наносистеми, наноматеріали, нанотехнології, (9, Вип. 4), pp. 819-830.
[56] Hurkx, G., Klaassen, D. and Knuvers, M., 1992, "A New Recombination Model for Device Simulation Including Tunneling," IEEE Transactions on Electron. Devices, 39(2), pp. 331-338.
[57] Patra, J. C. and Maskell, D.L., 2012, "Modeling of Multi-Junction Solar Cells for Estimation of EQE under Influence of Charged Particles using Artificial Neural Networks," Renewable Energy, 44, pp. 7-16.
[58] Li, X., et al., 2013, "Multi-Dimensional Modeling of Solar Cells with Electromagnetic and Carrier Transport Calculations," Prog. Photovoltaics Res. Appl., 21(1), pp. 109-120.

[59] Clugston, D. A. and Basore, P. A., 1997, "PC1D version 5: 32-bit Solar Cell Modeling on Personal Computers," Photovoltaic Specialists Conference, Conference Record of the Twenty-Sixth IEEE.
[60] Basore, P. A., 1990, "Numerical Modeling of Textured Silicon Solar Cells Using PC-1D," IEEE Transactions on Electron Devices, 37(2), pp. 337-343.
[61] Haug, H., et al., 2014, "Implementation of Fermi–Dirac Statistics and Advanced Models in PC1D for Precise Simulations of Silicon Solar Cells," Sol. Energy Mater. Sol. Cells., 131, pp. 30-36.
[62] Kurtz, S.R., et al., 2002, "Insights into the Electronic Properties of InGaAsN: the Effect of Nitrogen from Band Structure to Devices," Semicond. Sci. Technol., 17(8), pp. 843.
[63] Swatowska, B., Stapiński, T. and Zimowski, S., 2012, Properties of a-Si: N: H Films Beneficial For Silicon Solar Cells Applications," Opto-Electronics Rev., 20(2), pp. 168-173.
[64] Honsberg, C., et al. 2004, "InGaN–A New Solar Cell Materia,". Proc. 19th European Photovoltaic Science and Engineering Conference, Paris, France.
[65] Hossain, M., et al., 2014, "Design of High Efficient InN Quantum Dot Based Solar cell," Int. J. Sci. Eng. Technol., 3(4), pp. 346-349.
[66] Mehta, M., 2008, Modifying PC1D to Model Spontaneous & Piezoelectric Polarization in III-V Nitride Solar Cells, University of Delaware, Newark, Delaware.
[67] Yeon, D.H., et al., 2015, "Effect of Band-Aligned Double Absorber Layers on Photovoltaic Characteristics of Chemical Bath Deposited PbS/CdS Thin Film Solar Cells," Sci. Rep., 5, pp. 14353.
[68] Rover, D., Basore, P. and Thorson, G., 1985, "Solar Cell Modeling on Personal Computers," IEEE Photovoltaic Specialists Conference.
[69] Basore, P., 1991, "PC-1D version 3: Improved Speed and Convergence," Conference Record 22nd Photovoltaic Specialists Conference, IEEE.
[70] Basore, P. A. and Clugston, D. A., 1996, "PC1D Version 4 for Windows: from Analysis to Design," Conference Record 25th Photovoltaic Specialists Conference, IEEE.
[71] Basore, P. A. and Clugston, D. A. 2003, PC1D Version 5.9. University of New South Wales, Sydney, Australia.
[72] Tsai, H.-L., Tu, C.-S., and Su, Y.-J., 2008, "Development of Generalized Photovoltaic Model using MATLAB/SIMULINK," Proc. World Congress on Engineering and Computer Science, San Francisco, USA.
[73] Salmi, T., et al., 2012, "Matlab/Simulink Based Modeling of Photovoltaic Cell," Int. J. Renewable Energy Res., 2(2), pp, 213-218.
[74] Altas, I. and Sharaf, A., 2007, "A Photovoltaic Array Simulation Model for Matlab-Simulink GUI Environment," International Conference Clean Electrical Power, ICCEP'07, IEEE.
[75] Ghosh, P. and Kundu, P. K., 2017, "Modeling and Simulation of Solar Cell using Embedded MATLAB Simulink Tool," Int. J. Electron. Electr. Comput. Syst., 6(7), 101-114.
[76] Hussain, A.B., et al., 2017, "Modelling and Simulation of Single-And Triple-Junction Solar Cells using MATLAB/SIMULINK," Int. J. Ambient Energy., 38(6), pp. 613-621.
[77] Dehghanzadeh, A., Farahani, G. and Maboodi, M. 2017, "A Novel Approximate Explicit Double-Diode Model of Solar Cells for use in Simulation Studies," Renewable Energy, 103, pp. 468-477.
[78] Fonash, S., Analysis of Microelectronic and Photonic Structures (AMPS) Software, http://www.ampsmodeling.org/
[79] Hernandez-Como, N. and Morales-Acevedo, A., 2010, "Simulation of Hetero-Junction Silicon Solar Cells with AMPS-1D," Sol. Energy Mater. Sol. Cells., 94(1), pp. 62-67.
[80] Liu, Y., Heinzel, D. and Rockett. A., 2011, "A New Solar Cell Simulator: WxAMPS," Photovoltaic Specialists Conference (PVSC), 37th IEEE.
[81] Liu, Y., Sun, Y. and Rockett, A., 2012, "A New Simulation Software of Solar Cells—wxAMPS," Sol. Energy Mater. Sol. Cells., 98, pp. 124-128.
[82] Liu, Y., Heinzel, D. and Rockett, A., 2010, "A Revised Version of the AMPS Simulation Code," Proc. 35th Photovoltaic Specialists Conference (PVSC), IEEE.
[83] Messei, N., 2016, Study of the Effect of Grading in Composition on the Performance of Thin Film Solar Cells Based on AlGaAs and CZTSSe, a Numerical Simulation Approach. PhD thesis, Université Constantine 1, Canstantine, Algeria.
[84] Sayeed, M. A. and Salem, I. 2017, Design and Simulation of Efficient Perovskite Solar Cells, Master's thesis, East West University, Dhaka, Bangladesh.

[85] Chang, W.-R., et al., 2013, “Simulation of a Novel Single Junction Thin Film Solar Cell,” International Symposium Next-Generation Electronics (ISNE), IEEE.
[86] Levinshtein, M. and Mnatsakanov, T., 2002, “On the Transport Equations in Popular Commercial Device Simulators,” IEEE Transactions on Electron. Devices, 49(4), pp. 702-703.
[87] Kotov, I., et al., 2006, “Electric Fields in Nonhomogeneously Doped Silicon. Summary of Simulations,” Nucl. Instrum. Methods Phys. Res., Sect. A, 568(1), pp. 41-45.
[88] Algora, C., et al. 2004, “Pending Issues in the Modeling of Solar Cells,” 19th European Photovoltaic Conference, Paris.
[89] Kersys, T., Anilionis, R. and Eidukas, D., 2008, “Simulation of Doped Si Oxidation in Nano-dimension Scale,” Elektronika ir Elektrotechnika, 84(4), pp. 43-46.
[90] Garcia, B., 2007, “Indium gallium Nitride Multijunction Solar Cell Simulation Using Silvaco Atlas., Monterey California. Naval Postgraduate School.
[91] Jeong, S., et al., 2008, “Electrodeposited ZnO/Cu2O Heterojunction Solar Cells,” Electrochimica Acta, 53(5), pp. 2226-2231.
[92] Stangl, R., et al., 2007, “AFORS-HET 3.0: First Approach to a Two-Dimensional Simulation of Solar Cells,” Proc. 22nd European Photovoltaic Solar Energy Conference.
[93] Bingyan, R., Wang Minhua, Liu Xiaoping, Li Yanlin, Yang Jiankun, Li Xudong, Xu Ying, Li Hailing, Wang Wenjing, 2008, “Simulation of heterojuntion solar cell with AFORS-HET,” Acta Energiae Solaris Sinica, 2.
[94] Froitzheim, A., et al., 2003, “AFORS-HET: a Computer-Program for the Simulation of Heterojunction Solar Cells to be Distributed For Public Use,” Proc. 3rd World Conference Photovoltaic Energy Conversion, 2003. IEEE.
[95] Piprek, J., 2013, Semiconductor Optoelectronic Devices: Introduction to Physics and Simulation, Academic Press, Cambridge, Massachusetts, USA.
[96] Sheng, Y., et al., 2013, “Simulation of InGaN/GaN Light-Emitting Diodes with Patterned Sapphire Substrate,” Opt. Quantum Electron., 45(7), pp. 605-610.
[97] Krč, J., Smole, F. and Topič, M., 2003, Potential of Light Trapping in Microcrystalline Silicon Solar Cells with Textured Substrates. Prog. Photovoltaics Res. Appl., 11(7), pp. 429-436.
[98] Padmanabhan, B., et al., 2008, Modeling of solar cells, Master’s thesis, Arizona State University, Phoenix, Arizona, USA
[99] Zeman, M., et al., 1997, “Computer Modelling of Current Matching in a-Si: H/a-Si: H Tandem Solar Cells on Textured TCO Substrates,” Sol. Energy Mater. Sol. Cells, 46(2), p. 81-99.
[100] Zeman, M., et al., 2011, “Modeling of Advanced Light Trapping Approaches in Thin-Film Silicon Solar Cells,” MRS Online Proceedings Library Archive, 1321.

Chapter 6 Part 2: Modeling of properties of fabricated NiO/TiO_2 heterojunction solar cells

This chapter reports the modelling of the experimentally fabricated NiO/TiO2 heterojunction solar cells using SCAPxD.

To cite this article: Ukoba, O.K., and Inambao F.L. (2018) "Modeling of properties of fabricated NiO/TiO_2 heterojunction solar cells" ***International Journal of Applied Engineering Research,*** **Vol. 13, No. 11, pp. 9701 – 9705.**

International Journal of Applied Engineering Research ISSN 0973-4562 Volume 13, Number 11 (2018) pp. 9701-9705

Modeling of Fabricated NiO/TiO_2 P-N Heterojunction Solar Cells

Ukoba, O.K; and Inambao, F.L
Discipline of Mechanical Engineering, University of KwaZulu-Natal, Durban, South Africa.
Email :ukobaking@yahoo.com

Abstract

This paper reports modelling and theoretical validation of a fabricated NiO/TiO_2 P-N heterojunction solar cell. The solar cell equations were modelled and thereafter theoretical validation of the fabricated solar cells was performed. Modelling tools were used to validate the influence of NiO material features such as deposition temperature, voltage and defect densities on the performances of an ITO/TiO_2/NiO heterojunction solar cell structure. The working points used included a temperature of 350 ^oC, illumination of 1000 W/m^2 using an AM1.5 lamp, with voltage range of 0 to 1.5 volts. The output gave V_{oc} of 0.1445 V, J_{sc} of 247.959195E-6 mA/cm^2 and FF of 37.87 % and Voc 0.7056 and J_{sc} 28.366911 mA/cm2 when both contacts were added. This opens a new frontier for modelling of metal oxide based thin film solar cells especially NiO thin film solar cells. These findings enhance the quest to develop affordable and sustainable energy and encourage further research in solar cell technologies in low-income countries.

Keyword: NiO; solar cells; modelling; simulation

INTRODUCTION

Despite the potential that solar energy holds for being an environmentally benign and sustainable energy source [1], large-scale production and costs still hinder the usage, especially in low-income countries [2]. This may be attributed to the difficulty in scaling up existing methods or the expense and complexities associated with vacuum environment fabrication [3]. The way forward is to develop materials and techniques that will encourage low cost or focus on a few experimental techniques [4]. The latter can be achieved with more success when combined with modelling. The modelling of result improves the planning and implementation of the experiment.

Solar cells produce about 0.5 volts to 0.6 volts of open circuit voltage and 1 to 8 amps DC current depending on a range of factors but mainly related to the semiconductor used [5]. About 36 to 72 solar cells are stacked together in series to form a module which can produce meaningful output. A solar panel is an arrangement of solar modules either in series or parallel. When the solar modules are connected in parallel the currents are added while the voltage is the same, while for series the voltages are added and the current produced remains the same [6].

Solar cells can be grouped into monocrystalline, polycrystalline, and thin film technology [7]. Both monocrystalline and polycrystalline are referred to as traditional technologies of solar cells and collectively grouped as crystalline silicon. Solar cells can also be grouped by generations of the solar cells [8, 9]. The traditional technologies of solar cell manufacture use microelectronic manufacturing with an efficiency ranging from 10 % to 15 % and 9 % to 12 % for monocrystalline and polycrystalline respectively. Thin films' efficiency varies depending on the fabrication techniques and materials used. The monocrystalline solar cells tend to have the highest efficiency and are also very expensive.

Metal oxide heterojunction solar cells are currently attracting attention due to their potential [10]. Metal oxides offer great promise for being a solution to affordable, environmentally friendly, sustainable and viable energy, so ending the world energy problem, especially in developing and low-income countries [11, 12]. Metal oxides, especially NiO thin film, are the most promising materials to be used as solar cell absorber layers due to their excellent optical properties They have good band gaps, low cost and great absorption coefficients as well as constituents that are nontoxic and abundant naturally [13].

However, most of them still exhibit weak conversion efficiencies resulting in several experiments in the laboratory in an attempt to obtain the optimum power conversion efficiency with current levels being about 8.4 % [14] compared to those of other technological paths in the photovoltaic field like CIGS-based solar cells which reach record efficiencies of over 20 % [10]. However, despite the development of several physical and chemical fabrication techniques for PV [15-17], several reasons could explain this situation, such as various loss mechanisms due to absorber features.

Modelling has been used in other fields to reduce the amount of person-hours and resources spent performing experiments [18]. Modelling of solar energy spans many decades, with most models focusing on photovoltaic panels and modules. The few studies on solar cells are mainly on silicon and related solar cells [19-21]. There is, therefore, a need to explore ways of modelling metal oxide cells due to the increasing interest in them.

This study attempts to model metal oxides heterojunctions (NiO/TiO_2) using modelling tools (including SCAPS) which were successfully deployed in previous generations of solar cell research. SCAPs stands for Solar Cell Capacitance Simulator and is used for one or two-dimensional solar cell simulation. Therefore, a detailed analysis of the effect of deposition temperature, thickness, and defects densities of a NiO layer is necessary and has been presented in this work using the numerical simulation package SCAPS [22]. The results proposed in this study are a useful guideline for design of high performances NiO based solar cells.

METHODOLOGY

The Mathematical Model

A solar cell is basically a P-N heterojunction. Photovoltaic systems exhibit nonlinear I-V characteristics that vary with the temperature of the solar cell and the radiant intensity. Under ideal conditions, a solar cell can be theoretically modelled as a current source under a diode. A direct current is produced when the solar cell is exposed to light and this current varies linearly with the solar radiation. This is represented in Figure 1.

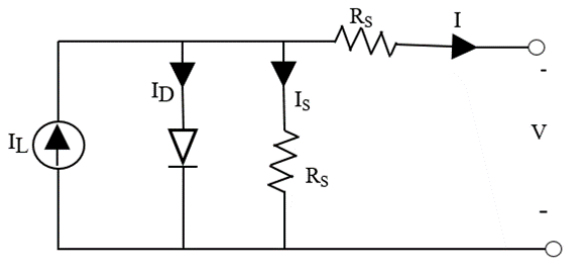

Figure 1. Solar cell model equivalent circuit

From the aforementioned, the characteristic equations are given as:

$$I_{ph} = \frac{I_r \times I_{sc}}{I_{ro}} \quad (1)$$

Equation (1) shows that the photocurrent depends on the temperature of the solar cell and solar insolation.

$$V_t = \frac{kT}{q} \quad (2)$$

$$I_s = I_{sc} \times \left(e^{\left(\frac{V_{OC}}{n.V_t}\right)} - 1 \right) \quad (3)$$

It can be seen from Equation (3) that the cell's saturation current varies with the cell temperature,

$$I_d = I_s \times \left(e^{\left(\frac{V + I.R_S}{n.V_t.N_S}\right)} - 1 \right) \quad (4)$$

Equation (4) gives the Shockley equation.

$$I = I_{ph} - I_d - I_{sh} \quad (5)$$

The output current of the solar cell is represented in Equation (5).

Equations (1) to (5) give the electrical behaviour and relationship between the current supplied and voltage, where; I_{ph} is photocurrent, I_{sc} is reverse saturation current, R_S and R_{sh} are inherent resistances in series and parallel associated with the cell, N_s is number of cells in series, q is the electron charge, K is Boltzmann's constant and A, the modified ideality factor. Table 1 shows the ideality factor of some of the solar cells.

Table 1. Ideality factor of some solar cells

S/N	Technology	Ideality factor (A)
1.	Monocrystalline silicon (Si Mono)	1.2
2.	Polycrystalline silicon (Si Poly)	1.3
3.	AsGa	1.3
4.	CIS	1.5
5.	CdTe	1.5
6.	a-Si:H	1.8
7.	a-Si: H tandem	3.3
8.	a-Si: H triple	5

The solar cell is not an active device in darkness but behaves as a diode in such an environment i.e. as a P-N junction. During this phase it does not produce current and voltage. Conversely, a current is generated when an external load is connected to the solar cells. This current is called diode current or dark current and the diode defines the I-V characteristics of the cell.

Therefore, from Figure 1 and from equation (5), the I-V characteristic equation of a solar cell can be expressed in Equation (6):

$$I = I_{ph} - I_s \left[e^{\left(\frac{q(V + R_s I_{pv})}{AkT_c}\right)} - 1 \right] - \frac{V + R_s I_{pv}}{R_{sh}} \quad (6)$$

Theoretical validation

SCAPS is a one-dimensional solar cell simulation program used for Opto-electrical simulation of the 1-D or 2-D structures of semiconductor layers [23-26]. SCAPS was originally developed for cell structures of the $CuInSe_2$ and the CdTe family. However, there have been improvements since then making room for other types of solar cells. SCAPS uses finite difference methods to solve the differential equations which, along with several relations from the physics of semiconductors, describe mathematically the performance of a solar cell. SCAPS performs a complete simultaneous numerical solution of the two continuity equations and Poisson's equation, conditional on the boundary conditions appropriate to one and two-dimensional cells [27]. The equations are expressed as shown in Equations (7-9).

$$\nabla^2 v = -\frac{q}{\epsilon}(p - n + N_D - N_A) \quad (7)$$

$$\nabla . J_p = q(G - R) \quad (8)$$

$$\nabla . J_n = q(R - G) \quad (9)$$

The general terms of Equations (8) and (9) can be represented as:

$$G(x) = \int_0^\infty \phi a e^{-ax} d\lambda \quad (10)$$

The hole and electron current densities which appear in Equations (8) and (9) are given by:

$$J_p = -q\mu_p p \nabla V_p - kT\mu_p \nabla_p \quad (11)$$

$$J_n = -q\mu_n n\nabla V_n + kT\mu_n\nabla_n \quad (12)$$

$$V_p = V - (1-\gamma)\frac{\Delta_G}{q} \quad (13)$$

$$V_n = V + \gamma\frac{\Delta_G}{q} \quad (14)$$

where v_p and v_n represent the effective potentials expressed in Equations (13) and (14), and Δ_G and γ account for variations in the band structure, such as density of states and band gap, and account for Fermi-Dirac statistics.

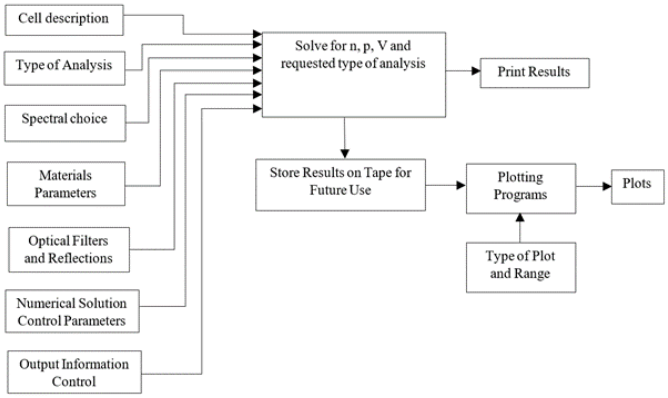

Figure. 2. Block Diagram of the structure of SCAP1D and SCAP2D

Figure 2 depicts the structure of the SCAPS programme, and summarizes the working of the programme. The operator inputs the information related to the materials' parameters, a description of the device to be analyzed, the type of analysis to be performed and the spectrum (optional). The results are printed in summary form and the detailed results of the calculation are stored. A separate plotting routine is used to access the information and to display the appropriate parameters. The plotting capability is one of the most valuable features of the code because it allows one to effectively have a microscopic view of most of the parameters of interest in the interior of the cell under operating conditions.

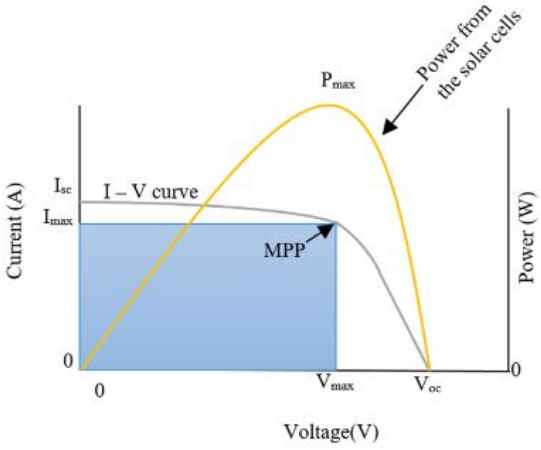

Figure 3. Typical characteristics of a solar cells

Figure 3 shows typical characteristics of solar cells. It shows the behaviour of the voltage and current with irradiation and the temperature of solar cells. The maximum power is obtained by computing the V_{max} and I_{max}. The maximum power point (MPP) technique is mainly used in computing the maximum power of solar module. The fundamental parameters related to the solar cell are short circuit current (I_{sc}), open circuit voltage (V_{oc}), and MPP [28, 29].

In this study, a temperature of 350 ^oC (623.15 K) was used as the working temperature. This was the temperature at which the experimental NiO/TiO_2 P-N heterojunction was spray pyrolysis deposited, while the illumination was done with AM1.5 using a lamp of 1000 W/m^2 with a voltage range of 0 volts to 1.5 volts as shown in Figure 4.

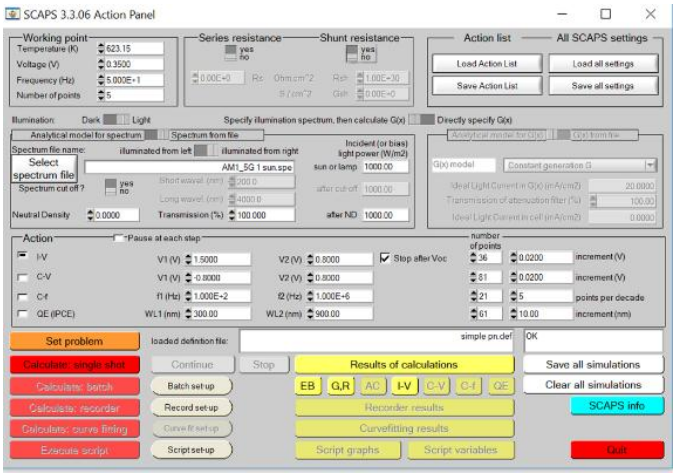

Figure 4. Defined parameters used for the modelling the solar cells

Figures 5 and 6 give the output of the I-V characteristics using SCAP-1D. Figure 5 varies the voltage from 0 volts to 1 volt while Figure 6 varies it from 0 volts to 1.5 volts. The generated plot of current density versus voltage corresponds to the typical I-V characteristic curve. The fill factor (FF) obtained was 37.87 % while the output voltage (V_{oc}) was 0.1445 volts. These parameters agree with the fabricated NiO/TiO2 solar cells with FF of 39 % [4].

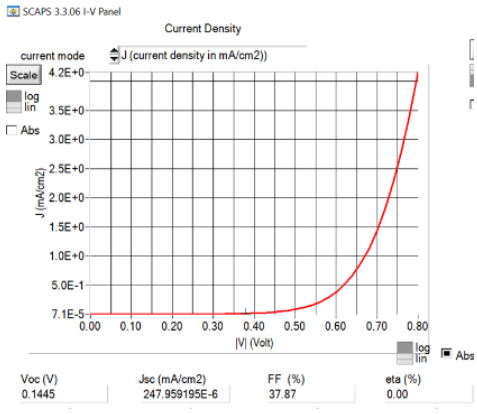

Figure 5. SCAP-1D generated I–V characteristic curve for the solar cells

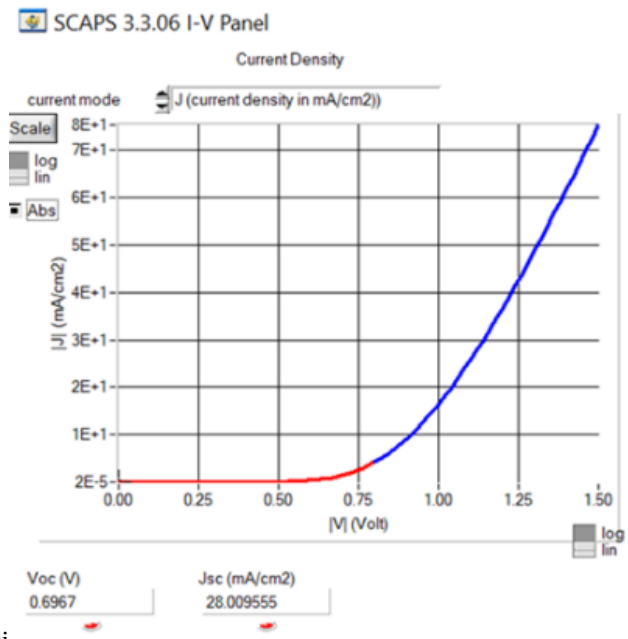

/ui

Figure 6. SCAP-1D generated I–V characteristic curve for the solar cells 0 to 1.5 v

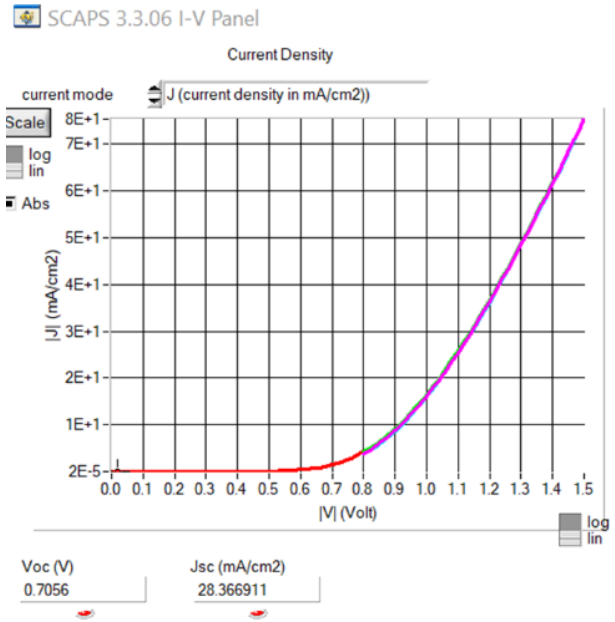

Figure 7. SCAP-1D generated I–V characteristic curve for the solar cells with gold and ITO added to 0 to 1.5V

Figure 7 shows the SCAP-1D generated I-V characteristic curve for the solar cells with gold and ITO added to 0 V to 1.5 V.

CONCLUSION

This paper was able to give the mathematical model and theoretical validation of a sprayed deposited NiO/TiO_2 heterojunction solar cell at 350 ºC. The model used the deposition parameters of the fabricated solar cell and generated the I-V characteristics of the solar cell. The results show excellent correspondence to reported experimental fabrication. The experimental fill factor obtained was 39 % while this study reported 37.87 %. This shows that this can be used to model another metal oxides especially NiO related solar cells. This will help to reduce several person-hours and resources spent on trying different optimization parameters in the laboratory. These findings enhance the quest to develop affordable and sustainable energy and encourages further research in solar cells technologies in low-income countries.

ACKNOWLEDGEMENT

The financial assistance of the National Research Foundation (NRF/TWAS) of South Africa towards this research under grant number 105492 is hereby acknowledged. Authors appreciate the SCAPS team for allowing us the usage of the program.

REFERENCE

[1] Kabir, E., Kumar, P., Kumar, S., Adelodun, A.A., and Kim, K.-H., 2018, “Solar Energy: Potential and Future Prospects,” Renewable Sustainable Energy Rev., 82, pp. 894-900.

[2] Ukoba, O., Inambao, F., and Eloka-Eboka, A., 2017, “Influence of Annealing on Properties of Spray Deposited Nickel Oxide Films for Solar Cells,” Energy Procedia, 142, pp. 244-252

[3] Ukoba, O.K., Eloka-Eboka, A.C., and Inambao, F.L., 2018, “Review of Nanostructured NiO Thin Film Deposition Using the Spray Pyrolysis Technique,” Renewable and Sustainable Energy Rev., 82, pp. 2900-915.

[4] Ukoba, K., Inambao, F., and Eloka-Eboka, A., 2018, “Fabrication of Affordable and Sustainable Solar Cells Using NiO/TiO_2 P-N Heterojunction,” Int. J. Photoenergy, Hindawi, 2018

[5] Cutter, A., 2012, The Electricians Green Handbook, Delmar, New York.

[6] Singla, V., and Garg, V.K., 2013, “Modeling of Solar Photovoltaic Module & Effect of Insolation Variation Using Matlab/Simulink,” Int. J. Adv. Eng. Tech., 4(3) pp.5-9.

[7] Xiao, W., Dunford, W.G., and Capel, A., 2004, “A Novel Modeling Method for Photovoltaic Cells,” Proc. 35th Annual IEEE Power Electronics Specialists Conference, Aachen, Germany, 20-25 June 2004; pp. 1950-1956.

[8] Bagher, A.M., Vahid, M.M.A., and Mohsen, M., 2015, “Types of Solar Cells and Application,” Am. J. Optics Photonics, 3(5), pp. 94-113.

[9] Liu, M., Johnston, M.B., and Snaith, H.J., 2013,

"Efficient Planar Heterojunction Perovskite Solar Cells by Vapour Deposition," Nature, 501(7467), pp. 395.

[10] Liu, H., Avrutin, V., Izyumskaya, N., Özgür, Ü., and Morkoç, H., 2010, "Transparent Conducting Oxides for Electrode Applications in Light Emitting and Absorbing Devices," Superlattices and Microstructures, 48, (5), pp. 458-484

[11] Omer, A.M., 2008, "Energy, Environment and Sustainable Development," Renewable Sustainable Energy Rev., 12(9), pp. 2265-2300.

[12] Özgür, Ü., Alivov, Y.I., Liu, C., Teke, A., Reshchikov, M., Doğan, S., Avrutin, V., Cho, S.-J., and Morkoc, H. 2005, "A Comprehensive Review of ZnO Materials and Devices," J. Appl. Phys., 98(4), p 11.

[13] Djinkwi Wanda, M., Ouédraogo, S., Tchoffo, F., Zougmoré, F., and Ndjaka, J., 2016, "Numerical Investigations and Analysis of Cu2ZnSnS4 Based Solar Cells by SCAPS-1D," Int. J. Photoenergy, 2016.

[14] Shin, B., Gunawan, O., Zhu, Y., Bojarczuk, N.A., Chey, S.J., and Guha, S., 2013, "Thin Film Solar Cell with 8.4% Power Conversion Efficiency Using an Earth-Abundant Cu2ZnSnS4 Absorber," Prog. Photovoltaics Res. Appl., 21(1) pp. 72-76.

[15] Katagiri, H., Jimbo, K., Yamada, S., Kamimura, T., Maw, W.S., Fukano, T., Ito, T., and Motohiro, T., 2008, "Enhanced Conversion Efficiencies of Cu2ZnSnS4-Based Thin Film Solar Cells by Using Preferential Etching Technique," Appl. Phys. Express, 1(4), p. 041201.

[16] Ahmed, S., Reuter, K.B., Gunawan, O., Guo, L., Romankiw, L.T., and Deligianni, H., 2012, "A High Efficiency Electrodeposited Cu2ZnSnS4 Solar Cell," Adv. Energy Mater., 2(2), pp. 253-259.

[17] Maeda, K., Tanaka, K., Fukui, Y., and Uchiki, H. 2011, "Influence of H2S Concentration on the Properties of Cu2ZnSnS4 Thin Films and Solar Cells Prepared by Sol-Gel Sulfurization," Sol. Energy Mater. Sol. Cells, 95(10), pp. 2855-2860.

[18] Arashpour, M., Wakefield, R., Blismas, N., and Minas, J., 2015, "Optimization of Process Integration and Multi-Skilled Resource Utilization in Off-Site Construction," Autom. Constr., 50, pp. 72-80.

[19] Altermatt, P.P., 2011, "Models for Numerical Device Simulations of Crystalline Silicon Solar Cells—A Review," J. Comput. Electron., 10(3), pp. 314-330.

[20] Fossum, J.G., 1976, "Computer-Aided Numerical Analysis of Silicon Solar Cells," Solid-State Electron., 19(4), pp. 269-277.

[21] Ingenito, A., Zeman, M., and Isabella, O., 2016, "Opto-Electrical Surface Engineering of Wafer-Based C-Si Solar Cells," Master's dissertation, Delft University of Technology, Delft, Netherlands.

[22] Degrave, S., Burgelman, M., & Nollet, P. 2003. "Modelling of Polycrystalline Thin Film Solar Cells: New Features in SCAPS Version 2.3," Proc. 3rd World Conference on Photovoltaic Energy Conversion, Osaka (Japan), May 2003.

[23] Burgelman, M., and Marlein, J., 2008, "Analysis of Graded Band Gap Solar Cells with SCAPS," Proc. 23rd European Photovoltaic Conference, Valencia, Spain, 2008.

[24] Burgelman, M., Nollet, P., and Degrave, S., 2000, "Modelling Polycrystalline Semiconductor Solar Cells," Thin Solid Films, 361, pp. 527-532.

[25] Decock, K., Khelifi, S., and Burgelman, M., 2011, "Modelling Multivalent Defects in Thin Film Solar Cells," Thin Solid Films, 519, pp. 7481-7484.

[26] Verschraegen, J., and Burgelman, M., 2007, "Numerical Modeling of Intra-Band Tunneling for Heterojunction Solar Cells in SCAPS," Thin Solid Films 515, pp. 6276-6279.

[27] Schwartz, R., Gray, J., and Lundstrom, M., 1985, "Current Status of One-And Two-Dimensional Numerical Models: Successes and Limitations," Proc. of the Flat-plate Solar Array Project Research Forum on High-efficiency Crystalline Silicon Solar Cells, JPL Publication 85-38.

[28] Mohammed, S.S., 2011, "Modeling and Simulation of Photovoltaic Module Using MATLAB/Simulink," Int. J. Chem. Environ. Eng., 2(5).

[29] Sahu, R., Sen, S.K., Kaushal, A., and Yadav, S., 2017, "Modelling of Photovoltaic Cell using Incremental Conductance MPPT Method," Int. J. Eng. Sci. Comp., 7(6), 13271-13275

CHAPTER 6 PART 3: SOLAR CELLS AND GLOBAL WARMING REDUCTION

This chapter proposes one way of addressing the issue of climate change and pollution using solar cells.

To cite this article: Ukoba, O.K. and Inambao F.L. (2018). "Solar cells and global warming reduction" *International Journal of Applied Engineering Research* ISSN 09734562 Volume 13, Number 10 (2018) pp. 8303-8310.

International Journal of Applied Engineering Research ISSN 0973-4562 Volume 13, Number 10 (2018) pp. 8303-8310

Solar Cells and Global Warming Reduction

[1]Ukoba, O. Kingsley and [2]Inambao, L. Freddie

[1,2] Mechanical Engineering, University of KwaZulu-Natal, Durban. South Africa.
inambaof@ukzn.ac.za, ukobaking@yahoo.com

Abstract

This study proposes one way of addressing the issue of climate change and pollution using solar cells. The quality of life in developing and low-income countries is on the decline because of air pollution. Energy has a role to play in the quality of life and reduction of air pollution especially in those countries. A reduction in the usage of fossil fuels and biomass in these countries will help decrease the air pollution and emissions generated by such energy sources. About 1 million solar lanterns are capable of reducing greenhouse gas emissions by over 30 000 tons. The role of eco-friendly solar cells in elimination of air pollution cannot be overstated.

Keywords: Solar; air pollution; developing countries; fossil fuels

INTRODUCTION

The quality of human life is affected by several factors of which access to a clean and reliable source of energy is at the forefront [1]. About one-fourth of earth's inhabitants lack access to electricity with little or no change of outlook over the last 40 years [2]. Several developing countries in Africa and elsewhere are struggling to deliver affordable and stable electricity [3]. These countries still use fossil fuels (Premium Motor Spirit, kerosene) and biomass (charcoal and wood) as their major sources of energy [4]. Although some of these are cheap and easily accessible, regular exposure to their usage poses health and social risks [5]. Energy insecurity and other human interaction have created a major challenge of climate change and pollution.

Pollution, especially air pollution, is ranked the sixth-leading cause of death world-side, responsible for about 2.4 million premature deaths annually [6]. Air pollution is a leading cause of respiratory illness, cardiovascular disease, cancer, hospitalization, work-days lost, and school-days lost [7, 8]. This is because climate change boosts disease, heat, glacier melting, and ocean acidity [9]. It also causes an imbalance in ecosystems, agriculture, and water supply. Carbon dioxide gas, fossil fuel [10], soot particles from biofuel [11], methane gas, halocarbons and nitrous oxide gas are the leading causes of global warming [12, 13]. Cooling aerosol particles mask more than half of the actual global warming as shown in Figure 1. Particles containing sulphates, chloride, ammonium, potassium, nitrates, certain organic carbons, and water, primarily, are called cooling aerosol particles. Although, their sources differ they are mainly from fossil-fuel and biofuel soot. Thus, removal of aerosol particles is critical for air pollution reduction.

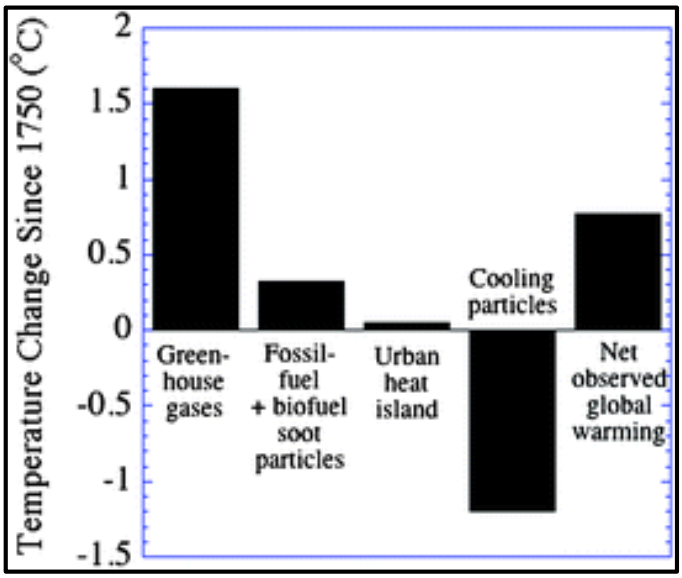

Figure 1. Primary contributions to observed global warming from 1750 to today from global model calculations

Apart from the seasonal scarcity of these fuels, they are expensive and prolonged exposure to them has adverse economic and health consequence. Kerosene is affordable and accessible in many countries due to the subsidization of the product by such countries [14]. However, kerosene lanterns emit both black carbon and carbon dioxide. Kerosene lamps emit 20 times more of these pollutants than previous estimates. They convert 7 % to 9 % of the fuel burned into black carbon particles. Black carbon particles are a major source of climate warming, second to CO_2 [15]. They do this by absorbing sunlight and heating the atmosphere. Black carbon combines with other pollutants to form 'short-lived climate pollutants' (SLCP). Table 1 illustrates the annual kerosene carbon emission in some Africa countries.

Table 1. Annual kerosene use and black carbon emissions by country

Country	Kerosene lamp-glass cover installed stock estimates (Million)			Kerosene lamp-simple wick installed stock estimates (Million)			Annual black carbon savings (tons)
	Households	Commercial	Total	Households	Commercial	Total	
Nigeria	39.8	3.8	43.6	17.8	0.3	18.1	52,680
Sudan	12.7	1.2	13.9	5.7	0.1	5.8	16,862
Kenya	14.0	1.3	15.3	6.3	0.1	6.4	19,629
Tanzania	11.7	1.6	13.3	5.9	0.2	6.1	18,335
Democratic Republic of Congo	4.1	1.3	5.4	20.3	1.2	21.5	49,964
Ethiopia	5.0	1.6	6.6	24.5	1.5	26	59,950

Fossil fuels are still being used for cooking and lighting in most developing countries as shown in Figures 2 and 3. Carbon is released when they are burnt thereby causing air pollution in the process.

(a) **(b)** **(c)**

Figure 2. Cooking with wood (a) Subsistence garri frying (b) Commercial garri frying (c) Food cooking (starch)

(a) **(b)**

Figure 3. Fossil fuel lightening (a) Reading with kerosene lamp (b) Suya meat vendor

At least 270 000 tons of black carbon per year is estimated to be emitted from kerosene lamps worldwide. Figure 4 shows the black carbon radiative forcing from kerosene lighting in residential. having a climate warming equivalent close to 240 million tons of CO_2, or roughly 4.5 % of the United States' CO_2 emissions. The warming impact of black carbon emissions from kerosene lamps is highest around source regions, reaching 0.5 W per square meter. Solar lanterns improve the quality of life for the people in Africa and Asia by reducing greenhouse gas emissions and providing greater access to energy.

Panasonic Electronics estimated that replacing kerosene lamps with 1 million solar lanterns will reduce greenhouse gas emissions by over 30 000 tons [16].

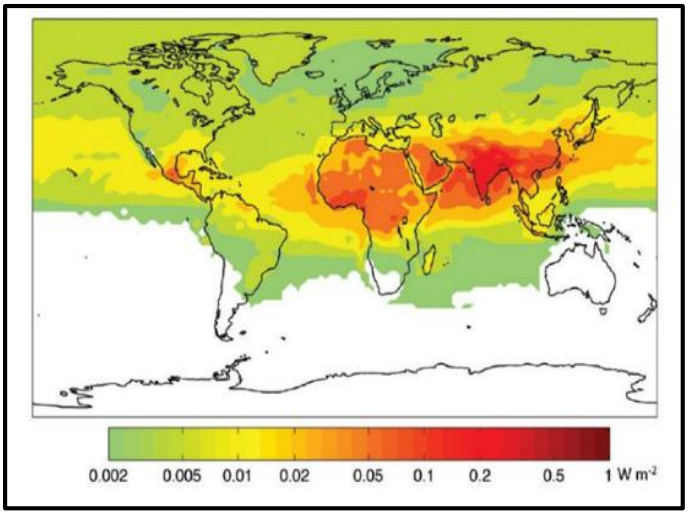

Figure 4. Black carbon radiative forcing from kerosene lighting in residential building (W/m^2)

The usage of renewable energy does not require the burning of fuels that emit carbon. This will help combat air pollution caused by fossil fuels and biomass. Sunlight has the most extensive range of applications for green households. The emerging range of materials for solar energy generation is environmentally friendly. This range includes metal oxide materials. Successful development and deployment in developing countries will help reduce the air pollution facing such countries. The impact is so noticeable that even a single household that has switched to solar energy can make a difference.

This study proposes one way of addressing the issue of climate change and pollution using solar technology.

SOLAR AND POLLUTION

Solar photovoltaics (PV)

These are arrays of cells containing a material that converts solar radiation into direct current (DC) electricity [17]. Different materials and methods are in use today. The materials include silicon (amorphous silicon, polycrystalline silicon, micro-crystalline silicon), cadmium telluride, and copper indium selenide/sulphide, metal oxides (plain or nanostructured), among others. These materials can also be doped to increase the number of positive (p-type) or negative (n-type) charge carriers. The resulting p- and n-type semiconductors are then joined to form a p–n junction that allows the generation of electricity when illuminated. Photovoltaics can be mounted on roofs or combined into farms [18].

Normalized distribution of radiation intensities for the sun and for a kerosene flame according to Planck's Law is shown in Figure 5. The non-normalized peak intensity of the Sun is a little over two orders of magnitude larger than that of kerosene [4]. Kerosene flame and sun estimated luminous efficacy values are 0.65 lm/W and 99 lm/W, respectively.

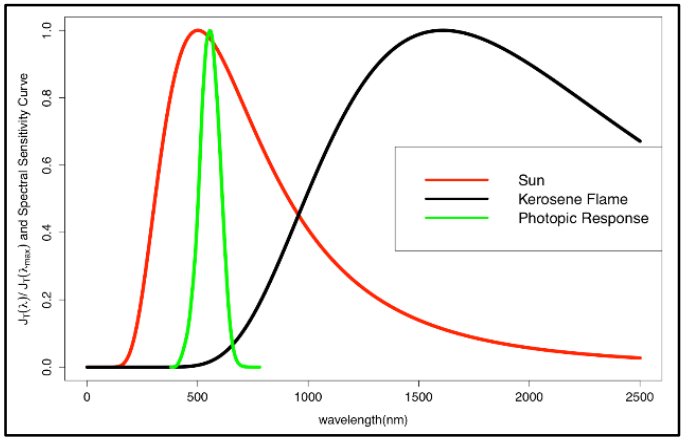

Figure 5. Normalized distribution of radiation intensities for the sun and kerosene flame according to Planck's Law, compared to the photopic spectral sensitivity of the eye

Lifecycle emissions from energy sources

Table 2 gives the ranges of the lifecycle CO_2e emission per kWh of electricity generated from most commonly used electricity sources. For the renewable electricity sources (wind, solar PV, CSP, tidal, wave, hydroelectric), climate-relevant lifecycle emissions take place only during the construction, installation, maintenance, and decommissioning of the technology. Emissions are caused by evaporation of dissolved CO_2 from hot water in geothermal flash- or dry-steam plants, but not in binary plants. Although, in the case of coal-carbon capture and storage (coal-CCS), nuclear, corn ethanol, and cellulosic ethanol additional emissions occur during the mining and production of the fuel. For biofuels and coal-CCS, emissions also occur as an exhaust component during combustion[18].

Table 2. Lifecycle emission of energy sources [18]

Technology	Lifecycle	Opportunity cost emissions due to delays	War/terrorism (nuclear) or CCS	Total
Solar Photovoltaic	19-59	0	0	19-59
Wind	2.8–7.4	0	0	2.8–7.4
Geothermal	15.1–55	1–6	0	16.1–61
Hydroelectric	17–22	31–49	0	48–71
Wave	21.7	20–41	0	41.7–62.7
Tidal	14	20–41	0	34–55
Nuclear	9–70	59–106	0–4.1	68–180.1
Coal-CCS	255–442	51–87	1.8–42	307.8–571

ENVIRONMENTAL BENEFITS OF SOLAR ENERGY

i. SOLAR ENERGY REDUCES AIR POLLUTION. Traditional electricity generation accounts for 31 % of greenhouse gas emissions in the United States [19]. Coal is used for electricity generation in some countries because it is a cheap form of electricity generation [20]. However, coal contains the most CO_2 per British thermal unit (BTU), and is the largest contributor to global warming [21]. Coal mining also has a severe impact on the environment and health of the workers and inhabitants around the mine. This contributes to air and water pollution. Metal oxide solar cells contain little or no toxic substance that causes air pollution. Electricity generation using solar will drastically reduce CO_2 emissions that pollute the air.

ii. SOLAR ENERGY REDUCES WATER POLLUTION AND CONSUMPTION. This is because water is not required for solar-based electricity generation, unlike natural gas and coal. A coal-fired power plant produces 72 % of water pollution. Most materials and methods used for solar cells contain little or no toxic materials. This helps to reduce water pollution.

iii. SOLAR REDUCES TOXIC WASTE. About 400 million tons of hazardous waste are produced every year mainly from fossil fuels. Coal-fired power plants release trace elements that are toxic [22]. Coal residues make up 90 % of all fossil fuel combustion wastes in the USA. However, only 20 % of those wastes are used with the rest deposited into landfills [23]. This constitutes a toxic waste. Solar eliminates this because fuel is not used and there is no need for waste disposal.

iv. SOLAR ENERGY HAS INFINITE USAGE. The solar system produces about 173 000 terawatts of solar energy per second. This value is 10 000 terawatts more than the total world energy needed.

Ways solar energy can reduce pollution

i. Vehicular emission reduction: Pollution from cars comes from by-products of the combustion process of fossil fuel (exhaust) and from evaporation of the fuel as shown in Figure 6.

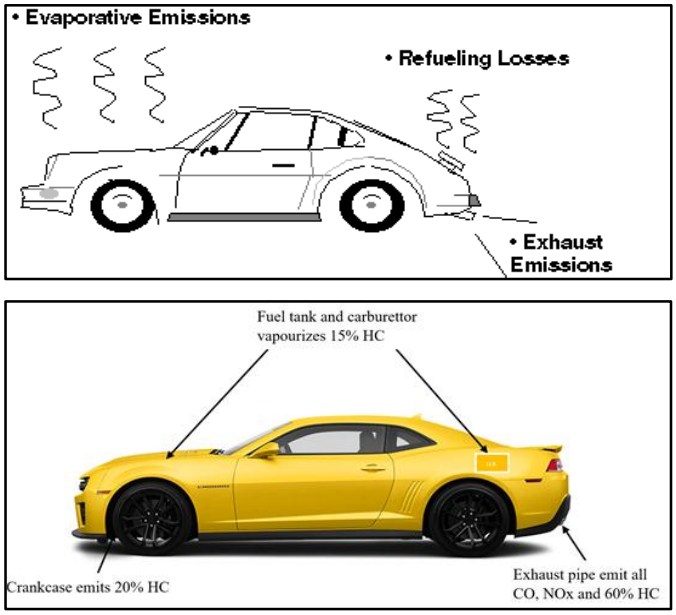

Figure 6. Sources of vehicle pollutants

The huge emission caused by fossil fuel powered cars, tricycles and motorcycles can be reduced with solar technology. Fossil fuel vehicles are sources of major air pollutants (such as carbon monoxide, nitrogen oxides, and other pollution) as shown in Table 3 [24]. Vehicles contribute about half of the carbon monoxide and nitrogen oxides emitted into the air [25, 26]. They also contribute about 25 % of the emitted hydrocarbons into the air [27, 28]. Particulate matter (soot and metals), nitrogen oxides, carbon monoxide, sulphur dioxide, hydrocarbons are the major air pollutants released by fossil fuel powered vehicles. Solar powered vehicles have little or no emissions. This will help reduced emission of the major pollutants causing global warming. Figure 7 illustrates t source of pollutants from a fossil fuel car and a solar car.

Figure 7. Vehicular emission (a) fossil fuel car emission (b) Solar car (zero emission)

Table 3. Vehicles pollutant emission factor

Pollutant	Bus	Motorcycle	Tricycle	Passenger	Luxury (car and SUV)	Commercial (Taxi)	Truck and Lorries	Goods Delivery	Heavy duty
Carbon dioxide (CO_2)	515.20	26.60	343.87	60.3	223.6	208.3	515.2	515.20	515.20
Carbon Monoxide (CO)	3.60	2.20	3.86	5.10	1.98	0.90	3.60	5.10	5.10
Nitrogen oxides (NOx)	12.00	0.19	3.89	1.28	0.20	0.50	6.30	1.28	1.28
Methane (CH_4)	0.09	0.18	0.11	0.18	0.17	0.01	0.09	0.09	0.09
Sulphur dioxide (SO_2)	1.42	0.01	1.94	0.03	0.05	10.30	1.42	1.42	1.42
Particulate matter	0.56	0.05	0.24	0.20	0.03	0.07	0.28	0.20	0.20
Hydrocarbons (HC)	0.87	1.42	0.54	0.14	0.25	0.13	0.87	0.14	0.14

ii. Solar lantern to replace a kerosene lantern. Quality of life will be improved by replacing kerosene lamps with solar lanterns. Kerosene lamps emit toxic fumes and pose a fire hazard, although the initial investment cost is more for solar lanterns compared to kerosene lamps. Figure 8 gives the cost obtained in 2005 by Mills [29].

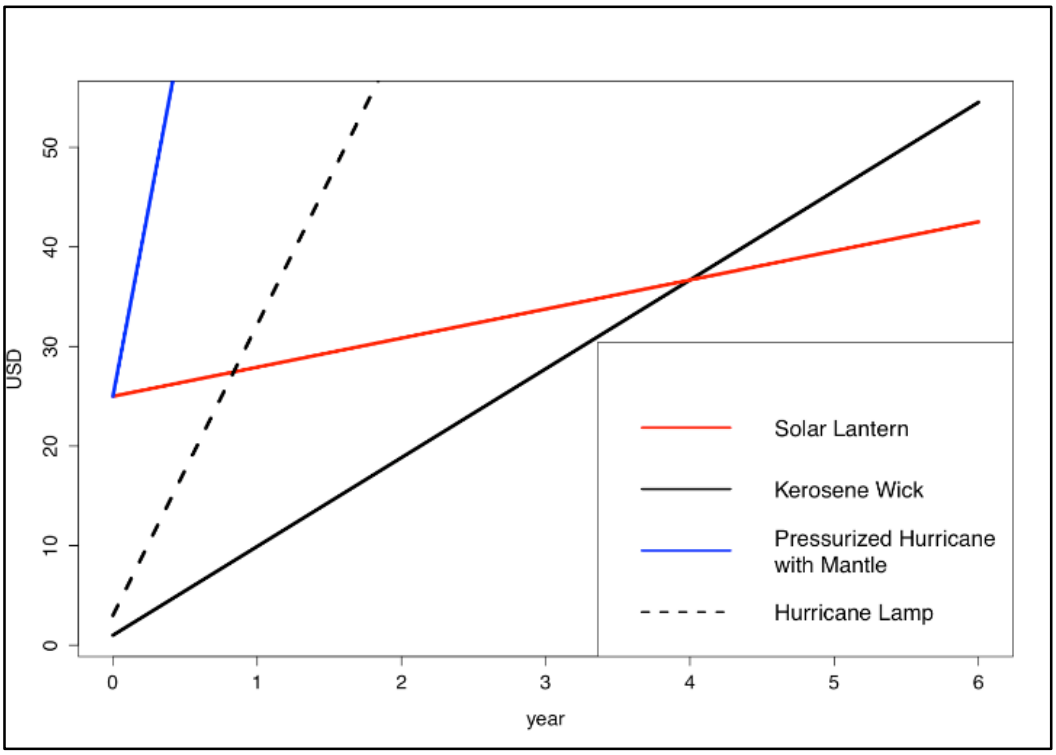

Figure 8. Accumulated costs of a solar lantern, kerosene wick lamp, hurricane wick lamp, and pressurized hurricane lamp with mantle

The health benefit of a solar lantern outweighs the costs when compared with a kerosene wick lamp. Subsidizing solar lanterns can encourage usage, and research into affordable yet efficient solar cells can help lower the cost.

iii. Cooking emission reduction: Solar cooking to replace biomass and other traditional cooking fuels. Air pollution can be reduced drastically when biomass and traditional cooking fuels are replaced with solar cookers. Solar cookers leverage on the sunlight to cook and boil water. This is achieved by using reflectors to heat an enclosed area that is different from the oven. This helps rural and low income communities that spend many hours each day searching for wood and other traditional fuels for cooking. It also encourages children to focus on studies and spend less time foraging for fuel [30]. This help saves resources, prevents health issues caused by fumes from fuels, saves money and encourages sustainable cooking. Figure 9 shows an annual solar cooking festival where people display and cook with different designs of solar cooker.

Figure 9. Solar cooking at a solar cooking festival

Solar water boiling will help reduce child mortality. It is estimated, by water.org, that a child dies every minute from disease related to water contamination [31]. Solar ovens help purify water polluted with microbes. These microbes are killed when the water is heated to certain temperatures. Water does not need to boil to eliminate dangerous microbes. Hepatitis A is killed at 65 °C, worms at 55 °C and *E. coli*, *Vibrio cholerae* (cholera) and *Salmonella typhi* (typhoid) bacteria at 60 °C. A water pasteurization indicator can be used to indicate the safety of the water. It consists of a small, less than 2-inch cylinder filled with wax. The water is safe for drinking when the wax melts. Although the water might still be brown, it will be safe to drink. Figure 10 gives an example of water boiling using solar energy.

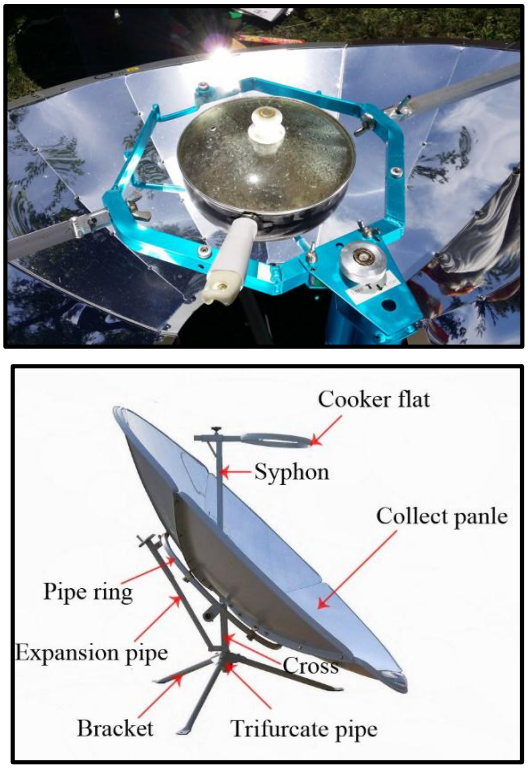

Figure 10. Solar water boiling and solar cooking panel

iv. Solar heating and cooling to replace traditional heating and cooling gas used for air conditioning: Most rural dwellers heat their water using wood collected from the farm. Urban residents heat up their home with coal during winter. These contribute to global warming. Demand for air conditioning is increasing due to the increase in global temperatures [32]. Agricultural produce and food items are stored and preserved using refrigerators and deep freezers. Air conditioners and refrigerator uses refrigerants. Refrigerants deplete the ozone and cause global warming. Refrigerants such as chlorofluorocarbons and hydrochlorofluorocarbons (HCFCS) have been replaced by hydrofluorocarbons (HFCS) in developed countries. Although HFCS do not deplete stratospheric ozone they have global warming potential [33].

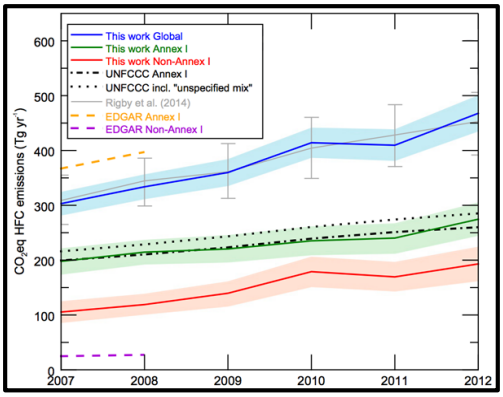

Figure 11. Hydrofluorocarbons (HFCS) from 2007 to 2012

Figure 11 shows the combined emissions of five hydrofluorocarbons from 2007 to 2012. The blue lines represent the world, green for developed countries, and a red line for developing countries. The dashed black lines and dotted gives the emissions reported to the UNFCCC (for developed countries only). The estimates from other studies are represented by grey, orange and purple lines [33]. The use of solar technology for heating and cooling will eliminate ozone depletion and greenhouse gas. Figure 12 shows solar heating for a swimming pool and for residential water heating.

(a) **(b)**

Figure 12. Solar heating (a) water heating for swimming pool (b) residential water heating

CONCLUSION

Air pollution threatens the very existence of humanity. Solar cells, and solar technology in general, are capable of reducing air pollution. Direct replacement of fossil powered cooking and

lightening by solar powered cooking and lighting can mitigate this pollution. Solar cells and solar energy have a great role in reduction and even elimination of air pollution and water pollution. The emerging generation of solar cells, especially nanostructured metal oxides, can help combat global warming.

ACKNOWLEDGEMENT

The financial assistance of the National Research Foundation and The World Academy of Science (NRF-TWAS) of South Africa is acknowledged.

REFERENCES

[1] Martinez, D.M., and B.W. Ebenhack, 2008, "Understanding the Role of Energy Consumption in Human Development Through the Use of Saturation Phenomena," Energy Policy, 36(4), pp. 1430-1435.

[2] Ukoba, O.K., Eloka-Eboka, A.C., and Inambao, F.L., 2018, "Review of Nanostructured NiO Thin Film Deposition Using the Spray Pyrolysis Technique," Renewable Sustainable Energy Rev., 82, pp. 2900 - 2915.

[3] Ebhota, W., Eloka-Eboka, A.C., and Inambao, F.L, 2014, "Energy Sustainability Through Domestication of Energy Technologies in Third World Countries in Africa," Proc. Industrial and Commercial Use of Energy, Cape Town, 19-20 August.

[4] Machala, M., 2011, "Kerosene Lamps vs. Solar Lanterns," coursework for PH240, Stanford University, Stanford, USA.

[5] Kim Oanh, N.T., Nghiem, L.H., and Phyu, Y.L., 2002, "Emission of Polycyclic Aromatic Hydrocarbons, Toxicity, and Mutagenicity from Domestic Cooking Using Sawdust Briquettes, Wood, and Kerosene," Environ. Sci. Technol., 36(5), pp. 833-839.

[6] World Health Organization (W.H.O), 2002, The World Health Report. p. Annex Table 9.

[7] Ostro, B.D., Tran, H., and Levy, J.I., 2006, "The Health Benefits of Reduced Tropospheric Ozone in California," J. Air Waste Manage. Assoc., 56(7), pp. 1007-1021.

[8] Pope III, C.A., and Dockery, D.W., 2006, "Health Effects of Fine Particulate Air Pollution: Lines That Connect," J. Air Waste Manage. Assoc., 56(6), pp. 709-742.

[9] Change, I.C., 2007, The Fourth Assessment Report of the Intergovernmental Panel on Climate Change, Geneva, Switzerland.

[10] Jacobson, M.Z., 2002, "Control of Fossil- Fuel Particulate Black Carbon and Organic Matter, Possibly the Most Effective Method of Slowing Global Warming," J. Geophys. Res. Atmos., 107(D19).

[11] Jacobson, M.Z., 2004, "Climate Response of Fossil Fuel and Biofuel Soot, Accounting for Soot's Feedback to Snow and Sea Ice Albedo and Emissivity," J. Geophys. Res. Atmos., 109(D21).

[12] Ramanathan, V., and Carmichael, G., 2008, "Global and Regional Climate Changes Due to Black Carbon," Nat. Geosci., 1(4), pp. 221.

[13] Chung, S.H., and Seinfeld, J.H., 2002 "Global Distribution and Climate Forcing of Carbonaceous Aerosols," J. Geophys. Res. Atmos., 107(D19).

[14] Lam, N.L., et al., 2012, "Household Light Makes Global Heat: High Black Carbon Emissions from Kerosene Wick Lamps," Environ. Sci. Technol., 46(24), pp. 13531-13538.

[15] Bond, T.C., et al., 2013 "Bounding the Role of Black Carbon in the Climate System: A Scientific Assessment," J. Geophys. Res. Atmos., 118(11), pp. 5380-5552.

[16] Corporation, P. (2014). Sustainability Report. Retrieved from Tokyo, Japan: https://www.panasonic.com/global/corporate/sustainability/pdf/sr2014e.pdf

[17] Masters, G.M., 2013 Renewable and Efficient Electric Power Systems, John Wiley & Sons.

[18] Jacobson, M.Z., 2009, "Review of solutions to global warming, air pollution, and energy security," Energ Environ Sci., 2(2), pp. 148-173.

[19] Dietz, T., et al., 2009, Household Actions Can Provide a Behavioral Wedge to Rapidly Reduce US Carbon Emissions. Proc. National Academy of Sciences, USA, 106(44), pp. 18452-18456.

[20] Sims, R.E., Rogner, H.-H., and Gregory, K., 2003, "Carbon Emission and Mitigation Cost Comparisons Between Fossil Fuel, Nuclear and Renewable Energy Resources for Electricity Generation," Energy Policy, 31(13), pp. 1315-1326.

[21] Jaramillo, P., Griffin, W.M,. and Matthews, H.S., 2007, "Comparative Life-Cycle Air Emissions of Coal, Domestic Natural Gas, LNG, and SNG for Electricity Generation," Environ. Sci. Technol., 41(17), pp. 6290-6296.

[22] Sushil, S., and Batra, V.S., 2006 "Analysis of fly Ash Heavy Metal Content and Disposal in Three Thermal Power Plants in India," Fuel, 85(17-18), pp. 2676-2679.

[23] Carlson, C.L., and Adriano, D.C., 1993 "Environmental Impacts of Coal Combustion Residues," J. Environ. Qual., 22(2), pp. 227-247.

[24] Singh, R., Sharma, C., and Agrawal, M., 2017 "Emission Inventory of Trace Gases From Road Transport in India," Transp. Res. Part D Transp. Environ., 52, pp. 64-72.

[25] Abam, F. ,and Unachukwu, G., 2009, "Vehicular

Emissions and Air Quality Standards in Nigeria," Eur. J. Sci. Res., 34(4), p. 550-560.

[26] Zhang, Q., et al., 2007, "NOx Emission Trends for China, 1995–2004: The View from the Ground and the View from Space," J. Geophys. Res. Atmos., 112(D22).

[27] Miguel, A.H., et al., 1998 "On-Road Emissions of Particulate Polycyclic Aromatic Hydrocarbons and Black Carbon from Gasoline and Diesel Vehicles," Environ. Sci. Technol., 32(4), pp. 450-455.

[28] Zhuo, S., et al., 2017 "Source-Oriented Risk Assessment of Inhalation Exposure to Ambient Polycyclic Aromatic Hydrocarbons and Contributions of Non-Priority Isomers in Urban Nanjing, a Megacity Located in Yangtze River Delta, China," Environ. Pollut., 224, pp. 796-809.

[29] Mills, E., 2005, The specter of Fuel-Based Lighting, American Association for the Advancement of Science.

[30] Cabraal, R.A., Barnes, D.F., and Agarwal, S.G., 2005 "Productive Uses of Energy for Rural Development," Annu. Rev. Environ. Resour., 30, pp. 117-144.

[31] Jahan, S., and Umana, A., 2003 "The Environment-Poverty Nexus," Dev. Policy J., 3(20), pp. 53-70.

[32] Davis, L.W., and Gertler, P.J., 2015 "Contribution of Air Conditioning Adoption to Future Energy Use Under Global Warming," Proc. of the National Academy of Sciences, 112(19), pp. 5962-5967.

[33] Lunt, M.F., et al., 2015 "Reconciling Reported and Unreported HFC Emissions with Atmospheric Observations," Proc. of the National Academy of Sciences, 112(19), pp. 5927-5931.

CHAPTER 7: CONCLUSION AND FUTURE WORK

7.1 Conclusion

The aims and objectives of this study which were to fabricate, characterize and model a nanostructured metal oxide thin film based solar cell with emphasis on NiO/TiO_2 p-n heterojunction have been explored. This has been with a view to providing affordable and sustainable energy to developing and low-income countries. The objective of the study focused on deposition of metal oxide thin films using NiO, characterizing the thin films and thereafter optimize the parameters. Experimental optimization was done on the films with focus on pre-deposition, deposition and post-deposition. These optimized results were then used to fabricate the metal oxide heterojunction device. The experimental results validated the theoretical model/result. These were achieved successfully as reflected in the peer-reviewed journal publications and conferences presentations documented in this thesis.

Chapter 2 did a comprehensive literature review on solar energy inclusion in developing and low-income countries with a focus on Africa. This laid the basis for the need for more affordable and sustainable energy to replace existing unstable energy in these countries. It established that developing countries can latch on the technology of solar energy to meet their energy needs. However, more research is needed to reduce the current cost, efficiency and sustainability of current solar technology in the market.

Chapter 3 did an extensive review of an alternate material (NiO) to existing silicon wafers solar cells and low-power consuming technique (SPT). This is because nanostructured metal oxides hold promise for a better replacement to silicon wafer solar cells. They are cheap, easy to optimize, sustainable and can be efficient. The chapter was able to establish that NiO deposited using spray pyrolysis technique can be used for development of affordable, efficient and sustainable solar cells in developing countries.

Chapter 4 did comprehensive optimization of NiO using spray pyrolysis technique with a view of using it for fabrication of the final solar cells device. The optimization covers pre-deposition, deposition and post-deposition.

Chapter 5 capitalized on the gains achieved in the optimization of the nanostructured NiO thin films to fabricate the solar cells. The fabricated solar cell exhibited 16.8 mA for the short circuit current, 350 mV open circuit voltage, 0.39 fill factor and conversion efficiency of 2.30 % under 100 mW/cm^2 illumination

Chapter 6 modelled the fabricate solar cells using SCAPs and also looked at using solar cells to reduce global warming.

The study has shown that affordable, sustainable and efficient solar cells can be developed in laboratories of developing and low-income countries with ease and without adverse effects on the environment and without incurring a huge cost due to use of low budget equipment and materials.

7.2 Future work

Photovoltaic solar cells is an evolving and dynamic area with huge potentials and opportunities. There is a great promise from this study for metal oxide heterojunction solar cells.

7.2.1 **Experimental:** more optimization can be done on the concentration and on combining with other low-cost deposition techniques. Ageing and other substrates can also be explored. More parameters can be explored during the course of the modelling and then validated via experimental results. Other metal oxides can also be investigated. There is also the possibility of doping with other materials. A different but cheap technique can also be studied or a possible development of hybrid technique can also be explored.

7.2.2 **Theoretical**: tuning can be done by varying simulation parameters. Other modelling tools and software can also be explored for formulating and validating results.

APPENDICES

APPENDIX A: SCHEMATIC OF THE DISSERTATION

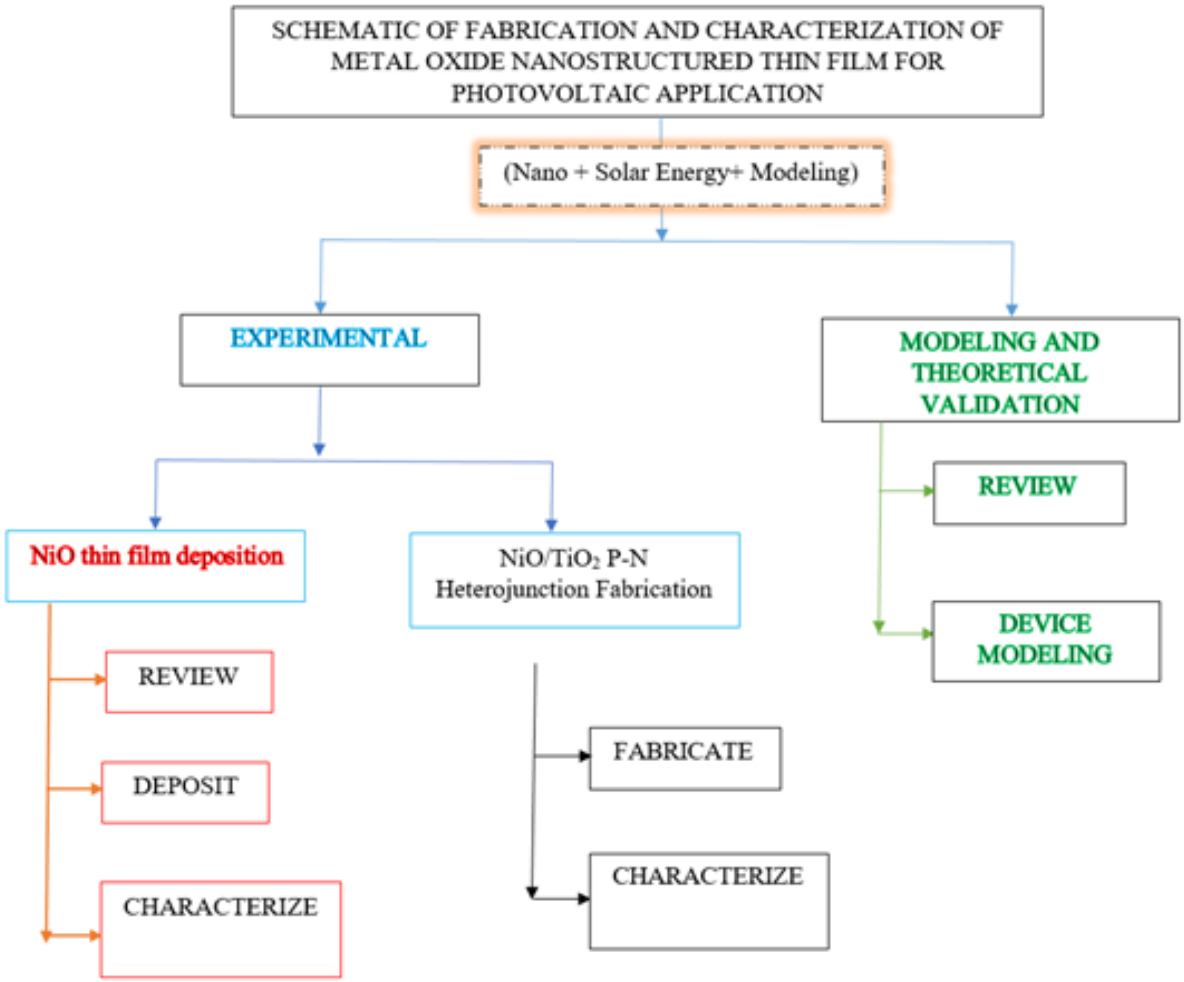

APPENDIX B: EQUIPMENT USED

FIG 1. FEGSEM

FIG 2. SAMPLE PREPARATION

FIG 3. FUME CHAMBER WITH CHEMICALS

FIG 4. EXPERIMENTAL SET UP

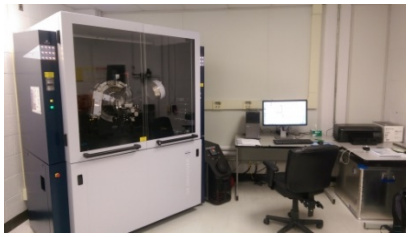

FIG 5. X-RAY DIFFRACTOMETER

FIG 6. UV-VIS-NIR SPECTROMETER

Fig. 7. Pictorial view of the Material (Metal Oxide) used

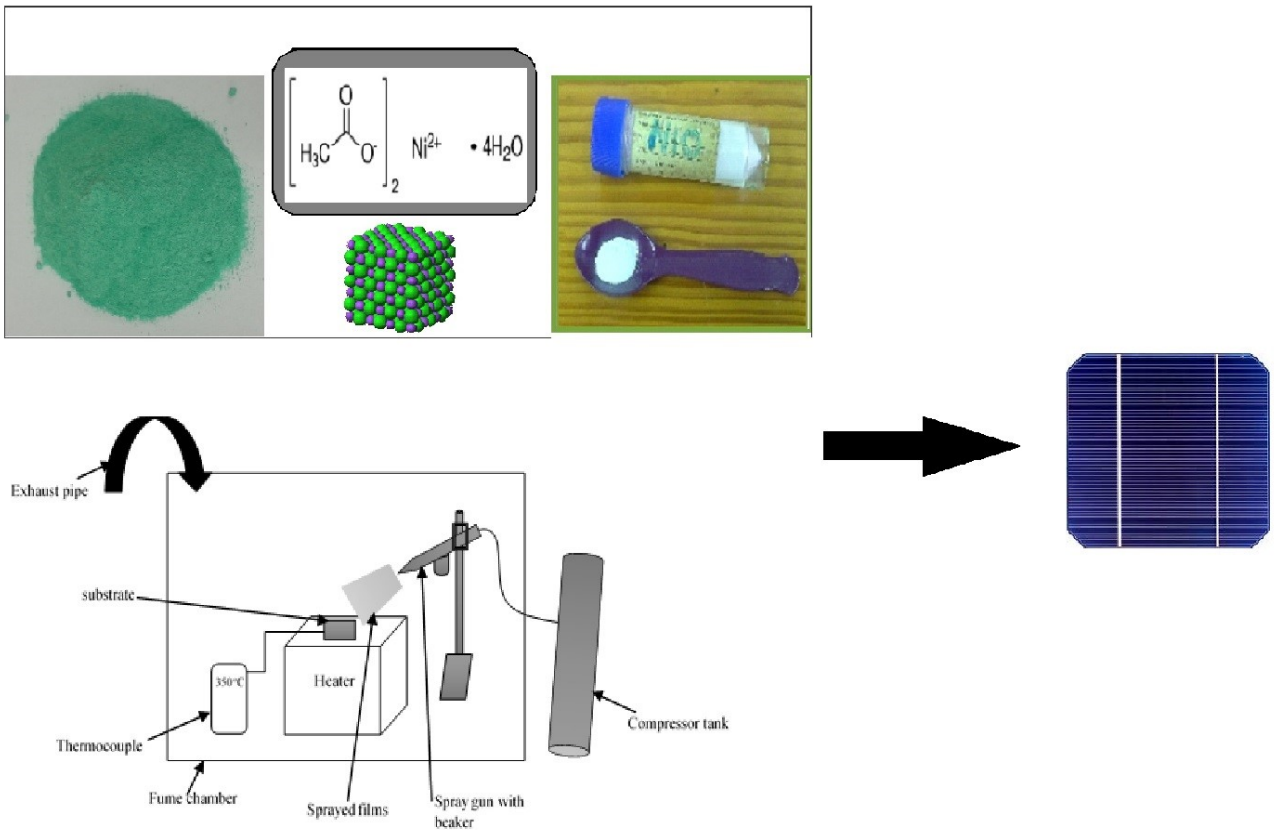

Fig 8. Overall schematic of the experimental